W physics in ATLAS

Fabrice Balli, CEA Saclay

THE XIV-th INTERNATIONAL SCHOOL-CONFERENCE
"THE ACTUAL PROBLEMS OF MICROWORLD PHYSICS"

Grodno, Belarus, 12–24 August , 2018

Outline

- Introduction
- Theoretical context of precise W measurements
  - Exemple physics motivation : m_W measurement
  - W production at LHC
  - W detection at ATLAS
- Recent ATLAS measurements
  - W cross-sections at 7 TeV
  - W+jets at 8 TeV
  - W mass measurement at 7 TeV
  - Wjj and aGC at 7 and 8 TeV
- Conclusive remarks

Introduction

The Standard Model (SM)

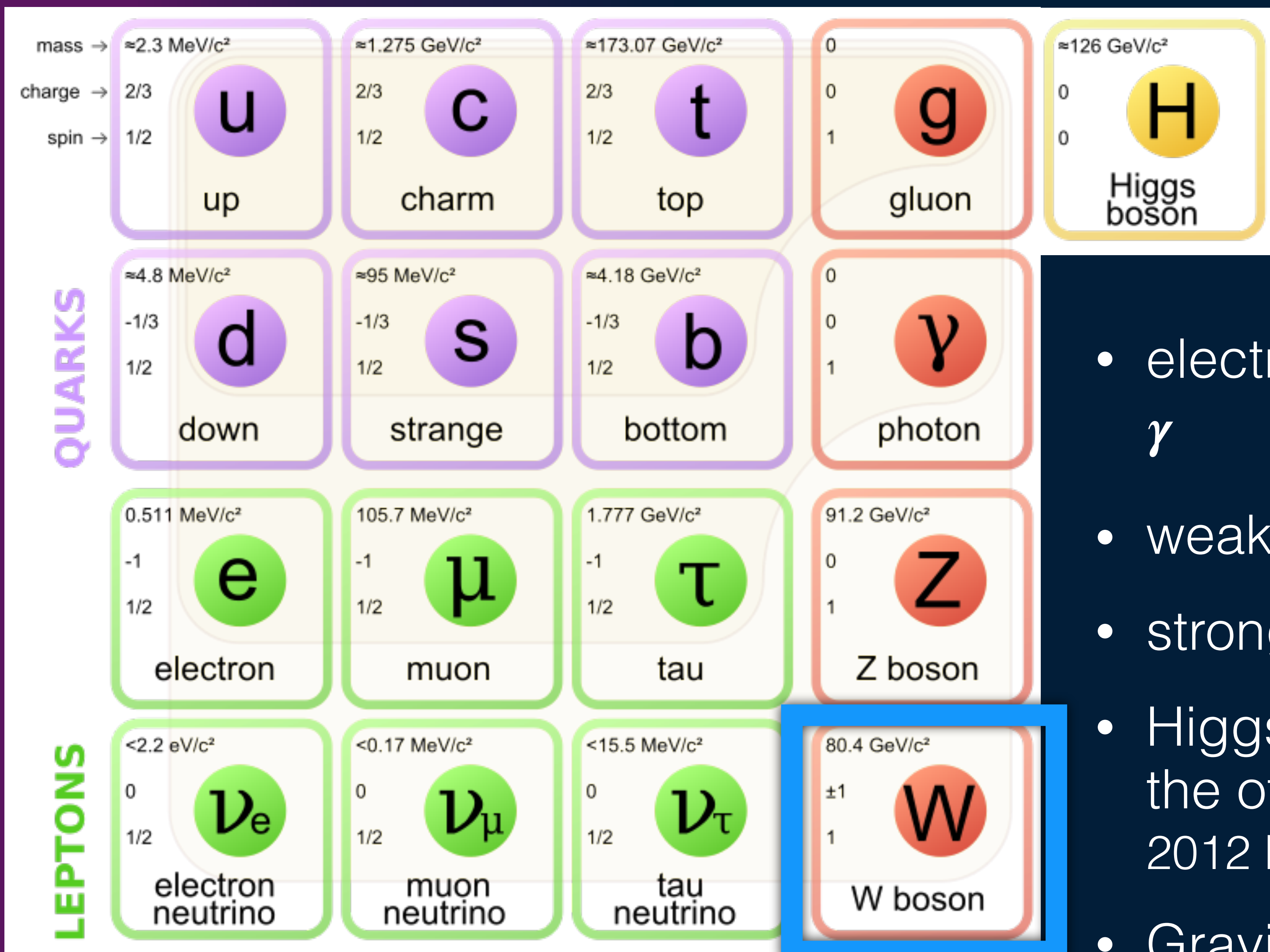

- Standard Model : basic model of elementary particle physics

- electromagnetic force — photon γ
- weak interaction — Z, W^+, W^-
- strong interaction — 8 gluons
- Higgs boson — confers mass to the other particles ; discovered in 2012 by ATLAS and CMS
- Gravitational interaction — not described by the SM

The W boson

- Discovered in UA1 and UA2 at CERN SPS in 1983
  - 1984 Nobel prize awarded to Carlo Rubbia and Simon van der Meer
- Charge : ±1e
- Width : 2.085±0.042 GeV
- Spin : 1
- Mass : 80.385±0.015 GeV
- Decay channels :
  - e, μ, τ : BR ~11 % each
  - hadrons : BR ~67 %

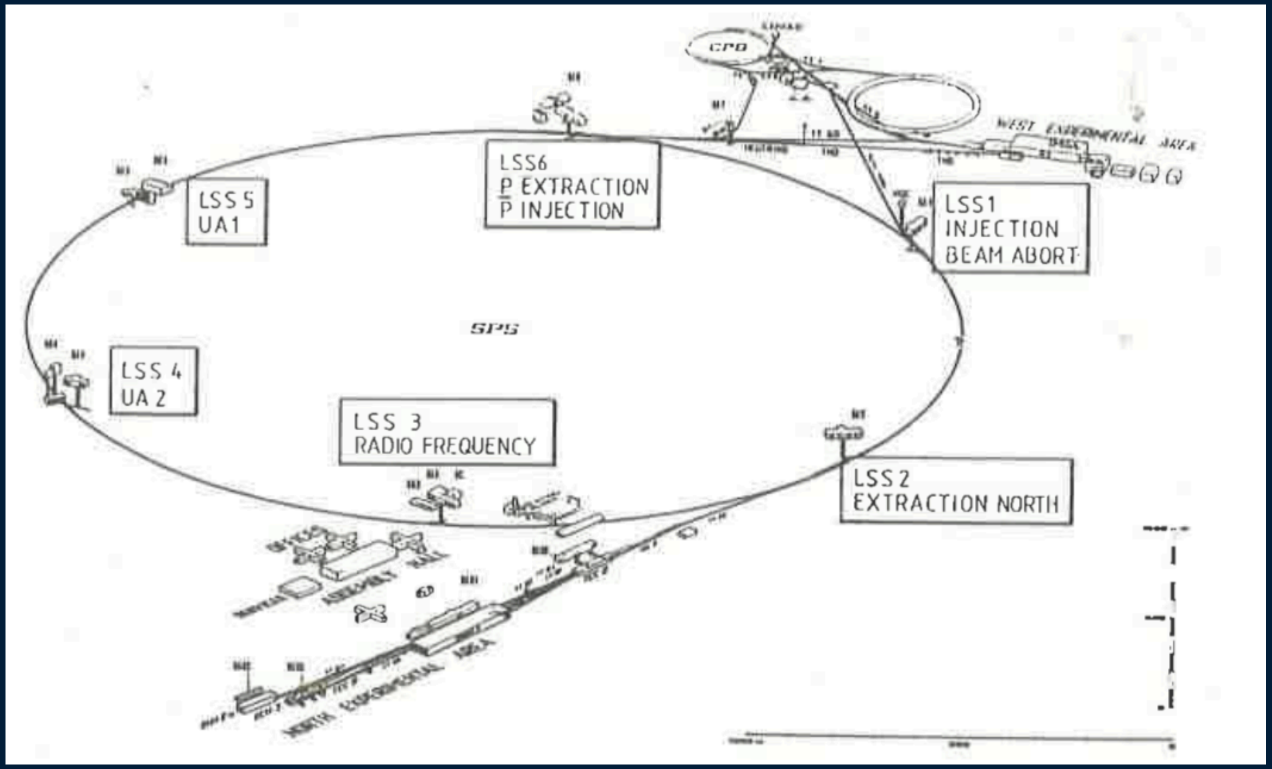

- A well-known pillar of SM : why worry about further measurements ?
  - Background to other processes (Higgs, ttbar…)
  - Stringent tests of SM consistency (EW fit), probe of pQCD, of anomalous gauge couplings —> **More precise** measurements of differential cross-sections and mass is **necessary**

The Large Hadron Collider at CERN

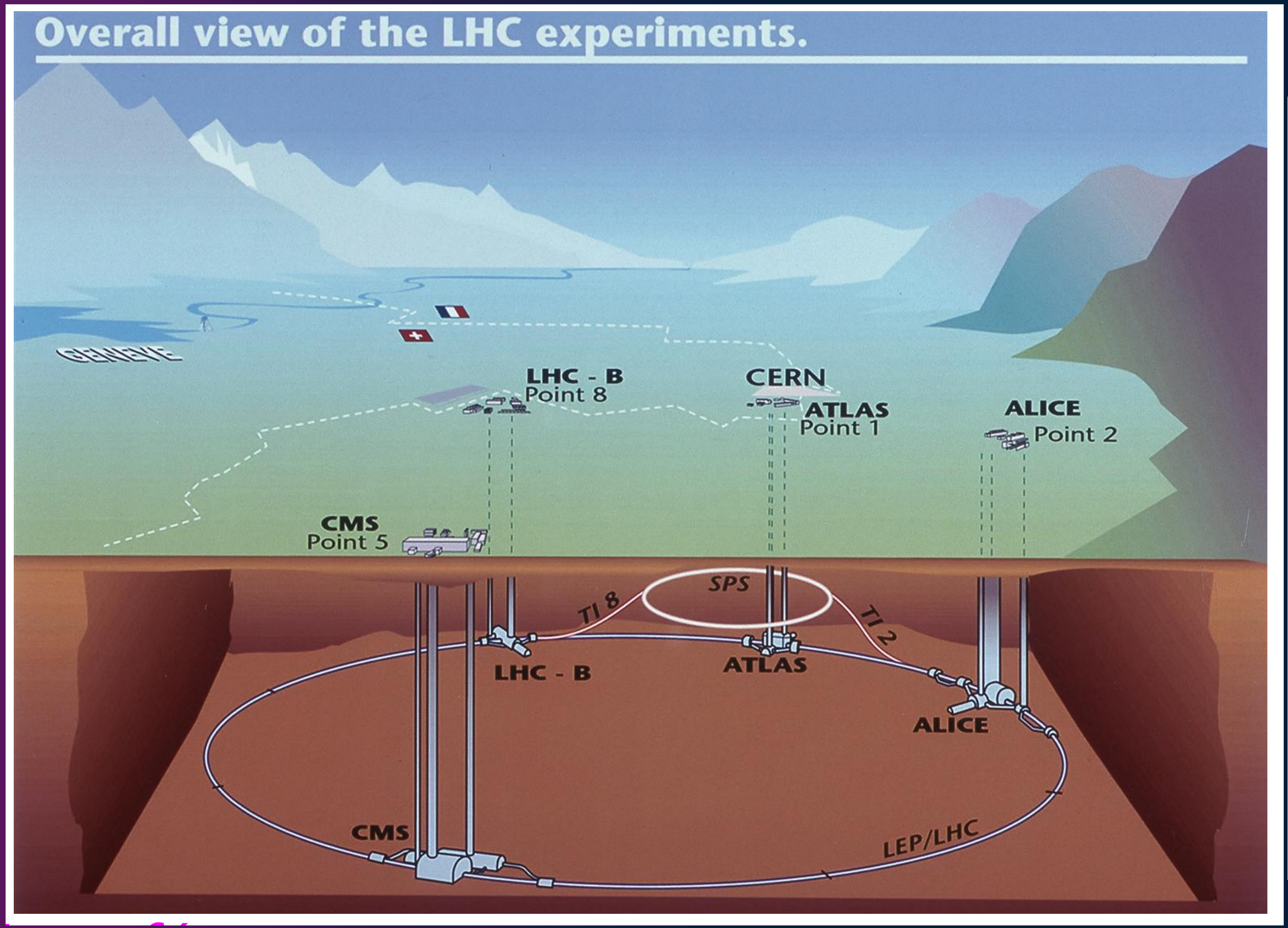

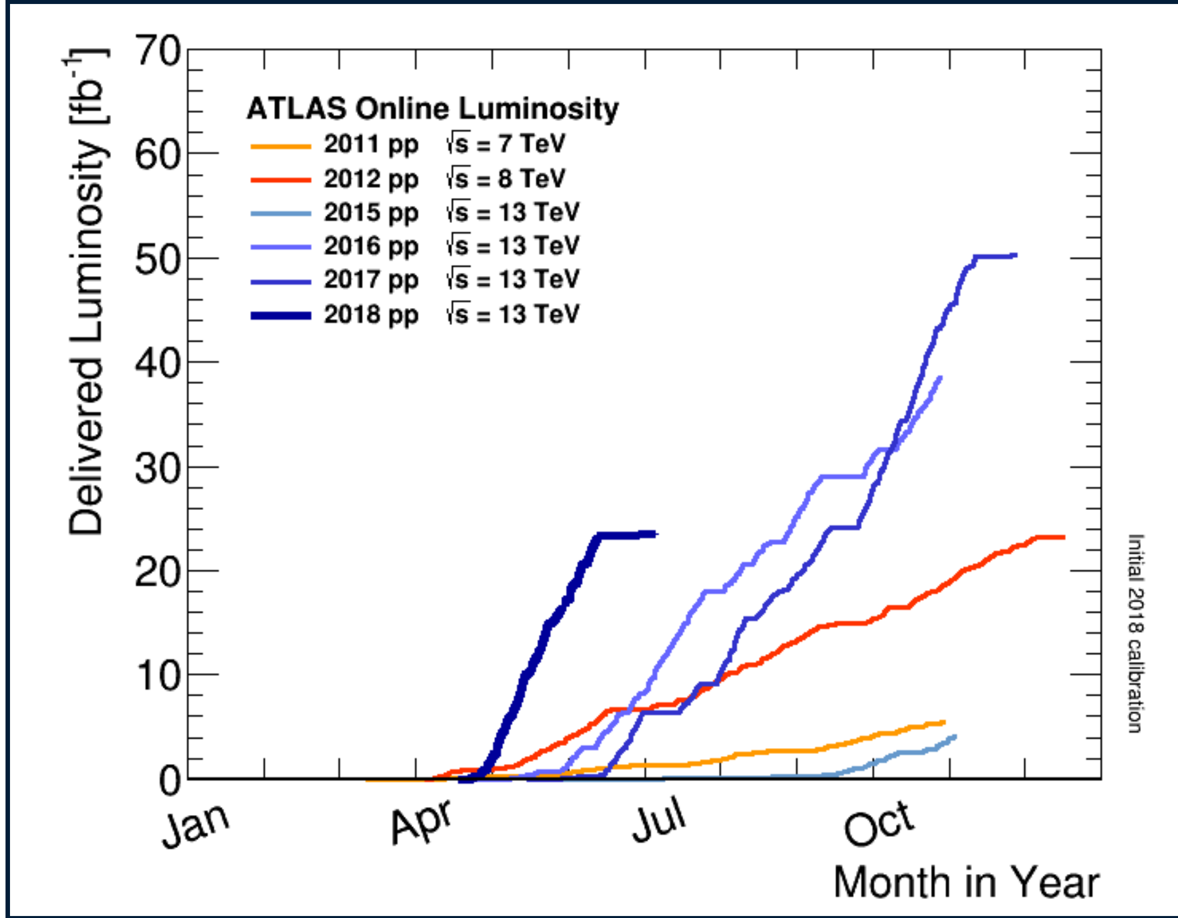

- 27 km circumference
- The only high-energy physics proton-proton collider currently running
- Has successfully delivered big amounts of collision data over the last 7 years to the 4 detectors : LHCb, ALICE, CMS and ATLAS
- Center of mass energy is **7 TeV (2011), 8 TeV (2012)**, 13 TeV (2015 - up to now)

The ATLAS experiment at LHC in Run1 (2011-2012)

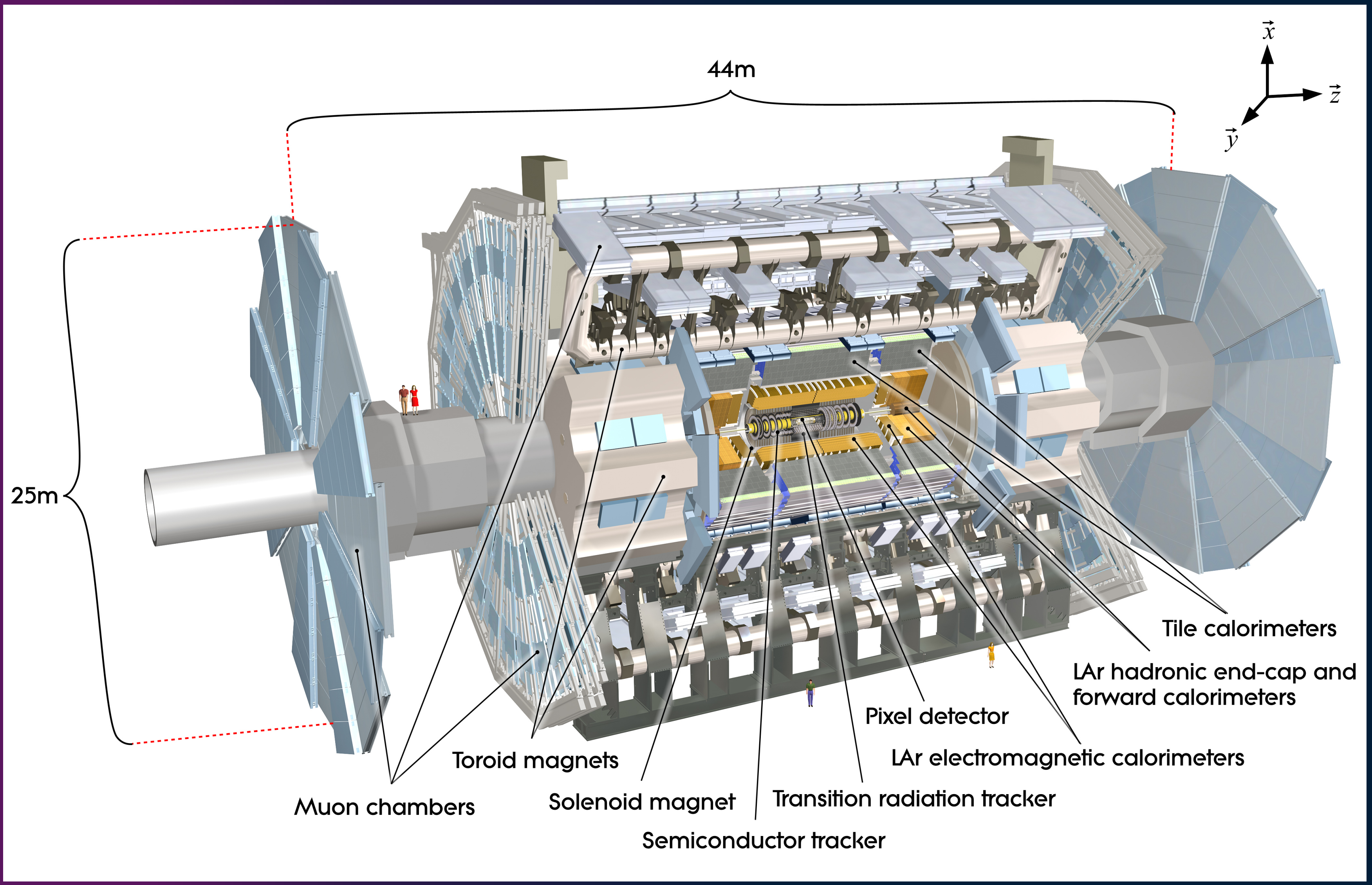

- Inner tracker - vertices reconstruction, charged tracks
- Electromagnetic calorimeter - electrons, photons
- Hadronic calorimeter - jets
- Muon spectrometer - in a toroidal magnetic field

Recorded 4.6/20.2 fb^{-1} luminosity in 2011/2012

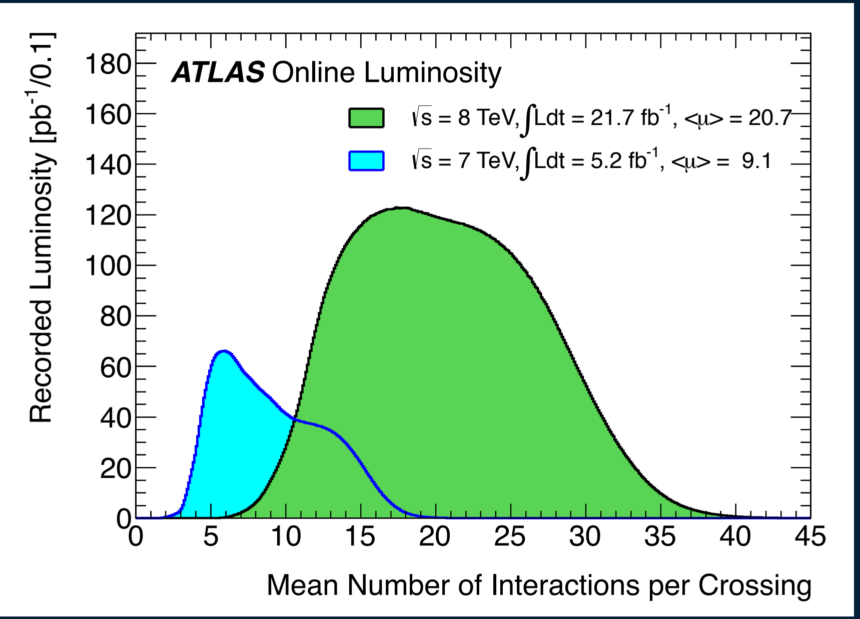

W events at ATLAS Run1

- W cross-section ~ 10^2 nb
  - —>7 TeV N_W ~ 470M
  - —>8 TeV N_W ~ 2.02B
  - cleanest signature : e, μ
    - ~47 (202) M events per channel
      - detector acceptance, event selection and reconstruction efficiencies to be taken into account (conservative factor 10 : still a few M just for 7 TeV)

W.J. Stirling, private communication

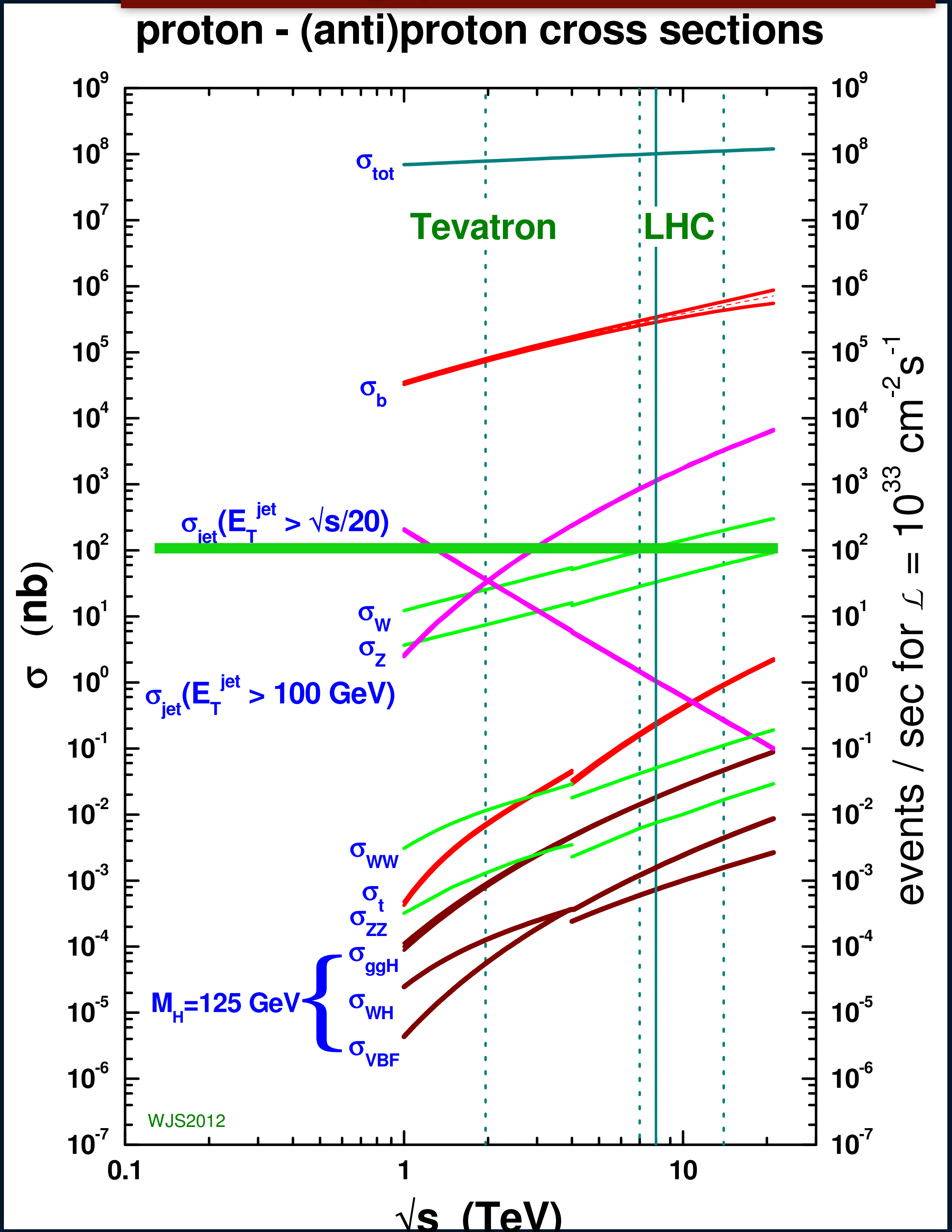

Recommended readings :
- CTEQ Lecture from Jeff Owens (2000)
- QCD and Collider Physics, R.K. Ellis, W.J. Stirling, and B.R. Webber

Theory context

(an experimentalist's view!)

- Theory motivation to m_W measurement
- W production at LHC
- W detection at ATLAS

m_W and the EW fit

One illustration : W mass (m_W) and the EW fit

- Electroweak theory (true at all orders) (1)
- Also, one has (2)
- After solving the 2nd order equation in m_W^2 one gets (3)

$$m_W^2 = \frac{\pi \alpha_{tree}}{\sqrt{2} G_\mu \sin^2 \theta_{W,tree}} \quad (1)$$

$$m_W^2 = \frac{g_W^2 v^2}{4}, \; m_Z^2 = \frac{g_W^2 v^2}{4 \rho_0 \cos^2 \theta_W} = \frac{m_W^2}{\rho_0 \cos^2 \theta_W} \quad (2)$$

$$\begin{aligned} m_W^2 &= \frac{m_Z^2}{2}\left(1 + \sqrt{1 - \frac{4\pi\alpha}{\sqrt{2} G_\mu m_Z^2}}\right) \\ &= \frac{m_Z^2}{2}\left(1 + \sqrt{1 - \frac{4\pi\alpha_{tree}}{\sqrt{2} G_\mu m_Z^2} \frac{1}{1 - \Delta r}}\right) \end{aligned} \quad (3)$$

- Where radiative corrections to the W boson propagator (dominated by top and Higgs contributions) can be expressed as :

$$\Delta r = \Delta \alpha - \frac{\cos^2 \theta_W}{\sin^2 \theta_W} \Delta \rho + \Delta r_{res},$$

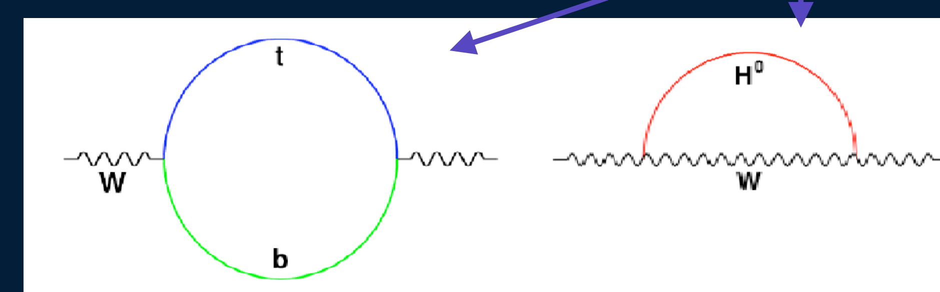

- Top quark mass dependence dominated by :

$$\Delta \rho^{top} \approx \frac{3\sqrt{2} G_\mu m_{top}^2}{16\pi^2}$$

G. Burgers and F. Jegerlehner
10.5170/CERN-1989-008-V-1.55

- Higgs boson mass dependence dominated by :

$$\Delta r_{res}^{Higgs} \approx \frac{\sqrt{2} G_\mu m_W^2}{16\pi^2}\left[\frac{11}{3}\left(\ln \frac{m_h^2}{m_W^2} - 5/6\right)\right].$$

Relationship between W mass, top mass and Higgs mass (and EW parameters) !

The global EW fit

arXiv:1803.01853

- Idea of electroweak fits
  - Measure many different observables in experiments
  - Calculate the relations between all observables in the Standard Model
  - Probe the consistency of the SM by predicting observables
- Input for the gobal electroweak fit mostly from
  - LEP: Z boson observables (e.g. $\sin^2\theta_W$)
  - Tevatron: W boson, top quark mass
  - LHC: Higgs boson, top quark mass
- Overall good consistency between indirect determination (i.e. physics parameter left free) and the direct measurements

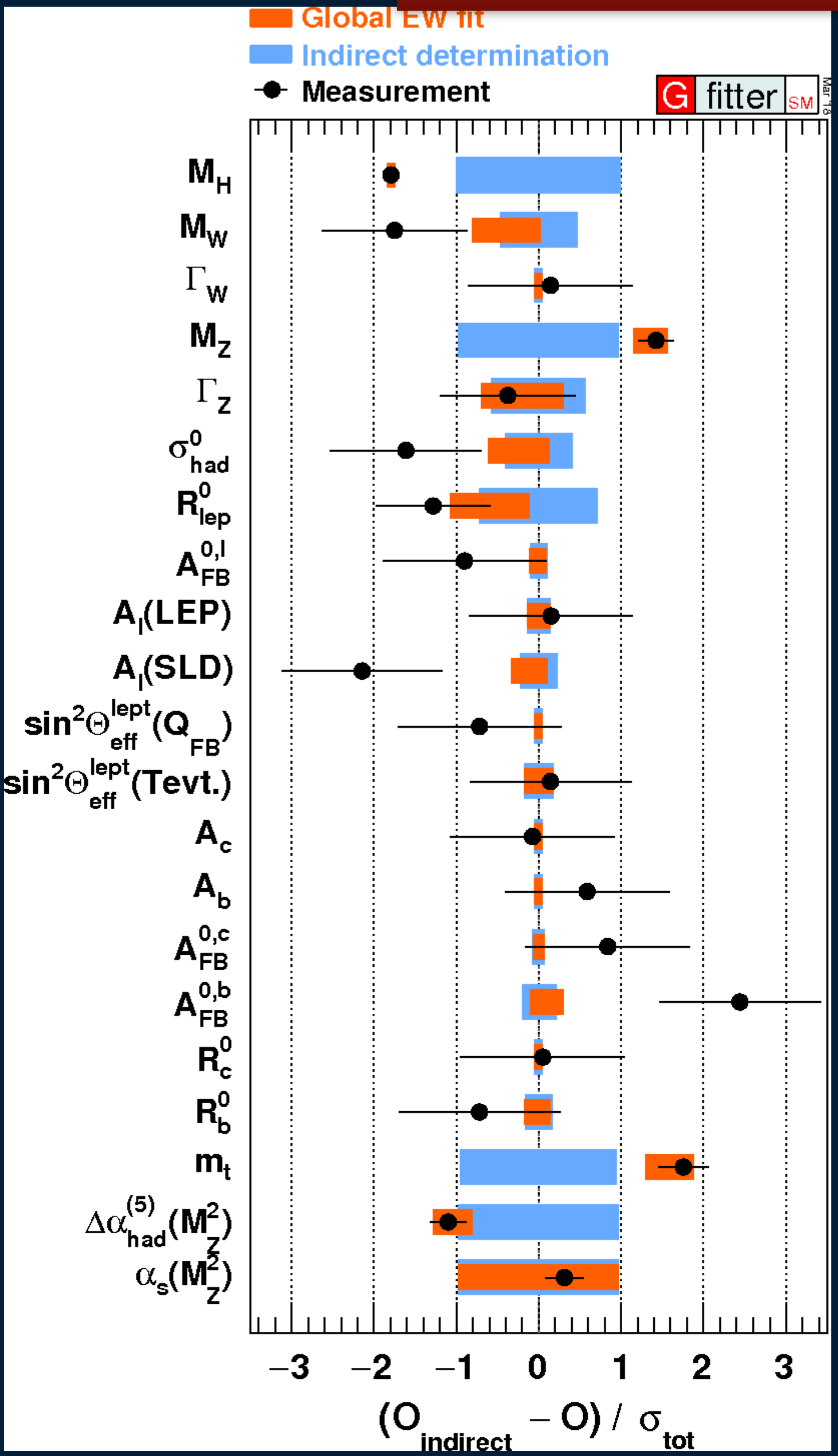

The global EW fit

- Test the consistency of the Standard Model
  - e.g. predict m_W, provided all other input measurements
- needs 7 MeV precision to compete with indirect determination from theory fit (10^{-4} relative uncertainty!)
- Electroweak precision measurements also sensitive to several new physics scenarios
  - For this, need a 5 MeV precision on m_W
- —>this measurement needs very accurate prediction for W production and kinematics of decay products :
  - W p_T and rapidity spectrum
  - polarisation (spin correlations)
  - high order EW (NLO)
- Proton PDFs are an essential ingredient for this
- It also needs detector calibration at the same level of precision!

arXiv:1803.01853

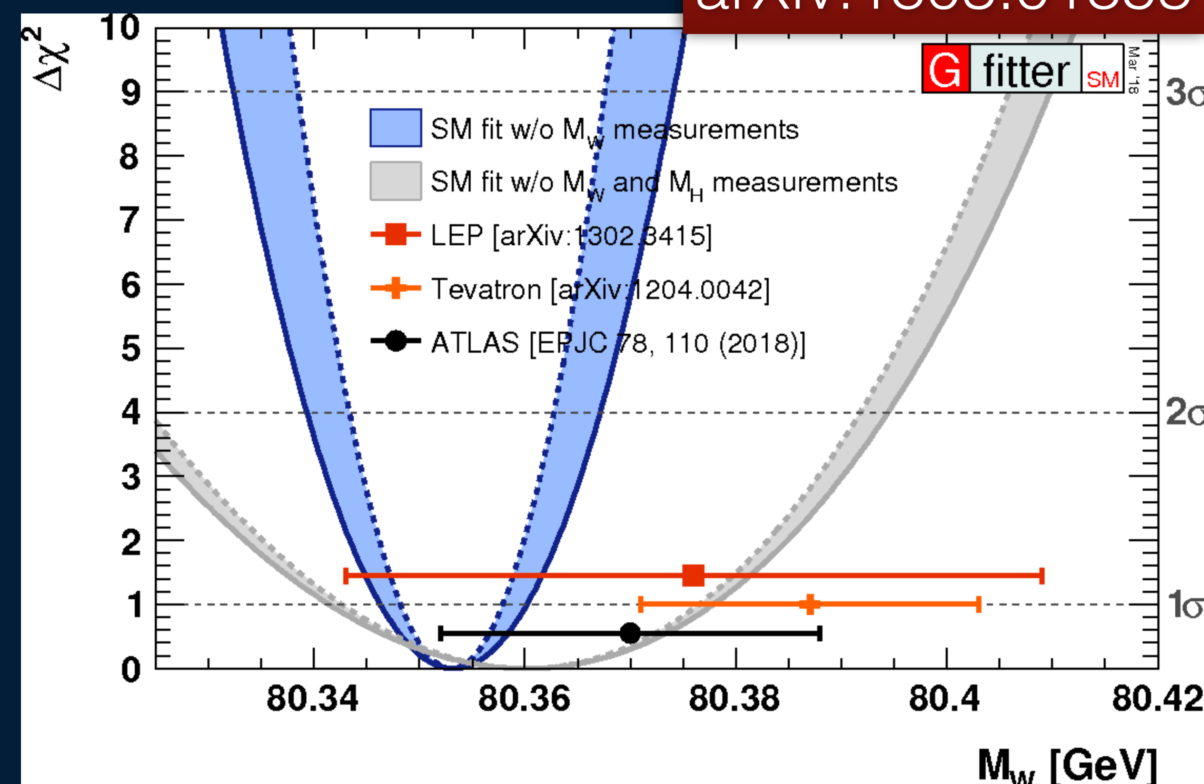

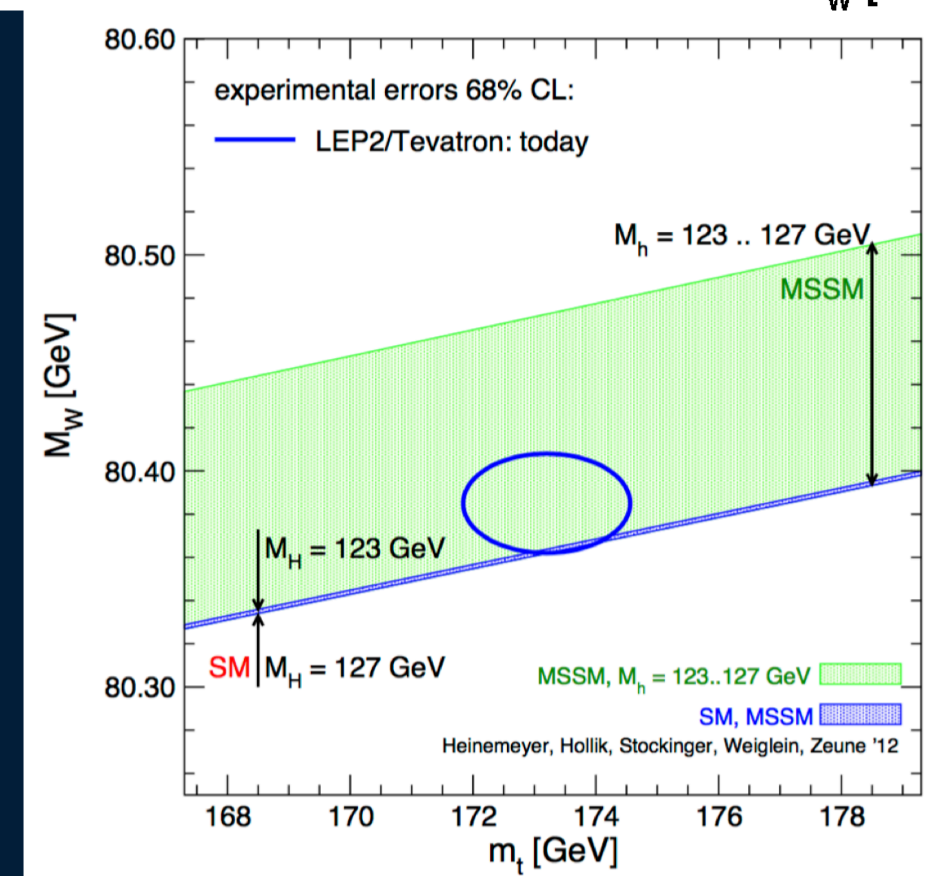

parenthesis : $\sin^2\theta_W$

- One of the key inputs to EW and BSM fits
- Observed tension between LEP and SLD measurements (~3 sigmas)
- New preliminary measurement from ATLAS

ATLAS-CONF-2018-037

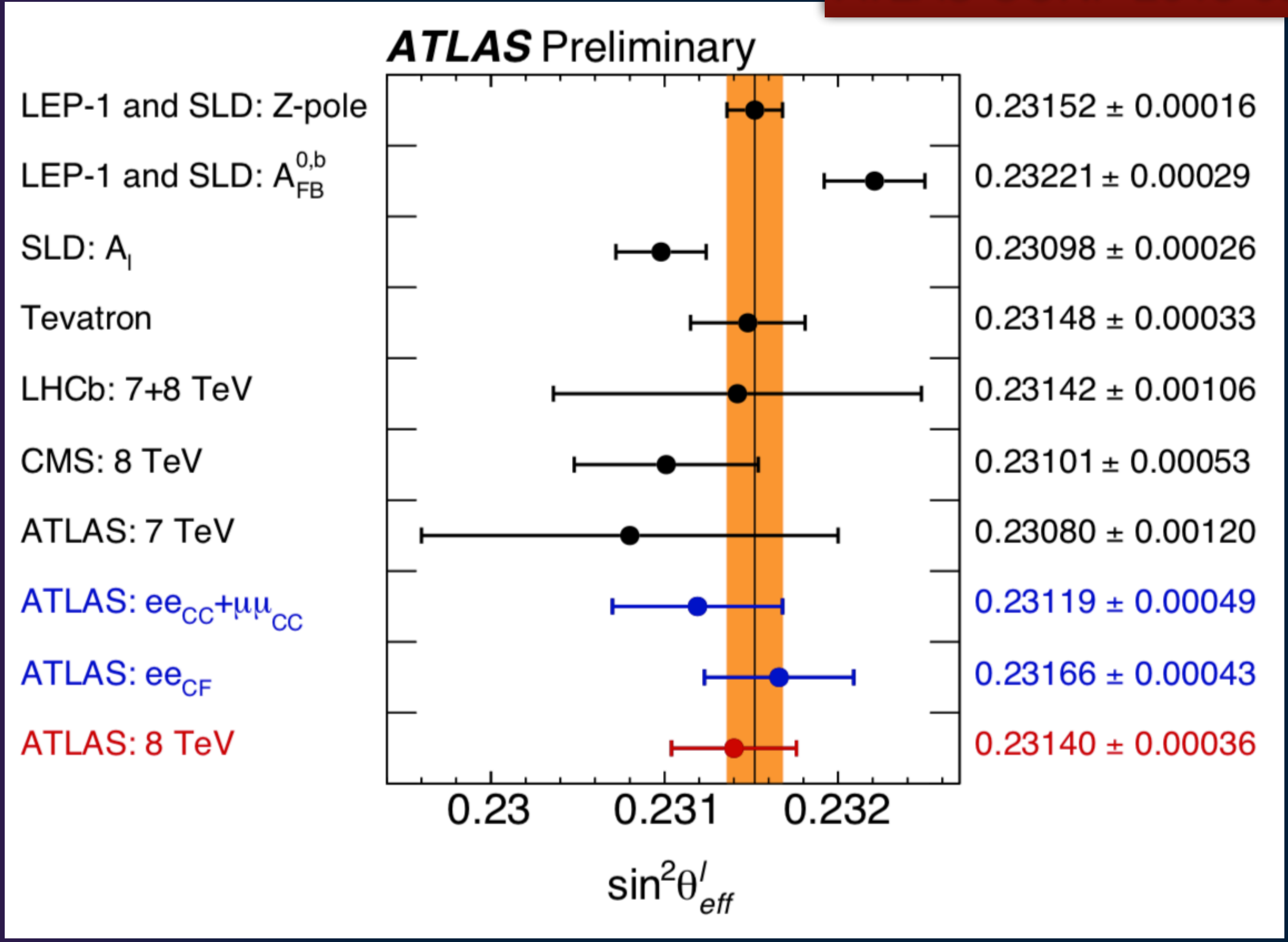

W production

Drell-Yan production

- factorization theorem :

$$\sigma_{pp\to X}(\alpha_s, Q^2) = \sum_{a,b}\int_0^1 f_a(x_1, Q^2) f_b(x_2, Q^2) \times \hat{\sigma}_{ab\to X}(\alpha_s, Q^2) dx_1 dx_2$$

- weight the partonic cross-section by non-perturbative fonctions (parton distribution functions, PDFs) considered at high scale $Q^2 = \mu_F^2$ (separates perturbative and non-perturbative regime)
- partonic cross-section can be calculated perturbatively and is only known up to NNLO and thus depends on a renormalisation scale μ_R^2 (=Q^2):

$$\hat{\sigma}_{\mathrm{ab}\to\mathrm{X}}(\hat{s}) = \underbrace{\hat{\sigma}_0(\hat{s})}_{\mathrm{LO}} + \underbrace{\alpha_s(\mu_R^2)\hat{\sigma}_1(\hat{s})}_{\mathrm{NLO}} + \underbrace{\alpha_s^2(\mu_R^2)\hat{\sigma}_2(\hat{s})}_{\mathrm{NNLO}} + \mathscr{O}(\alpha_s^3)$$

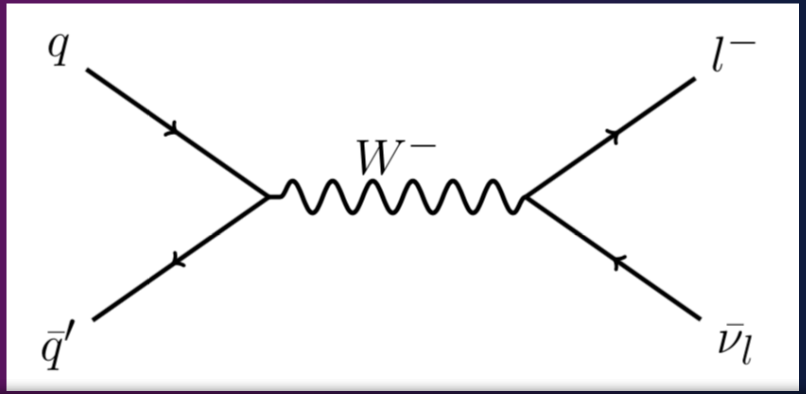

tree level W production (LO)

$$\mathscr{M} = i[\frac{g}{\sqrt{2}} V_{q\bar{q}'}\bar{v}(k_b)\varepsilon^*_{\lambda,\mu}\gamma^\mu(1-\gamma^5)u(k_a)]\left\{\frac{1}{\hat{s}-M_W^2+(iM_W\Gamma_W)}\right\}[\frac{g}{\sqrt{2}}\bar{u}(p_a)\varepsilon_{\lambda,\nu}\gamma^\nu(1-\gamma^5)v(p_b)]$$

- the spinors
- coupling (V-A)
- polarisation
- ‘Breit Wigner’ with W mass and width
- CKM matrix element
- Gauge coupling constant $g^2 = \frac{8G_F M_W^2}{\sqrt{2}}$

W production : PDFs

W.J. Stirling, private communication

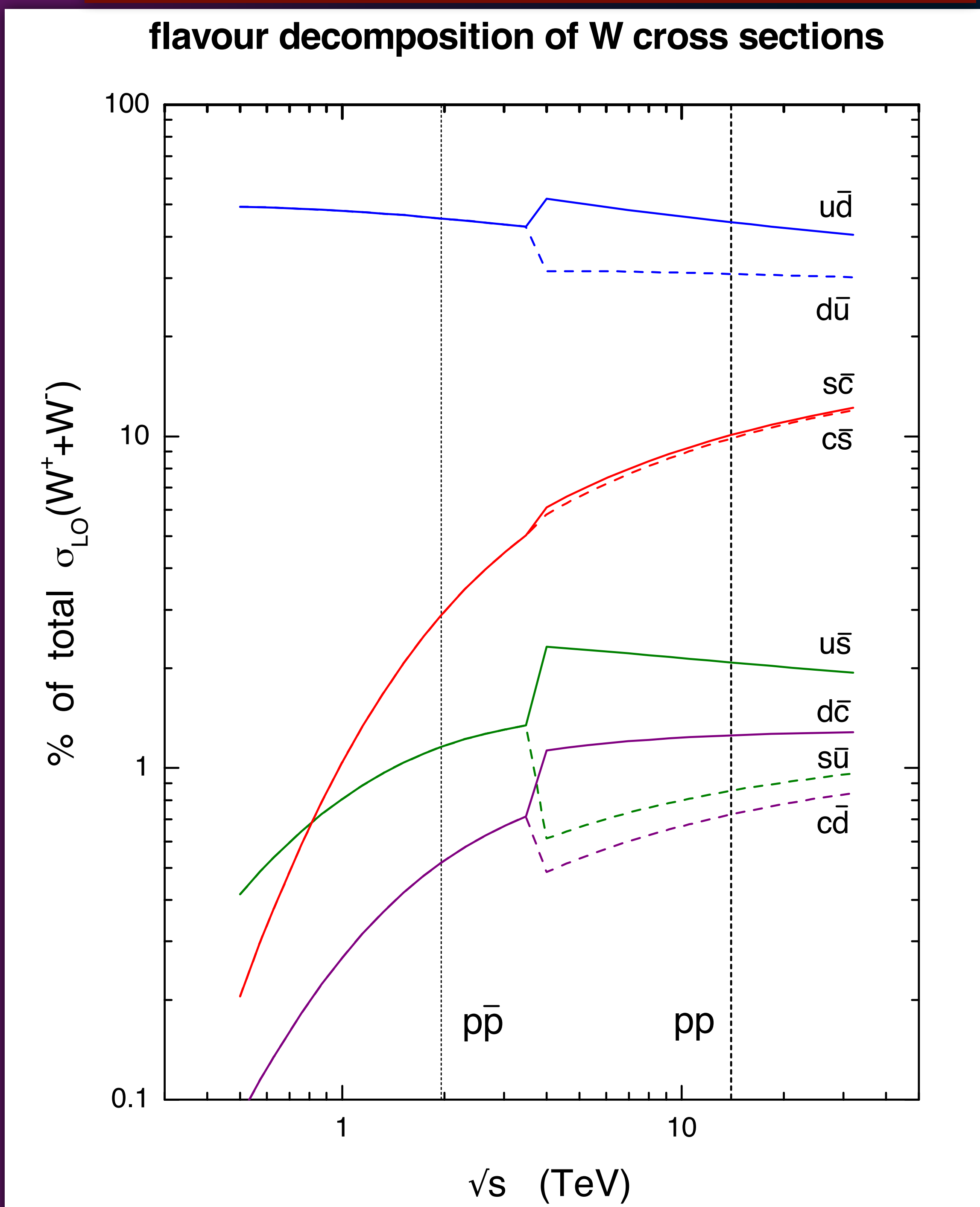

- W^+(W^-) production is dominated by u$\bar{d}$ (d$\bar{u}$)
- u_v is higher at high x —> increase of W^+ production at high rapidities (next slide)
- Contribution from 2nd quark generation is not negligible : ~25%
  - induces larger uncertainties than in p$\bar{p}$
- Gluon contribution starting at NLO

PDF $f_{q/g}(x, Q^2)$ = probability for a parton q/g to carry a fraction x of the proton momentum for a hard process with scale Q^2

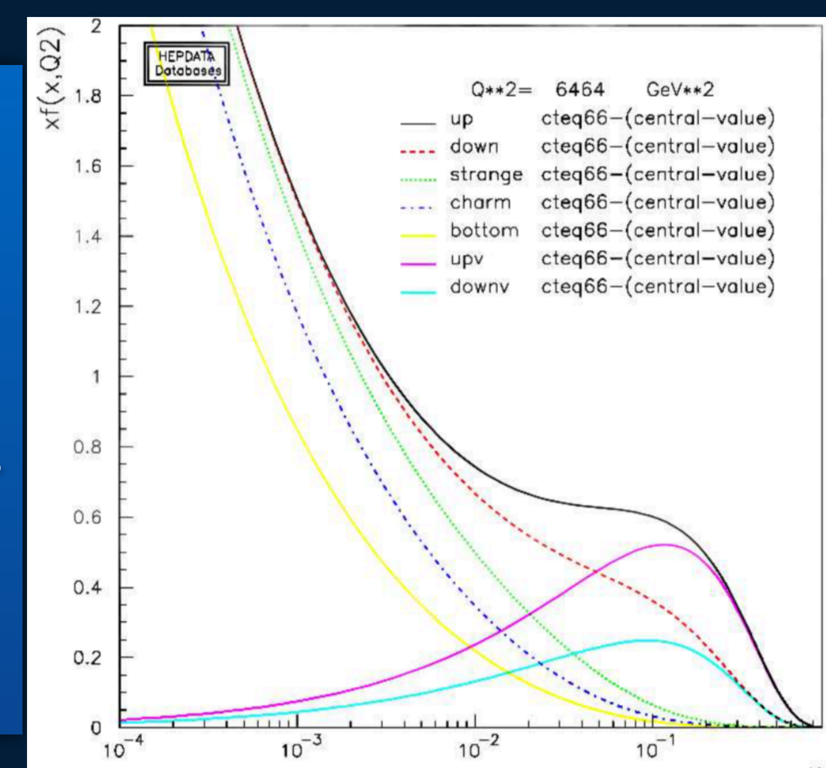

W production : rapidity

- Rapidity y is defined as : $y = 1/2 \ln [(E+p_z)/(E-p_z)]$
- Assuming intrinsic transverse momentum of partons $k_T=0$, we have (in center of mass frame) : $p_a = \sqrt{s}/2 * x_a (1,0,0,1)$ and $p_b = \sqrt{s}/2 * x_b (1,0,0,-1)$
- —>$y = 1/2 \ln (x_a/x_b)$
- Leading to : $x_a = \frac{M}{\sqrt{s}} e^{y}$ $x_b = \frac{M}{\sqrt{s}} e^{-y}$

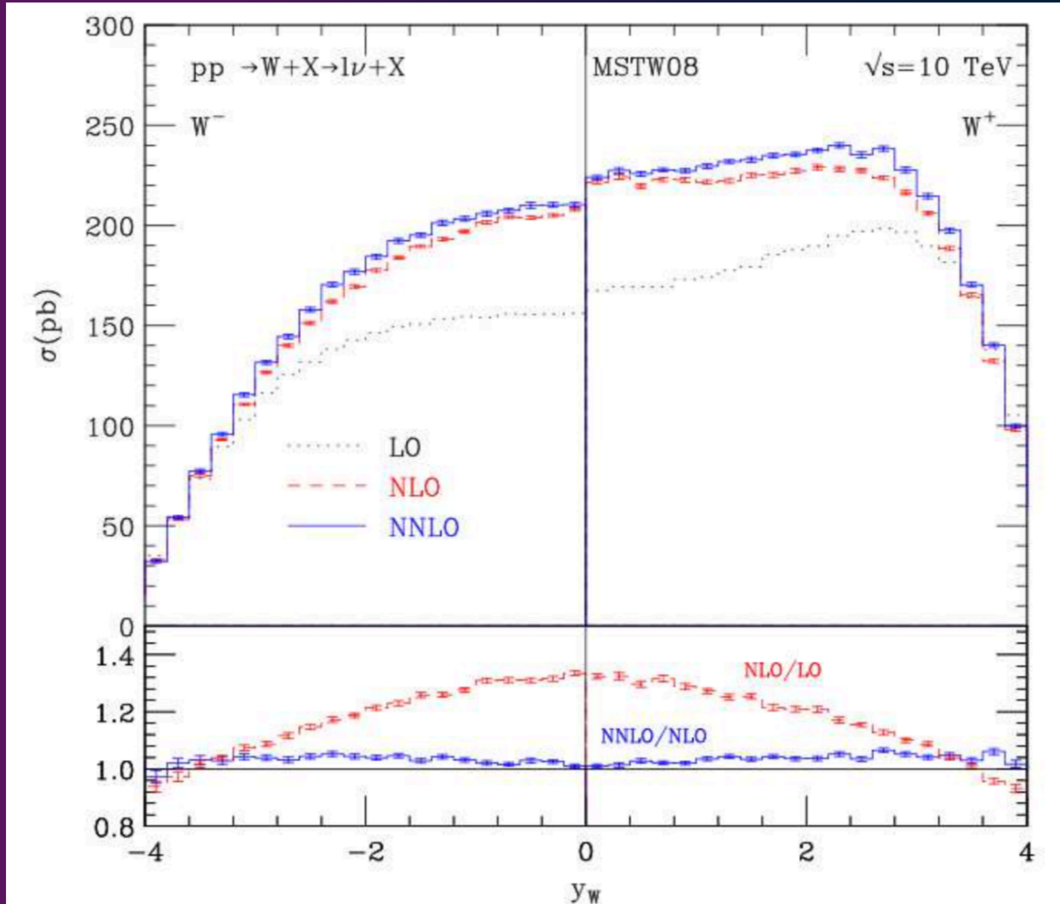

- low |y| : mainly sea quarks ($x \sim 10^{-2}$)
- high |y| : 1 sea quark and 1 valence quark ($x \sim 10^{-4}$, a few 0.1)
- One has at lowest order :

$$\frac{d\sigma}{dy} = \frac{1}{s} \sum_{a,b} \sigma_0^{ab \to W}(M) f_a(x_a, M^2) f_b(x_b, M^2)$$

- Boson rapidity directly sensitive to PDFs
- allows to constrain them from differential cross-section measurements

W p_T : where does it come from ?

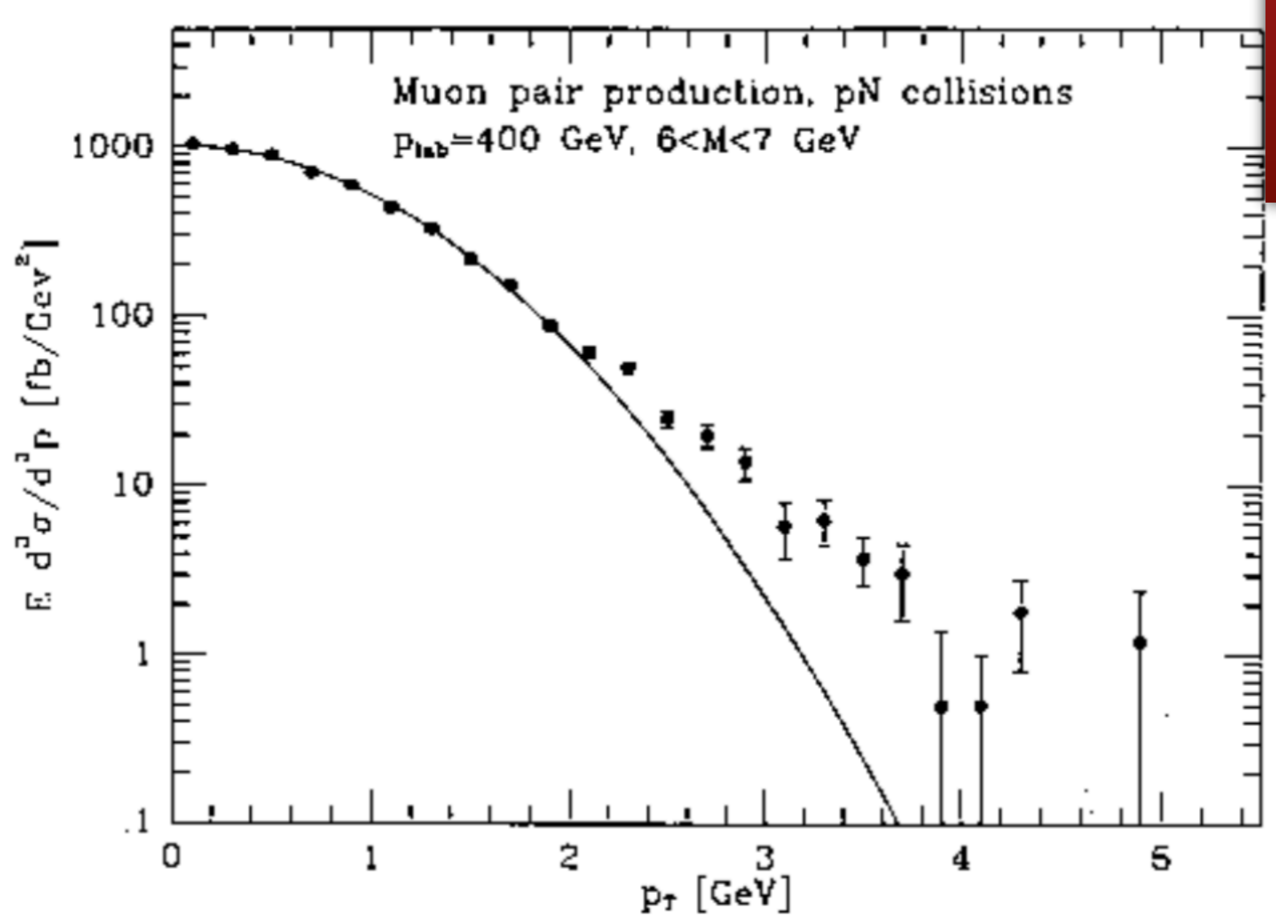

Fig. 9.2. The lepton pair transverse momentum from the CFS collaboration [4]. The curve corresponds to a Gaussian intrinsic k_T distribution for the annihilating partons.

QCD and Collider Physics, R.K. Ellis, W.J. Stirling, and B.R. Webber

- Intrinsic k_T of the partons : good agreement with the data (fixed-target pn collisions) up to p_T ~ 2 GeV —>assume Gaussian form with < k_T(parton)> ~ 760 MeV
- Not sufficient to describe higher values of W p_T

W p_T : where does it come from ?

- Need additional hard parton emissions to explain higher p_T region
  - NLO (qg—>Wq, qq'—>Wg), NNLO QCD
  - NNLO diagrams are typically :

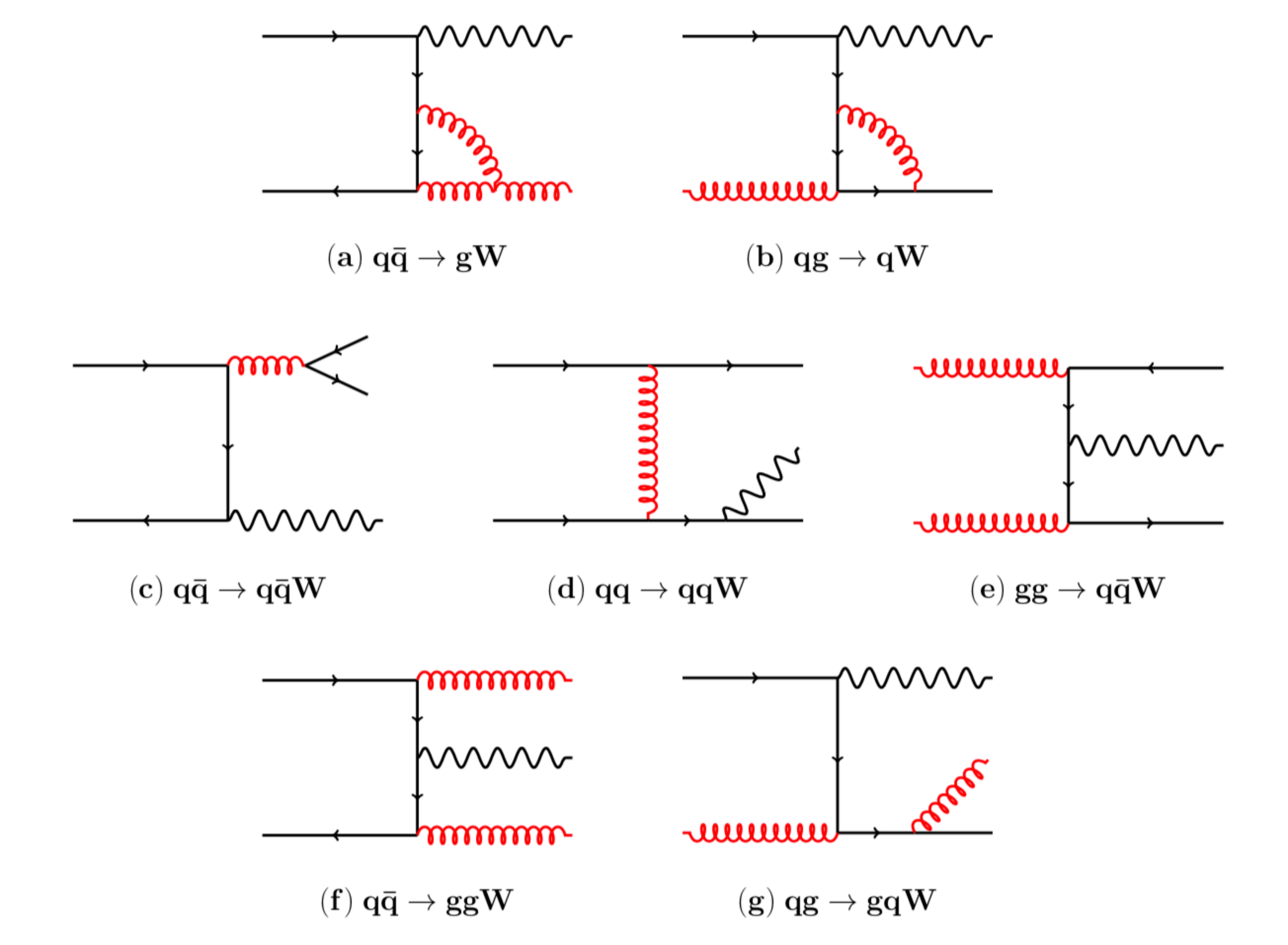

W p_T : let's diverge a little bit

ATL-PHYS-PUB-2014-015

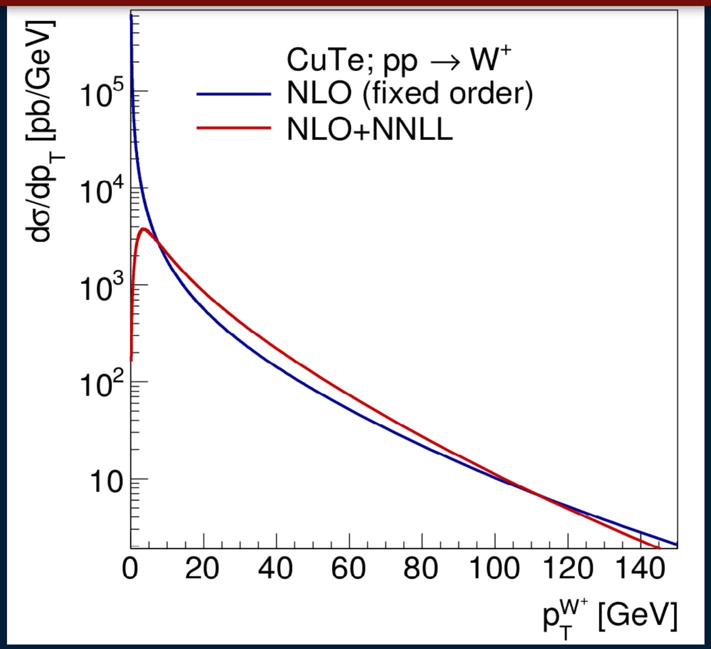

- Pure fixed-order NNLO predictions : diverge when $p_T \to 0$ ($p_T \ll M$) due to the presence of soft and collinear emissions — spoiled by large logarithms of the type $\alpha_S^n \ln^m(M^2/p_T^2)$
- This can (has to) be resummed at all orders and gives

$$\frac{d\sigma}{d\tau dy dp_T^2} = \left(\frac{d\sigma}{d\tau dy}\right)_{Born} \frac{4\alpha_s}{3\pi} \frac{\ln s/p_T^2}{p_T^2} \exp\left(-\frac{2\alpha_s}{3\pi} \ln^2 s/p_T^2\right)$$

- Where the exponential is referred to as the 'Sudakov form factor'
- However, does not include the cases where multiple gluons are emitted with $k_T \sim p_T$, nor the cases where gluon momenta add to 0.
- Several resummation formalisms and calculations to resum the leading, next-to-leading and next-to-next-to leading logs
  - e.g., RESBOS, DYRES, Geneva, RADISH…
- Can also use parton showers (typically done in simulations) : Sherpa, Pythia, Herwig…
  - Evolution of fragmentation functions through DGLAP formalism

W p_T : summary

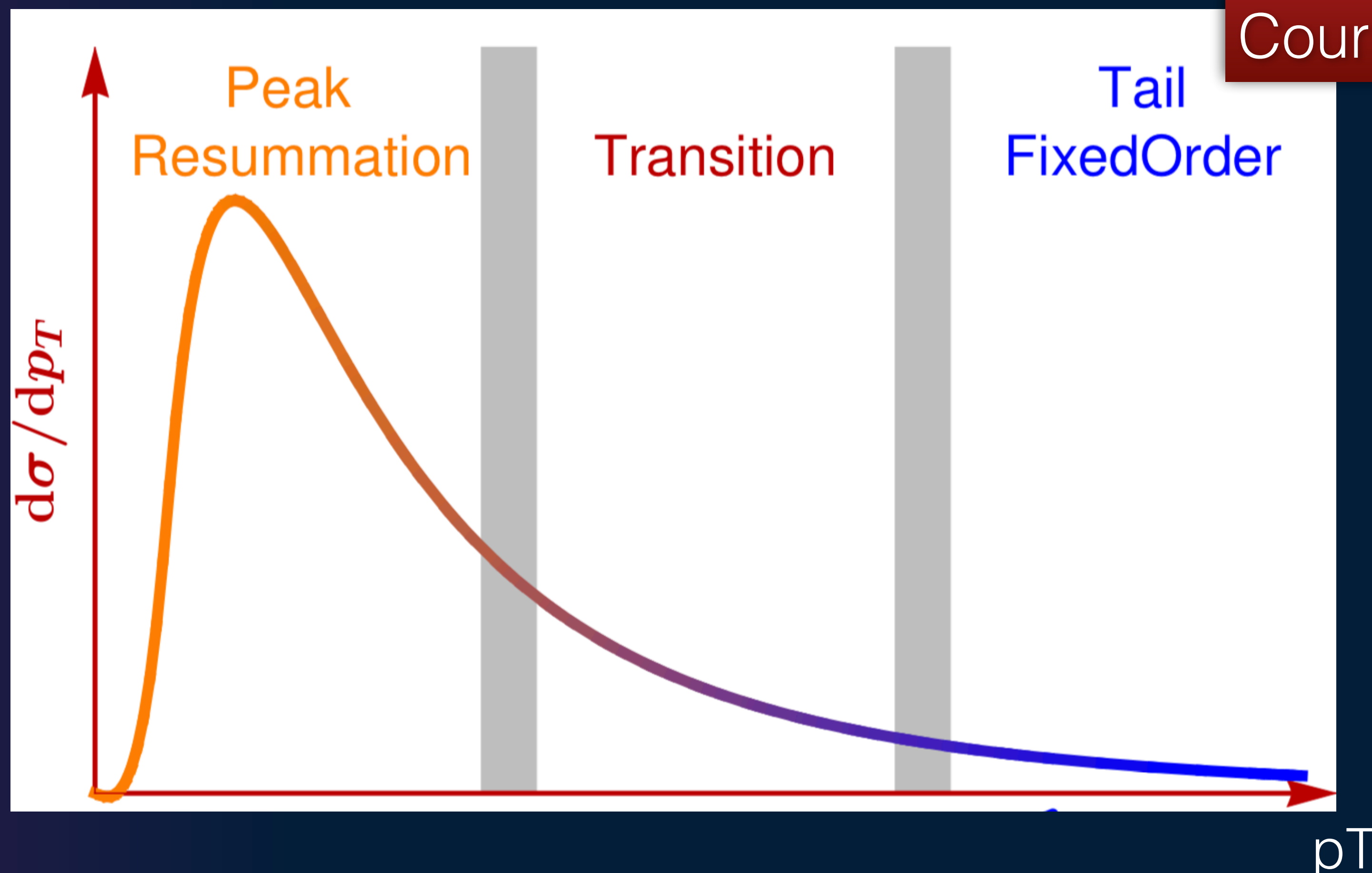

Courtesy of F. Tackmann

- high p_T~M : fixed-order V+1 jet (MC : fixed-order matrix elements) ; resummation does not work
  - $d\sigma/dp_T^2$ goes as $1/p_T^2$
- low p_T << M : fixed-order breaks down, resummation comes in (MC : Parton showers)
- Transition region : no fixed boundary
  - resummation works but fixed-order gives sensible results as well
    - Best prediction from consistent combination of the two
  - MC : Matrix element + parton shower merging/matching

NLO EW emissions

- Corrections to W production take into account O(α_{EM}) corrections : photon radiation (ISR, FSR), loop corrections (pure weak), ISR/FSR interference (IFI)

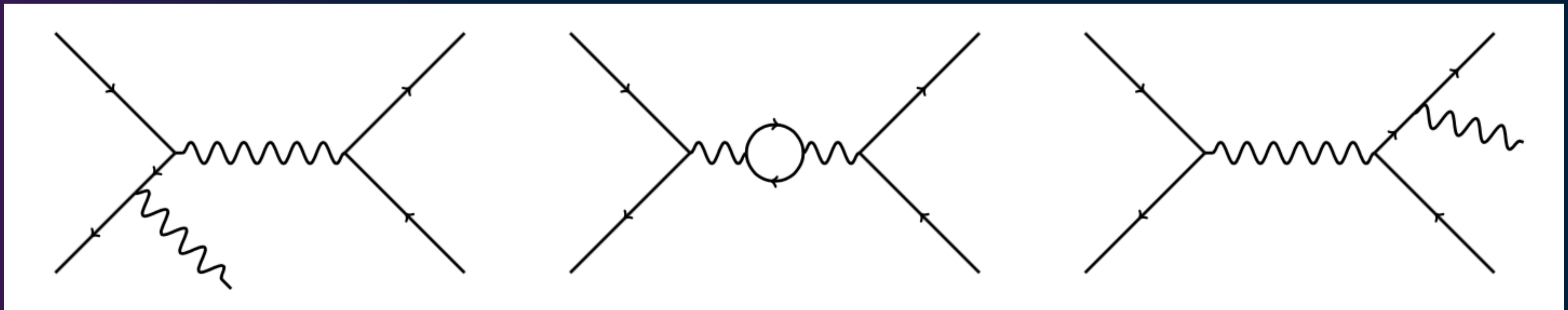

- ISR factorised in the PDF evolution, FSR is the most important numerically among the rest
- Several tools to handle this. In ATLAS W/Z simulated samples, typically :
    - Pythia8 parton shower handles the ISR
    - Photos handles FSR and electron pair emissions from virtual photon (higher order, uncertainty only)
    - pure weak and IFI corrections not included but impact is estimated with other tools (YFS, Winhac…) (and often simply added as uncertainty)

W detection

Event topology, definitions of observables

- Detect single (inclusive) W boson decaying into a lepton and a neutrino
- The ATLAS detector measures :
  - The **lepton** charge and 4-vector (transverse momentum $\vec{p}_{T\ell}$)
  - The activity recoiling against the W **(hadronic recoil $\vec{u}_T$)**
    - measures additional jets from signal
    - Sensitive to additional interactions (pile-up) and underlying event
    - Enables to indirectly reconstruct the neutrino transverse momentum $\vec{p}_T^{miss} = -(\vec{u}_T + \vec{p}_{T\ell})$
    - Some analyses use a direct reconstruction of p_T^{miss}, some use a direct reconstruction of the recoil —> different algorithms, impact is significant ~only for m_W here

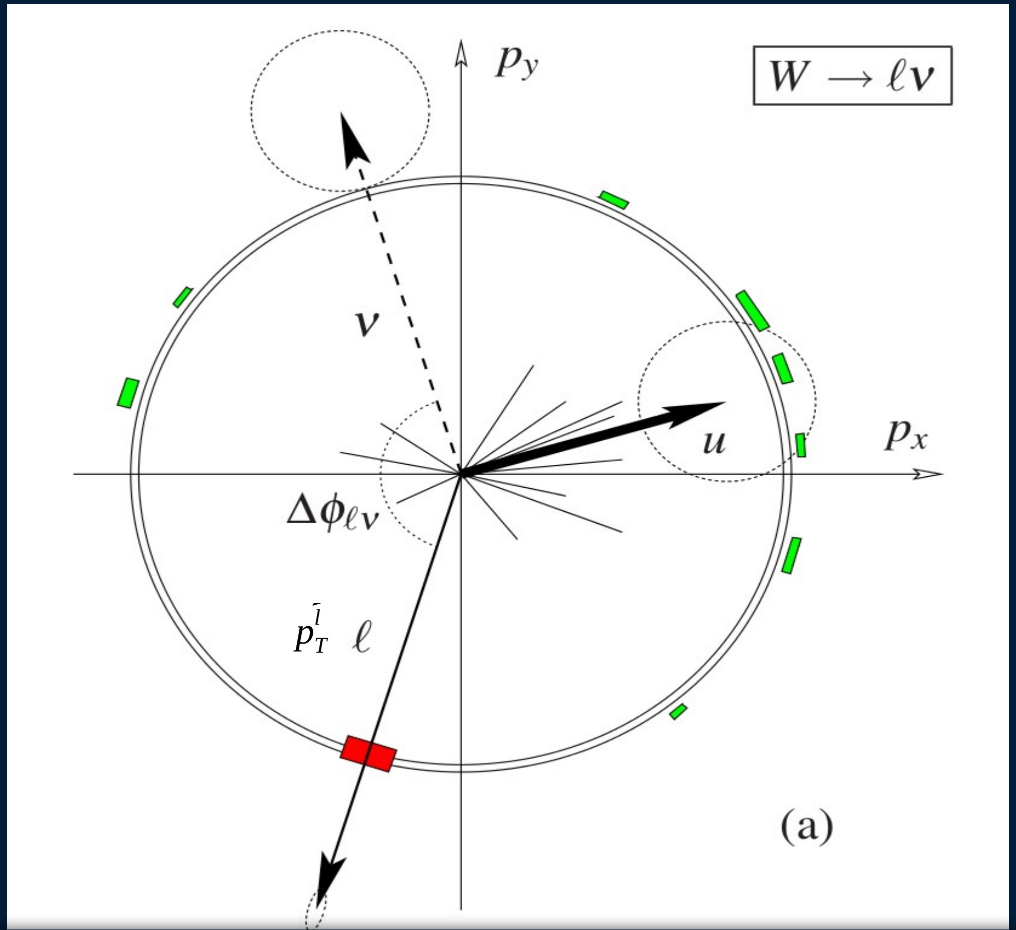

$\vec{u}_T$: vector sum of calorimeter deposits excluding lepton deposits

$m_T = \sqrt{[2\, p_{T\ell}\, p_T^{miss}\, (1-\cos\Delta\phi)]}$

Impossible to fully reconstruct m_W because of the neutrino

The Jacobian peaks : m_T and lepton p_T

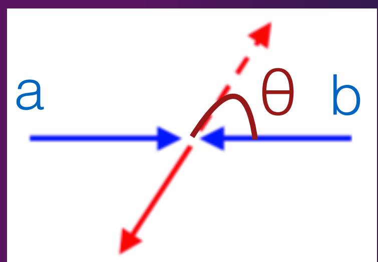

- In the W rest frame (assume $p_T(W)$ =0) :

$$|\overrightarrow{p^{\ell}}| = |\overrightarrow{p^{\nu}}| = \frac{m_W}{2} \quad \text{hence} \quad p_T^{\ell} \leq \frac{m_W}{2} \qquad \hat{s} = (p_a + p_b)^2$$

$$p_{a,b} = \frac{\sqrt{\hat{s}}}{2}(1,0,0,\pm 1) \quad \text{Actually} \quad p_T^{\ell 2} = \frac{\hat{s}}{4}\sin^2\theta \quad \text{Thus} \quad \cos\theta = \sqrt{1 - \frac{4p_T^{\ell 2}}{\hat{s}}}$$

$$\frac{d\cos\theta}{dp_T^{\ell 2}} = \frac{2}{\hat{s}\times\cos\theta}$$

- Singularity at θ = $\pi/2$!

$$\frac{d\sigma}{dp_T^{\ell 2}} = \frac{d\sigma}{d\cos\theta} \times \frac{d\cos\theta}{dp_T^{\ell 2}}$$

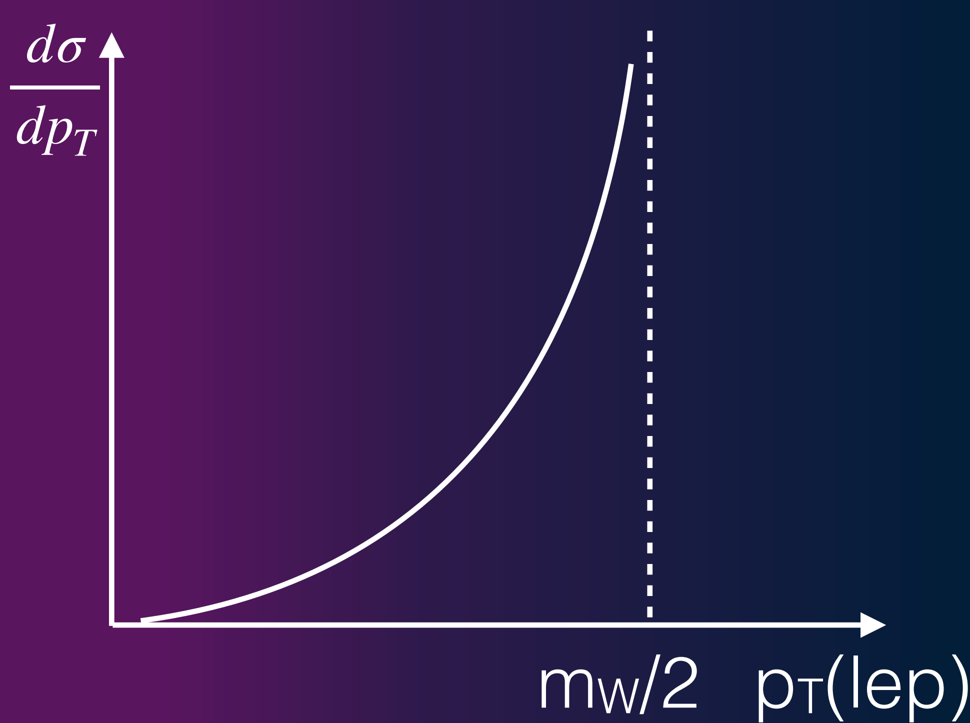

- Jacobian peak at p_T = $m_W/2$
- Transverse momentum of the W
- Finite W decay width
- —>

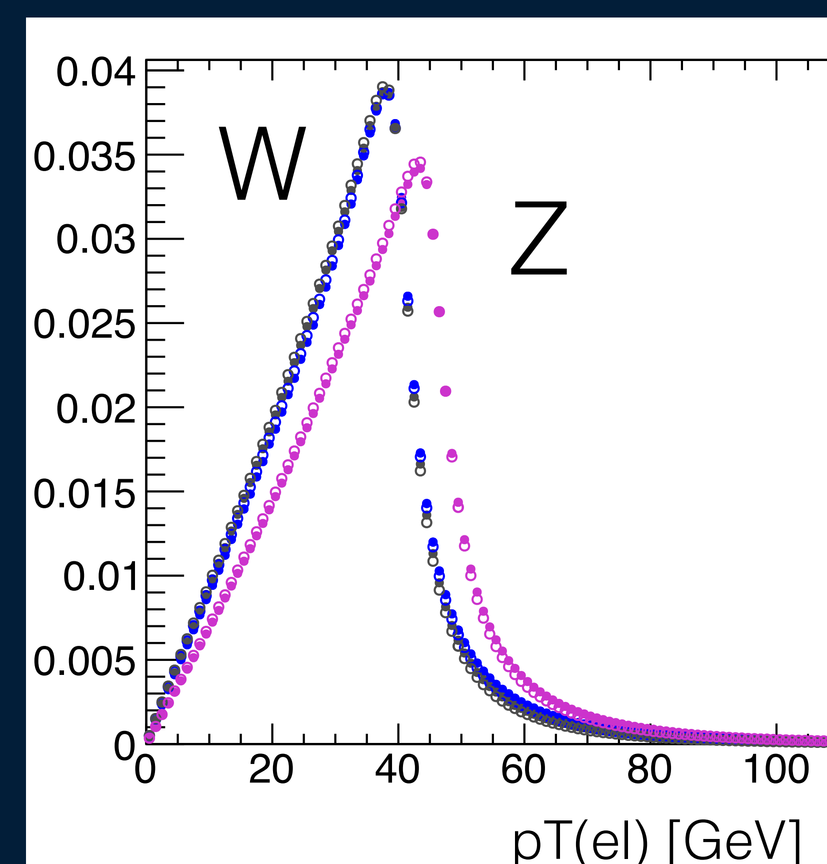

The Jacobian peaks : m_T and lepton p_T

- Unlike the Z, not possible to fully reconstruct the W mass due to neutrino
- One can use the transverse mass $m_T(\ell\nu)$:

$$m_T(\ell\nu)^2 = (|\overrightarrow{p_T^{\ell}}| + |\overrightarrow{p_T^{\nu}}|)^2 - (\overrightarrow{p_T^{\ell}} + \overrightarrow{p_T^{\nu}})^2 = 2|\overrightarrow{p_T^{\ell}}||\overrightarrow{p_T^{\nu}}|(1 - \cos\Delta\phi_{\ell\nu})$$

- Can be compared to the invariant mass :

$$m(\ell\nu) = (|\overrightarrow{p^{\ell}}| + |\overrightarrow{p^{\nu}}|)^2 - (\overrightarrow{p^{\ell}} + \overrightarrow{p^{\nu}})^2$$

- For small $p_T(W)$, m_T is invariant to leading order
- Jacobian peak at m_W

- In the context of m_W measurement :
  - lepton p_T sensitive to modelling of W p_T and not so much to detector resolution
  - m_T is not sensitive to W p_T but is very sensitive to MET resolution

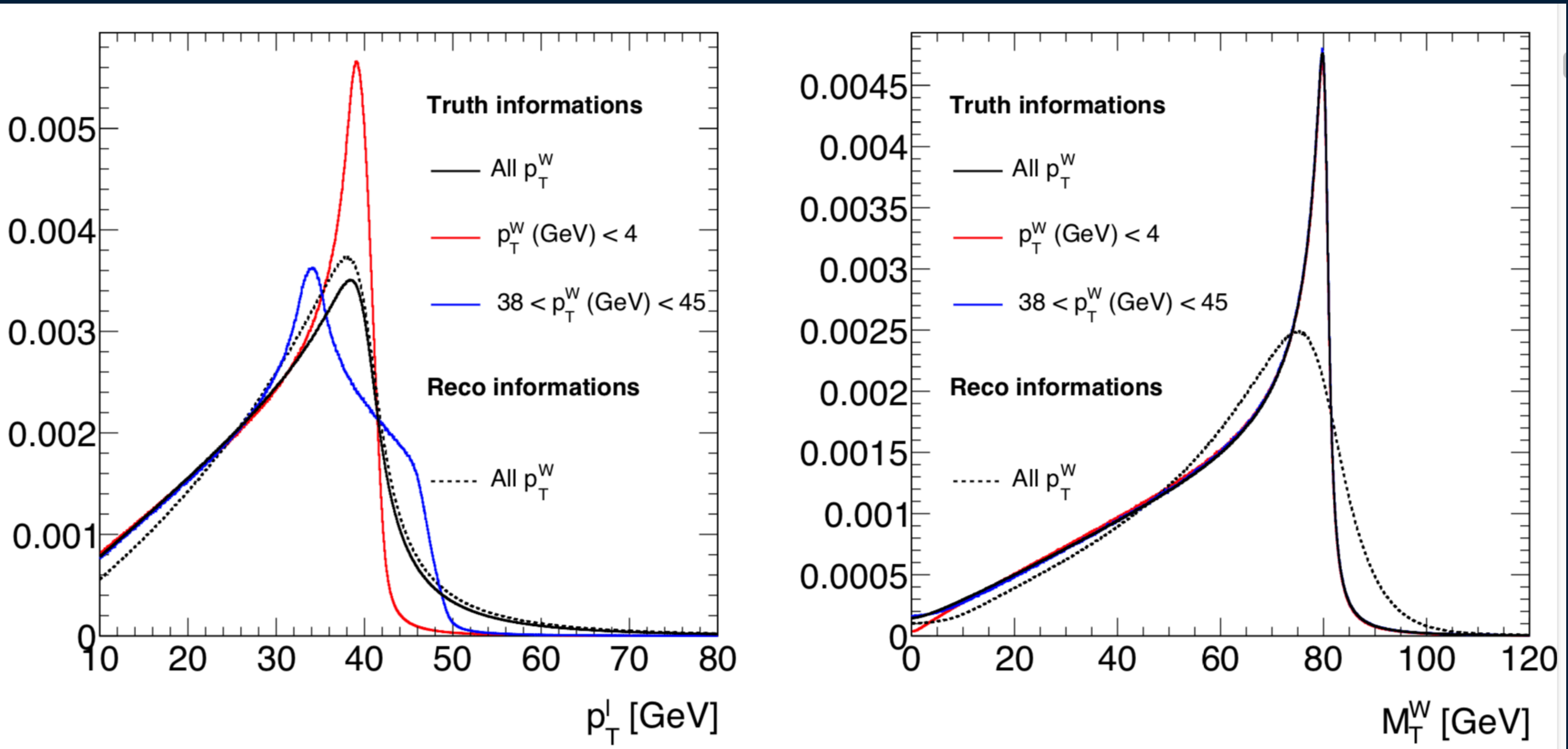

Recent ATLAS measurements

W cross-sections at 7 TeV

Eur. Phys. J. C (2017) 77:367

W cross-sections at 7 TeV : introduction

- Very precise measurement (<1%) of W and Z cross-sections at 7 TeV
- W cross-section is measured in a fiducial volume, extrapolated to full phase-space and differentially in lepton η absolute value, $|\eta_\ell|$
- QCD analysis : PDF fits, strange-quark density, determination of CKM matrix $|V_{cs}|$

- Signal MC sample : Powheg+Pythia6 using CT10 NLO PDF set for the matrix element, CTEQ6L1 for the parton shower
  - Assess uncertainties with alternative samples : MC@NLO+Herwig, Powheg+Herwig : matrix element variation, parton shower/underlying event
  - W p_T is reweighed to Powheg+Pythia8AZNLO, generator tuned to ATLAS Z data
  - Normalised to NNLO prediction from FEWZ with a 5% uncertainty (PDF, scales)
- Background is also using simulated samples except for multi-jet (data-driven)

Event selection

- at least one primary vertex with 3 tracks of p_T >500 MeV
- MET > 25 GeV
- m_T > 40 GeV
- electron channel :
  - single electron trigger with medium ID and p_T >20 or 22 GeV (depending on the period)
    - Identification (ID) : based on shower shape, track properties and track-to-cluster matching
  - Calorimeter isolation : upper limit on sum of energy in a cone of size ΔR = 0.2 ('topoetcone20')
  - Tracking isolation : upper limit on sum of p_T of tracks in a 0.4 cone ('ptvarcone40')
  - exactly one tight ID electron that matches the trigger, in the acceptance ($|\eta| < 1.37$ or $1.52<|\eta| < 2.47$, with p_T >25 GeV
  - reject events with >=1 medium ID electron with p_T >20 GeV (cuts the Z background)
- Charge-separated analyses (W^+ vs W^-) : sensitive to charge misID
  - Evaluated from same-sign Z—>ee events in the data and the MC as a function of η, corrected for in the MC

$$\Delta R = \sqrt{\Delta\phi^2 + \Delta y^2}$$

Event selection

- Muon channel
  - single muon trigger with $p_T > 18$ GeV
  - reconstructed using a combination of muon spectrometer and inner detector information
  - $|z_0 - z_{PV}| < 1$cm (remove background from cosmic rays) : z extrapolated to the beam line
  - $p_T > 25$ GeV, $|\eta| < 2.4$
  - isolation : ptvarcone40/p_T < 0.1
  - events with >= 1 muon with p_T >20 GeV are rejected (cuts the Z background)
  - charge misID negligible

Fiducial volume : phase-space to where the distributions are unfolded at generation level (i.e. remove detector effects):

- lepton $p_T > 25$ GeV, lepton $|\eta| < 2.5$ — Born level for the leptons
- $p_T^{\nu} > 25$ GeV
- $m_T > 40$ GeV
- 11 lepton $|\eta|$ bins (common to electron and muon channels) : [0.00, 0.21, 0.42, 0.63, 0.84, 1.05, 1.37, 1.52, 1.74, 1.95, 2.18, 2.50]

Muon calibration

- Use a combination of ID and MS, calibrate transverse momentum as a function of η
  - Momentum resolution : obtained by fitting the Z invariant mass, as well as $1/p_T^{ID} - 1/p_T^{MS}$ for both μ^+ and μ^- in Z and W
  - Momentum scale : compare Z peak in data and MC
- **longitudinal biases (sagitta biases**, from systematic misalignment modes)
  - muon sagitta bias correction uses W events (E/p) and Z events
- Momentum corrections at the level of 0.1-0.4% and uncertainty of ~2.10^{-4}
- Use tag-and-probe methods (Z—>$\mu\mu$) for the scale factors (reconstruction, trigger, isolation) and uncertainties
  - Same level of correction, a bit higher for trigger, 5-10% (still known with a relative uncertainty of 0.1-0.8%)

momentum scale

momentum resolution

$$p_T^{\rm MC,corr} = p_T^{\rm MC} \times [1 + \alpha(\eta,\phi)] \times \left[1 + \beta_{\rm curv}(\eta) \cdot G(0,1) \cdot p_T^{\rm MC}\right]$$

$$p_T^{\rm data,corr} = \frac{p_T^{\rm data}}{1 + q \cdot \delta(\eta,\phi) \cdot p_T^{\rm data}},$$

sagitta bias correction

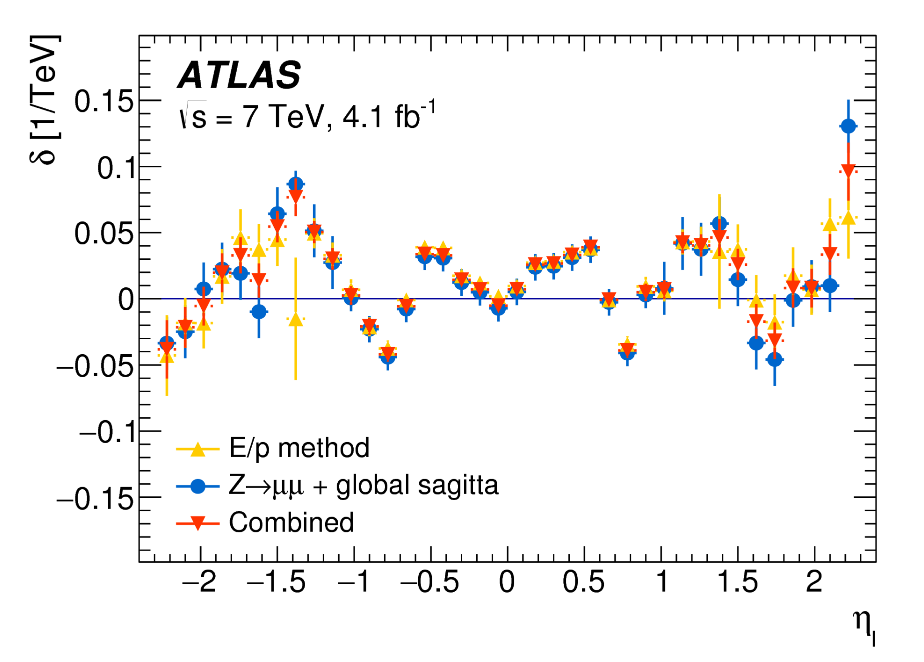

Electron calibration

- Electron measurement : energy from the EM calorimeter; eta and phi from the ID
- Calibration sequence :
  - Calorimeter longitudinal intercalibration using muon energy deposits (Z—>$\mu\mu$ events)
  - Passive material and presampler response corrections derived using longitudinal shower profiles of electrons and photons
  - Overall energy scale and resolution from Z—>ee decays
- Selection efficiencies for reconstruction, identification, trigger, isolation
  - use tag-and-probe methods (Z—>ee) for the scale factors and uncertainties

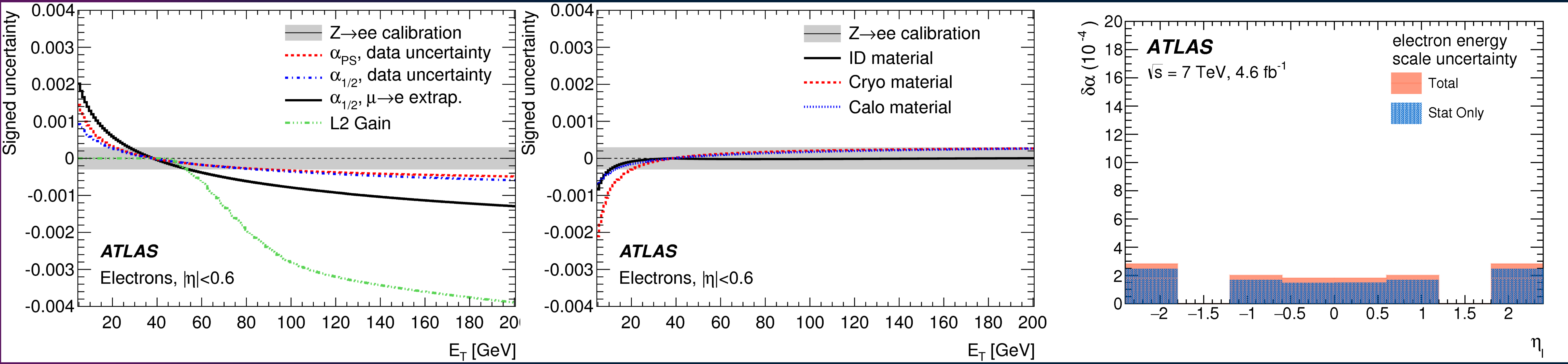

MET calibration

- MET built from a soft term (tracks) + hard term that comprises leptons and jets
- Uncertainties from each hard object is propagated to the hard term
- Soft term uncertainty is obtained by looking at Z in MC and data (response and resolution)

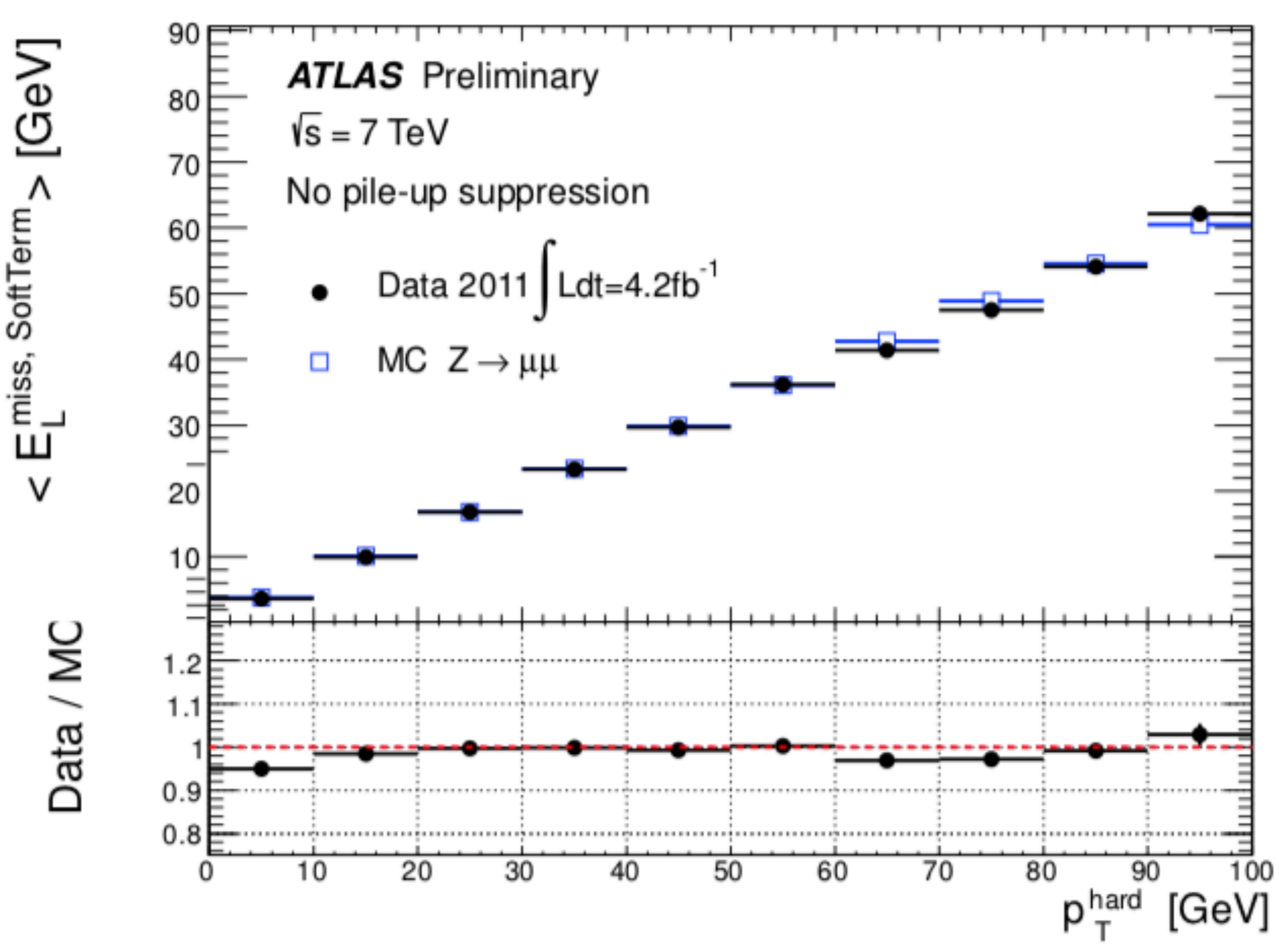

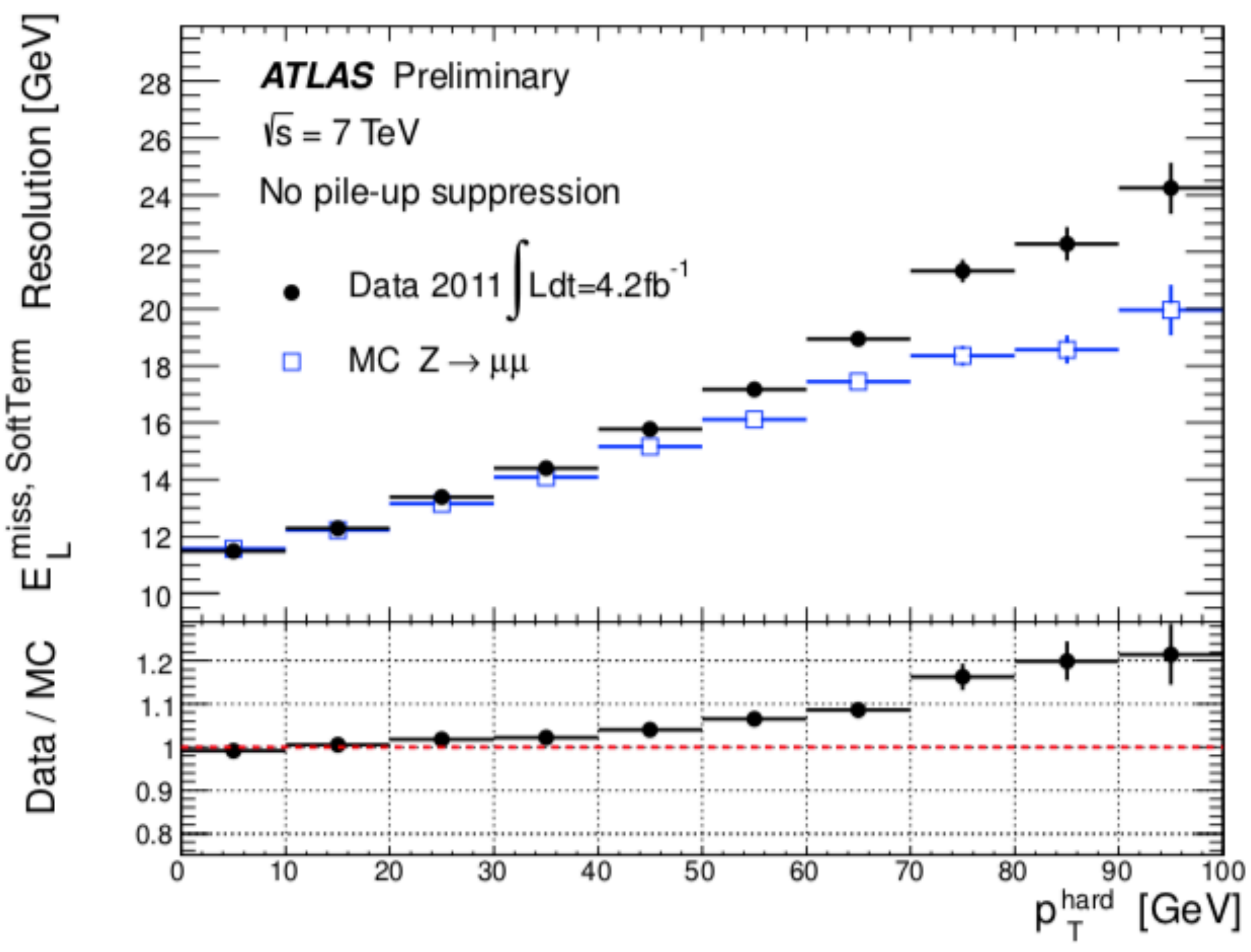

Multijet background (QCD)

- non-isolated electrons, converted photons or hadrons misidentified as signal electrons, or heavy quarks or hadron decays into muons + MET cut is passed thanks to neutrinos from hadron decays/resolution effect
- multijet is poorly modelled in most ATLAS analyses (huge cross-section, tiny selection efficiency, bad modelling of non-prompt muons…)
  - Need to use the data to estimate its contribution
- Use a control region (CR) enriched in multijet to build shape templates
  - loosen lepton ID and invert isolation requirement, subtract EW/top contributions
- Fit the fraction in a ‘normalization (or fit) region’ == signal region with relaxed m_T and MET cuts (enriched in QCD)
- Extrapolate the fitted fraction to the signal region by taking into account the selection efficiency
- Scan in m_T/MET relaxing cut values —> dependence —>additional linear extrapolation to signal region (10% correction, added as uncertainty here)
- Additional uncertainties for the template shapes : different requirements for CR, detector calibration uncertainties, alternative signal MC

Analysis method

- Measured fiducial cross-section where :
  - L is the integrated luminosity N_W is the total number of events, B_W is the estimated background, C_W is defined as :

$$\sigma_W^{fiducial,e/\mu} = \frac{N_W - B_W}{C_W \times L}$$

$$C_W = \frac{N_W^{MC,reconstructed}}{N_W^{MC,generated,fiducial}}$$

- Then extrapolated to common fiducial volume, where E_W accounts for the different eta acceptances

$$\sigma_W^{fiducial,\ell\nu} = \frac{\sigma_W^{fiducial,e/\mu}}{E_W^{e/\mu}}$$

- Total cross-sections can be then inferred from :

$$\sigma_W^{total,\ell\nu} = \frac{\sigma_W^{fiducial,\ell\nu}}{A_W}$$

- where

$$A_W = \frac{N_W^{MC,generated,fiducial}}{N_W^{MC,generated,total}}$$

- Luminosity uncertainty is 1.8%
- Theory uncertainties relate to : PDF, NLO ME/PS matching, hadronisation, underlying event

- C_W uncertainties amount to ~0.2(0.6)% in the μ (e) channel
- E_W has small uncertainties w.r.t. experimental
- A_W has larger uncertainties : 1.5-2%

Results

Process	N events	N Background	C
$W^+ \longrightarrow \mu\nu$	9 225 887	683 000 ± 32 000	0.656 ± 0.003
$W^- \longrightarrow \mu\nu$	6 260 198	598 000 ± 20 000	0.649 ± 0.003
$W^+ \longrightarrow e\nu$	7 552 884	515 000 ± 48 000	0.572 ± 0.004
$W^- \longrightarrow e\nu$	5 286 997	468 000 ± 40 000	0.586 ± 0.005

- Combine using technique introduced at HERA
- Properly taking into account the correlations between the measurements
- χ^2 minimisation allowing to have contributions of the correlated uncertainty sources to shift

	$\sigma^{\text{fid}}_{W\to\ell\nu}$ (pb)
$W^+ \to e^+\nu$	2939 ± 1 (stat) ± 28 (syst) ± 53 (lumi)
$W^+ \to \mu^+\nu$	2948 ± 1 (stat) ± 21 (syst) ± 53 (lumi)
$W^+ \to \ell^+\nu$	2947 ± 1 (stat) ± 15 (syst) ± 53 (lumi)
$W^- \to e^-\bar{\nu}$	1957 ± 1 (stat) ± 21 (syst) ± 35 (lumi)
$W^- \to \mu^-\bar{\nu}$	1964 ± 1 (stat) ± 13 (syst) ± 35 (lumi)
$W^- \to \ell^-\bar{\nu}$	1964 ± 1 (stat) ± 11 (syst) ± 35 (lumi)
$W \to e\nu$	4896 ± 2 (stat) ± 49 (syst) ± 88 (lumi)
$W \to \mu\nu$	4912 ± 1 (stat) ± 32 (syst) ± 88 (lumi)
$W \to \ell\nu$	4911 ± 1 (stat) ± 26 (syst) ± 88 (lumi)

Results

	$\sigma^{\text{tot}}_{W\to\ell\nu}$ (pb)
$W^+ \to \ell^+\nu$	$6350 \pm 2\,(\text{stat}) \pm 30\,(\text{syst}) \pm 110\,(\text{lumi}) \pm 100\,(\text{acc})$
$W^- \to \ell^-\bar{\nu}$	$4376 \pm 2\,(\text{stat}) \pm 25\,(\text{syst}) \pm 79\,(\text{lumi}) \pm 90\,(\text{acc})$
$W \to \ell\nu$	$10720 \pm 3\,(\text{stat}) \pm 60\,(\text{syst}) \pm 190\,(\text{lumi}) \pm 130\,(\text{acc})$

$$R_W = \frac{\sigma^{\text{fid,e}}_{W\to e\nu}/E^{\text{e}}_W}{\sigma^{\text{fid},\mu}_{W\to\mu\nu}/E^{\mu}_W} = \frac{\sigma^{\text{fid}}_{W\to e\nu}}{\sigma^{\text{fid}}_{W\to\mu\nu}} = \frac{BR(W\to e\nu)}{BR(W\to\mu\nu)}$$
$$= 0.9967 \pm 0.0004\,(\text{stat}) \pm 0.0101\,(\text{syst})$$
$$= 0.997 \pm 0.010.$$

- Integrated cross-section : dominated by luminosity and acceptance factor uncertainties
- Test of lepton universality
  - Ratio result is more precise than LEP result of 1.007 ± 0.019

Systematic uncertainties : electron channel

	$\delta\sigma_{W+}$ (%)	$\delta\sigma_{W-}$ (%)
Trigger efficiency	0.03	0.03
Reconstruction efficiency	0.12	0.12
Identification efficiency	0.09	0.09
Forward identification efficiency	–	–
Isolation efficiency	0.03	0.03
Charge misidentification	0.04	0.06
Electron p_T resolution	0.02	0.03
Electron p_T scale	0.22	0.18
Forward electron p_T scale + resolution	–	–
E_T^{miss} soft term scale	0.14	0.13
E_T^{miss} soft term resolution	0.06	0.04
Jet energy scale	0.04	0.02
Jet energy resolution	0.11	0.15
Signal modelling (matrix-element generator)	0.57	0.64
Signal modelling (parton shower and hadronization)	0.24	0.25
PDF	0.10	0.12
Boson p_T	0.22	0.19
Multijet background	0.55	0.72
Electroweak+top background	0.17	0.19
Background statistical uncertainty	0.02	0.03
Unfolding statistical uncertainty	0.03	0.04
Data statistical uncertainty	0.04	0.05
Total experimental uncertainty	0.94	1.08
Luminosity	1.8	1.8

- Dominated by multijet background and signal modelling (MC@NLO vs Powheg)
- Luminosity dominates
- Total experimental uncertainty (excluding luminosity) is ~1%

Systematic uncertainties : muon channel

	$\delta\sigma_{W+}$ (%)	$\delta\sigma_{W-}$ (%)
Trigger efficiency	0.08	0.07
Reconstruction efficiency	0.19	0.17
Isolation efficiency	0.10	0.09
Muon p_{T} resolution	0.01	0.01
Muon p_{T} scale	0.18	0.17
$E_{\mathrm{T}}^{\mathrm{miss}}$ soft term scale	0.19	0.19
$E_{\mathrm{T}}^{\mathrm{miss}}$ soft term resolution	0.10	0.09
Jet energy scale	0.09	0.12
Jet energy resolution	0.11	0.16
Signal modelling (matrix-element generator)	0.12	0.06
Signal modelling (parton shower and hadronization)	0.14	0.17
PDF	0.09	0.12
Boson p_{T}	0.18	0.14
Multijet background	0.33	0.27
Electroweak+top background	0.19	0.24
Background statistical uncertainty	0.03	0.04
Unfolding statistical uncertainty	0.03	0.03
Data statistical uncertainty	0.04	0.04
Total experimental uncertainty	0.61	0.59
Luminosity	1.8	1.8

- Dominated by multijet background, followed by various uncertainties ~at the same level
- Total uncertainty excluding luminosity is ~0.6%

Results : unfolded differential distributions

- Bayesian unfolding, purity > 90%
  - Unfolding is almost an efficiency correction

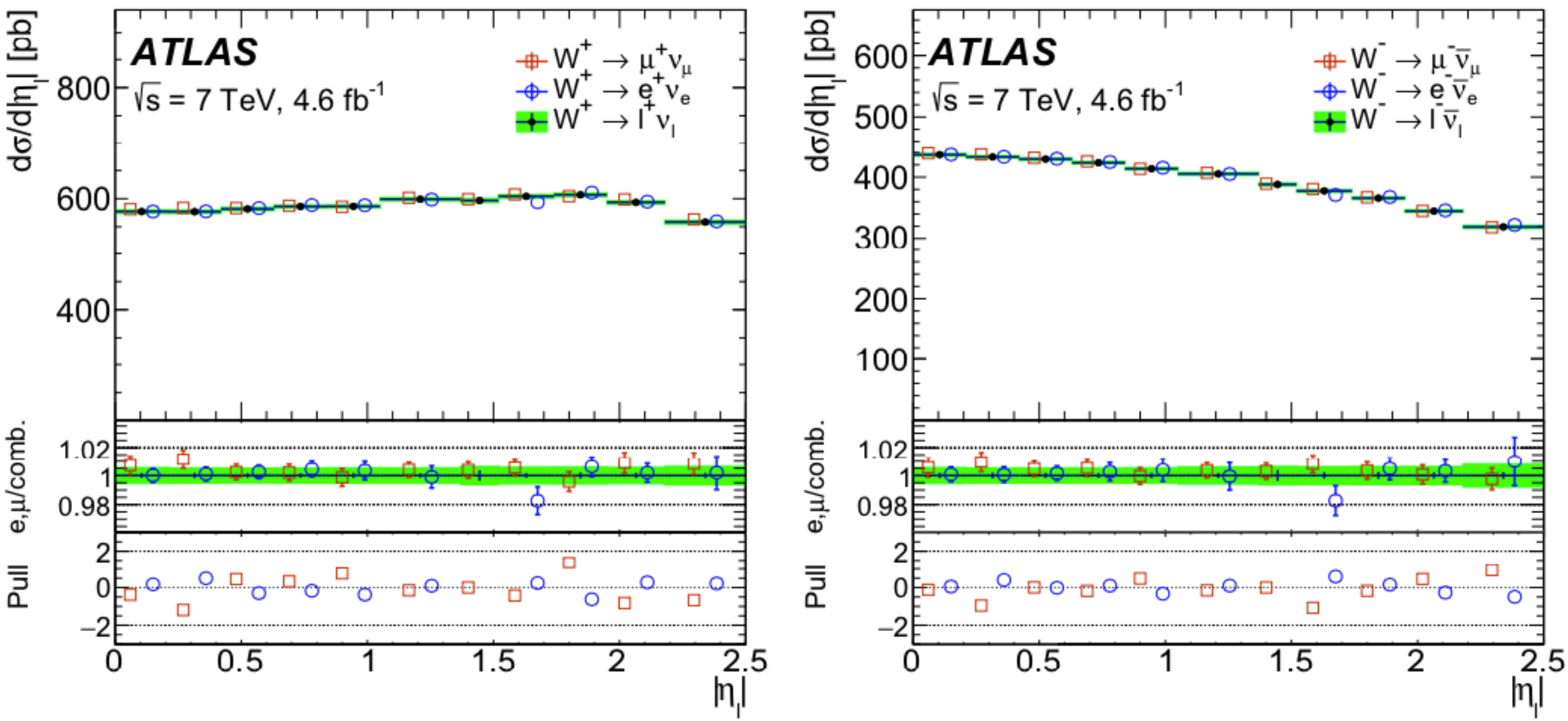

Comparison with theory

- Fixed-order NNLO QCD predictions use DYNNLO 1.5 (baseline) and FEWZ 3.1.b2 (used for NNLO uncertainty evaluation)
    - NLO EW corrections provided by MCSANC
- In DY cross-section calculations the value of α_{EW} can be fixed in different input-parameter schemes
    - Here ‘Gμ’ scheme (primary parameters are particle masses and Fermi constant with values taken from PDG) —>see Dittmaier, S. & Huber, M. J. High Energ. Phys. (2010) 2010: 60
- Uncertainties in these plots is the dominating PDF uncertainty only
- Good potential to discriminate between different PDF choices and to provide information to reduce PDF uncertainties

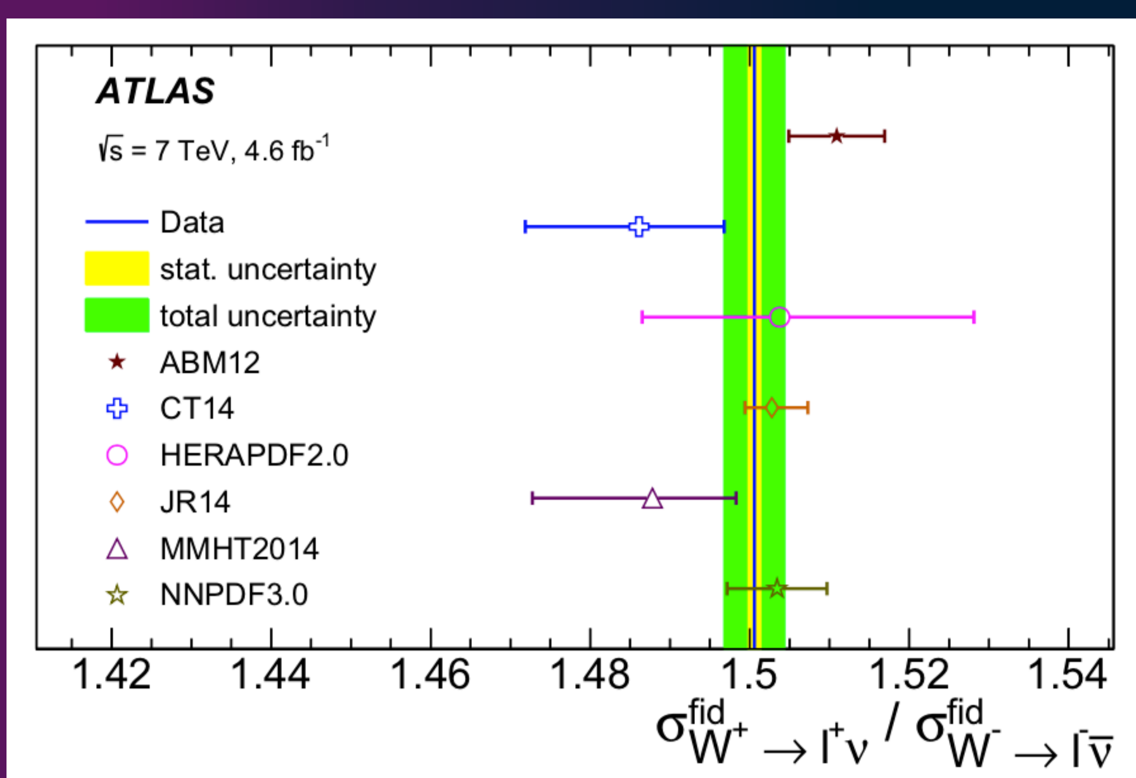

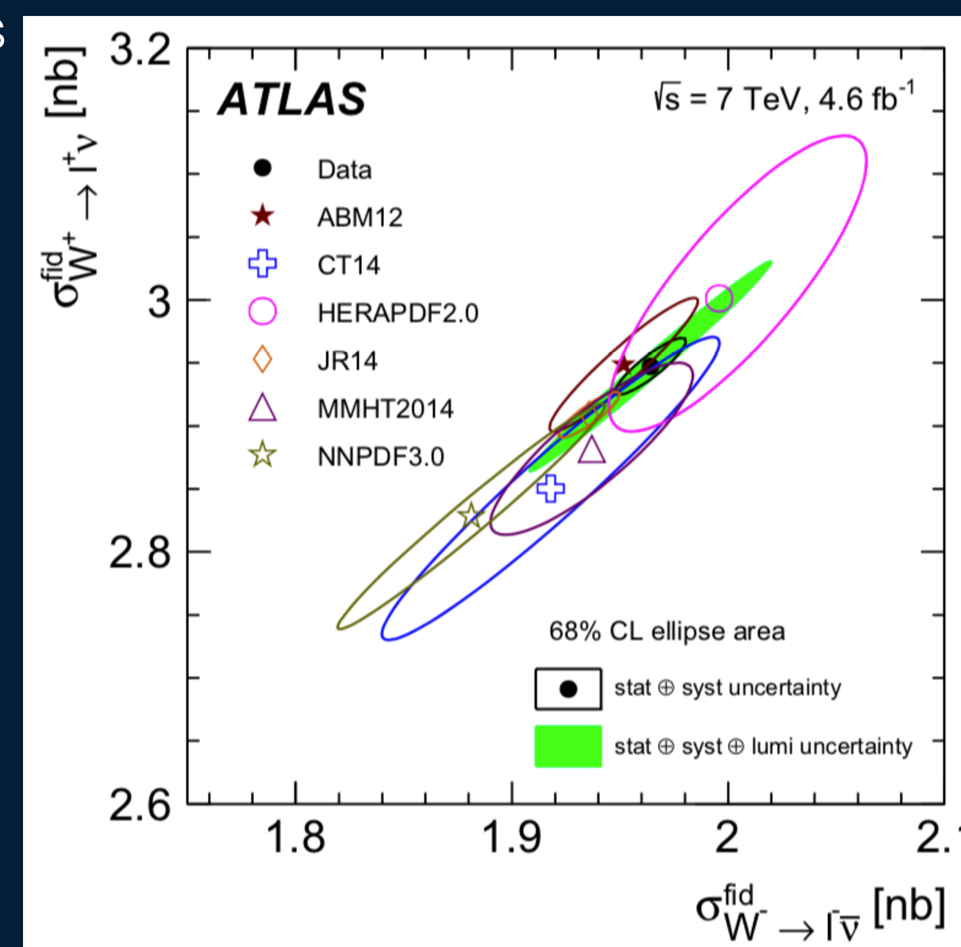

Comparison with theory : lepton η and asymmetry

- Lepton charge asymmetry defined as :

$$A_\ell = \frac{d\sigma_{W+}/d|\eta_\ell| - d\sigma_{W-}/d|\eta_\ell|}{d\sigma_{W+}/d|\eta_\ell| + d\sigma_{W-}/d|\eta_\ell|}$$

  - Significant constrain on u/d PDFs between x ~ 10^{-1} and 10^{-3}
- Data overall well described (luminosity uncertainty of 1.8% is excluded in the plots)
- HERAPDF2.0, NNPDF3.0, MMHT14 and CT14 more or less agree with the data within uncertainties
  - ABM12 remarkably good, but does a poorer job describing Z distributions

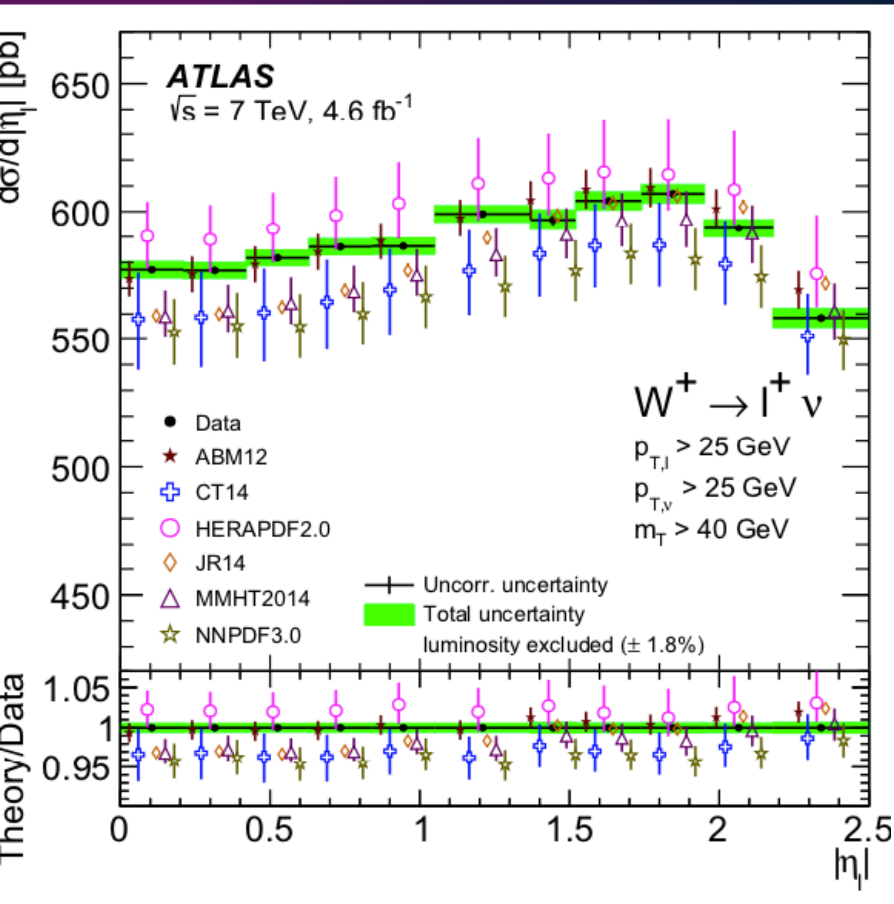

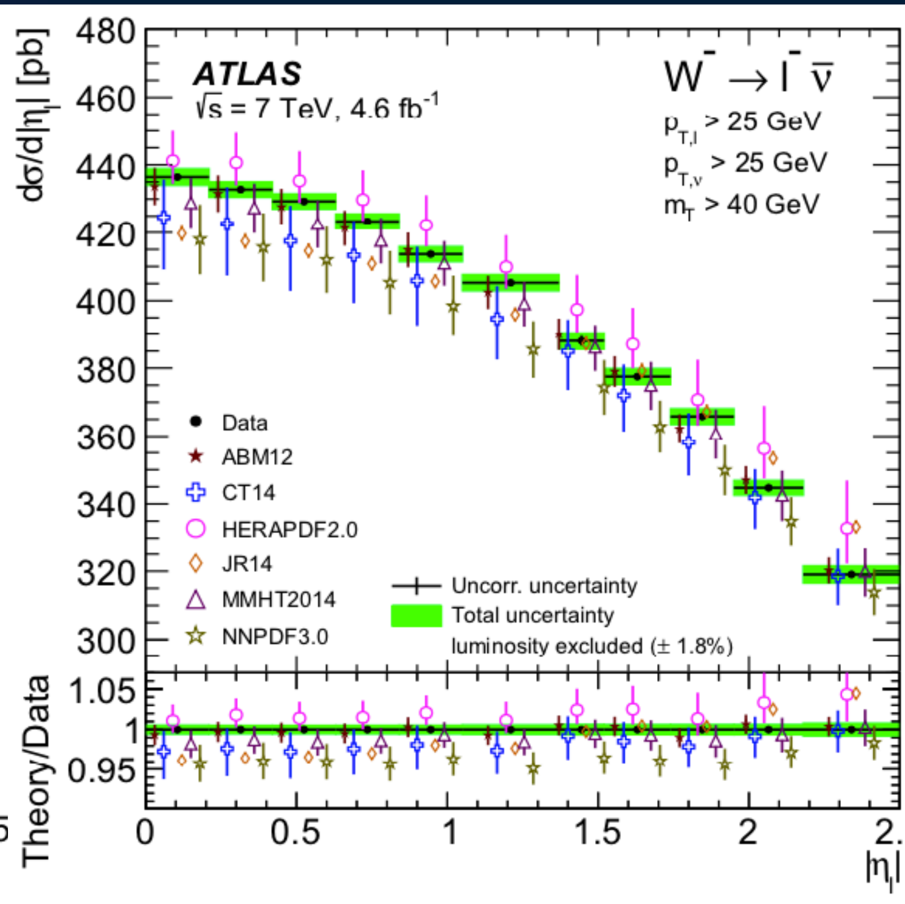

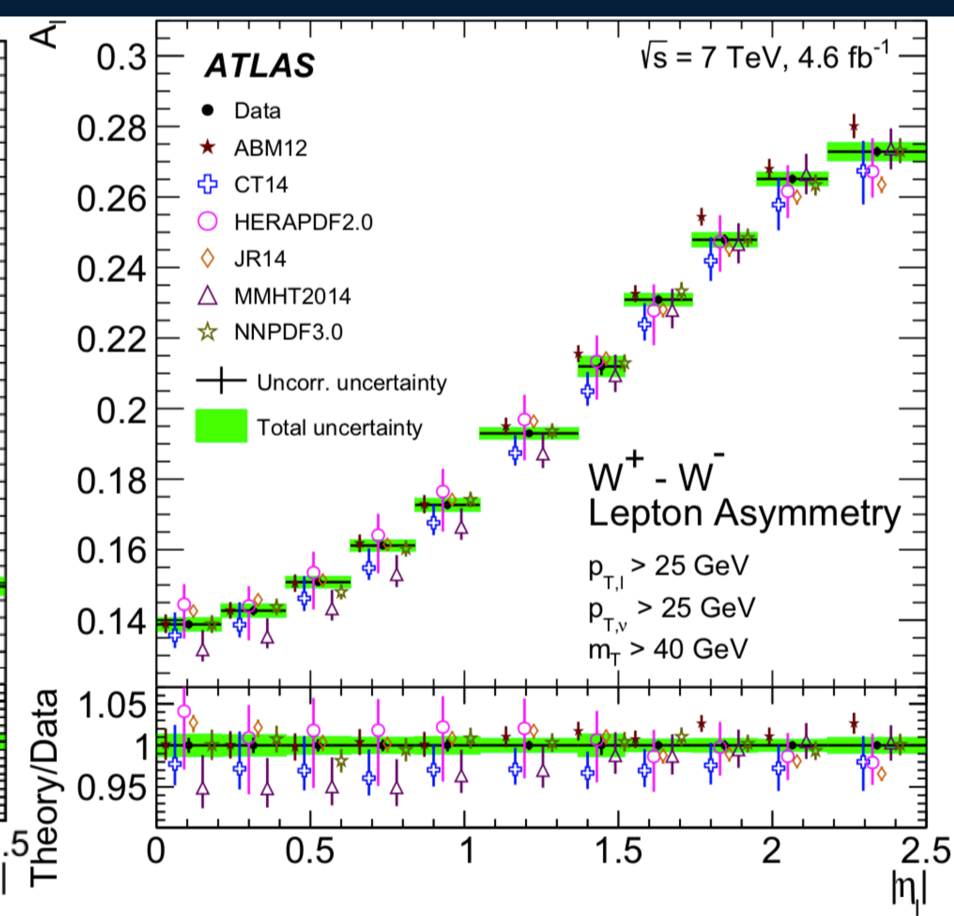

PDF profiling : methodology

- PDF profiling and full PDF fits heavily rely on methods used in previous experiments (Tevatron, HERA) and global PDF fit groups, see e.g

Eur. Phys. J. C **75**, 458 (2015), JHEP **12**, 100 (2014), JHEP **09**, 061 (2012)

- Use of APPLGRID for theory predictions, together with k-factors from the accurate theory tools described before (NNLO QCD from DYNNLO 1.5, NLO EW from PHOTOS and MCSANC)
- Use of xFitter software
    - start from existing PDF sets
    - Use a $\chi^2(b_{exp}, b_{th})$ that minimises difference between observed and predicted cross-section allowing nuisance parameters (b_{exp}, b_{th}) to shift
    - Allows for quantitative estimate of the agreement between the data and the PDF sets from global fits, and study further constraining power from the new measurement
        - Best χ^2 is obtained with CT14nnlo, CT10nnlo, and reasonable with MMHT14nnlo

PDF profiling results (exemple of MMHT14)

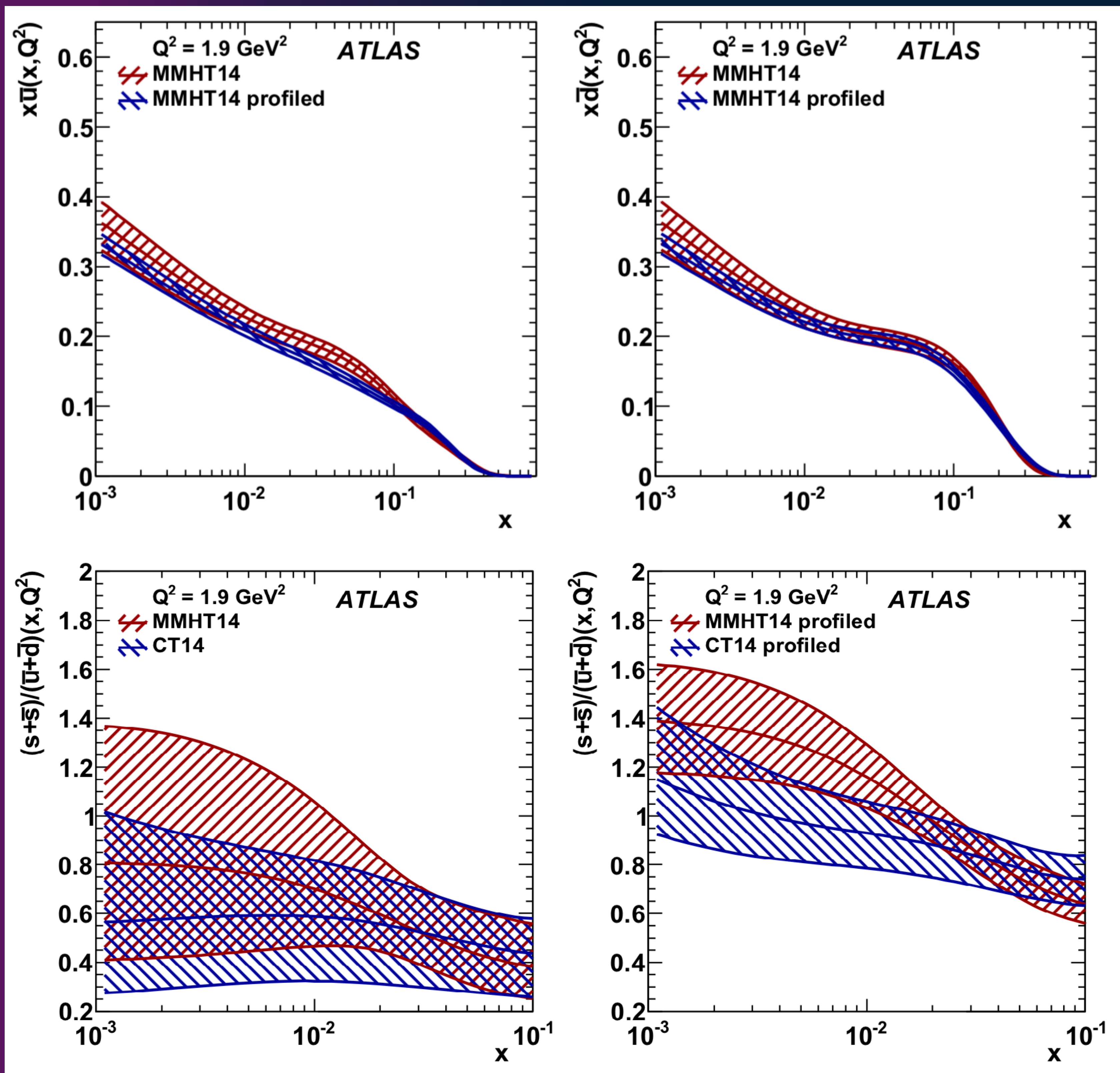

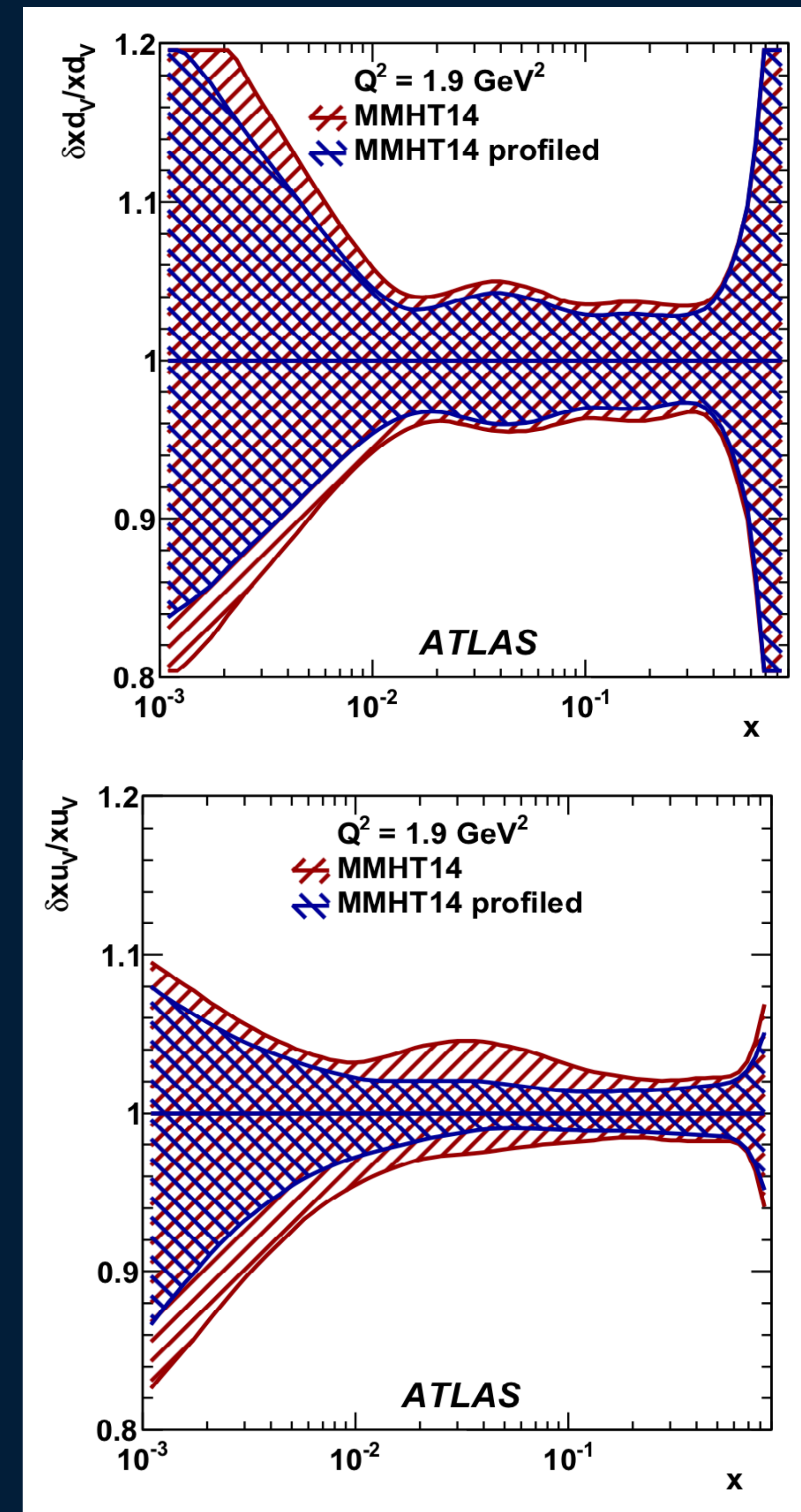

Full PDF fit

- More complex than PDF profiling
  - Requires parametrisation of the PDFs at a starting scale $Q_0^2 = 1.9 GeV^2$

$$
\begin{aligned}
xu_v(x) &= A_{u_v} x^{B_{u_v}} (1-x)^{C_{u_v}} (1 + E_{u_v} x^2), \\
xd_v(x) &= A_{d_v} x^{B_{d_v}} (1-x)^{C_{d_v}}, \\
x\bar{u}(x) &= A_{\bar{u}} x^{B_{\bar{u}}} (1-x)^{C_{\bar{u}}}, \\
x\bar{d}(x) &= A_{\bar{d}} x^{B_{\bar{d}}} (1-x)^{C_{\bar{d}}}, \\
xg(x) &= A_g x^{B_g} (1-x)^{C_g} - A'_g x^{B'_g} (1-x)^{C'_g}, \\
x\bar{s}(x) &= A_{\bar{s}} x^{B_{\bar{s}}} (1-x)^{C_{\bar{s}}},
\end{aligned}
$$

- PDFs are evolved to the scale of the measurements and convolved with hard-scattering coefficients to obtain the theoretical cross-section predictions
- Then, fit using similar (but different) χ^2 as in profiling, with parameters left free
- Fit done with HERA and new ATLAS data
  - New set termed ATLAS-epWZ16
  - Includes experimental and theory uncertainties

Full PDF fit : result

- Theory uncertainties include : variation on the heavy quark masses, on Q_0, on Q_{min} (smallest scale for HERA data), different parametrisation, $\alpha_S(m_Z)$ (= 0.118 ± 0.002), NLO EW, FEWZ vs DYNNLO
- Experimental uncertainties on the new PDF set greatly reduced by a factor 3 w.r.t. the previous one (ATLAS-epWZ12)
- Data well described by the theory

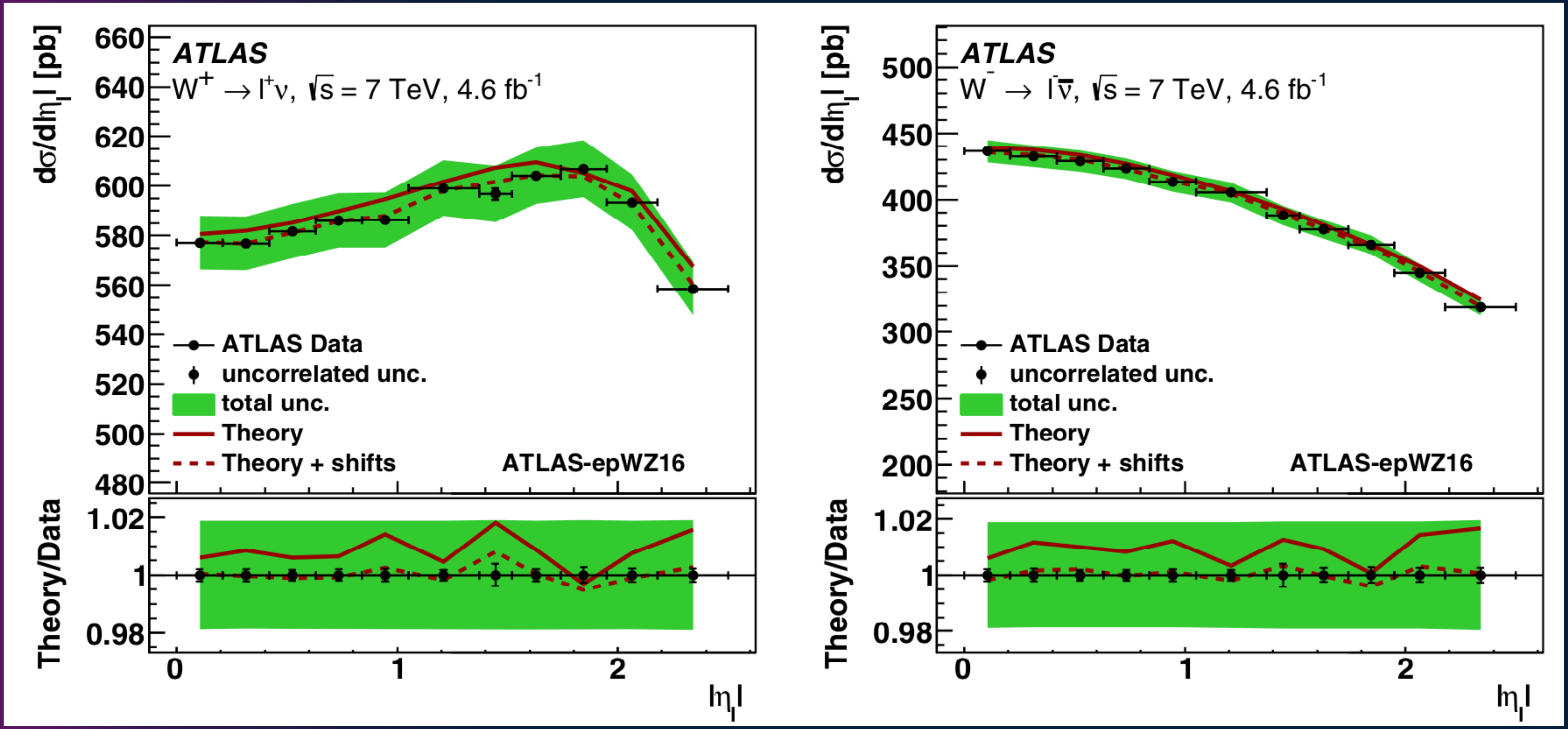

strange quark density

- ATLAS 2010 W,Z : unsuppressed strangeness at $x \approx 0.023$ and $Q^2 = 1.9$ GeV^2, —> strange, down and up sea quarks of similar strength in that kinematic range
  - Supported by ATLAS W+c measurement
  - Not expected from neutrino scattering experiments, which have big weight in global PDF fits

$$r_s = \frac{s+\bar{s}}{2\bar{d}}$$

$$r_s = 1.19 \pm 0.07\,(\text{exp})\,^{+0.13}_{-0.14}\,(\text{mod}+\text{par}+\text{thy})$$

- Many checks were performed :
  - remove the constraint $\bar{u} = \bar{d}$ for x—>0
  - Inclusion of E866 data for which there are tensions ($\bar{u} - \bar{d}$)
  - remove low/high mass Drell-Yan
  - How much the χ^2 increases when imposing suppressed strangeness ($r_s = 0.5$ and $C_{\bar{s}} = C_{\bar{d}}$)
- Everything points to strangeness values consistent with this measurement

strange quark density

- Uncertainties include :
  - experimental
  - model variations (heavy quark masses, starting scale, minimum scale of HERA data)
  - **PDF parametrisation**
  - α_S
  - EW corrections
- **factorisation and renormalisation scales**
- **FEWZ vs DYNNLO**

$$R_s = \frac{s + \bar{s}}{\bar{u} + \bar{d}}$$

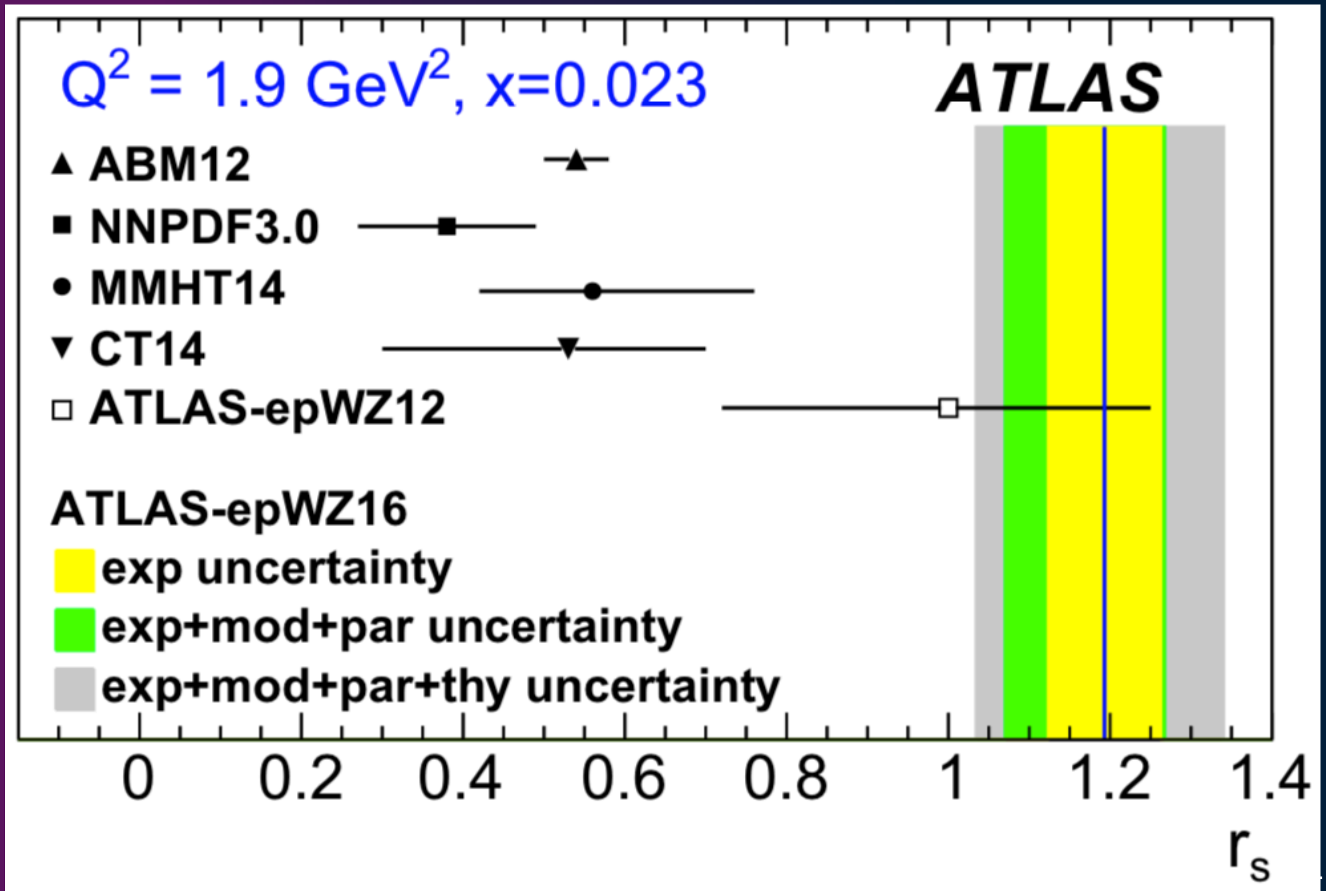

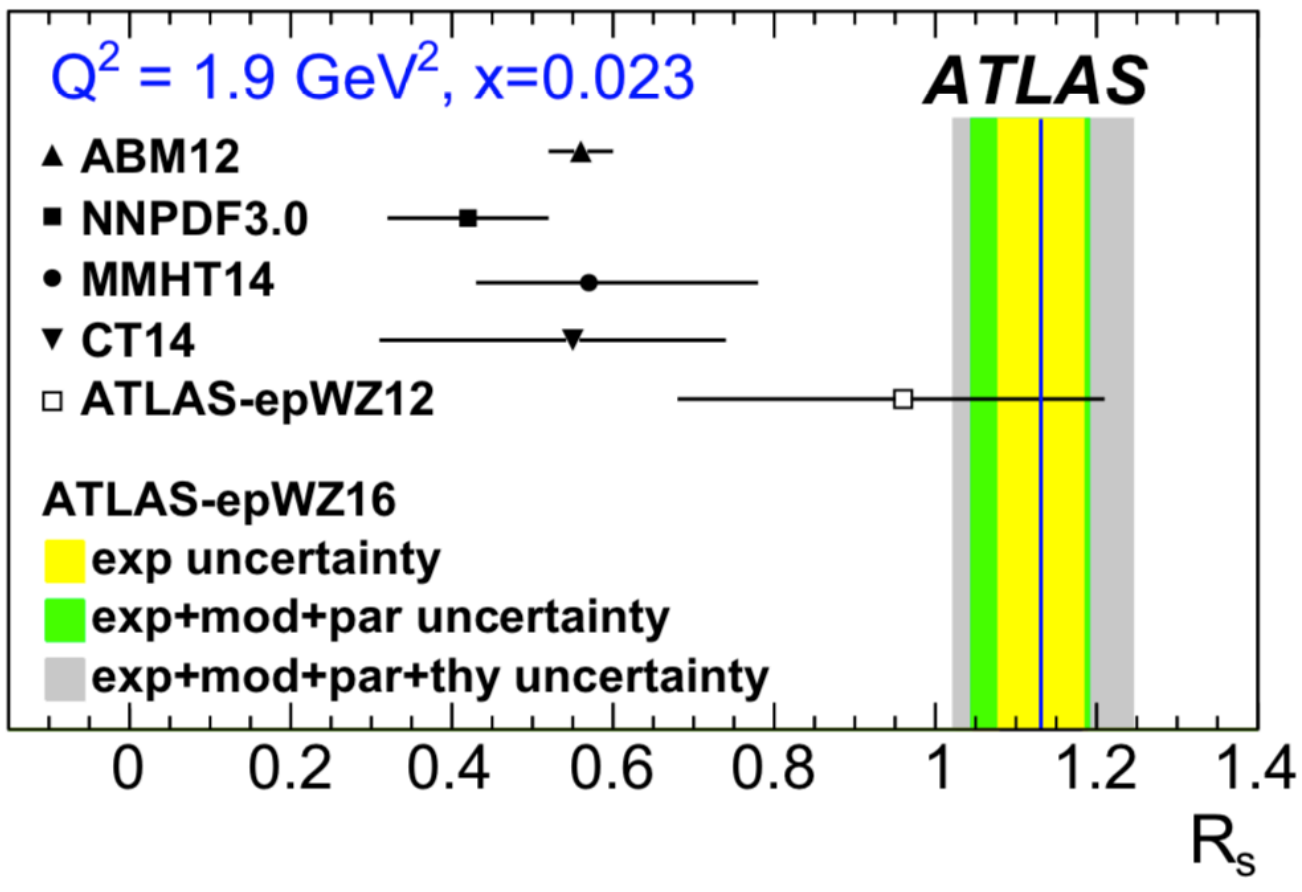

$|V_{cs}|$ measurement

- W production mainly from ud and cs quarks
  - $|V_{ud}|$ already measured with high precision, but not $|V_{cs}|$
  - W production rate and lepton η distributions are sensitive to $|V_{cs}|$
  - —>PDF fit with $|V_{cs}|$ allowed to vary (other CKM matrix elements fixed to the 2012 PDG value)
  - parametrisation variations —>Dominant uncertainty
  - Competitive with other measurements

$$|V_{cs}| = 0.969 \pm 0.013\,(\mathrm{exp})\,^{+0.006}_{-0.003}\,(\mathrm{mod})\,^{+0.003}_{-0.027}\,(\mathrm{par})\,^{+0.011}_{-0.005}\,(\mathrm{thy}).$$

	$\lvert V_{cs}\rvert$
Central value	0.969
Experimental data	± 0.013
Model (m_b, Q^2_{min}, Q^2_0 and m_c)	$^{+0.006}_{-0.003}$
Parameterization	$^{+0.003}_{-0.027}$
α_S	± 0.000
EW corrections	± 0.004
QCD scales	$^{+0.000}_{-0.003}$
FEWZ 3.1b2	$+0.011$
Total uncertainty	$^{+0.018}_{-0.031}$

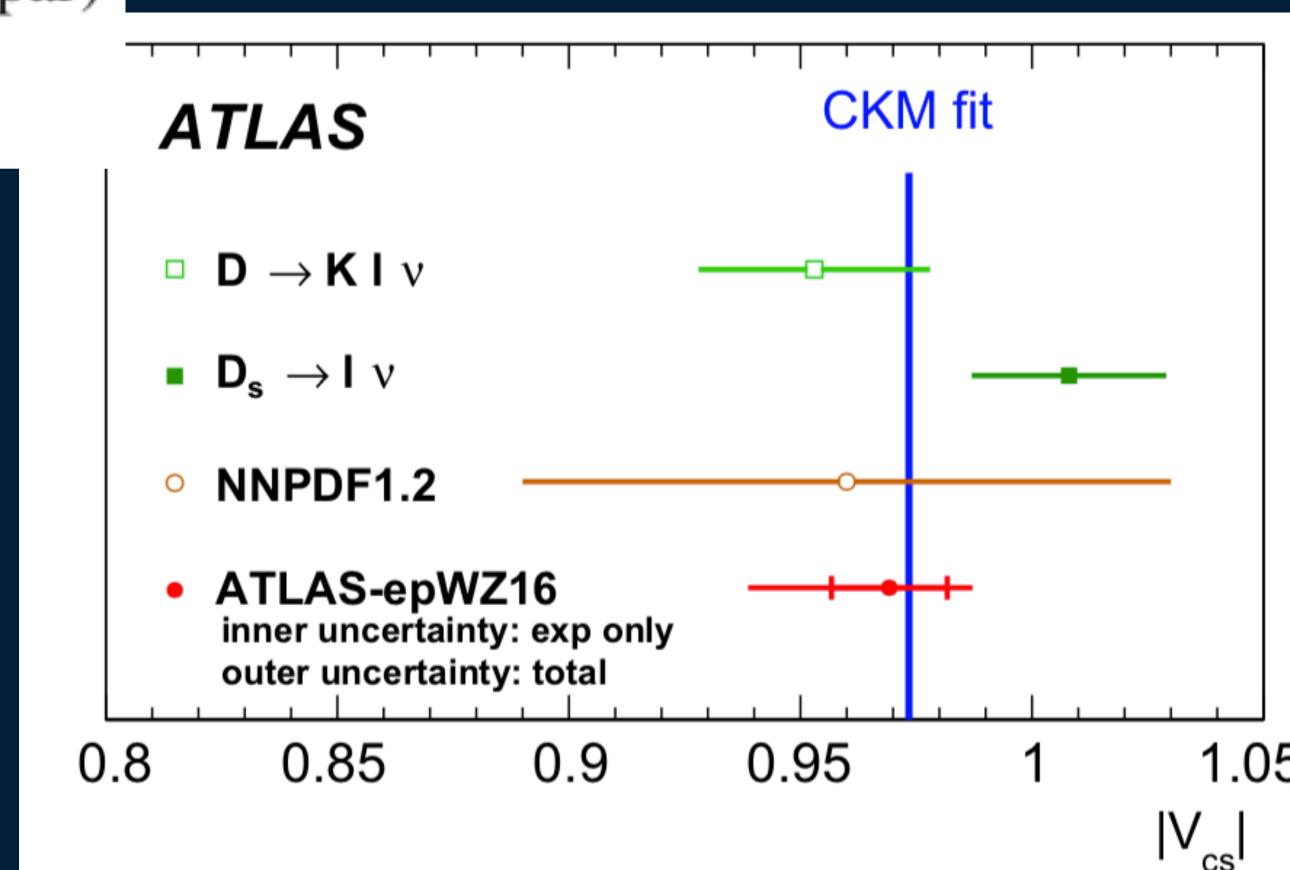

W cross-section at 13 TeV

Physics Letters B 759 (2016) 601–621

- Shorter analysis was performed using $81 pb^{-1}$ of early Run2 2015 data : W,Z fiducial and inclusive cross-sections
- Peak delivered instantaneous luminosity was $L = 1.7 \times 10^{33}\ cm^{-1}\ s^{-1}$, $\langle\mu\rangle = 19$.
- measurement compared with NNLO fixed-order predictions from DYNNLO using different PDF sets
- Dominant uncertainty from MET

	Measured cross section $\times$ BR($W \to \ell\nu$, $Z \to \ell\ell$) [nb] (value $\pm$ stat $\pm$ syst $\pm$ lumi)	
Channel	Fiducial	Total
W^-	$3.50 \pm 0.01 \pm 0.07 \pm 0.07$	$8.79 \pm 0.02 \pm 0.24 \pm 0.18$
W^+	$4.53 \pm 0.01 \pm 0.09 \pm 0.10$	$11.83 \pm 0.02 \pm 0.32 \pm 0.25$
$W^\pm$	$8.03 \pm 0.01 \pm 0.16 \pm 0.17$	$20.64 \pm 0.02 \pm 0.55 \pm 0.43$

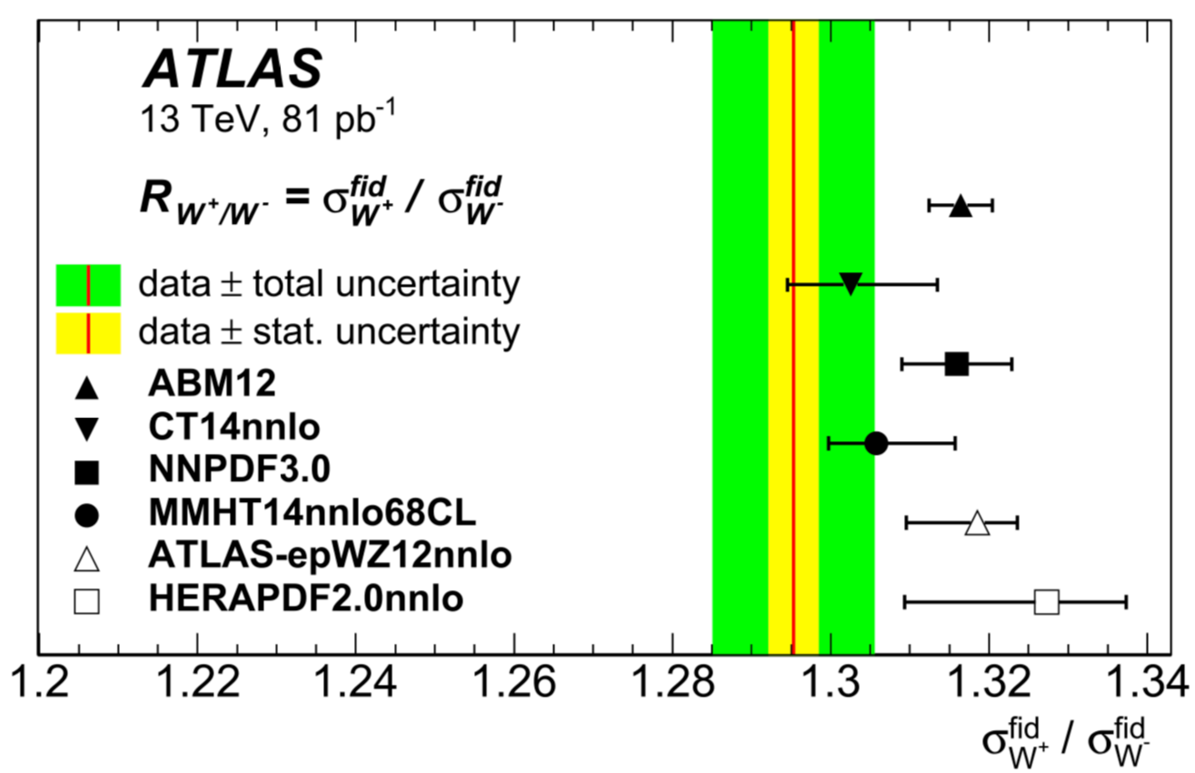

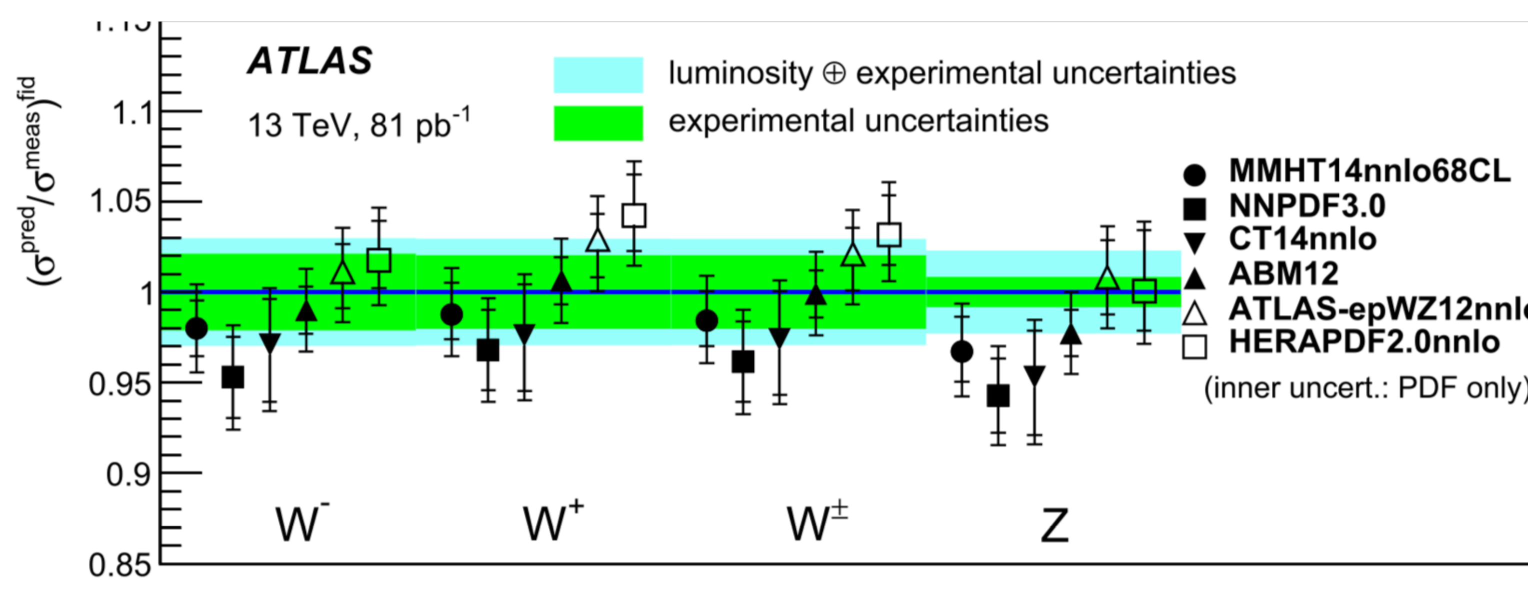

W cross-section : conclusion and summary

- Remarkable precision on Drell-Yan cross-section, below 1% (when excluding luminosity uncertainty) even for W
- Allows for stringent tests of Standard Model
- High number of experimental points is a good input to constrain parton distribution functions and thus reduce their related uncertainty
  - Key ingredient for most physics analyses
- Competitive measurement of $|V_{CS}|$ CKM matrix element

W+jets at 8 TeV

JHEP05(2018)077

W+jets at 8 TeV : introduction

- Several differential cross-sections for W + ≥ 1 jet in the electron channel
  - H_T (scalar sum of the transverse momenta of electron, neutrino and jets), $p_T(W)$, $p_T(j1)$, $y(j1)$ (transverse momentum and rapidity of the leading jet, i.e. with highest p_T)
- And for W+ ≥ 2 jets
  - $p_T(j2)$, $y(j2)$, $\Delta R(j1,j2)$, M_{jj}
- W^+/W^- cross-section ratio
  - Cancelling of dominant systematic uncertainties
- Motivation : stringent tests of pQCD, constraints to PDFs fits, sensitivity to ME/PS matching schemes

- detector calibration for reconstructed objects (leptons, jets, missing E_T) are all from standard Combined Performance groups
- Main signal MC sample is Alpgen+Pythia6 with up to 5 partons in the ME
- All backgrounds estimated with MC except for multi jet (data driven)

W+jets at 8 TeV : event selection

- Trigger : electron, isolated (p_T>24 GeV) or not (p_T>60 GeV)
- exactly 1 electron with p_T>25 GeV, within detector acceptance and matching the trigger
  - 'tight' identification
  - cut on impact parameters of associated track
  - isolation : ptvarcone30/p_T < 0.07, topoetcone30/p_T < 0.14
  - no other 'medium' electron with p_T>20 GeV
- Anti-k_T jets with R=0.4, p_T>30 GeV, |y|<4.4, separated from the electron
  - pile-up rejection for jets within tracking acceptance ('JVF' cut)
  - Veto on events with b-tagged jets (p_T >20 GeV, $|\eta|$ <2.5) —>rejects $t\bar{t}$
- jets-electron overlap removal
- MET > 25 GeV, m_T > 40 GeV

W+jets at 8 TeV : event yields

N_{jets}	0	1	2	3	4	5	6	7
$W \to e\nu$	94 %	86 %	75 %	67 %	57 %	47 %	40 %	35 %
Multijet	3 %	8 %	15 %	16 %	16 %	16 %	14 %	14 %
$t\bar{t}$	< 1 %	< 1 %	1 %	6 %	16 %	27 %	36 %	43 %
Single t	< 1 %	< 1 %	1 %	1 %	2 %	2 %	2 %	1 %
$W \to \tau\nu$	2 %	2 %	2 %	2 %	2 %	1 %	1 %	1 %
Diboson	< 1 %	< 1 %	1 %	1 %	1 %	1 %	< 1 %	< 1 %
$Z \to ee$	< 1 %	3 %	5 %	6 %	6 %	6 %	5 %	5 %
$Z \to \tau\tau$	< 1 %	< 1 %	< 1 %	< 1 %	< 1 %	< 1 %	< 1 %	< 1 %
Total predicted	54 310 000	7 611 700	2 038 000	478 640	120 190	30 450	7430	1735
	±22 000	±4000	±1700	±720	±320	±150	±63	±20
Data observed	56 342 232	7 735 501	2 070 776	486 158	120 943	29 901	7204	1641

- Dominant background is multijet for lower jet multiplicity, $t\bar{t}$ becomes more important for events with higher multiplicity

W+jets at 8 TeV : comparison to various predictions

- All observables use Bayesian unfolding to account for detector effects (bin migrations)
- Comparison to various prediction (first 3 have non-perturbative corrections using Sherpa 2.2.1 to account for hadronisation and underlying event)
- NLO EW corrections investigated with Sherpa 2.2.1, PDF sensitivity investigated with MCFM
- Theory uncertainties include : renormalisation/factorisation scale variations, α_S, PDF uncertainties (only statistical uncertainty is shown for LO generators)

Program	Order in α_S	$N_{\text{partons}}^{\text{max}}$ at highest order	PDF set
N_{jetti}	NNLO	1	CT14
BlackHat+Sherpa	NLO	1, 2 or 3	CT10
MCFM 6.8	NLO	1	CT10 + 3 more
Powheg+Pythia 8	NLO	1	CT14
Sherpa 2.2.1	NLO	2	CT10
Sherpa 2.2.1	LO	2 (3)	NNPDF 3.0
Alpgen+Pythia 6	LO	5	CTEQ6L1 (LO)
Alpgen+Herwig	LO	5	CTEQ6L1 (LO)
Sherpa 1.4.1	LO	4	CT10

Theoretical predictions

	Electron criteria
Electron p_T	$p_T > 25$ GeV
Electron pseudorapidity	$\|\eta\| < 2.5$
	W criteria
Electron decay	Exactly one electron
Missing transverse momentum	$E_T^{\text{miss}} > 25$ GeV
Transverse mass	$m_T > 40$ GeV
	Jet criteria
Jet p_T	$p_T > 30$ GeV
Jet rapidity	$\|y\| < 4.4$
Jet-electron distance	$\Delta R(e, \text{jet}) \geq 0.4$

Fiducial phase space

W+jets cross-section and W+/W- ratio

- Overall good agreement of measured values with predictions
- NLO vs LO improves agreement (Sherpa 2.2.1)
- Better agreement for the ratio
  - —>probable cancelling of theoretical mismodeling (jet emission)

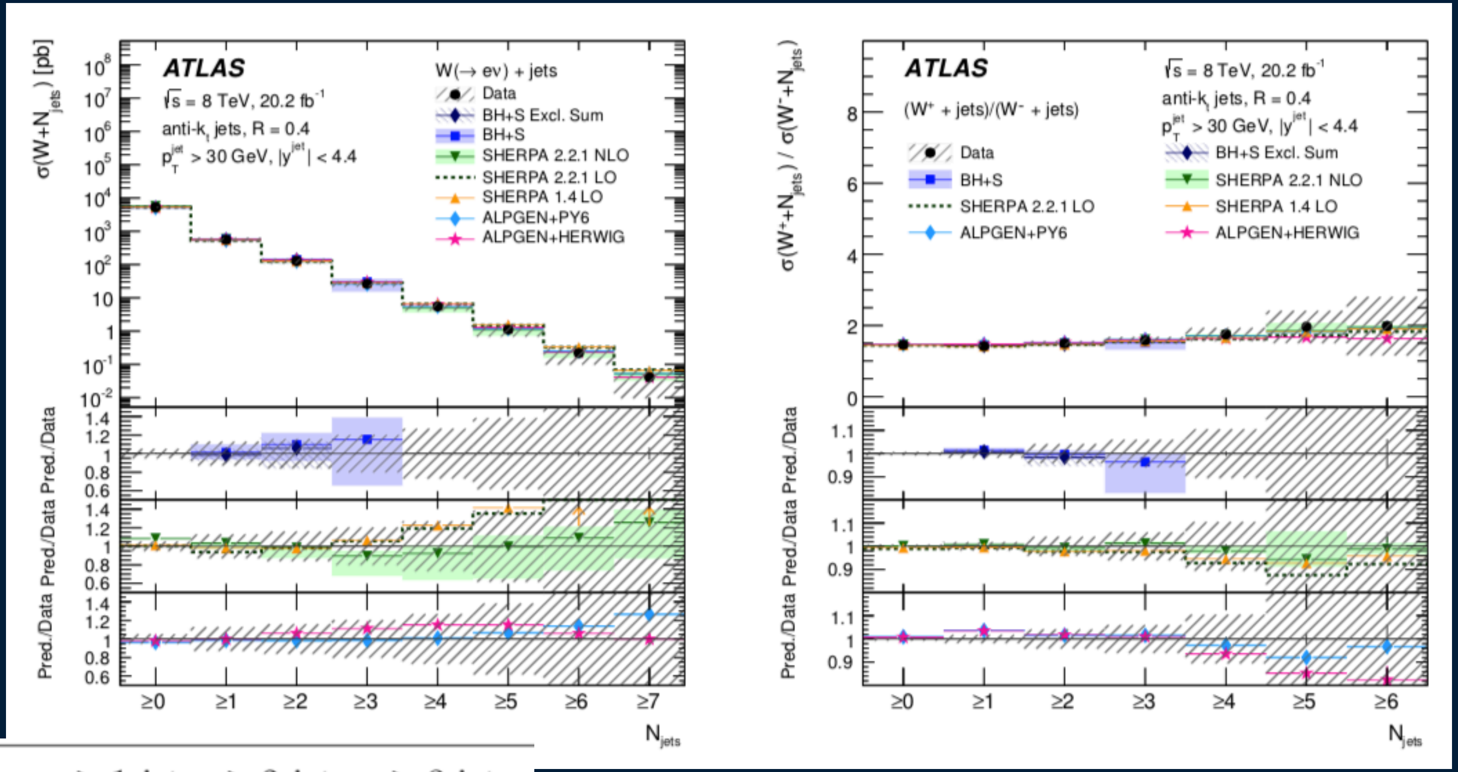

	Inclusive	$\geq$ 1 jet	$\geq$ 2 jets	$\geq$ 3 jets
Jet energy scale	<0.1	0.3	1.2	2.3
Jet energy resolution	0.1	0.7	1.6	2.5
b-tagging	<0.1	0.2	0.5	1.5
Electron	0.1	0.1	0.1	0.1
$E_{\mathrm{T}}^{\mathrm{miss}}$	0.1	0.8	1.9	2.8
Multijet background	0.3	1.2	2.9	3.2
Top quark background	<0.1	0.1	0.3	1.2
Other backgrounds	<0.1	0.1	0.2	0.3
Unfolding	0.6	0.5	0.6	0.7
Other	<0.1	0.1	0.3	0.9
Luminosity	<0.1	<0.1	0.1	0.2
Total systematic uncert.	0.7	1.8	4.1	5.9

W cross-section ratio uncertainties

Inclusive	$\geq$ 1 jet	$\geq$ 2 jets	$\geq$ 3 jets
0.1	7.5	10	14
0.5	8.8	9.9	12
0.1	0.5	1.5	3.8
1.1	1.4	1.4	1.5
1.1	2.6	4.2	5.5
0.5	1.3	2.1	2.6
<0.1	0.2	0.8	2.5
<0.1	0.1	0.2	0.3
4.7	4.1	4.9	4.4
0.3	0.8	1.0	2.1
0.1	0.2	0.4	0.7
5.0	13	16	20

W cross-section

- High gain in precision from the ratio
- multijet uncertainty dominant at large jet multiplicity (ratio)
- Significant impact of jet energy scale at high multiplicity (dominant for W cross-section)

W+jets at 8 TeV : differential cross-sections

- Just a few exemples of distributions : W p_T for W + ≥ 1 jet (W and ratio), ΔR, M_{jj} for W + ≥ 2 jets
- W p_T : sensitive to PDFs, interesting for fits
  - best described by Alpgen+Pythia and LO Sherpa 1.4
  - Ratio : most predictions are off
- ΔR, M_{jj} : test hard parton radiation at large angles and matrix-element/ parton-shower matching
  - Good description from BlackHat+Sherpa
  - Much better description of large M_{jj}/ΔR values from Sherpa 2.2.1 as compared to Sherpa 1.4

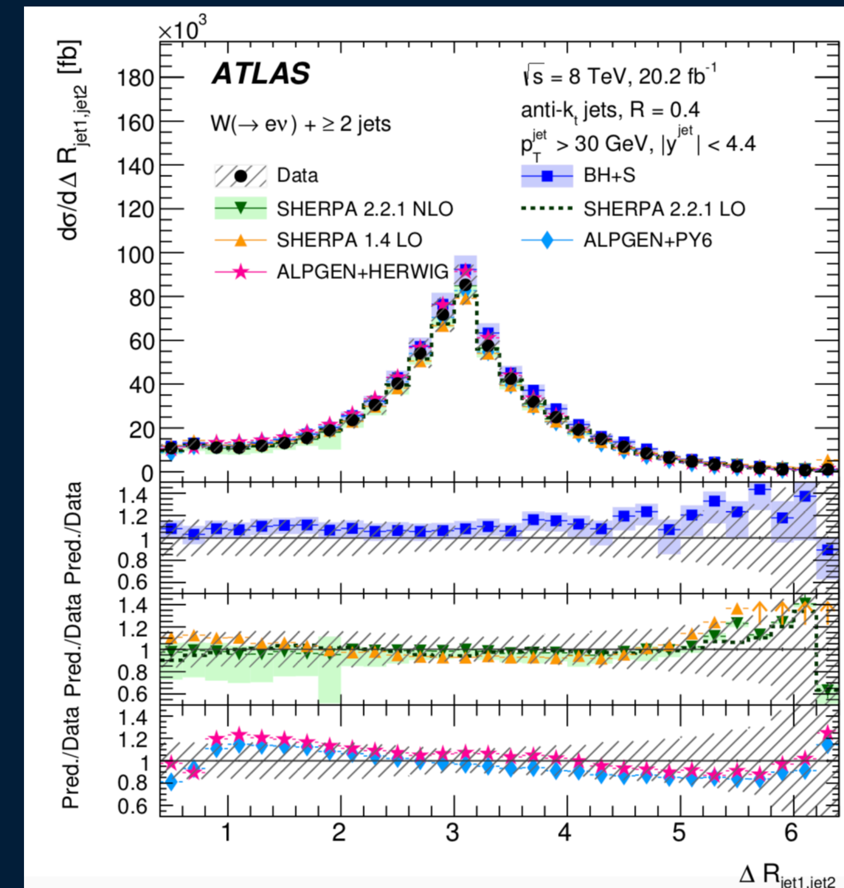

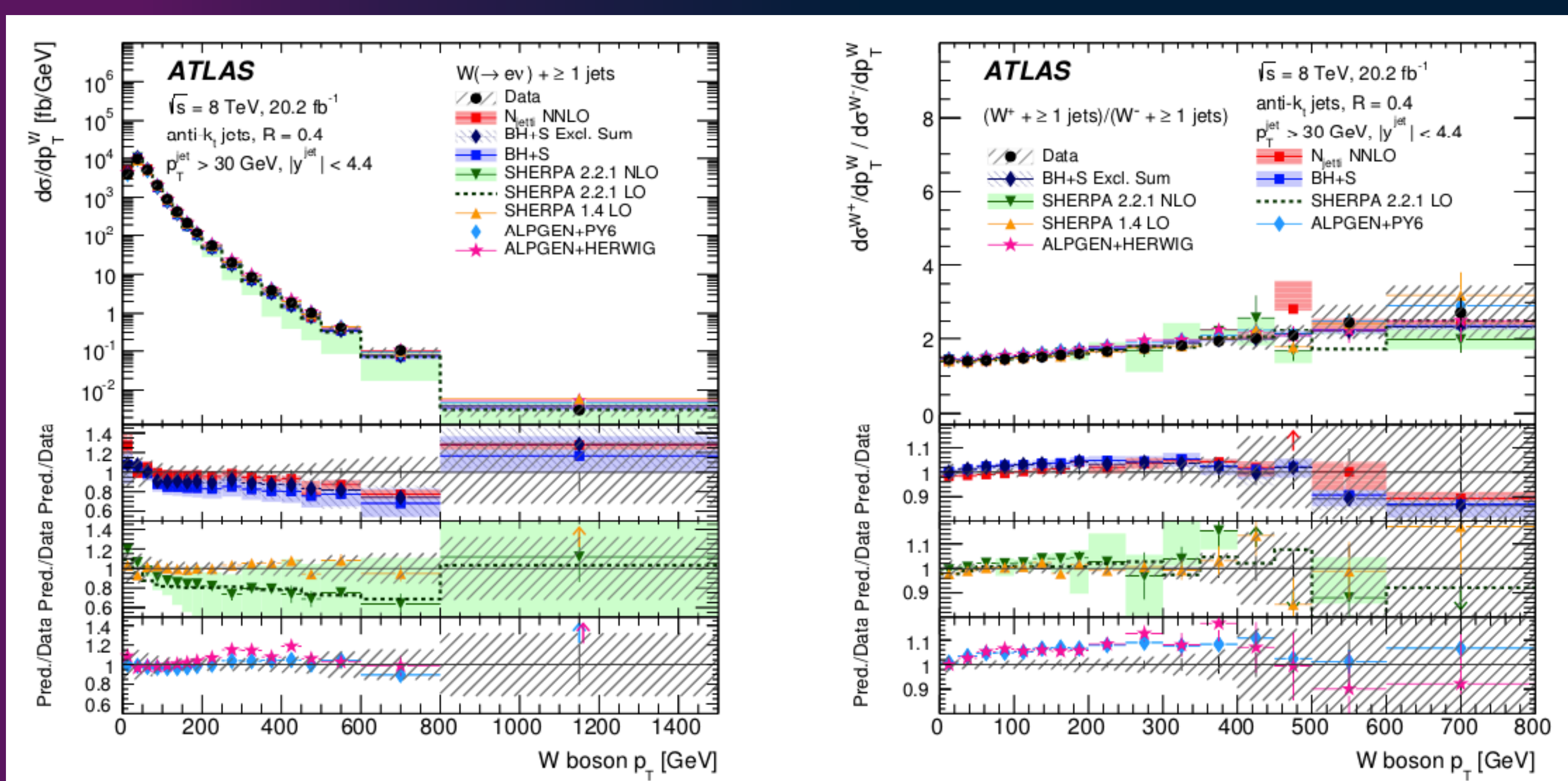

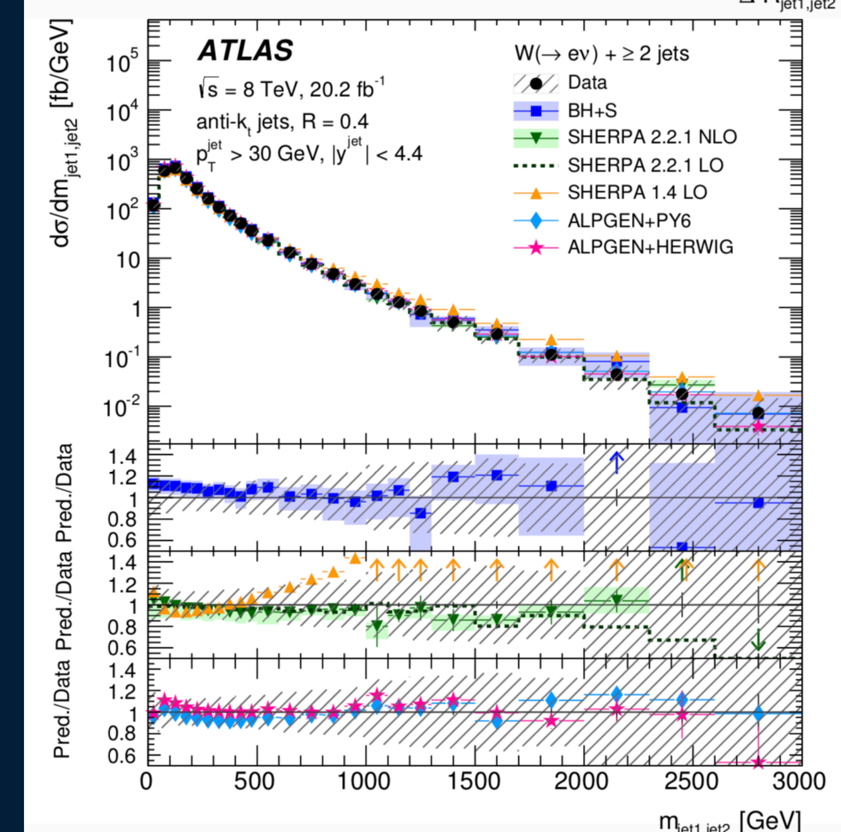

W+jets at 8 TeV : a few conclusions

- High precision reached especially for the W+/W- ratio
- Overall good agreement between the data and the theory predictions
- Degradation at large jet rapidity, angular separation and energy
- Sensitivity of W+/W- ratio to PDFs
- Multi-leg generators (Alpgen, Sherpa) do best in many places
    - High multiplicities in the ME
- No single prediction describes each and every measured observable

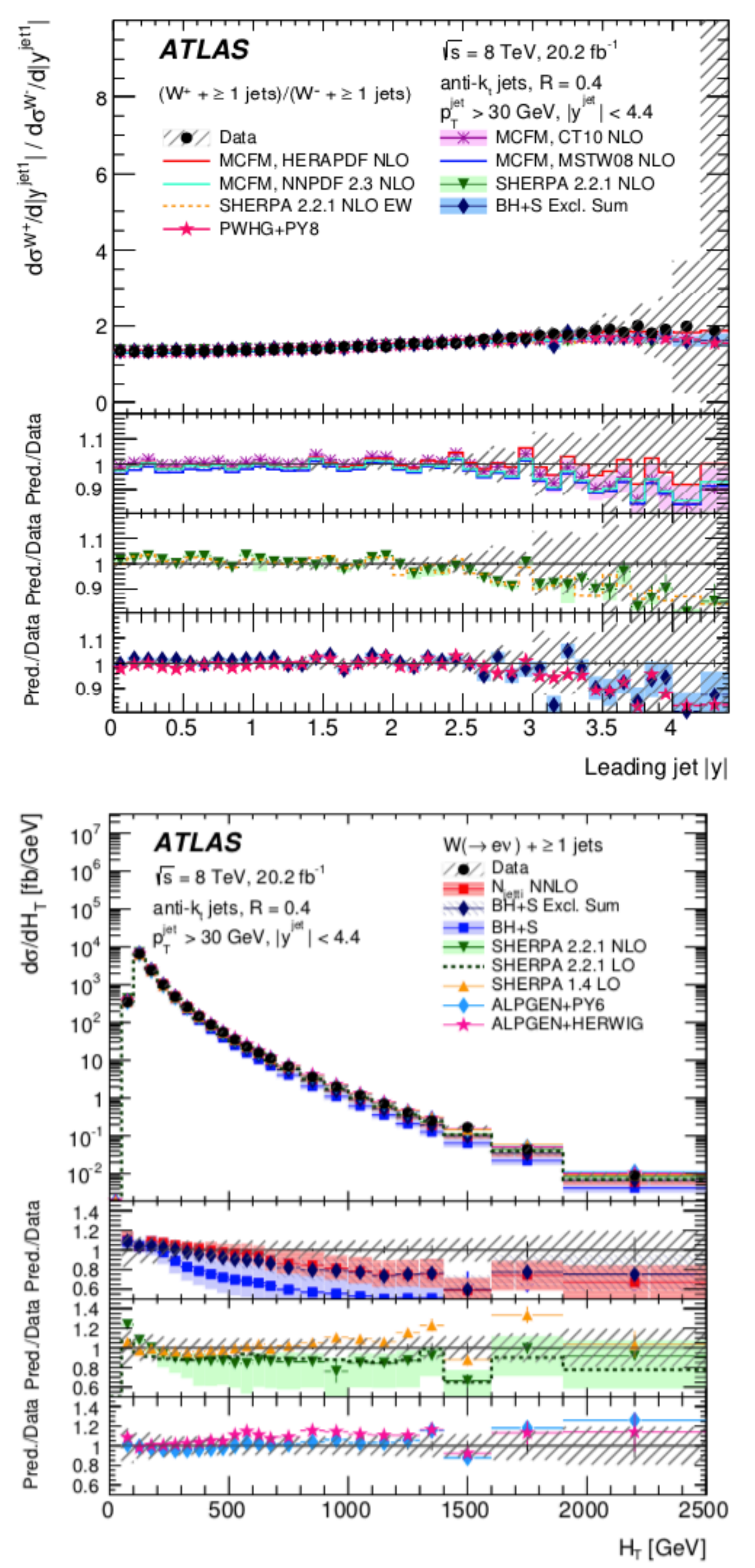

W cross-section : conclusion and summary

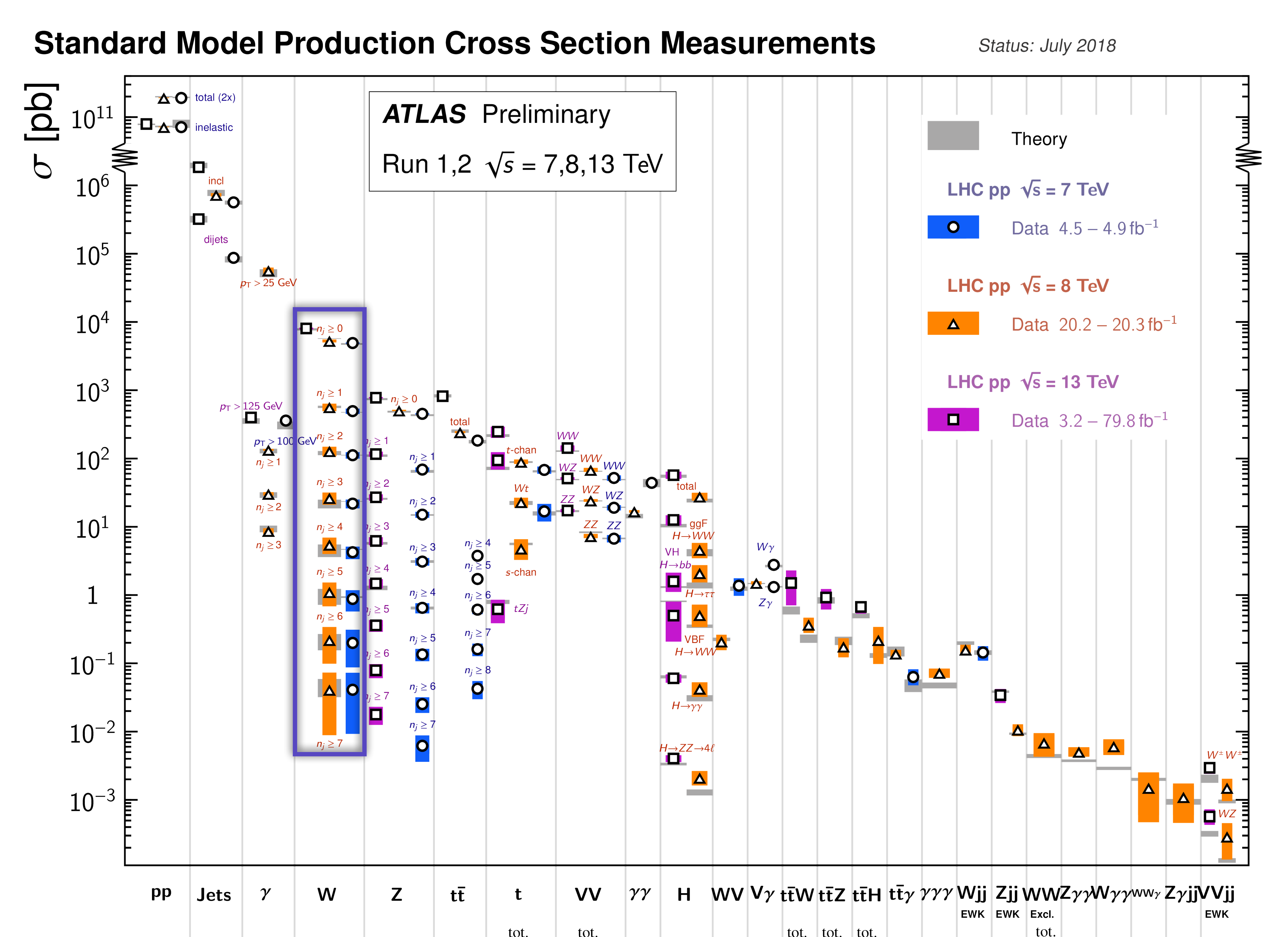

W mass at 7 TeV

Eur.Phys.J. C78 (2018) no.2, 110

Analysis strategy

- Measurement's methodology :
  - obtain predictions with simulated events for signal and background (except data-driven multijet background)
  - to extract the result, compare data and predictions for distributions sensitive to m_W by performing a template $\chi 2$ fit
- Very simple in principle, but extremely challenging in practice as it requires at the 1/10,000 level :
  - Accurate theoretical description of W production and decay kinematics in the simulation
  - Precise calibration of the detector
- Fully reconstructed mass in Z-boson sample to validate the analysis and to provide significant experimental and theoretical constraints (ancillary measurements)

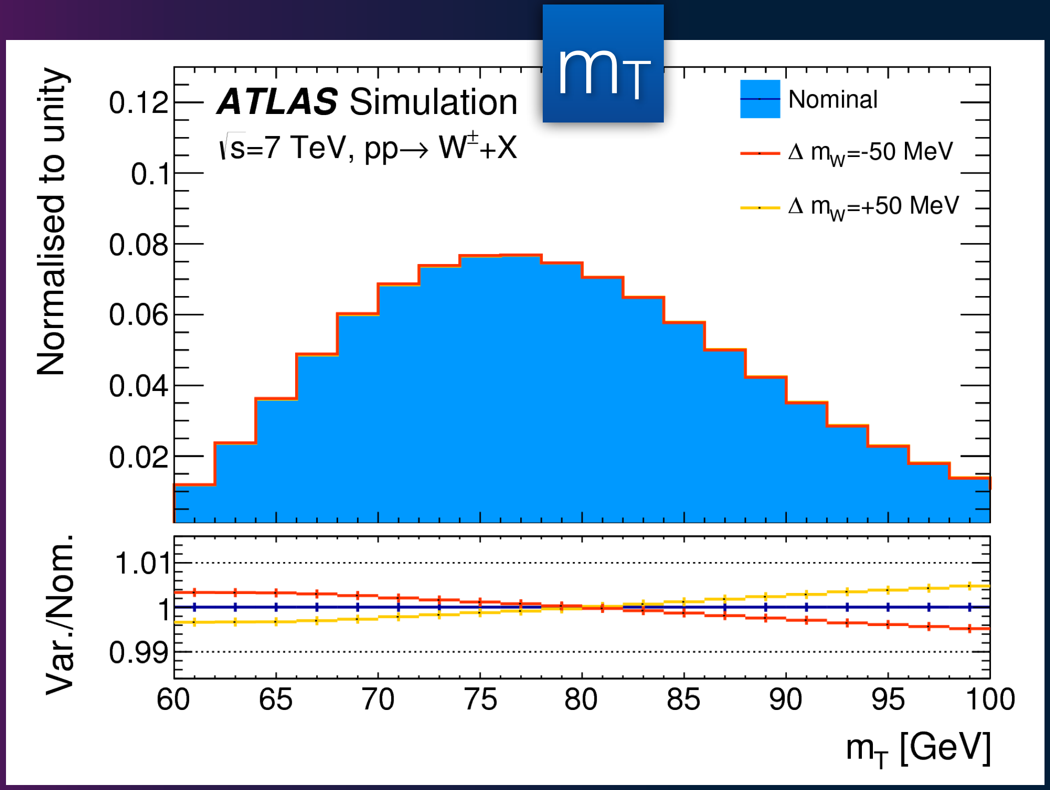

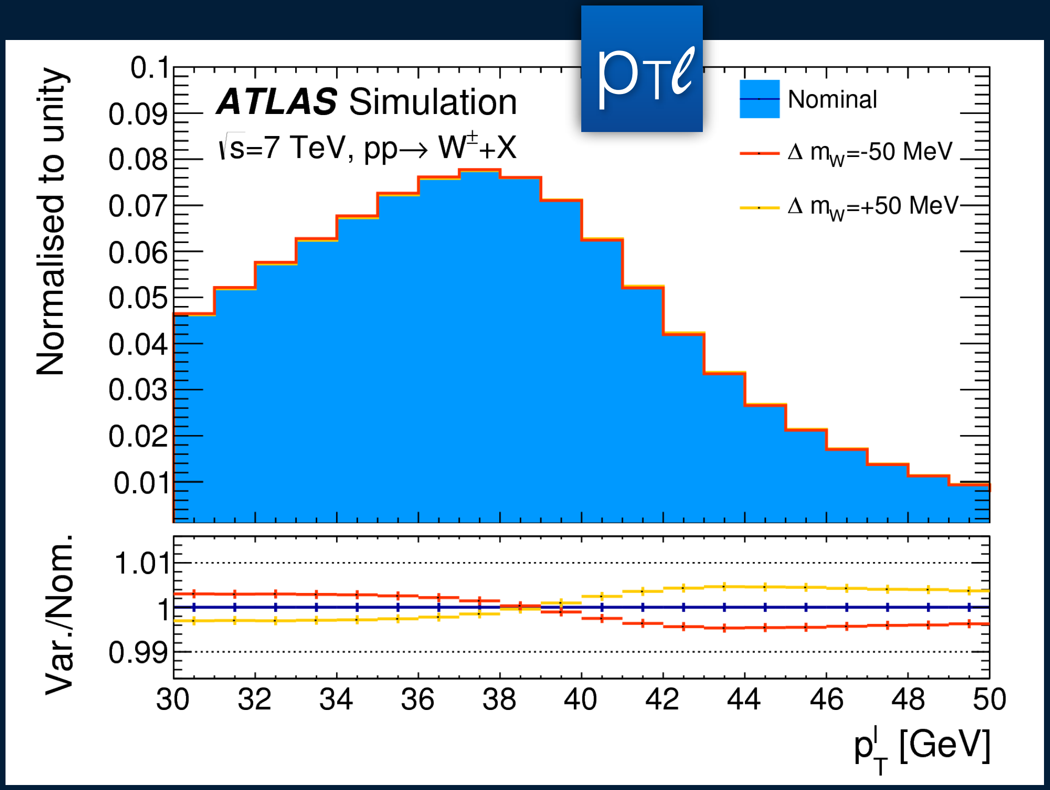

Measurement's categories

Decay channel	$W \to e\nu$	$W \to \mu\nu$
Kinematic distributions	p_T^ℓ, m_T	p_T^ℓ, m_T
Charge categories	W^+, W^-	W^+, W^-
$\|\eta_\ell\|$ categories	$[0, 0.6]$, $[0.6, 1.2]$, $[1.8, 2.4]$	$[0, 0.8]$, $[0.8, 1.4]$, $[1.4, 2.0]$, $[2.0, 2.4]$

- Measurement performed in 2 channels, using 2 observables, 2 charge categories, 3 (4) |η(lepton)| bins in the electron (muon) channel
  - In total, 28 different values of m_W are extracted
  - Allows to :
    - Thoroughly validate the physics modelling
    - benefit from different sensitivities to systematic uncertainties

Motivation

arXiv:1803.01853

- See Introduction
- Current world average (Tevatron + LEP) provides the most precise value :
  - m_W = 80.385 ± 0.015 GeV
- The natural goal for the measurement's precision is set by the EW fit prediction's uncertainty (7 MeV)

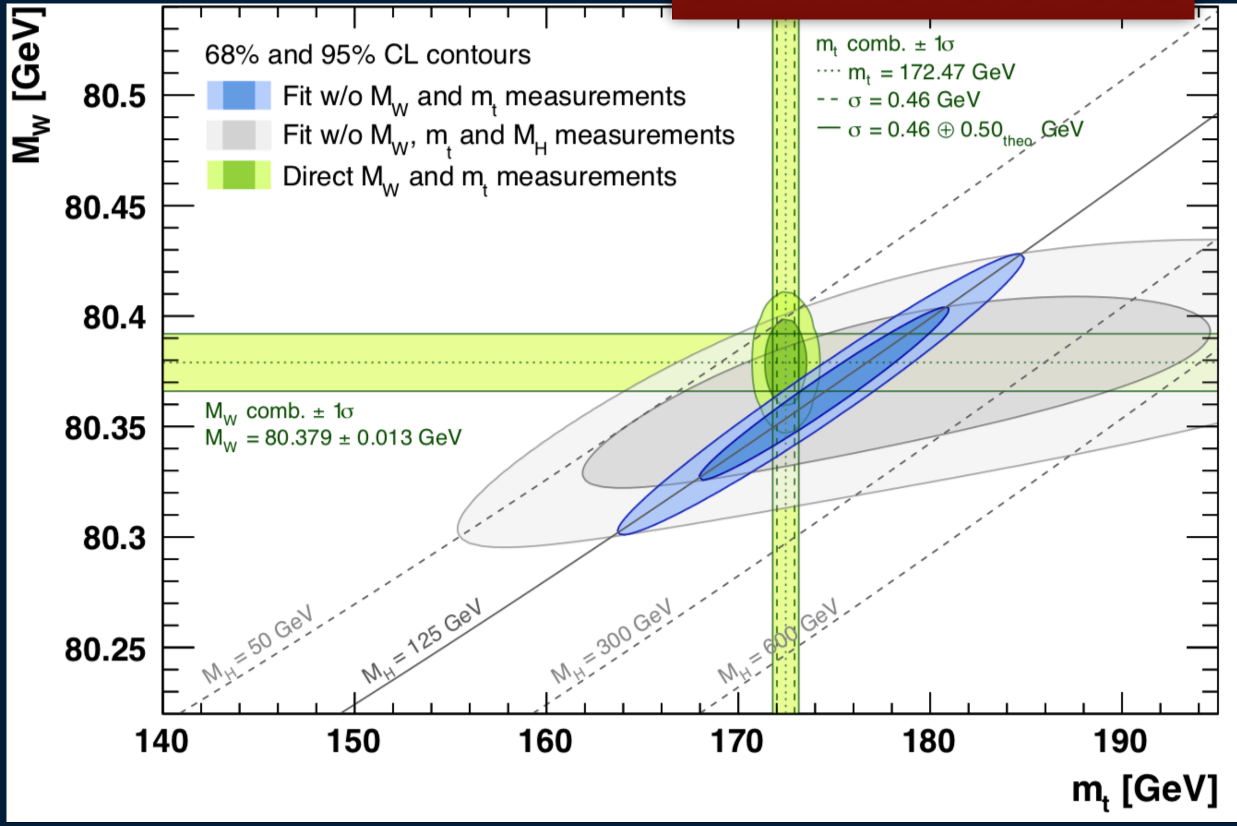

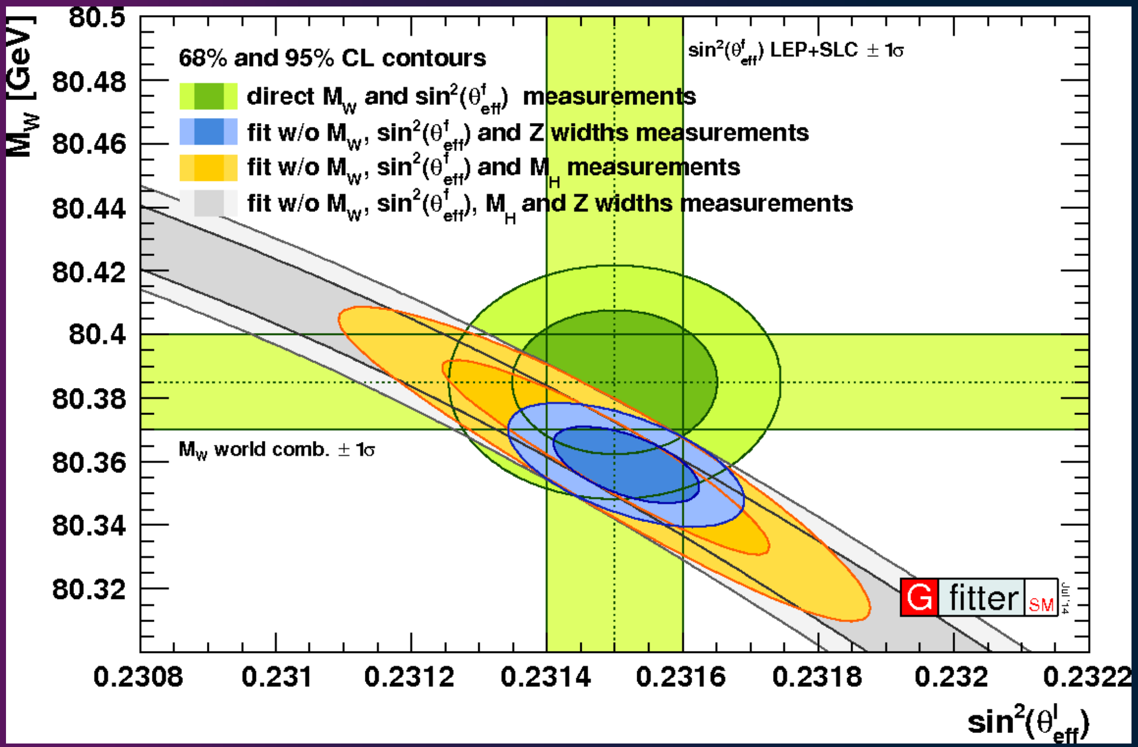

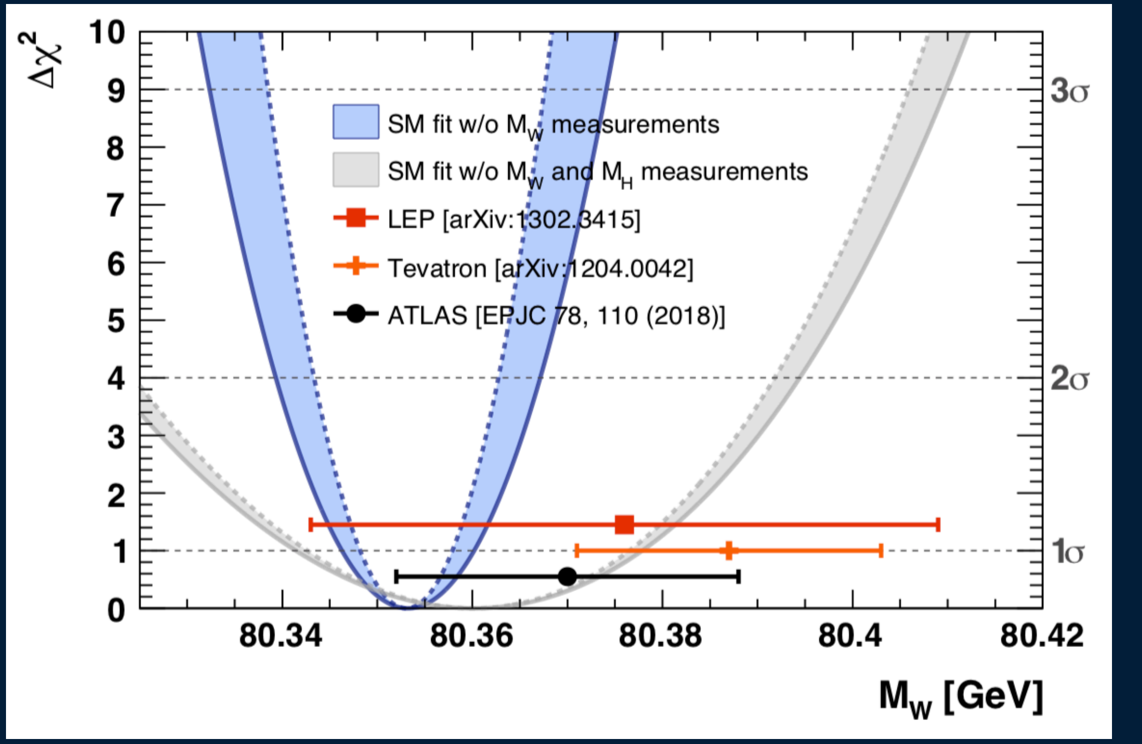

W mass at LHC : more data, larger challenges

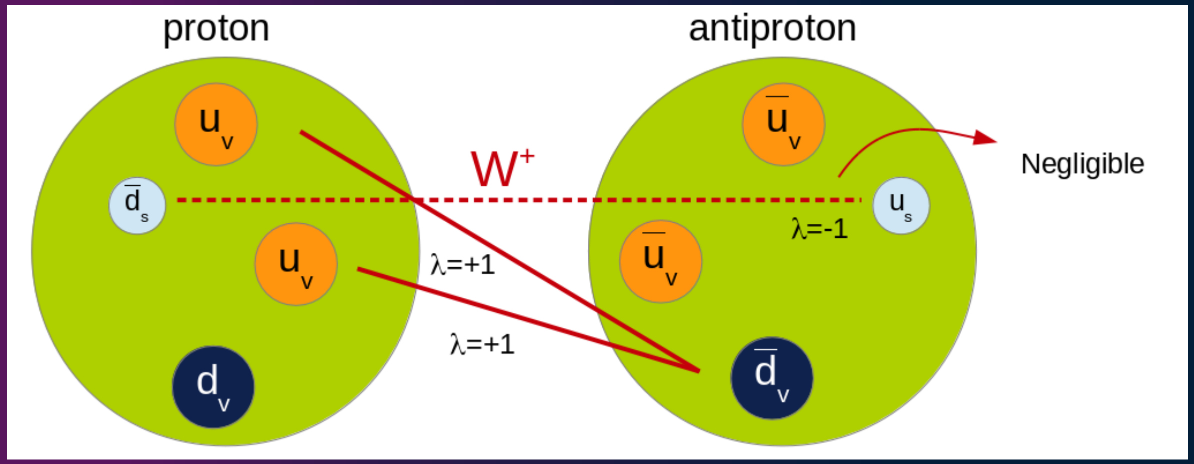

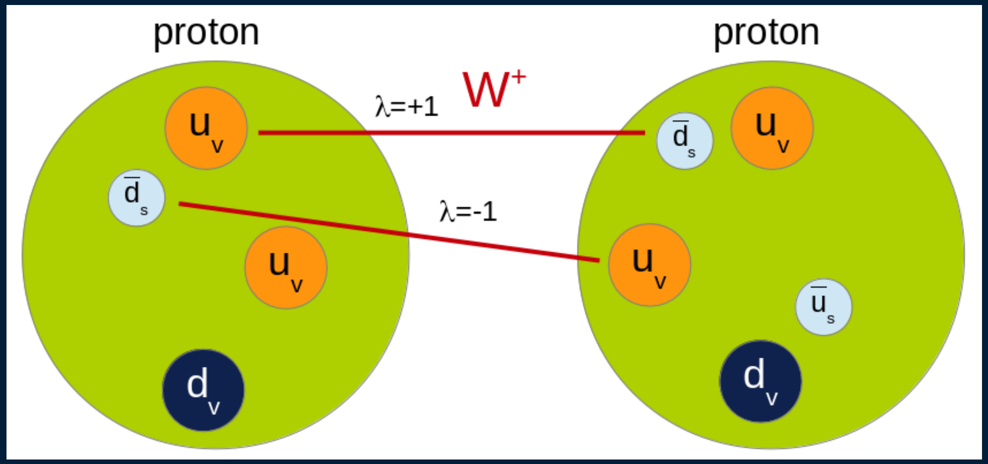

- In proton-proton, W+/W- boson production is asymmetric
  - Different contributions from sea/valence quarks
    - Charge dependence of p_T spectrum and thus on the $p_{T\ell}$ and m_T observables
- More heavy flavour initiated production (25% of the W production is induced by at least one second generation quark s or c)
- W+, W- and Z are produced by different light flavour fractions
- Larger gluon-induced W production
- Large PDF-induced W-polarisation uncertainty (valence vs sea quarks)
- Strange quark pdf uncertainty —> uncertainty on the relative fraction of charm-initiated W boson —> alter the balance between valence quark and sea quark

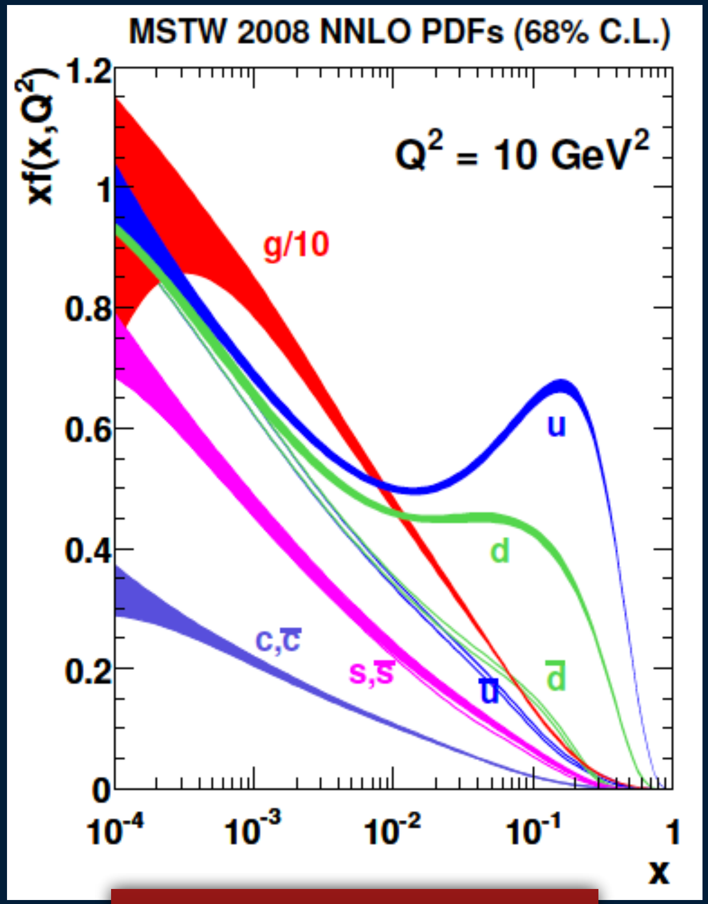

arXiv:0901.0002

Spectra differences between ‘purely sea’ and ‘standard’ quark induced W production

Eur. Phys. J. C (2010) 69: 379–397

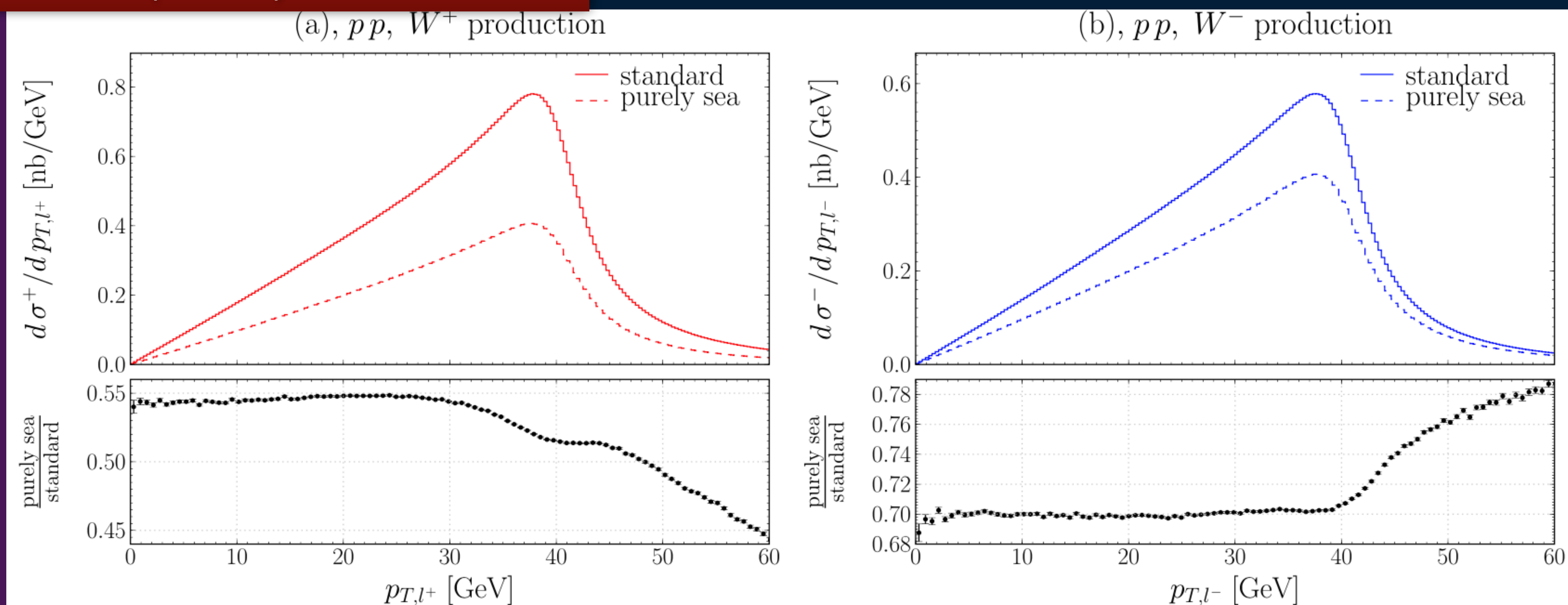

- Uncertainty on sea and valence PDFs —>on the measured spectra

$$\sigma_{W^+}(y) \propto u(x_1)\cdot \bar{d}(x_2) + \bar{d}(x_1)\cdot u(x_2)$$
$$\sigma_{W^-}(y) \propto d(x_1)\cdot \bar{u}(x_2) + \bar{u}(x_1)\cdot d(x_2)$$

MODELING ASPECTS

Introduction to the modeling

- Factorisation of cross-section under 4 terms
  - Approximation checked and valid at 2 MeV level for m_W

spherical harmonics

$$\frac{d\sigma}{dp_1\,dp_2} = \left[\frac{d\sigma(m)}{dm}\right]\left[\frac{d\sigma(y)}{dy}\right]\left[\frac{d\sigma(p_T, y)}{dp_T\,dy}\left(\frac{d\sigma(y)}{dy}\right)^{-1}\right]\left[(1+\cos^2\theta) + \sum_{i=0}^{7} A_i(p_T, y)P_i(\cos\theta, \phi)\right]$$

- $d\sigma(m)/dm$ modeled with Breit Wigner
- Other terms : reweight MC according to various predictions
  1. dσ(y)/dy : fixed-order NNLO prediction (DYNNLO)
  2. p_T at a given y : Pythia8 with ‘AZ’ tune
  3. polarisation Ai : fixed-order NNLO prediction (DYNNLO)
  - (NB : baseline MC is Powheg+Pythia)

Validity check of the reweighting

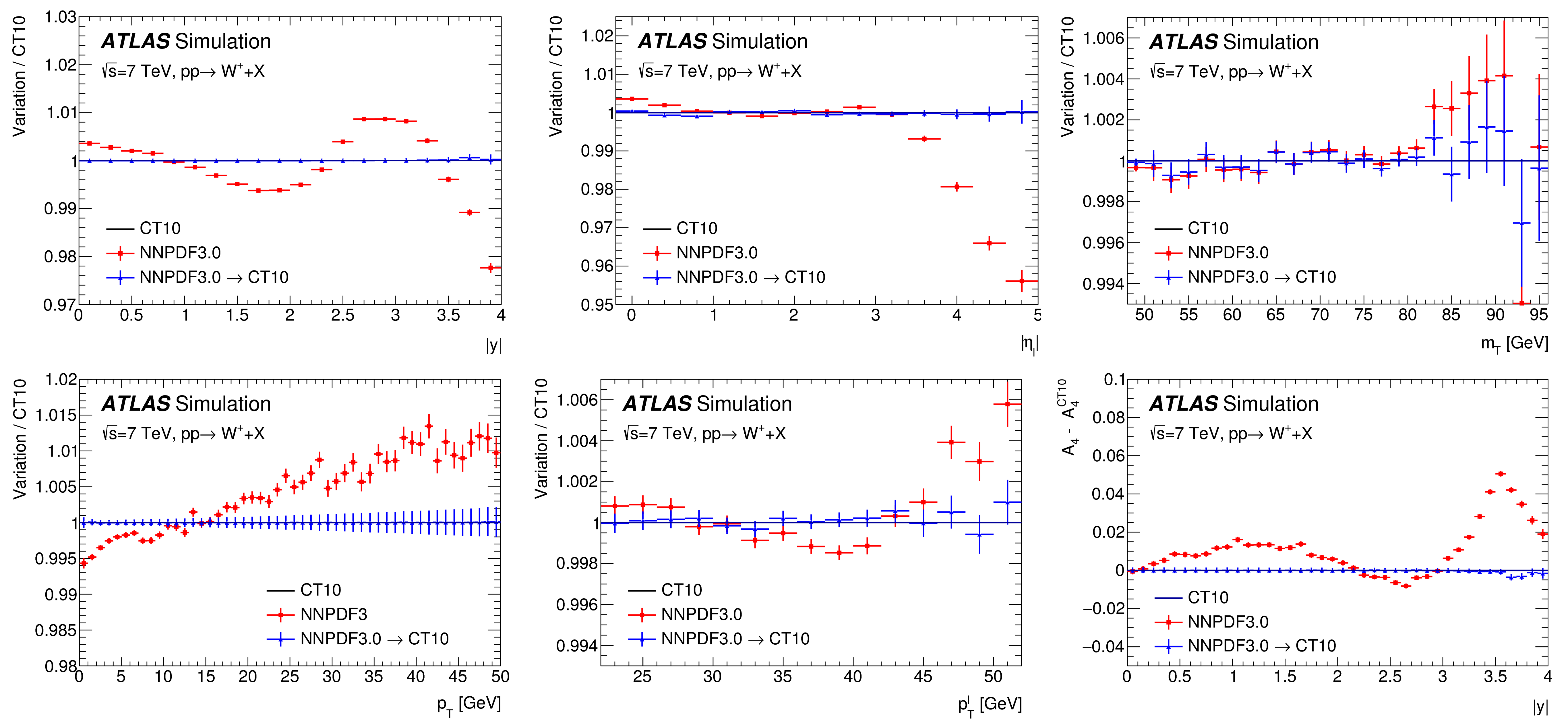

Use NNPDF3 prediction as pseudo-data, perform the various reweightings (y, p_T, polarisation) to CT10 sample : strongly validates the modeling procedure

$\Delta m_W = 1.5 \pm 2.0$ MeV

Rapidity

- Use of DYNNLO (Fixed-order pQCD, NNLO)
- Validate against 7 TeV ATLAS W, Z cross-section measurements
  - Distributions sensitive to PDF effects, critical for validation

Eur. Phys. J. C 77 (2017) 367

- PDF set : CT10nnlo (best agreement), MMHT14nnlo and CT14nnlo used for uncertainties (other global sets disfavoured by the data)

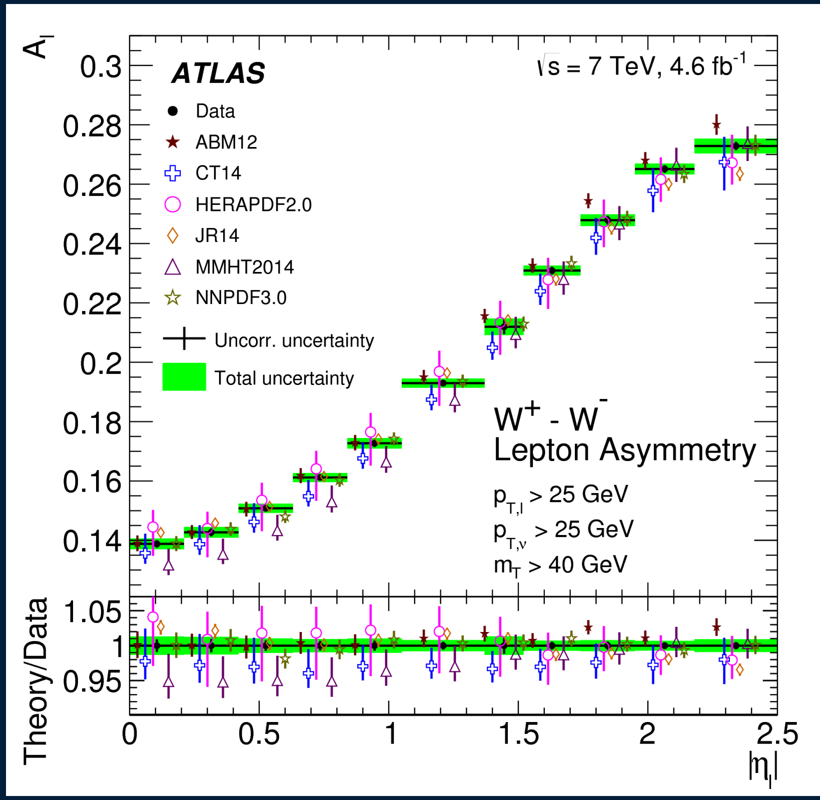

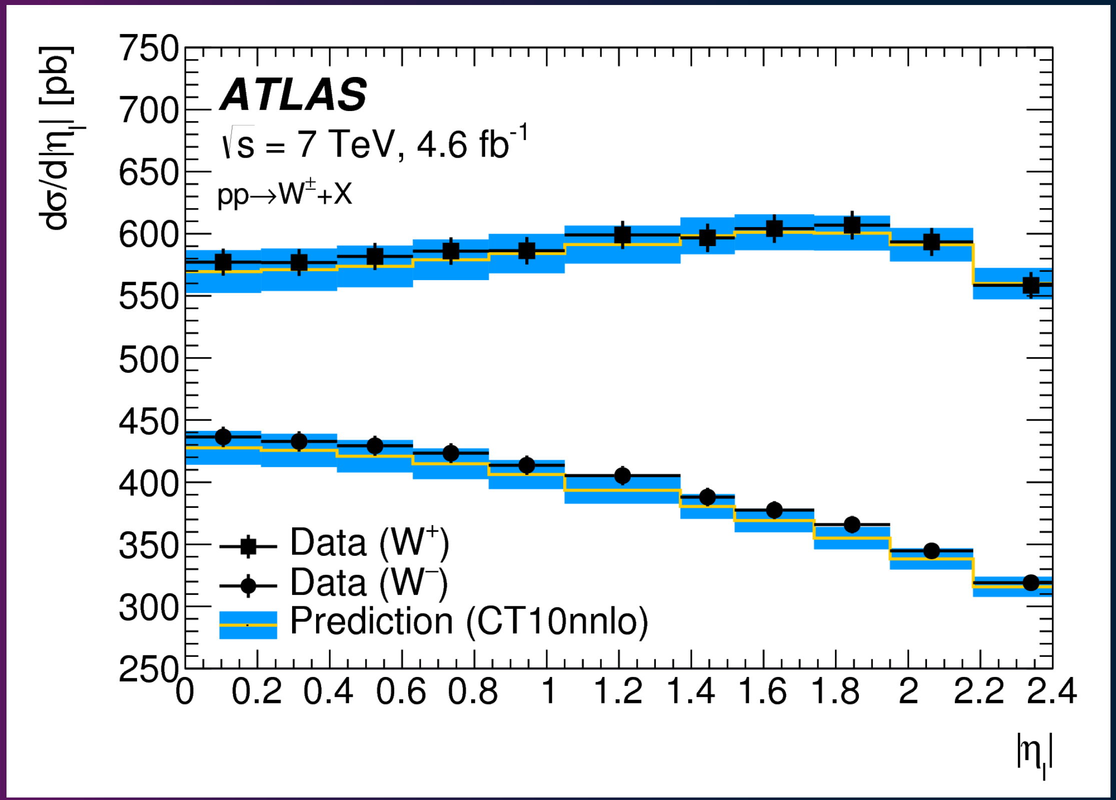

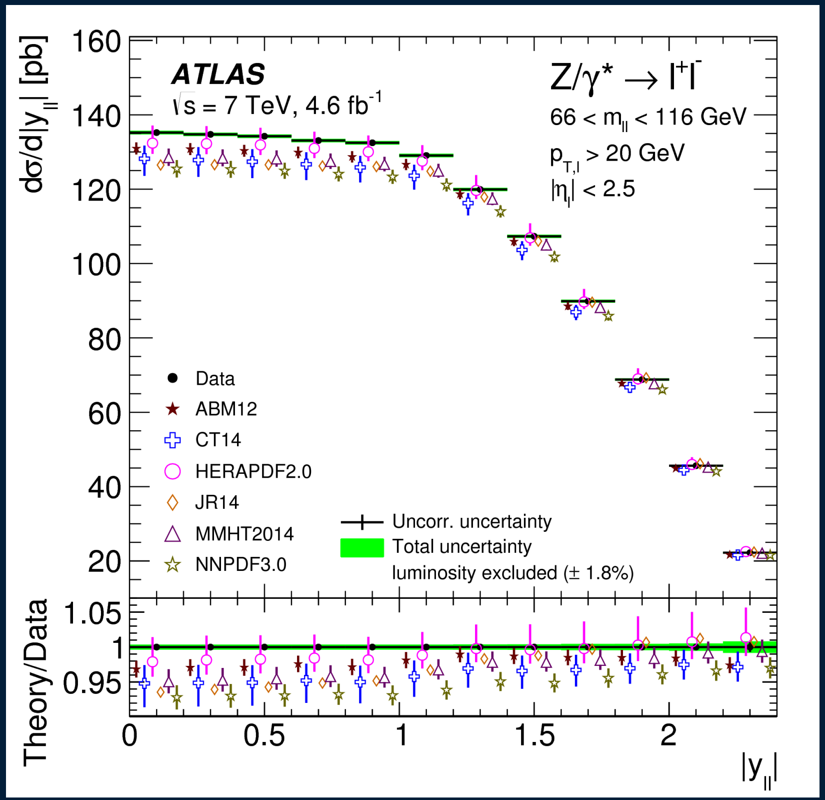

W/Z polarisation

- Kinematic of the decay leptons depend on polarisation of the (W or Z) boson
  - NLO QCD brings p_T to boson, in turn affecting polarisation
- Full 5-dimensional cross-section can be written as :

$$\frac{d\sigma}{dp_T^2\,dy\,dM\,d\cos\theta\,d\phi} = \frac{3}{16\pi}\frac{d\sigma}{dp_T^2\,dy\,dM} \times [(1+\cos^2\theta) + A_0\,\frac{1}{2}(1-3\cos^2\theta) + A_1\,\sin 2\theta\cos\phi + A_2\,\frac{1}{2}\sin^2\theta\cos 2\phi + A_3\,\sin\theta\cos\phi + A_4\,\cos\theta + A_5\,\sin^2\theta\sin 2\phi + A_6\,\sin 2\theta\sin\phi + A_7\,\sin\theta\sin\phi]$$

$$A_0 = \frac{2}{3} + \frac{10}{3} < (1-3\cos^2\theta) >$$
$$A_1 = 5 < \sin 2\theta\cos\phi >$$
$$A_2 = 10 < \sin^2\theta\cos 2\phi >$$
$$A_3 = 4 < \sin\theta\cos\phi >$$
$$A_4 = 4 < \cos\theta >$$
$$A_5 = 5 < \sin^2\theta\sin 2\phi >$$
$$A_6 = 5 < \sin 2\theta\sin\phi >$$
$$A_7 = 4 < \sin\theta\sin\phi >$$

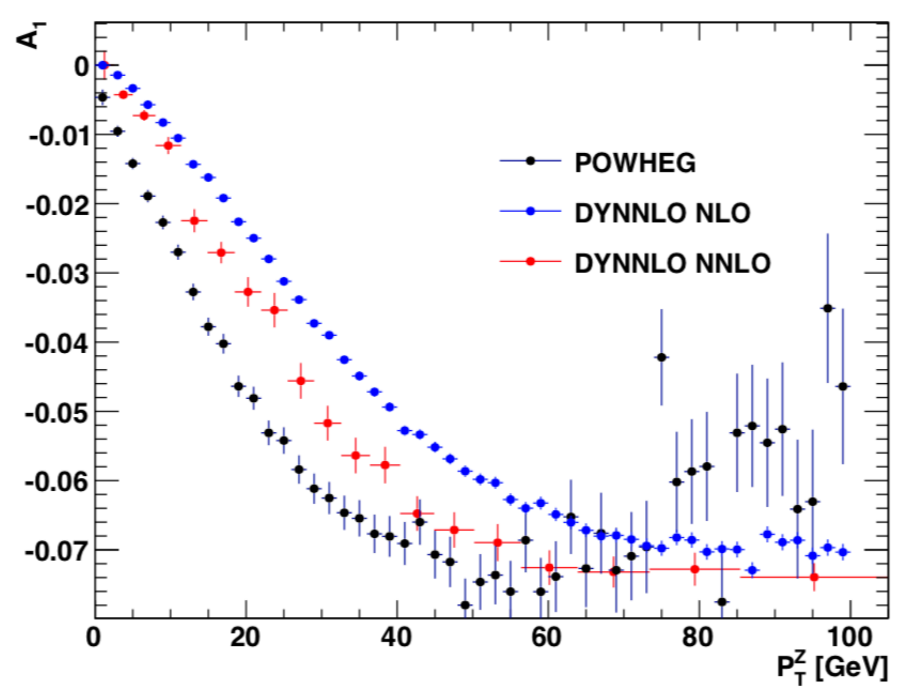

- θ and ϕ : angles of the charged lepton (W^-, Z) or neutrino (W^+) in the rest frame of the boson
- $A_i(m, y, p_T)$: dimensionless angular coefficients (m dependence is small)
  - A_i—>0 when p_T~0 except for A_4 (responsible of forward-backward lepton asymmetry, sensitive to $\sin^2\theta_W$)
  - A_5-A_7 small, only appear at NNLO in α_S

Polarisation

ATLAS-PHYS-PUB-2014-015

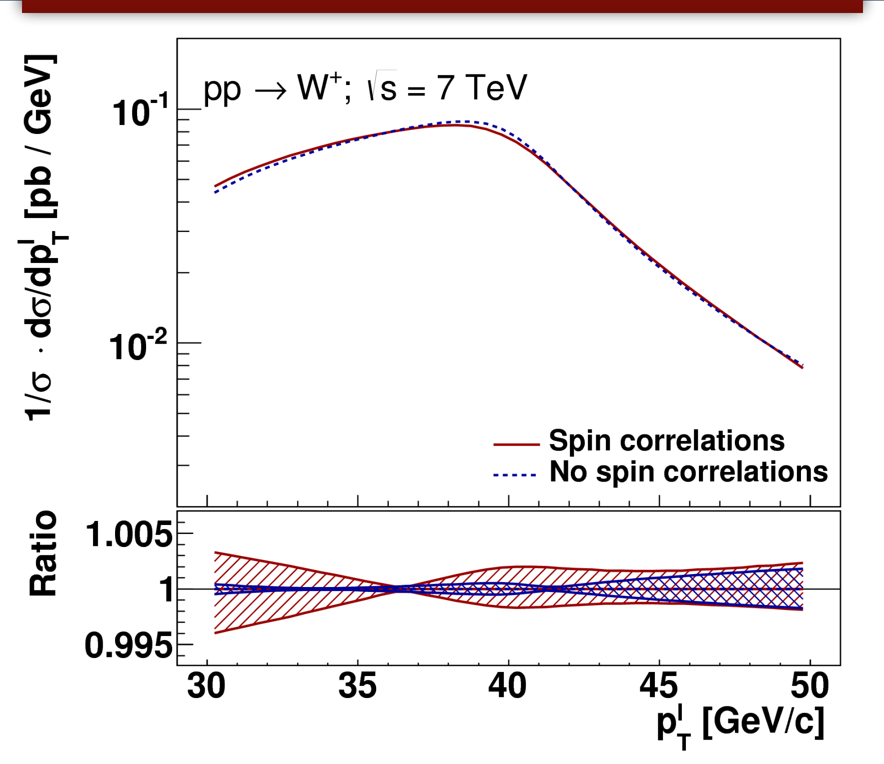

- Crucial to get right in *pp* collisions, otherwise miss some effects
- ATLAS measurement of Z angular coefficients validates fixed-order pQCD NNLO prediction
  - except for A_2 : additional uncertainty
    - data/prediction difference is added to the uncertainty ; pseudo-experiments show no correlation with other coefficients
  - Uncertainties on the Z measurement are propagated to the W

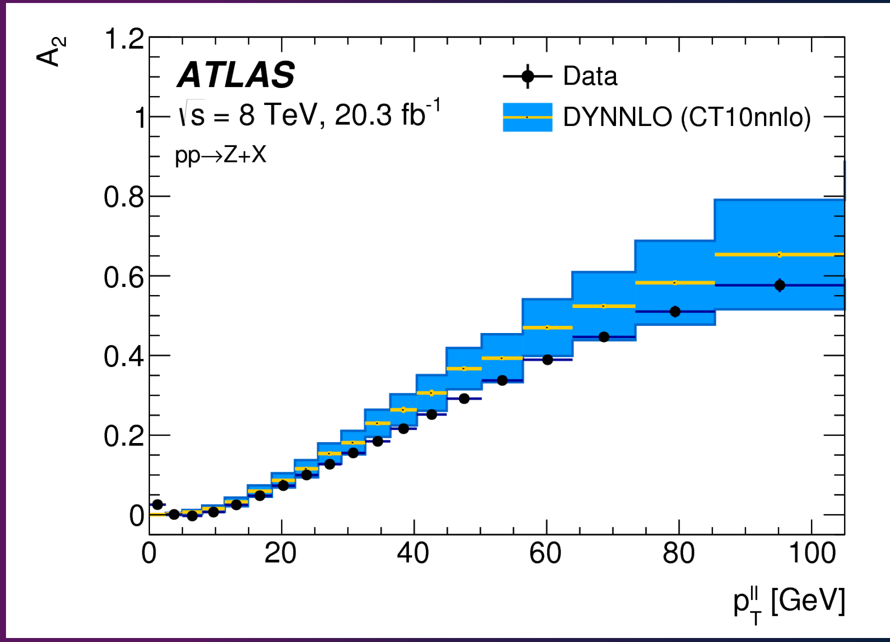

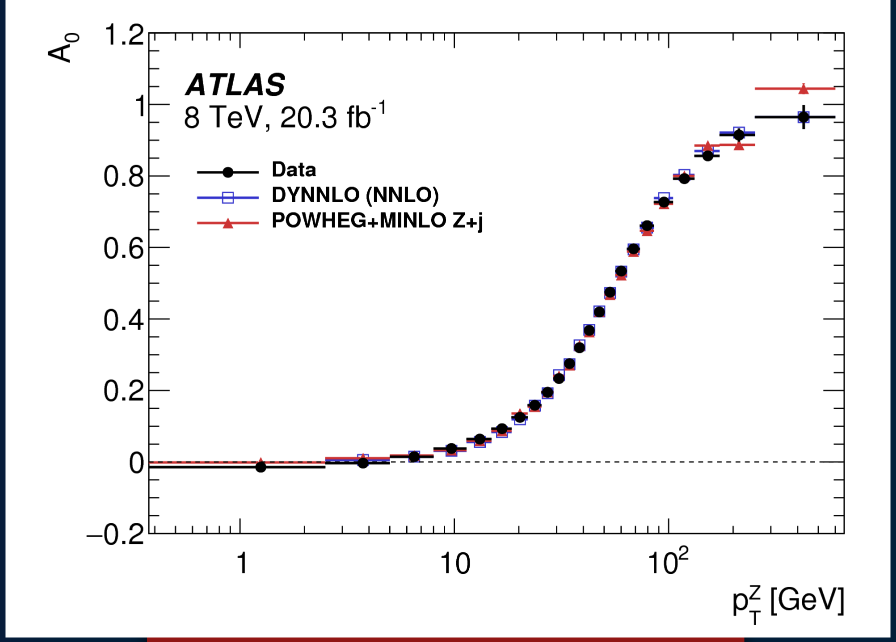

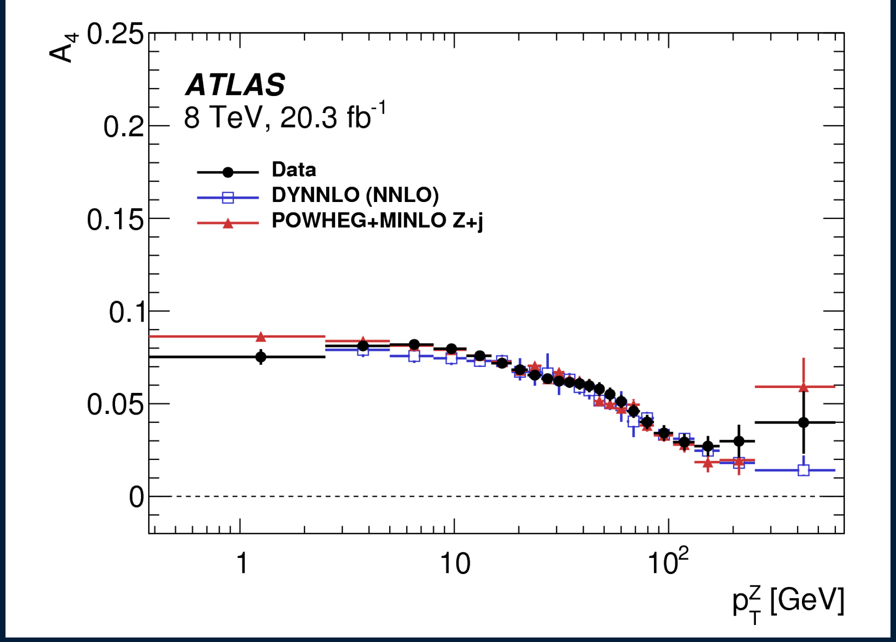

JHEP 08 (2016) 159

W boson transverse momentum

- Pythia8 tuned on Z p_T ATLAS data (AZ tune)

	PYTHIA8
Tune Name	AZ
Primordial k_T [GeV]	1.71 ± 0.03
ISR $\alpha_S^{ISR}(m_Z)$	0.1237 ± 0.0002
ISR cut-off [GeV]	0.59 ± 0.08
χ^2_{min}/dof	45.4/32

JHEP 09 (2014) 145

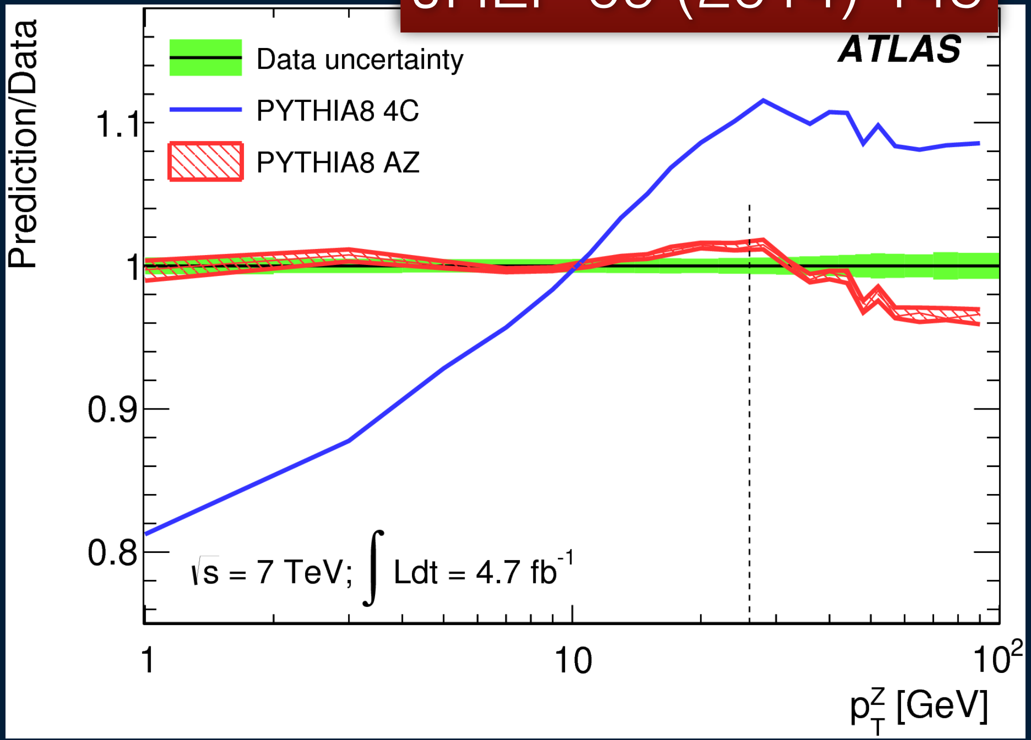

- Good agreement is obtained for the ratio of differential cross-sections using this tune:

$$R_{W/Z}(p_T) = \left(\frac{1}{\sigma_W} \cdot \frac{d\sigma_W(p_T)}{dp_T}\right)\left(\frac{1}{\sigma_Z} \cdot \frac{d\sigma_Z(p_T)}{dp_T}\right)^{-1}$$

- $p_T(W)$ is obtained via the product of the predicted ratio and the experimental Z p_T spectrum
  - The total uncertainty being the sum in quadrature of these two components, ~1-2%

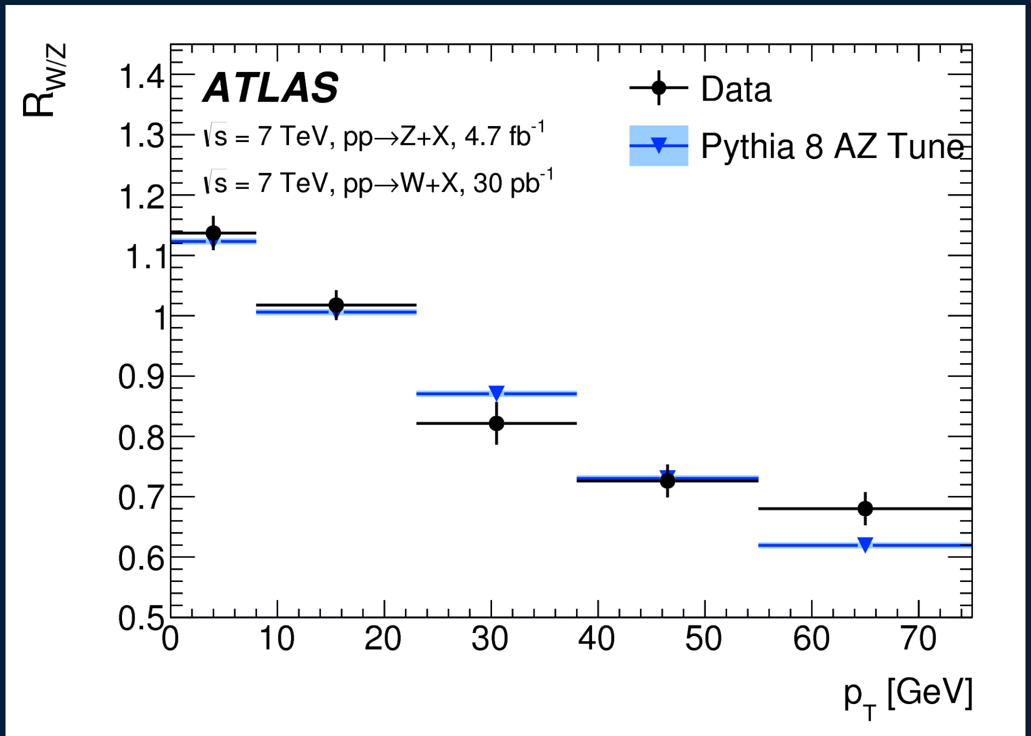

Uncertainties to $p_T(W)$

- Only modelling uncertainties which are uncorrelated between Z and W give sizeable uncertainties on the measurement
  - Induced by heavy flavour initiated production : 6/3% of cc/bb for Z, 20% of cs for W production
- Missing higher orders in QCD ISR : factorisation scale (μ_F) variations taken as correlated between W and Z for light quark, independently for heavy quarks
- other sources : uncertainty on m_C, choice of parton shower LO PDF
- Central prediction and uncertainty well validated with the recoil distribution in the data

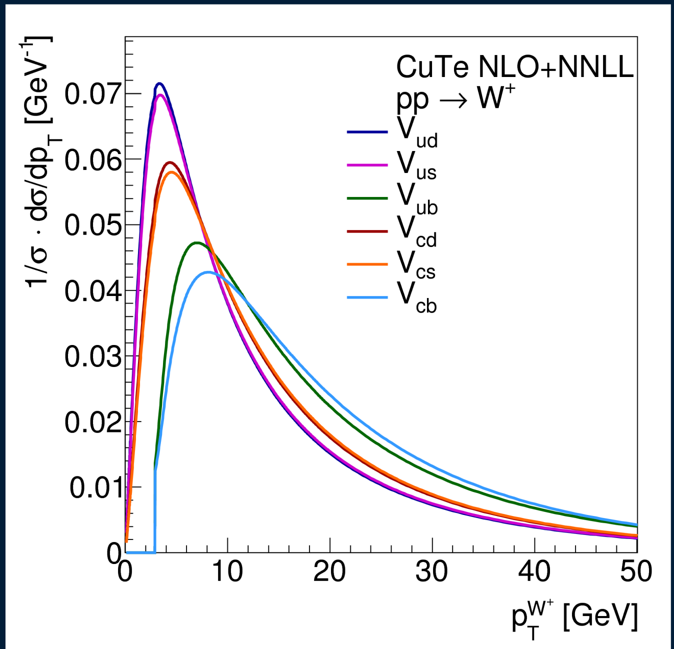

μ_F variations

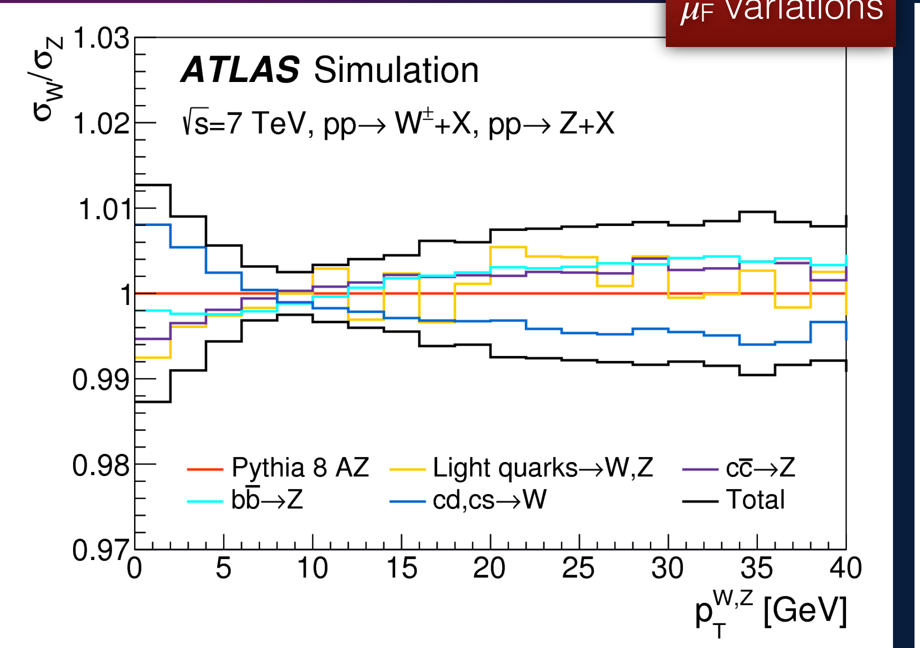

all uncertainties

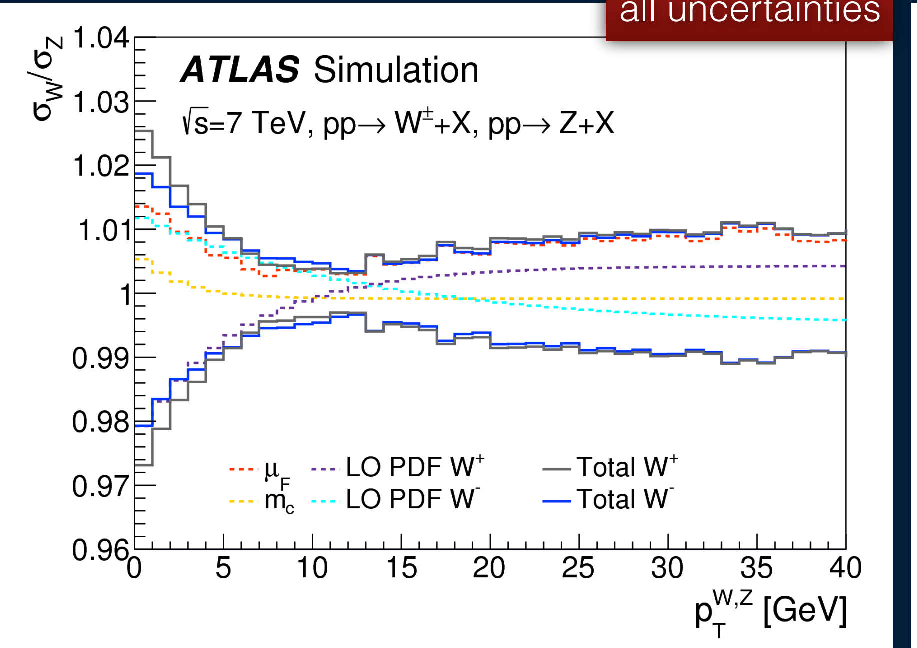

Validation in the data

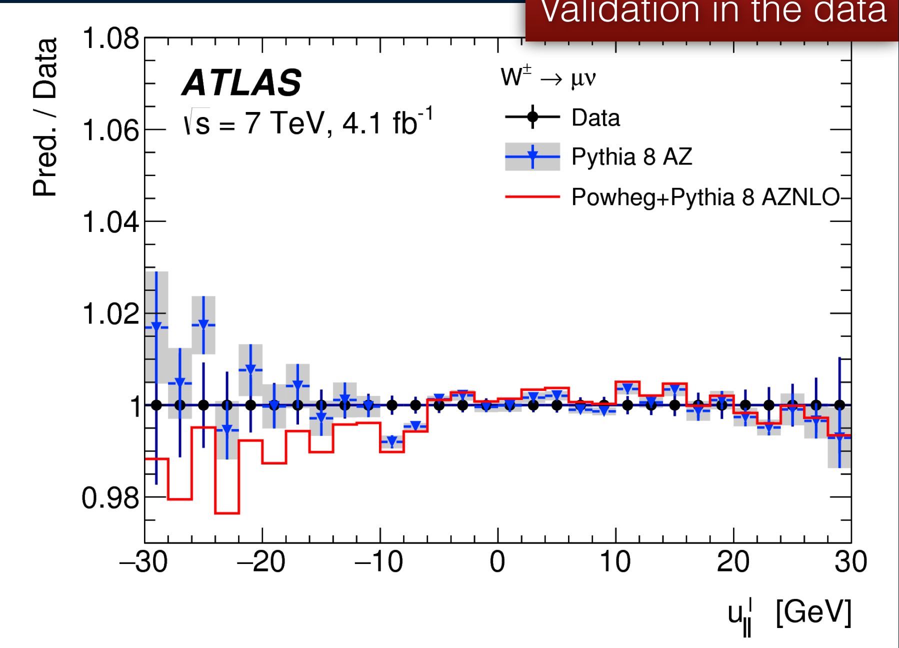

Uncertainty from the PDFs

- Each PDF uncertainty eigenvector from CT10nnlo propagated simultaneously to Ai, rapidity and pT reweighing distributions
  - Overall uncertainty evaluated with the Hessian method
  - Consider MMHT14nnlo and CT14nnlo as alternative
- For $p_T(W)$, only relative variations of $p_T(W)$ and $p_T(Z)$ are considered, reducing the impact of this uncertainty

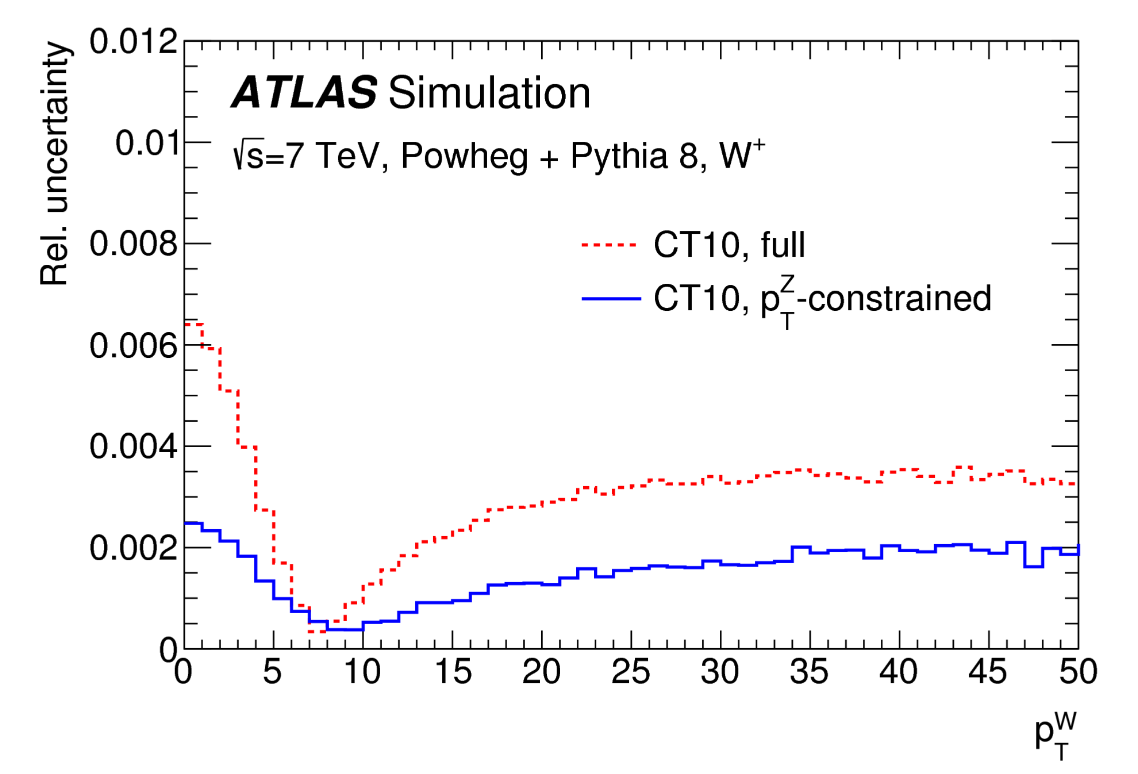

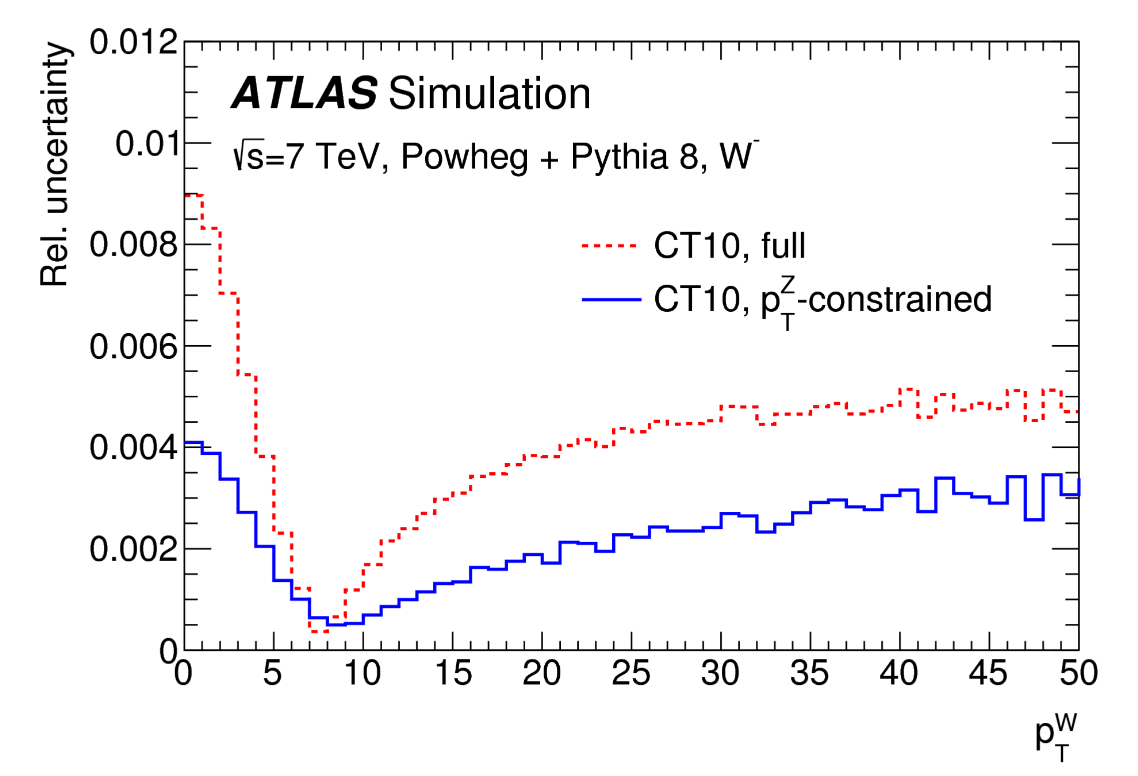

QCD modelling uncertainties

- Biggest uncertainties arise from the PDFs, modelling of $p_T(W)$ and polarisation
  - Strong anti-correlated effect of PDF on W+ vs W- !
- May be further reduced in the future thanks to :
  - More ancillary measurements : polarisation @13 TeV (higher statistics, uncorrelated systematics), direct W p_T measurement (requires a low pile-up run at LHC)
  - Simultaneous profiling of the PDFs in the fit

W-boson charge	W^+		W^-		Combined	
Kinematic distribution	p_T^ℓ	m_T	p_T^ℓ	m_T	p_T^ℓ	m_T
δm_W [MeV]						
Fixed-order PDF uncertainty	13.1	14.9	12.0	14.2	8.0	8.7
AZ tune	3.0	3.4	3.0	3.4	3.0	3.4
Charm-quark mass	1.2	1.5	1.2	1.5	1.2	1.5
Parton shower μ_F with heavy-flavour decorrelation	5.0	6.9	5.0	6.9	5.0	6.9
Parton shower PDF uncertainty	3.6	4.0	2.6	2.4	1.0	1.6
Angular coefficients	5.8	5.3	5.8	5.3	5.8	5.3
Total	15.9	18.1	14.8	17.2	11.6	12.9

Electroweak uncertainties

- QED FSR photons implemented with Photos, negligible uncertainty on it
- FSR pair production impact checked with Photos and Sanc, taken as uncertainty
  - can be implemented in the baseline MC for future measurements (Photospp 3.61)
- Combined NLO EW⊗QCD corrections are assessed with Winhac and taken as an uncertainty - they include IFI + pure weak corrections but need to be checked using a realistic p_T (NLO in QCD)
  - same remark (available recently in Powheg-EW)

Decay channel	$W \to e\nu$		$W \to \mu\nu$	
Kinematic distribution	p_T^ℓ	m_T	p_T^ℓ	m_T
δm_W [MeV]				
FSR (real)	< 0.1	< 0.1	< 0.1	< 0.1
Pure weak and IFI corrections	3.3	2.5	3.5	2.5
FSR (pair production)	3.6	0.8	4.4	0.8
Total	4.9	2.6	5.6	2.6

EXPERIMENTAL ASPECTS

Event selection

- Lepton selection
  - muon : p_T > 30 GeV, |η| < 2.4, track-based isolation
  - electron : p_T > 30 GeV, |η| < 1.2 or 1.8 < |η| < 2.4, track and calorimeter-based isolation
- Kinematic requirements :
  - Recoil : u_T < 30 GeV
  - m_T > 60 GeV, p_T^{miss} > 30 GeV

$\lvert\eta_\ell\rvert$ range	0–0.8	0.8–1.4	1.4–2.0	2.0–2.4	Inclusive
$W^+ \to \mu^+\nu$	1 283 332	1 063 131	1 377 773	885 582	4 609 818
$W^- \to \mu^-\bar{\nu}$	1 001 592	769 876	916 163	547 329	3 234 960
$\lvert\eta_\ell\rvert$ range	0–0.6	0.6–1.2		1.8–2.4	Inclusive
$W^+ \to e^+\nu$	1 233 960	1 207 136		956 620	3 397 716
$W^- \to e^-\bar{\nu}$	969 170	908 327		610 028	2 487 525

7.8M events

5.9M events

Background fractions

$W \to \mu\nu$						
Category	$W \to \tau\nu$	$Z \to \mu\mu$	$Z \to \tau\tau$	Top	Dibosons	Multijet
$W^{\pm}$ $0.0 < \|\eta\| < 0.8$	1.04	2.83	0.12	0.16	0.08	0.72
$W^{\pm}$ $0.8 < \|\eta\| < 1.4$	1.01	4.44	0.11	0.12	0.07	0.57
$W^{\pm}$ $1.4 < \|\eta\| < 2.0$	0.99	6.78	0.11	0.07	0.06	0.51
$W^{\pm}$ $2.0 < \|\eta\| < 2.4$	1.00	8.50	0.10	0.04	0.05	0.50
$W^{\pm}$ all η bins	1.01	5.41	0.11	0.10	0.06	0.58
W^{+} all η bins	0.99	4.80	0.10	0.09	0.06	0.51
W^{-} all η bins	1.04	6.28	0.14	0.12	0.08	0.68

$W \to e\nu$						
Category	$W \to \tau\nu$	$Z \to ee$	$Z \to \tau\tau$	Top	Dibosons	Multijet
$W^{\pm}$ $0.0 < \|\eta\| < 0.6$	1.02	3.34	0.13	0.15	0.08	0.59
$W^{\pm}$ $0.6 < \|\eta\| < 1.2$	1.00	3.48	0.12	0.13	0.08	0.76
$W^{\pm}$ $1.8 < \|\eta\| < 2.4$	0.97	3.23	0.11	0.05	0.05	1.74
$W^{\pm}$ all η bins	1.00	3.37	0.12	0.12	0.07	1.00
W^{+} all η bins	0.98	2.92	0.10	0.11	0.06	0.84
W^{-} all η bins	1.04	3.98	0.14	0.13	0.08	1.21

Electron calibration

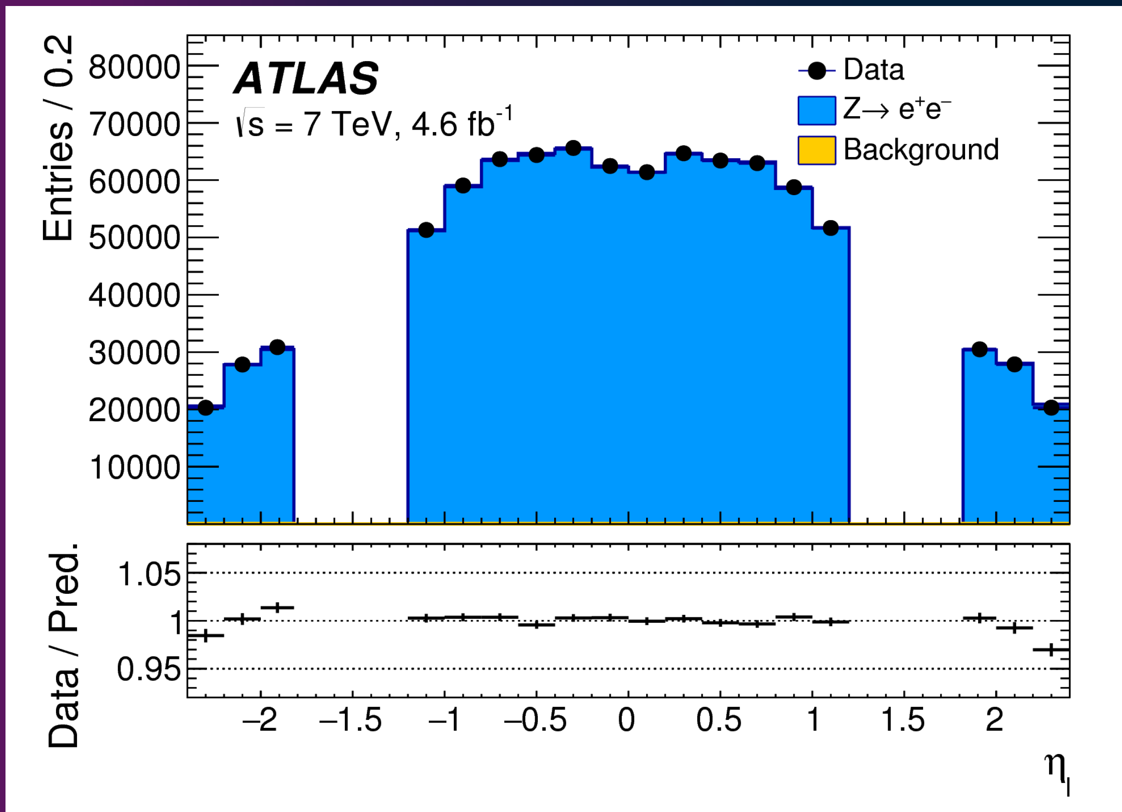

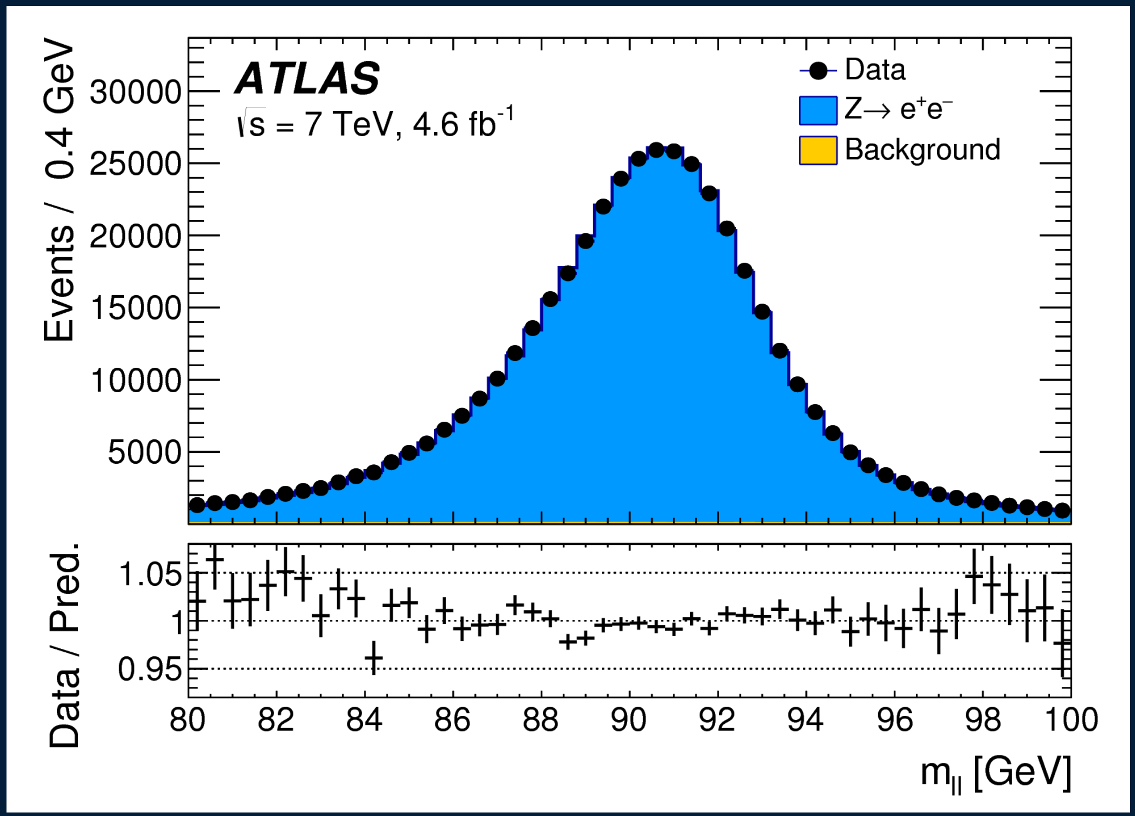

- ϕ modulation due to mechanical deformation under gravity of the calorimeter ('pear-shape') corrected with W and Z events

$\|\eta_\ell\|$ range	[0.0, 0.6]		[0.6, 1.2]		[1.82, 2.4]		Combined	
Kinematic distribution	p_T^ℓ	m_T	p_T^ℓ	m_T	p_T^ℓ	m_T	p_T^ℓ	m_T
δm_W [MeV]								
Energy scale	10.4	10.3	10.8	10.1	16.1	17.1	8.1	8.0
Energy resolution	5.0	6.0	7.3	6.7	10.4	15.5	3.5	5.5
Energy linearity	2.2	4.2	5.8	8.9	8.6	10.6	3.4	5.5
Energy tails	2.3	3.3	2.3	3.3	2.3	3.3	2.3	3.3
Reconstruction efficiency	10.5	8.8	9.9	7.8	14.5	11.0	7.2	6.0
Identification efficiency	10.4	7.7	11.7	8.8	16.7	12.1	7.3	5.6
Trigger and isolation efficiencies	0.2	0.5	0.3	0.5	2.0	2.2	0.8	0.9
Charge mismeasurement	0.2	0.2	0.2	0.2	1.5	1.5	0.1	0.1
Total	19.0	17.5	21.1	19.4	30.7	30.5	14.2	14.3

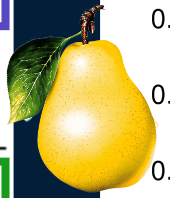

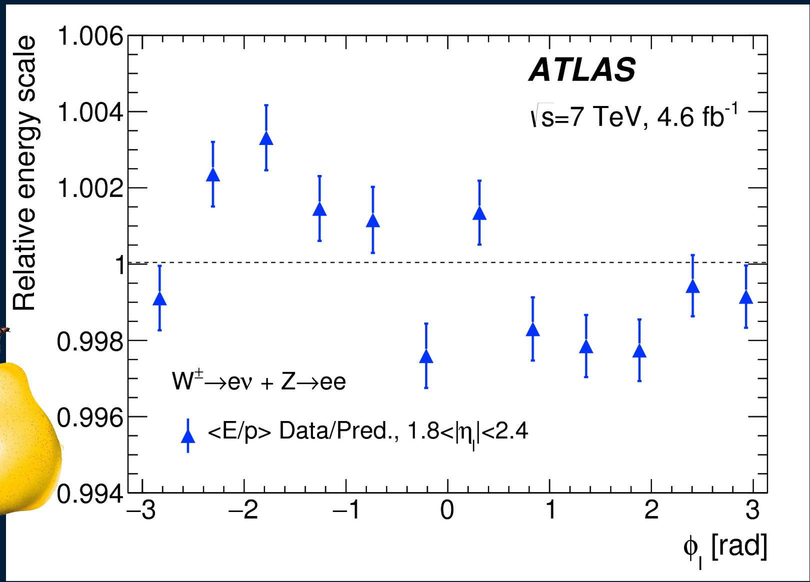

Muon calibration

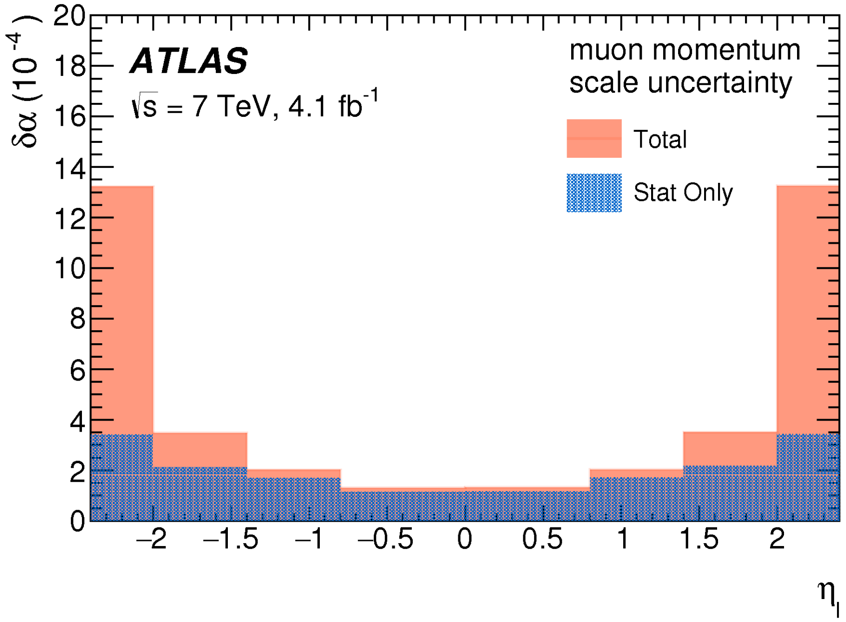

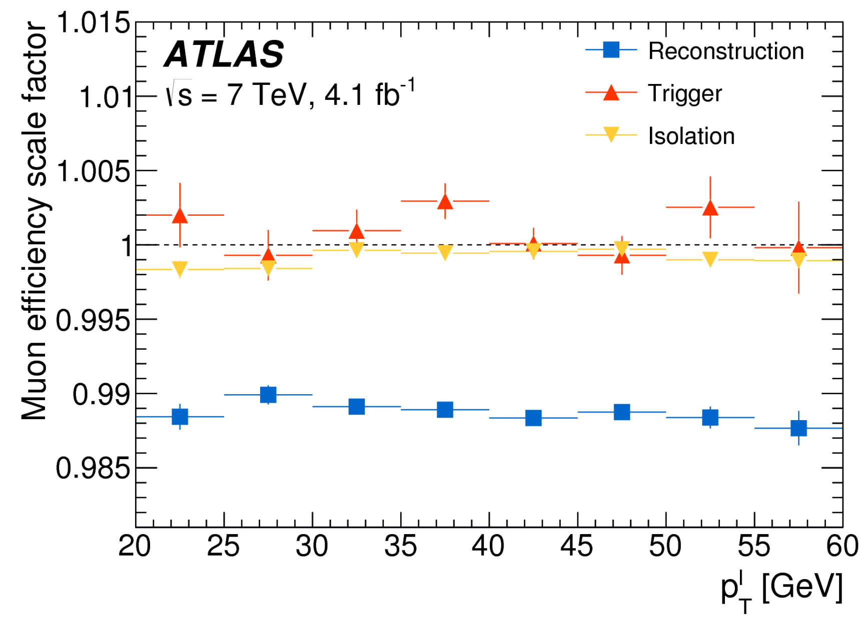

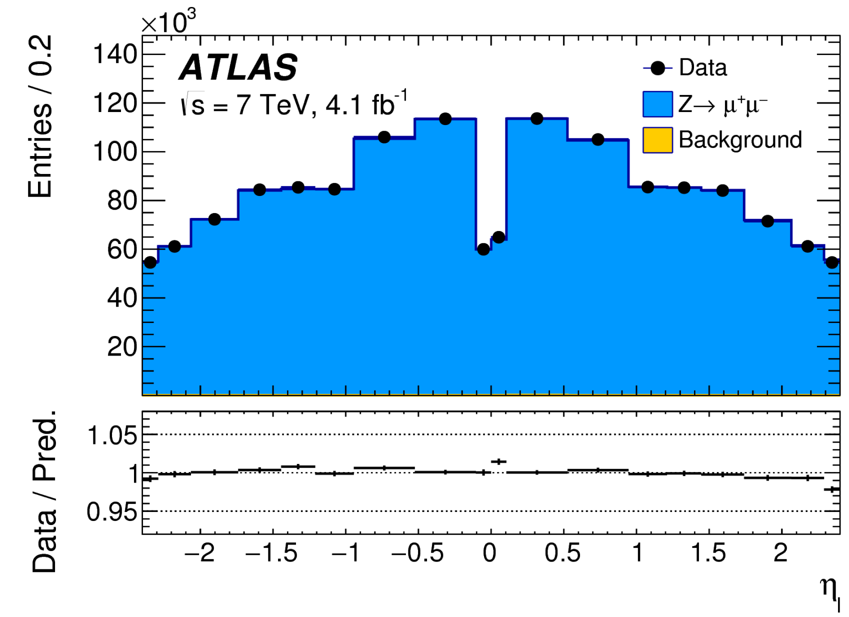

$\lvert\eta_\ell\rvert$ range	[0.0, 0.8]		[0.8, 1.4]		[1.4, 2.0]		[2.0, 2.4]		Combined	
Kinematic distribution	p_T^ℓ	m_T	p_T^ℓ	m_T	p_T^ℓ	m_T	p_T^ℓ	m_T	p_T^ℓ	m_T
δm_W [MeV]										
Momentum scale	8.9	9.3	14.2	15.6	27.4	29.2	111.0	115.4	8.4	8.8
Momentum resolution	1.8	2.0	1.9	1.7	1.5	2.2	3.4	3.8	1.0	1.2
Sagitta bias	0.7	0.8	1.7	1.7	3.1	3.1	4.5	4.3	0.6	0.6
Reconstruction and isolation efficiencies	4.0	3.6	5.1	3.7	4.7	3.5	6.4	5.5	2.7	2.2
Trigger efficiency	5.6	5.0	7.1	5.0	11.8	9.1	12.1	9.9	4.1	3.2
Total	11.4	11.4	16.9	17.0	30.4	31.0	112.0	116.1	9.8	9.7

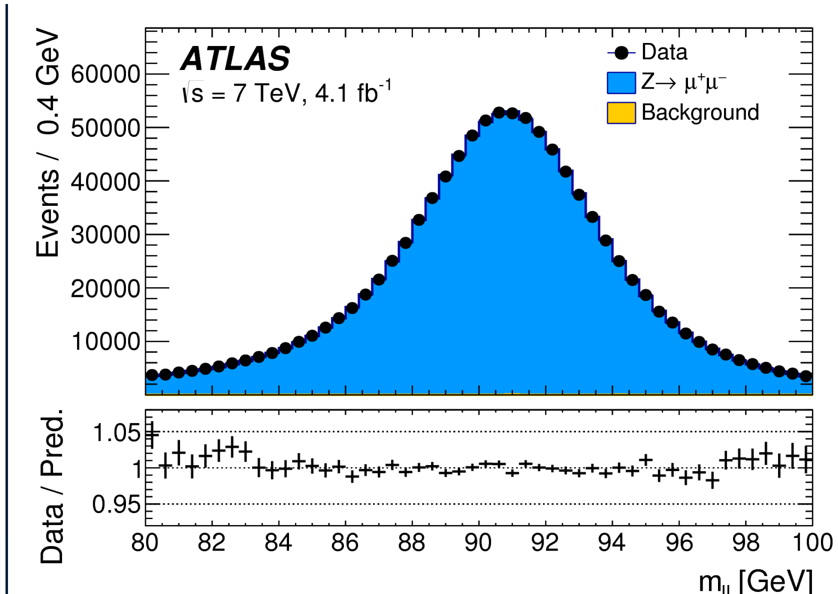

- As expected, uncertainties are smaller than for electron

Hadronic recoil calibration

- Several steps of the correction :
  - Correct pile-up activity
  - Correct ΣE_T distribution in p_T bins
  - residual response and resolution corrections in Z events, extrapolated to W
    - Includes a correction of recoil phi

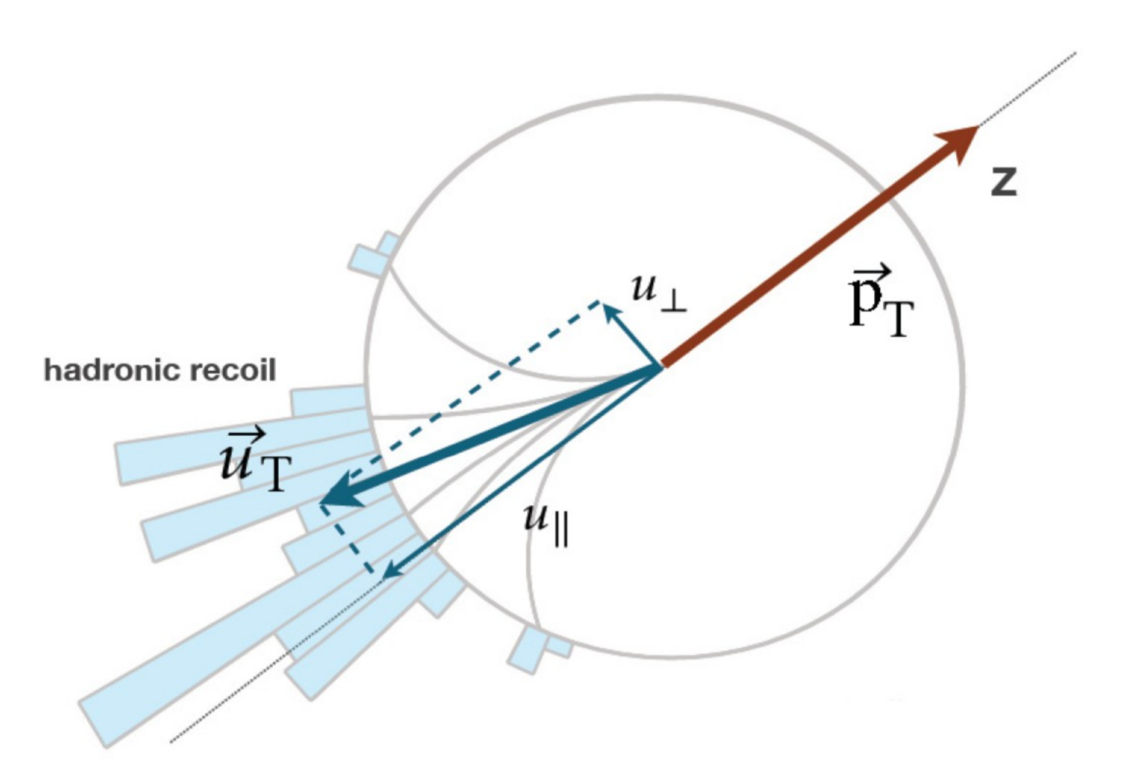

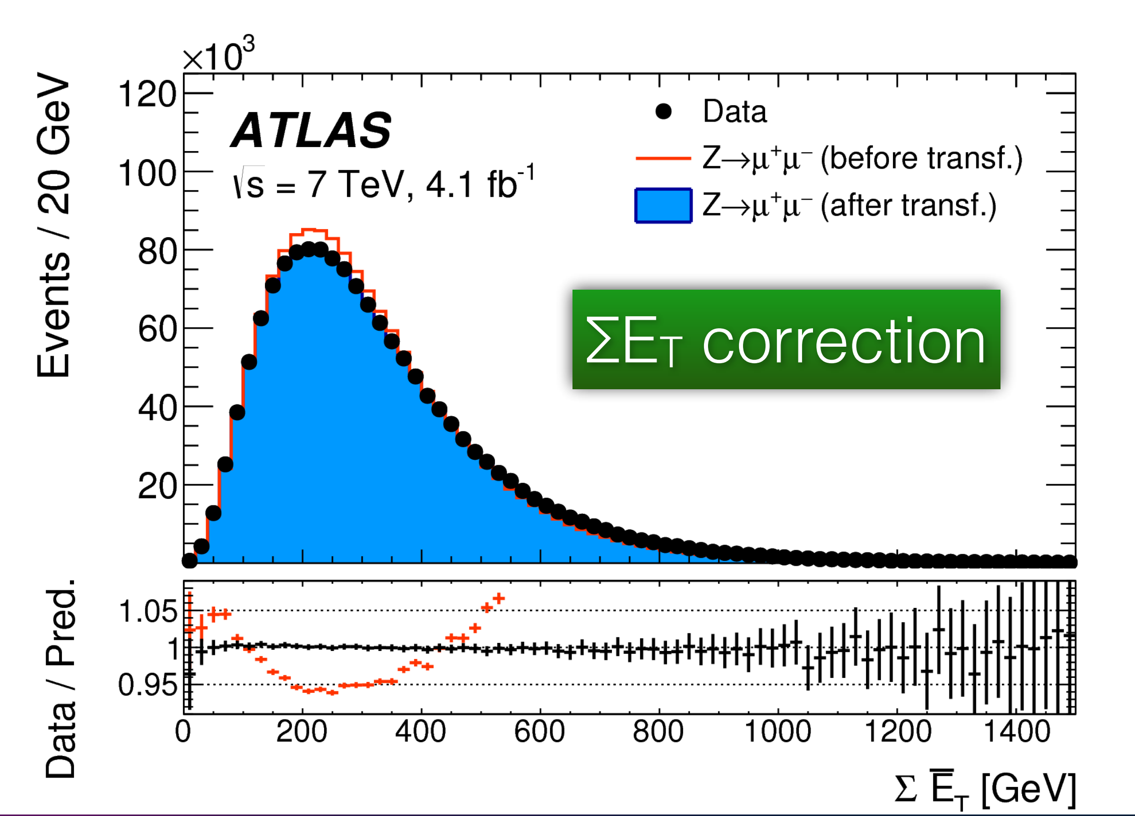

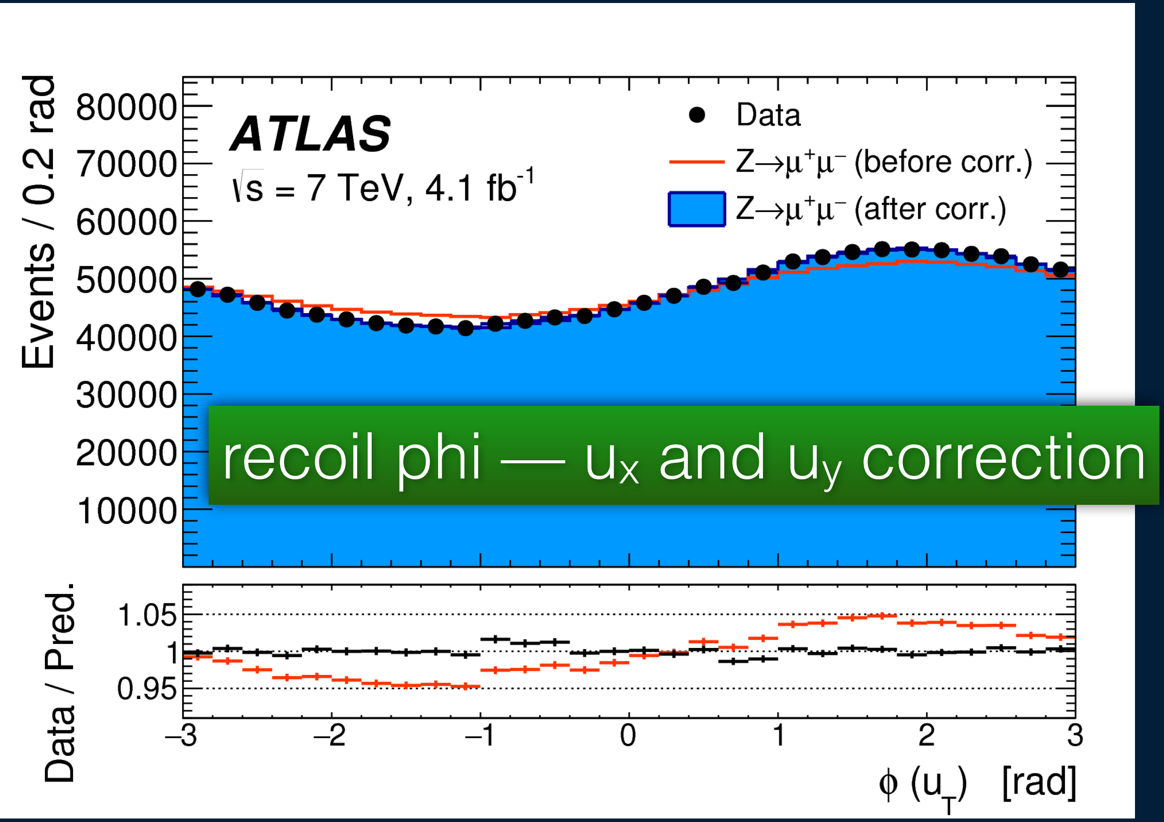

Hadronic recoil calibration

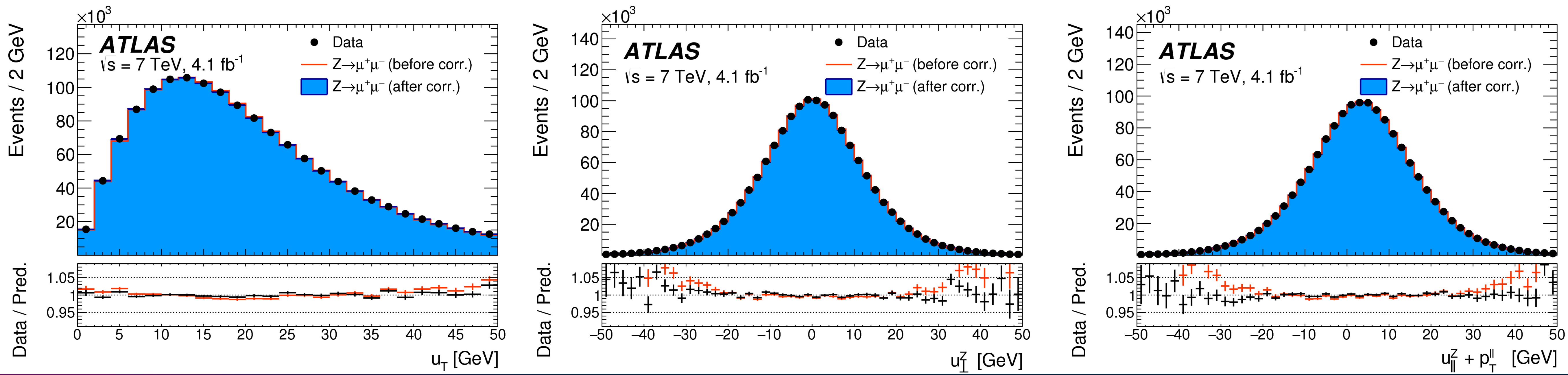

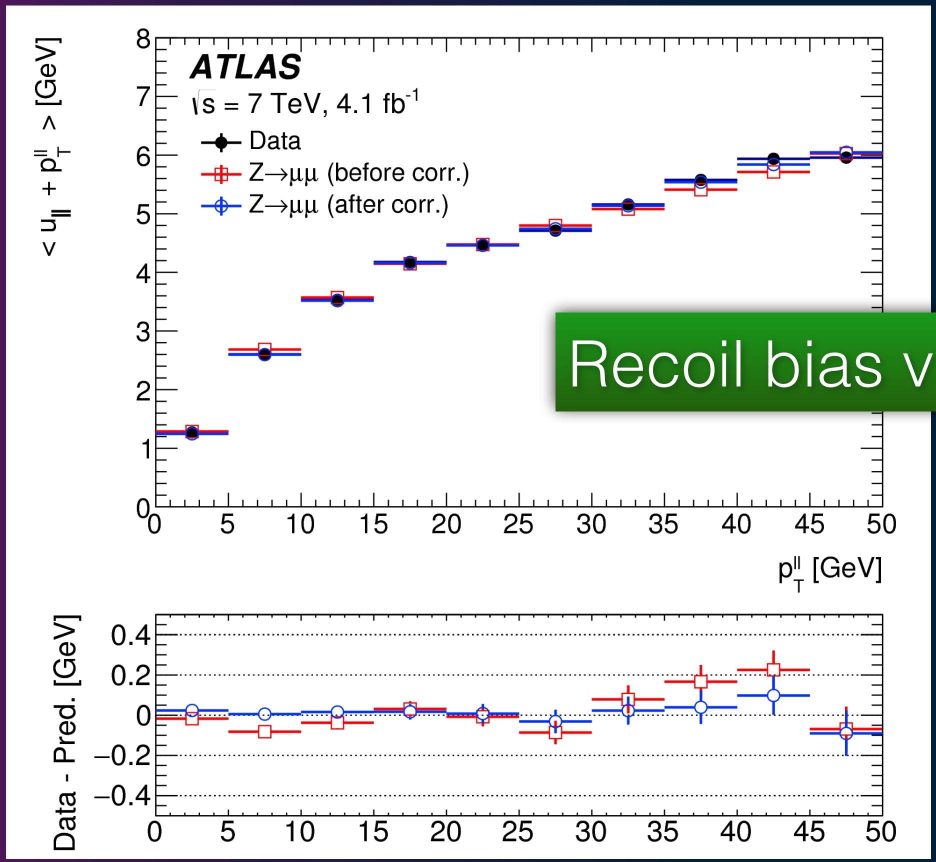

Recoil bias vs p_T^Z

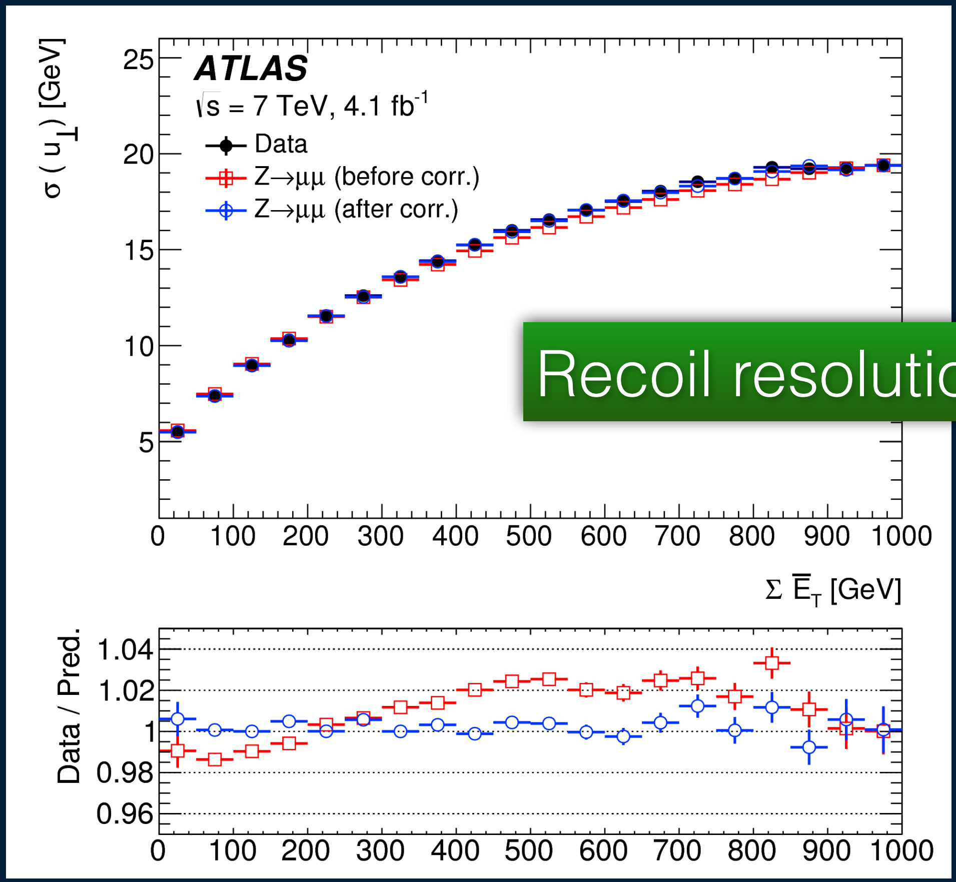

Recoil resolution vs ΣE_T

Hadronic recoil calibration

- Validation check using Powheg+Herwig6 as pseudo-data

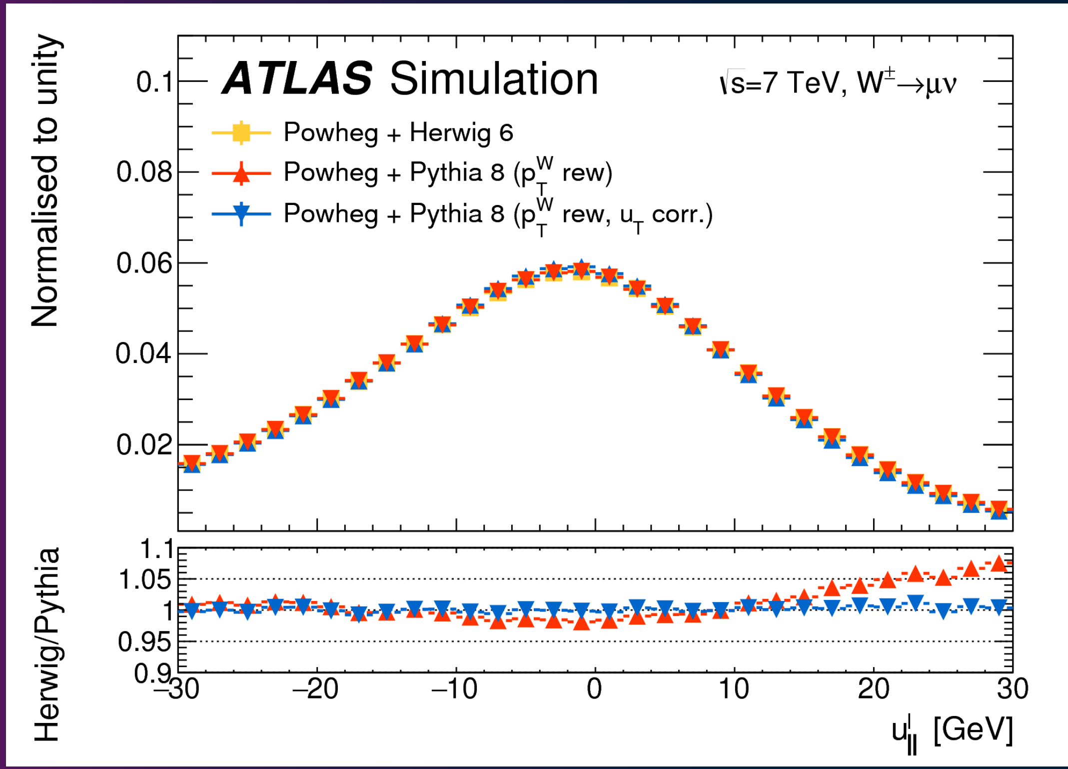

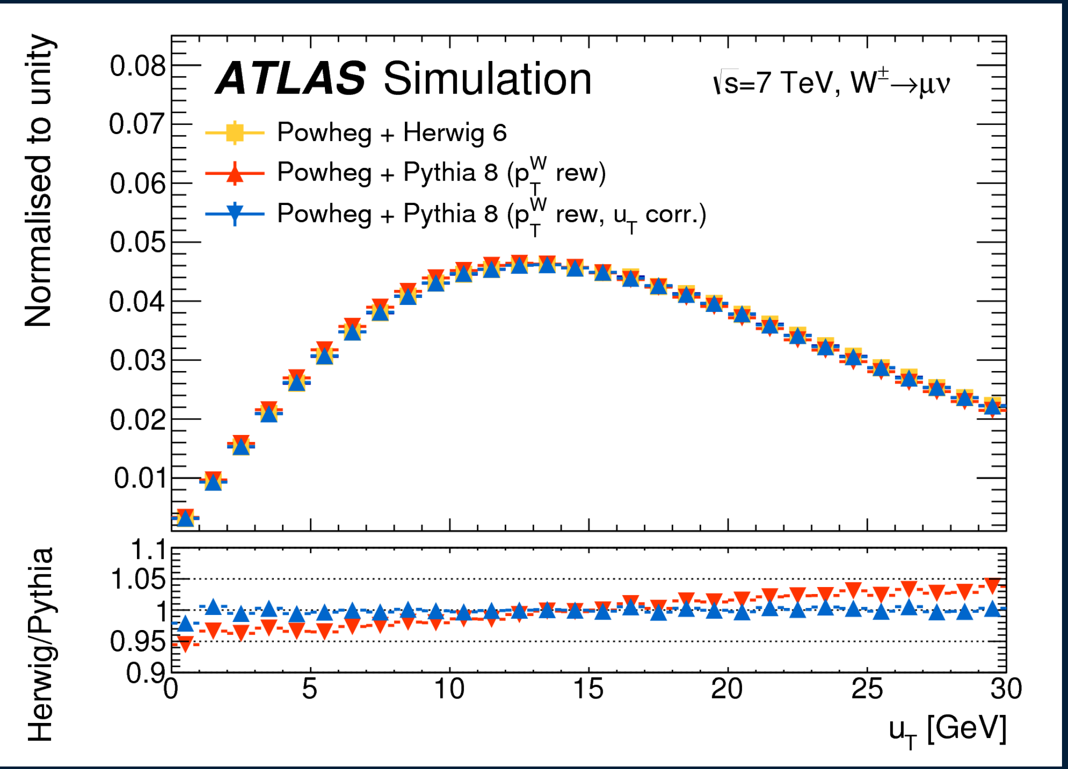

W-boson charge	W^+		W^-		Combined	
Kinematic distribution	p_T^ℓ	m_T	p_T^ℓ	m_T	p_T^ℓ	m_T
δm_W [MeV]						
$\langle\mu\rangle$ scale factor	0.2	1.0	0.2	1.0	0.2	1.0
$\Sigma \bar{E}_T$ correction	0.9	12.2	1.1	10.2	1.0	11.2
Residual corrections (statistics)	2.0	2.7	2.0	2.7	2.0	2.7
Residual corrections (interpolation)	1.4	3.1	1.4	3.1	1.4	3.1
Residual corrections ($Z \to W$ extrapolation)	0.2	5.8	0.2	4.3	0.2	5.1
Total	2.6	14.2	2.7	11.8	2.6	13.0

Multijet background

- Use of a data-driven technique :
  - 2 different fitting regions to extract multijet fraction (FR1, FR2) — mainly for uncertainty purposes
    - Templates obtained in an MJ enriched region by reverting isolation
      - EW and top contamination subtracted with MC estimation
    - Scan in lepton isolation variable for MJ shape template building
  - 3 different observables : m_T, $p_{T\ell}/m_T$, p_T^{miss}
  - Fitted fraction corrected for signal region selection efficiency
  - linear extrapolation to signal region

Cuts	Lepton isolation		E_T^{miss}	m_T^W	p_T^W
Selection	SR sample	CR sample			
Signal region			$E_T^{miss} > 30\text{GeV}$	$m_T^W > 60\text{GeV}$	$p_T^W < 30\text{GeV}$
FR1	$Iso < 0.1$	$0.2 < Iso < 0.4$	-	-	$p_T^W < 30\text{GeV}$
FR2			-	-	-

Multijet background

- Differences in the extrapolation to signal region are taken as (main) fraction uncertainty
- Shapes of observables obtained by an linear extrapolation from CR to SR using the ratio of different anti-isolated regions
  - Uncertainty dominated by statistics, evaluated by fluctuating the bin contents within stat. uncertainty before extrapolation

- Background fraction (η-dependent)
  - 0.6 - 1.7 % (e channel)
  - 0.5 - 0.7 % (mu channel)

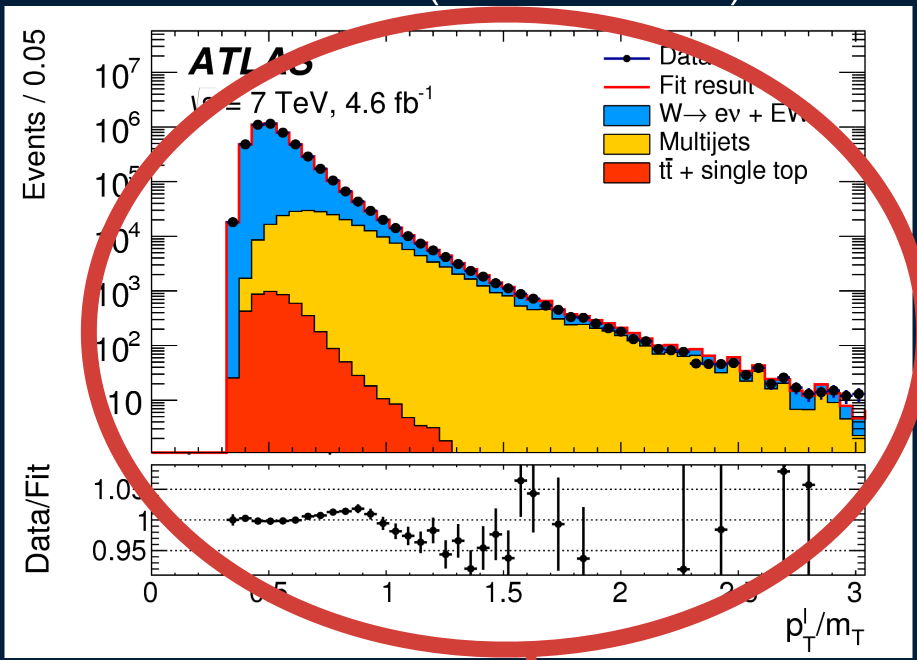

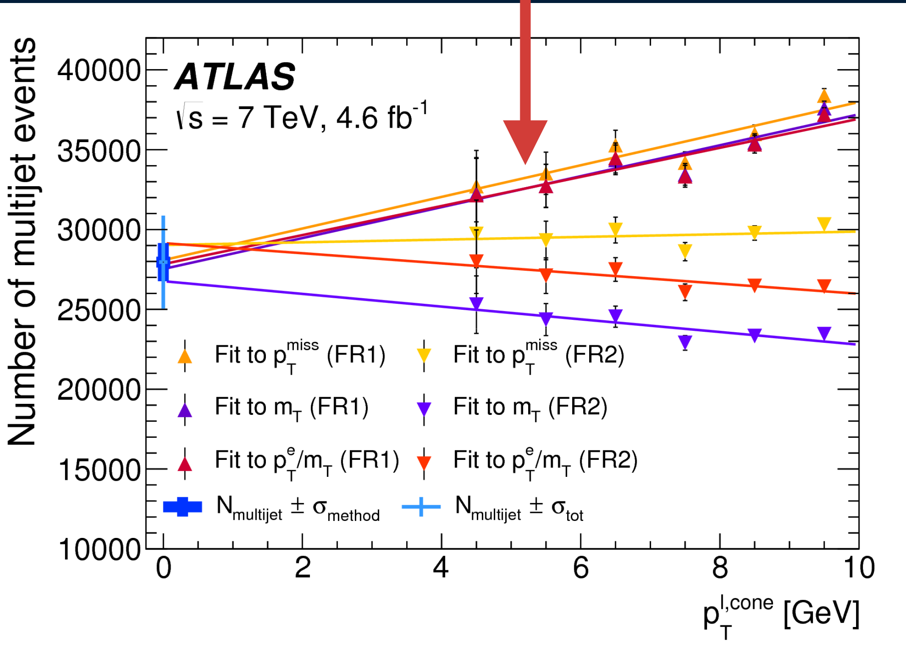

Kinematic distribution	p_T^ℓ				m_T			
Decay channel	$W \to e\nu$		$W \to \mu\nu$		$W \to e\nu$		$W \to \mu\nu$	
W-boson charge	W^+	W^-	W^+	W^-	W^+	W^-	W^+	W^-
δm_W [MeV]								
$W \to \tau\nu$ (fraction, shape)	0.1	0.1	0.1	0.2	0.1	0.2	0.1	0.3
$Z \to ee$ (fraction, shape)	3.3	4.8	–	–	4.3	6.4	–	–
$Z \to \mu\mu$ (fraction, shape)	–	–	3.5	4.5	–	–	4.3	5.2
$Z \to \tau\tau$ (fraction, shape)	0.1	0.1	0.1	0.2	0.1	0.2	0.1	0.3
WW, WZ, ZZ (fraction)	0.1	0.1	0.1	0.1	0.4	0.4	0.3	0.4
Top (fraction)	0.1	0.1	0.1	0.1	0.3	0.3	0.3	0.3
Multijet (fraction)	3.2	3.6	1.8	2.4	8.1	8.6	3.7	4.6
Multijet (shape)	3.8	3.1	1.6	1.5	8.6	8.0	2.5	2.4
Total	6.0	6.8	4.3	5.3	12.6	13.4	6.2	7.4

Extraction of m_W

Preliminary cross-check with Z

- Several cross-checks :
  - $\chi 2$ template fit to the reconstructed m_{ll} distribution : Δm_Z = 1(3) ± 3(5) MeV for the electron (muon) channel
  - Treat alternatively the negative or positive lepton as 'invisible' to mimic a neutrino,
    - fit to $p_{T\ell}$ and m_T distributions as in W analysis
- Results consistent with combined LEP value of m_Z within experimental uncertainties

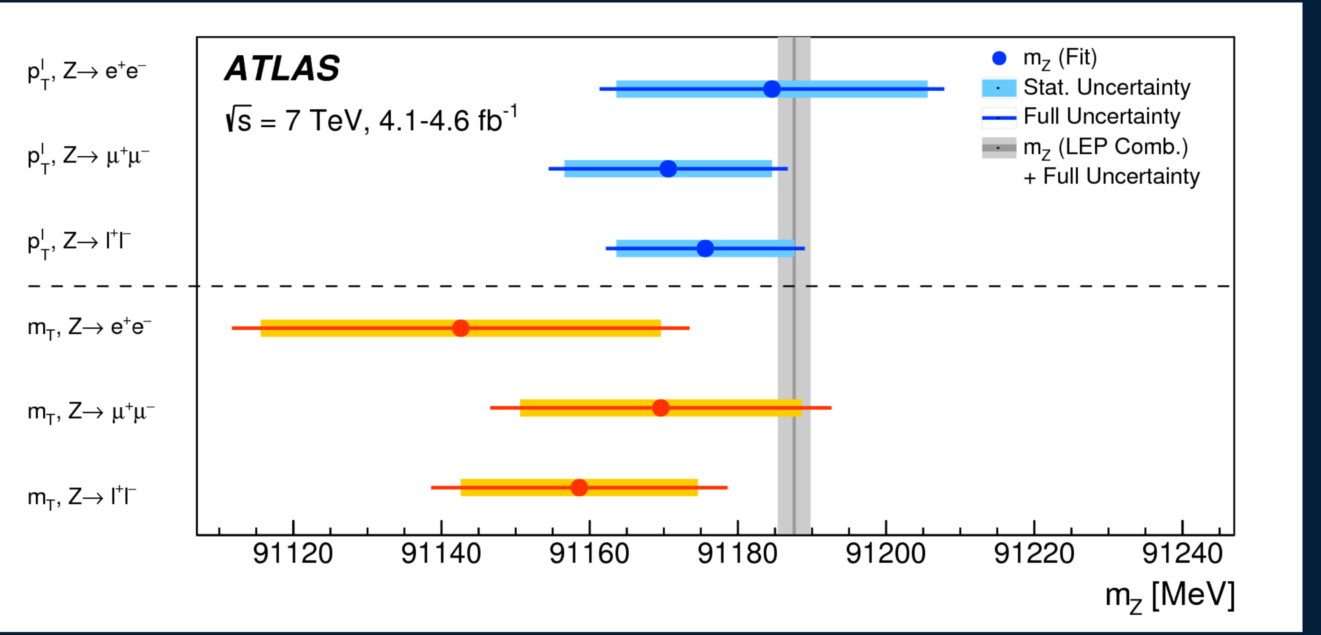

Lepton charge	ℓ^+		ℓ^-		Combined	
Distribution	p_T^ℓ	m_T	p_T^ℓ	m_T	p_T^ℓ	m_T
Δm_Z [MeV]						
$Z \to ee$	$13 \pm 31 \pm 10$	$-93 \pm 38 \pm 15$	$-20 \pm 31 \pm 10$	$4 \pm 38 \pm 15$	$-3 \pm 21 \pm 10$	$-45 \pm 27 \pm 15$
$Z \to \mu\mu$	$1 \pm 22 \pm 8$	$-35 \pm 28 \pm 13$	$-36 \pm 22 \pm 8$	$-1 \pm 27 \pm 13$	$-17 \pm 14 \pm 8$	$-18 \pm 19 \pm 13$
Combined	$5 \pm 18 \pm 6$	$-58 \pm 23 \pm 12$	$-31 \pm 18 \pm 6$	$1 \pm 22 \pm 12$	$-12 \pm 12 \pm 6$	$-29 \pm 16 \pm 12$

Difference between measured Z boson mass in ATLAS and the combined LEP result

Z ee plots after all corrections

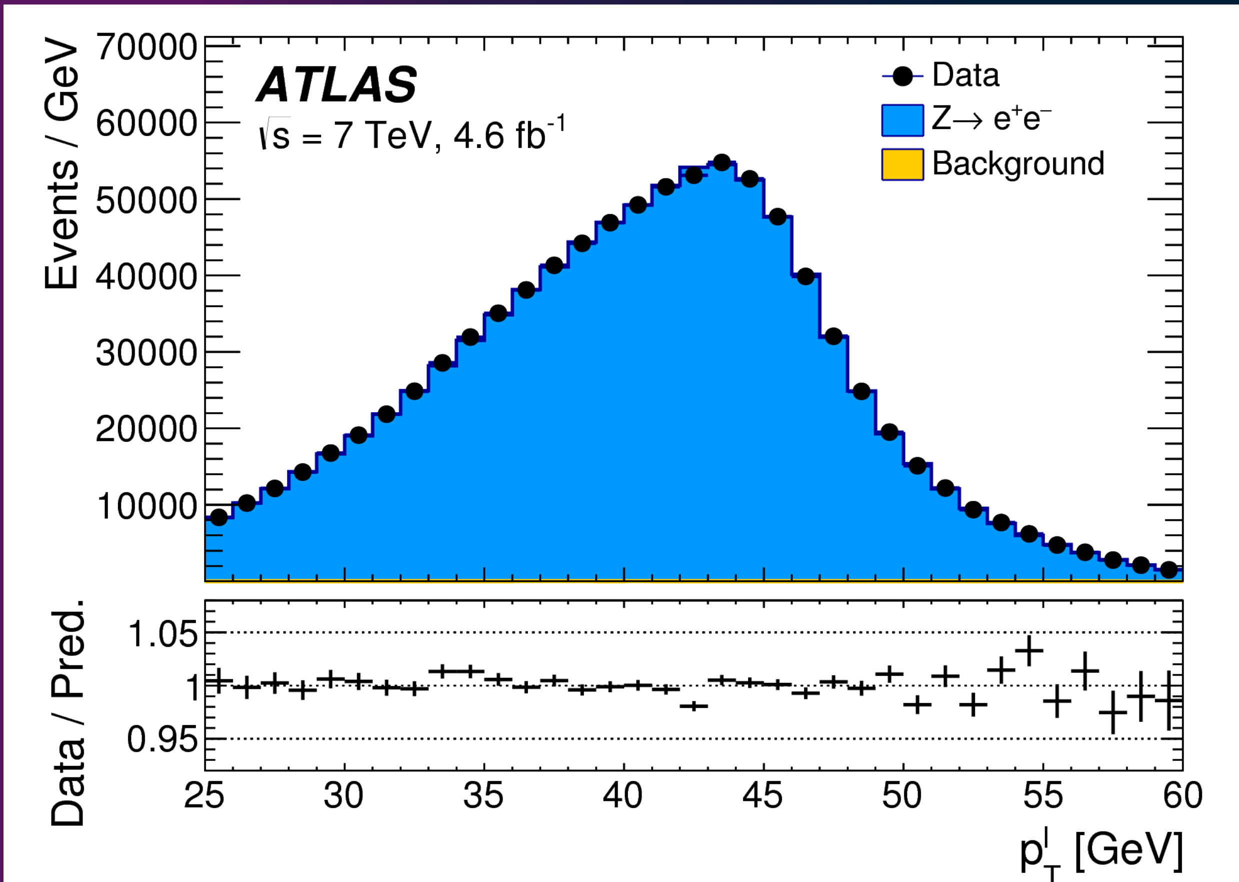

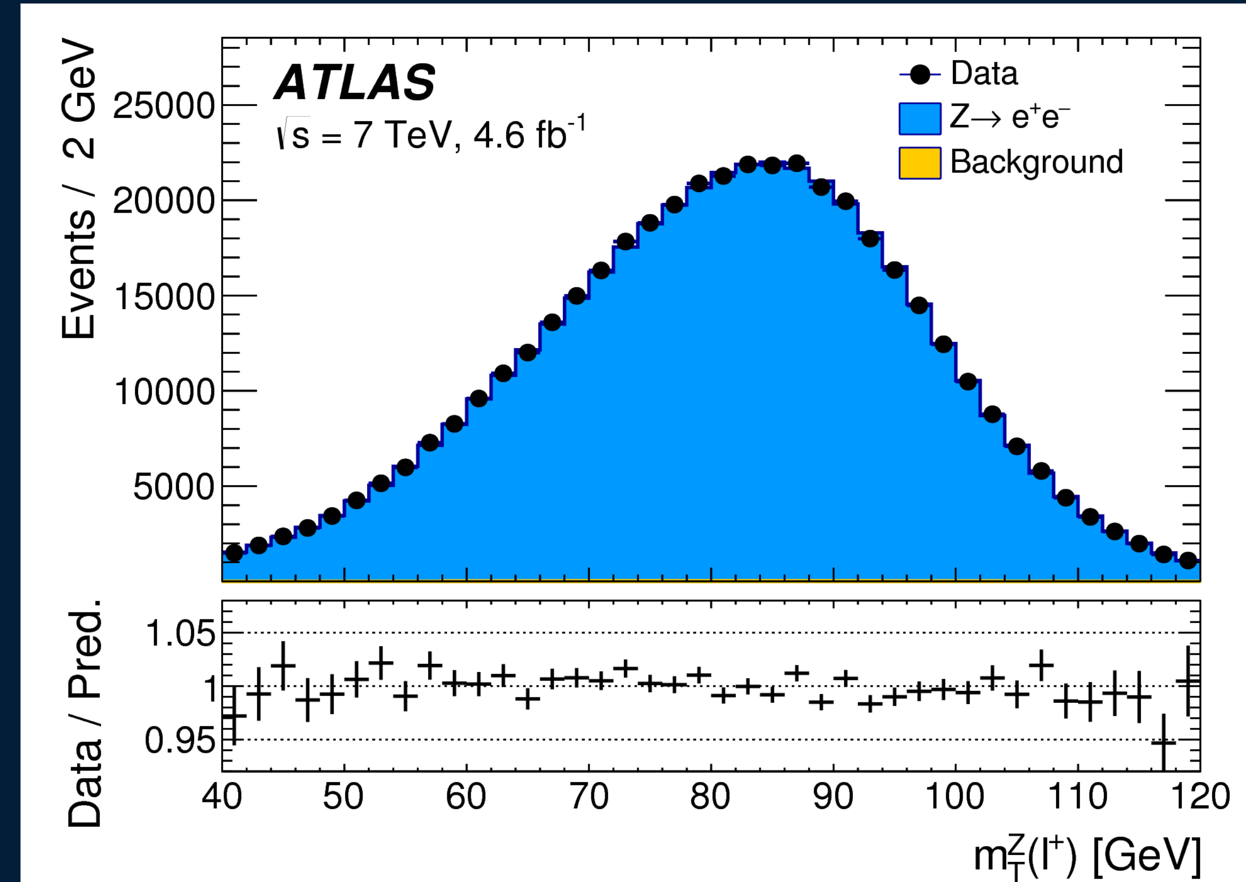

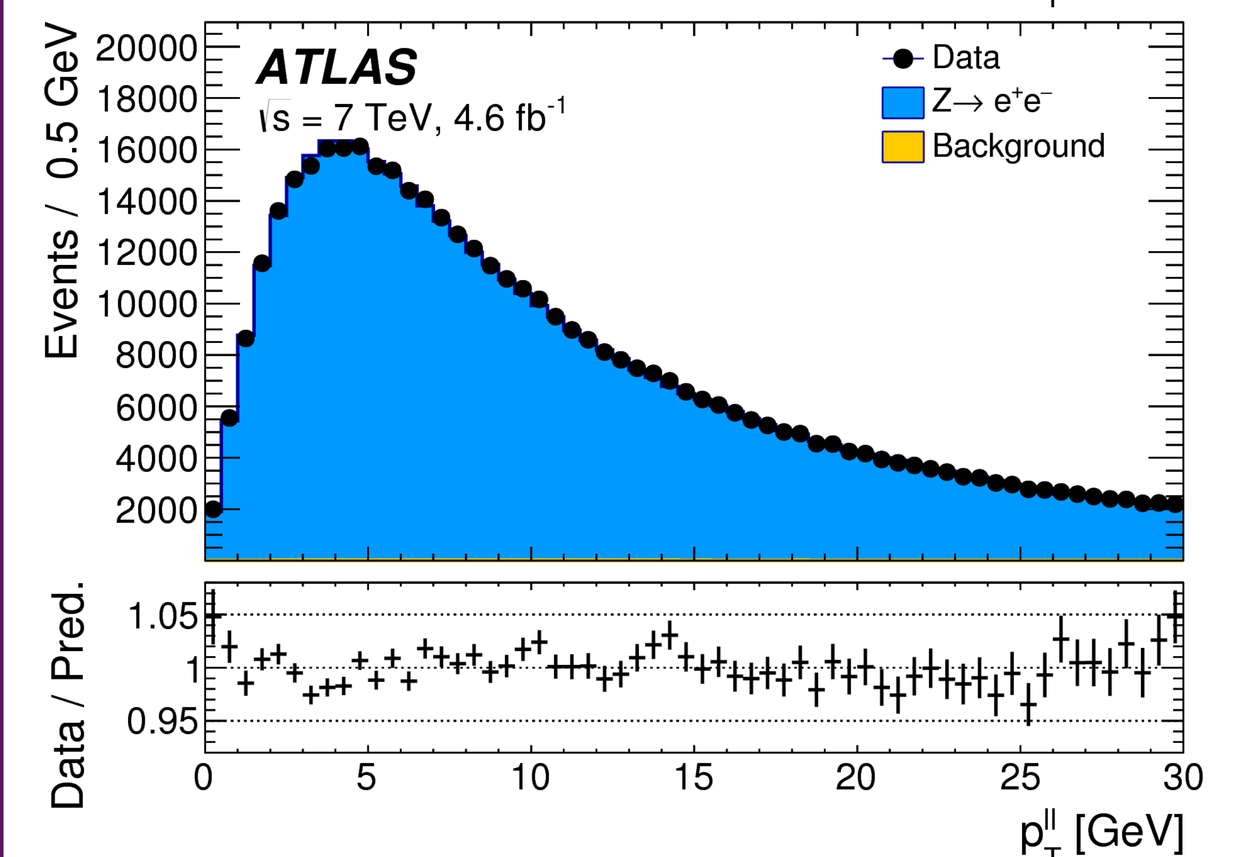

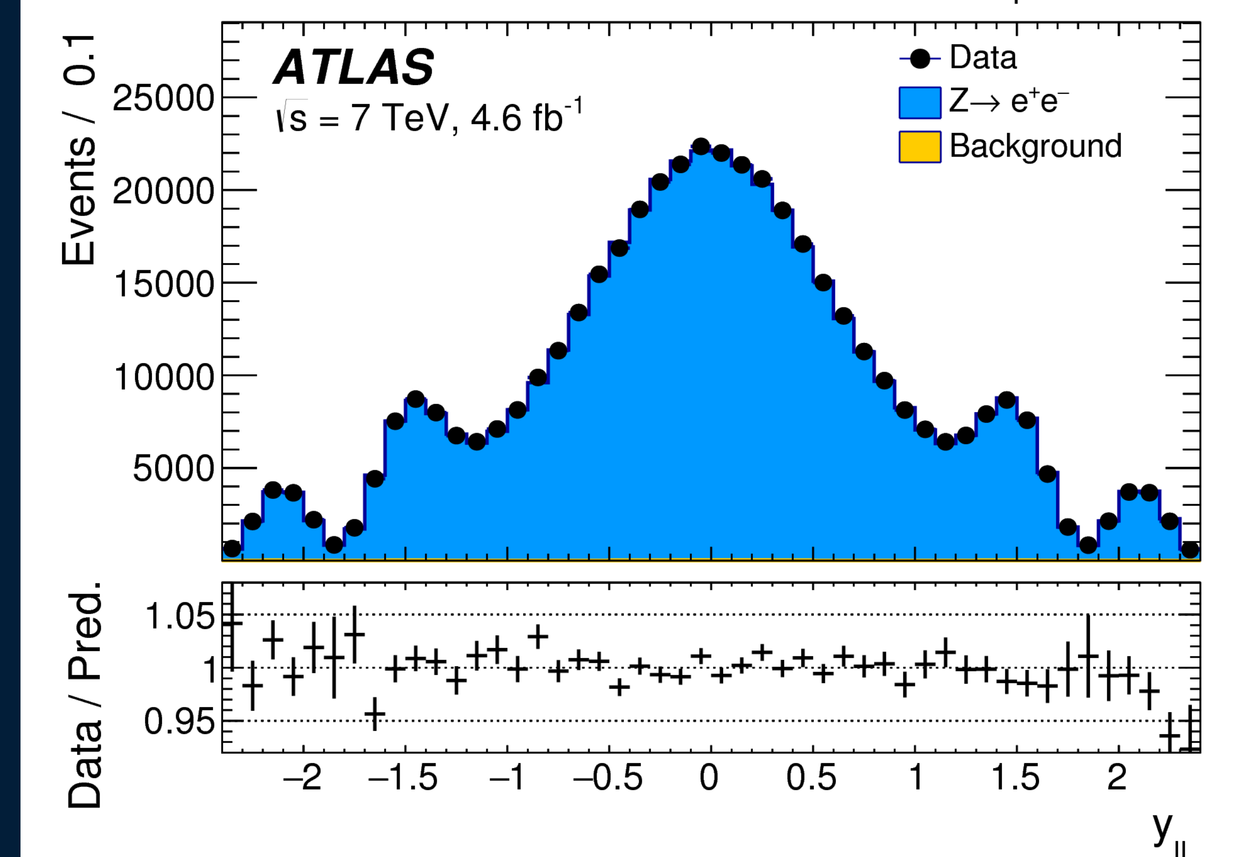

Z mumu plots after all corrections

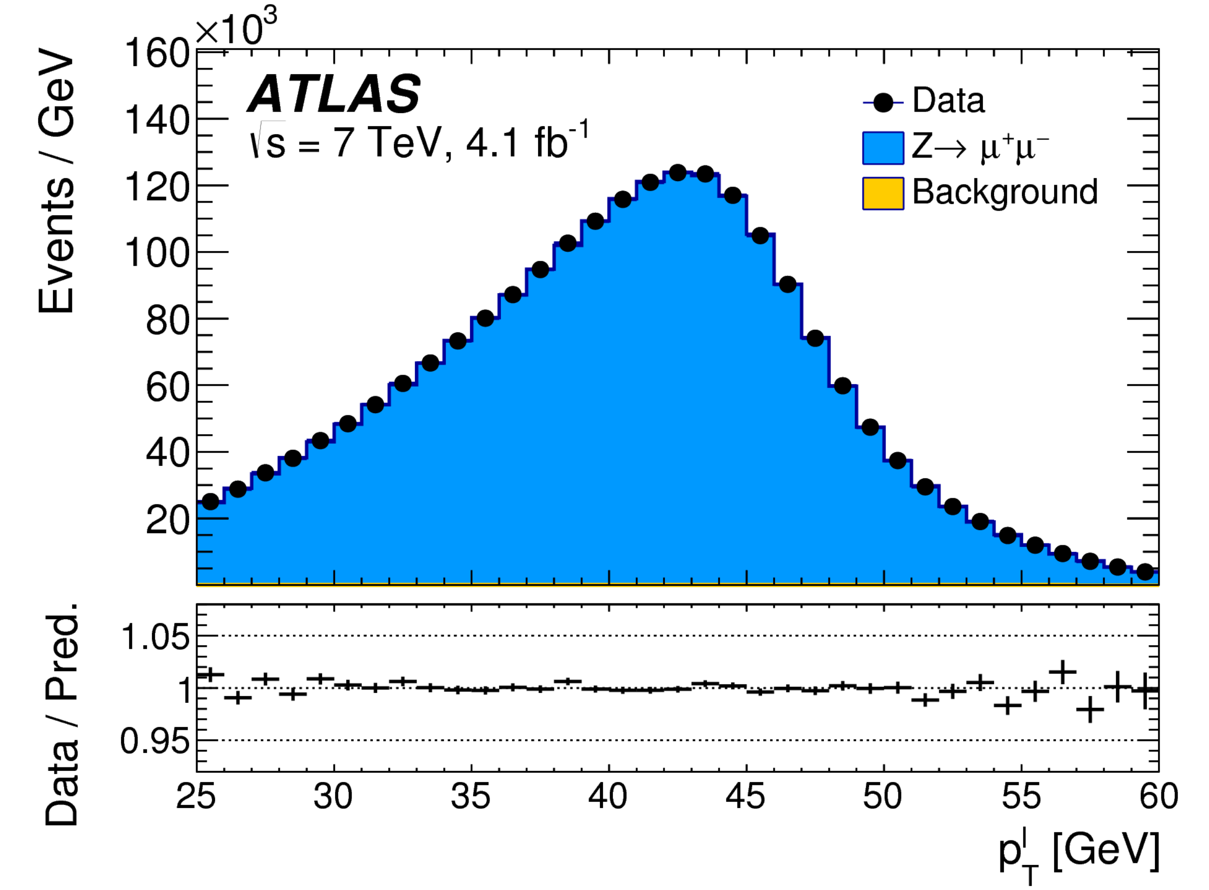

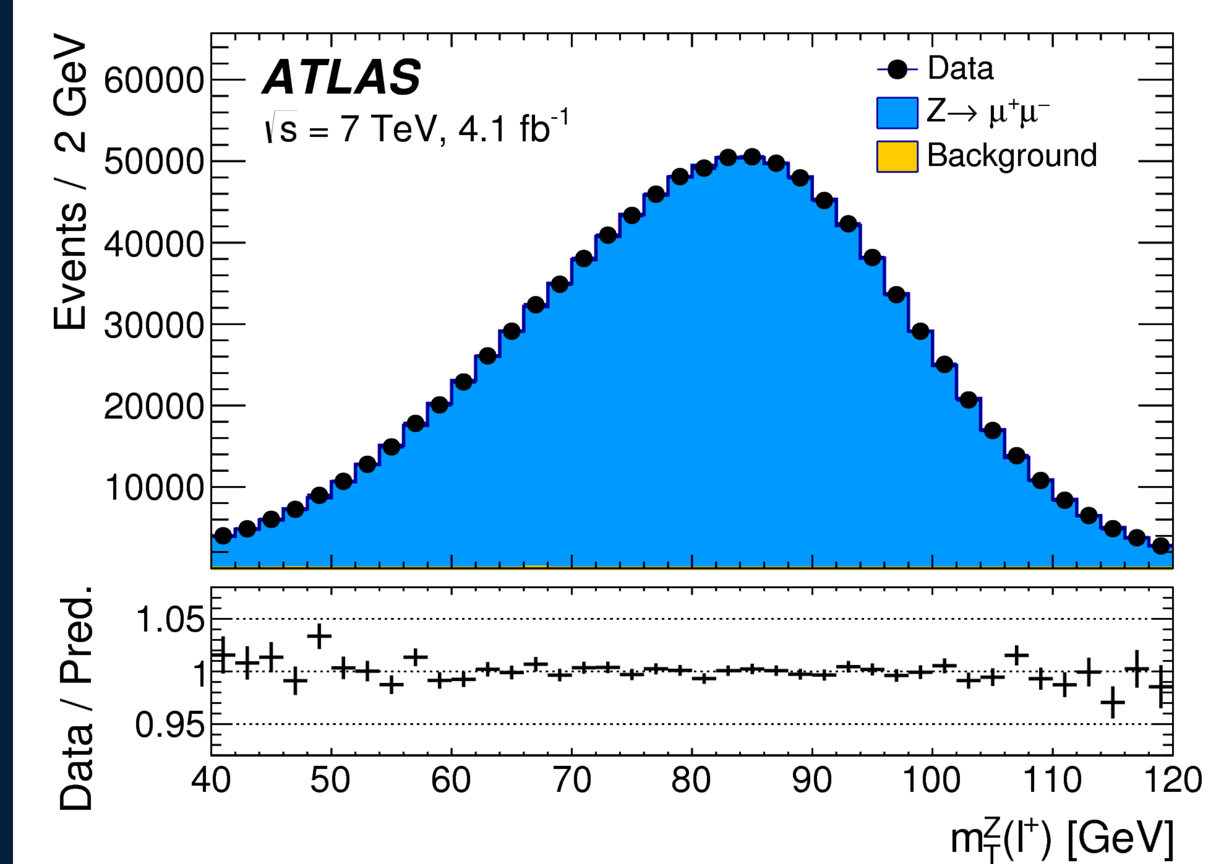

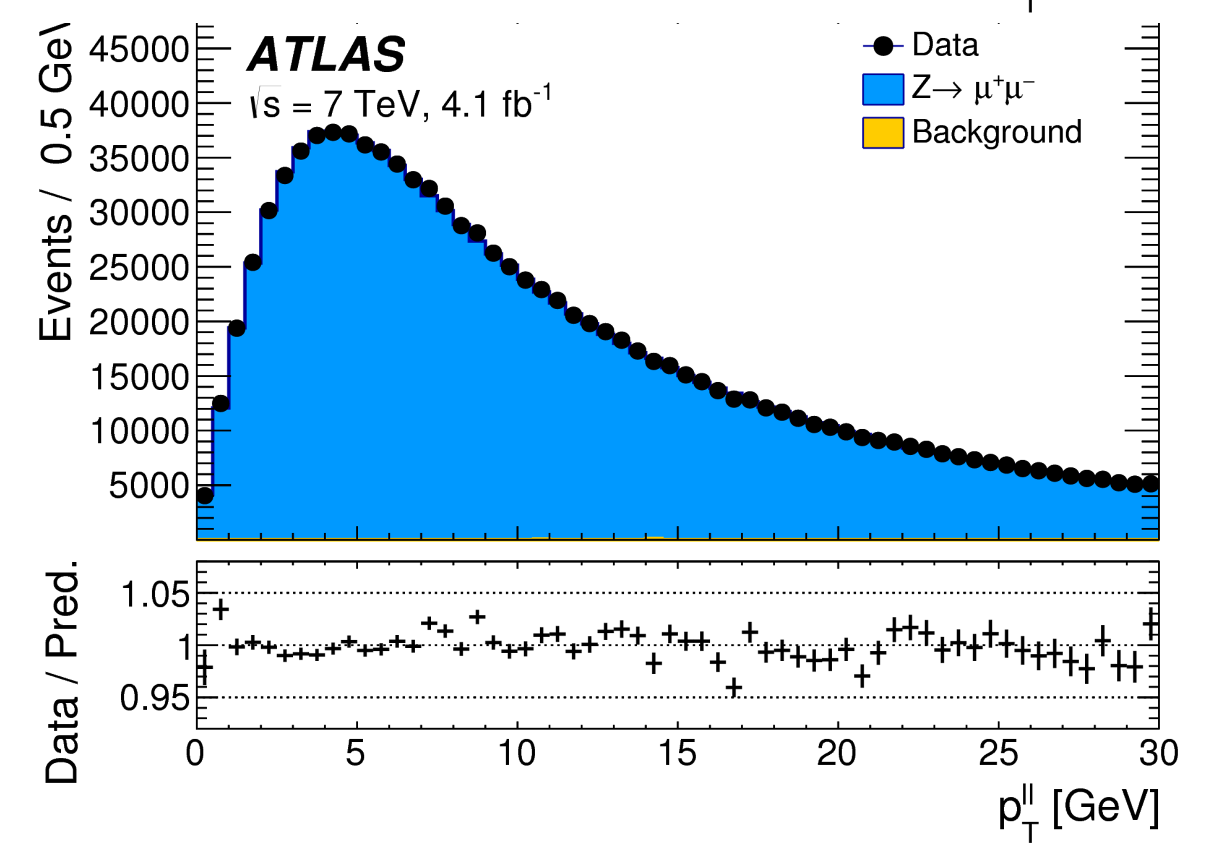

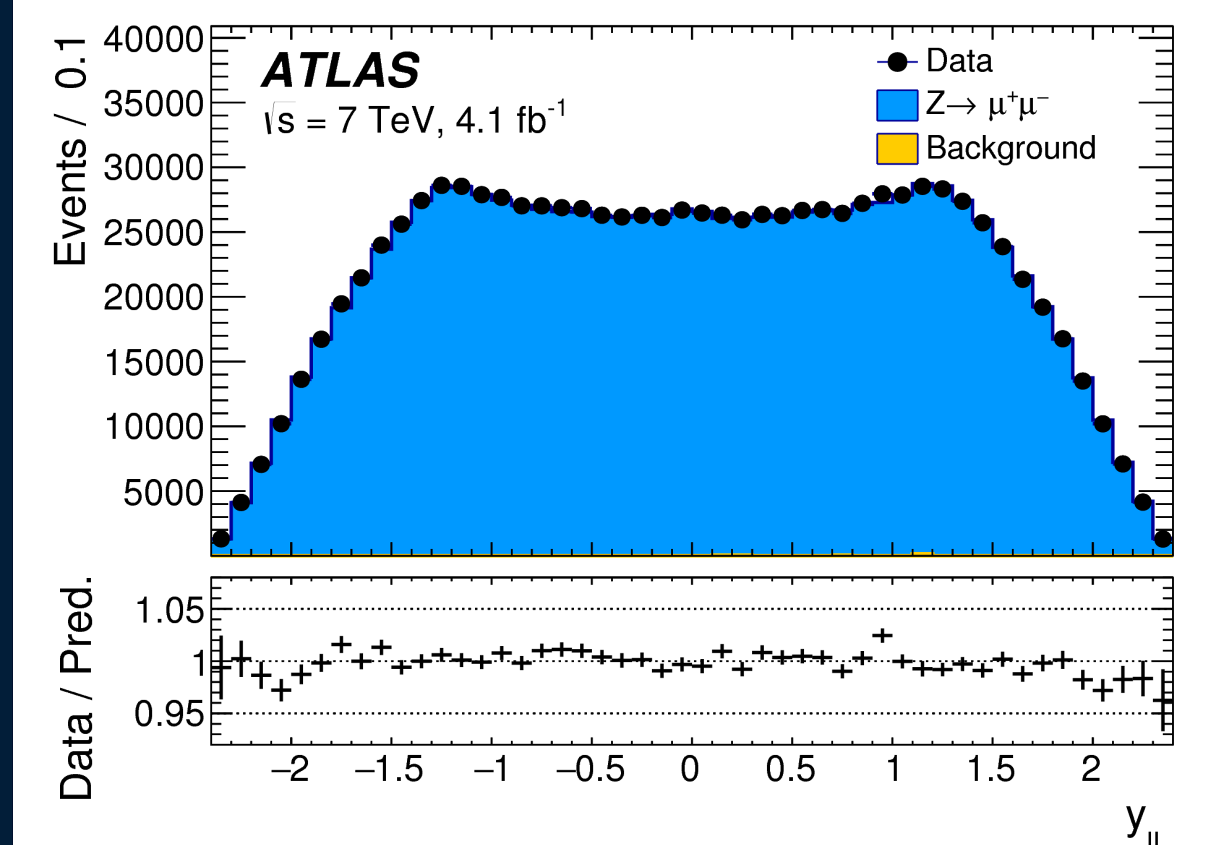

Fitting range stability

- Fitting range of the distributions optimised in the simulation
- Check the stability of the full combination when varying either m_T or $p_{T\ell}$ fitting range
  - Check that the result on the difference with respect to the central value is within ~1-2 standard deviations (fully uncorrelated uncertainty)

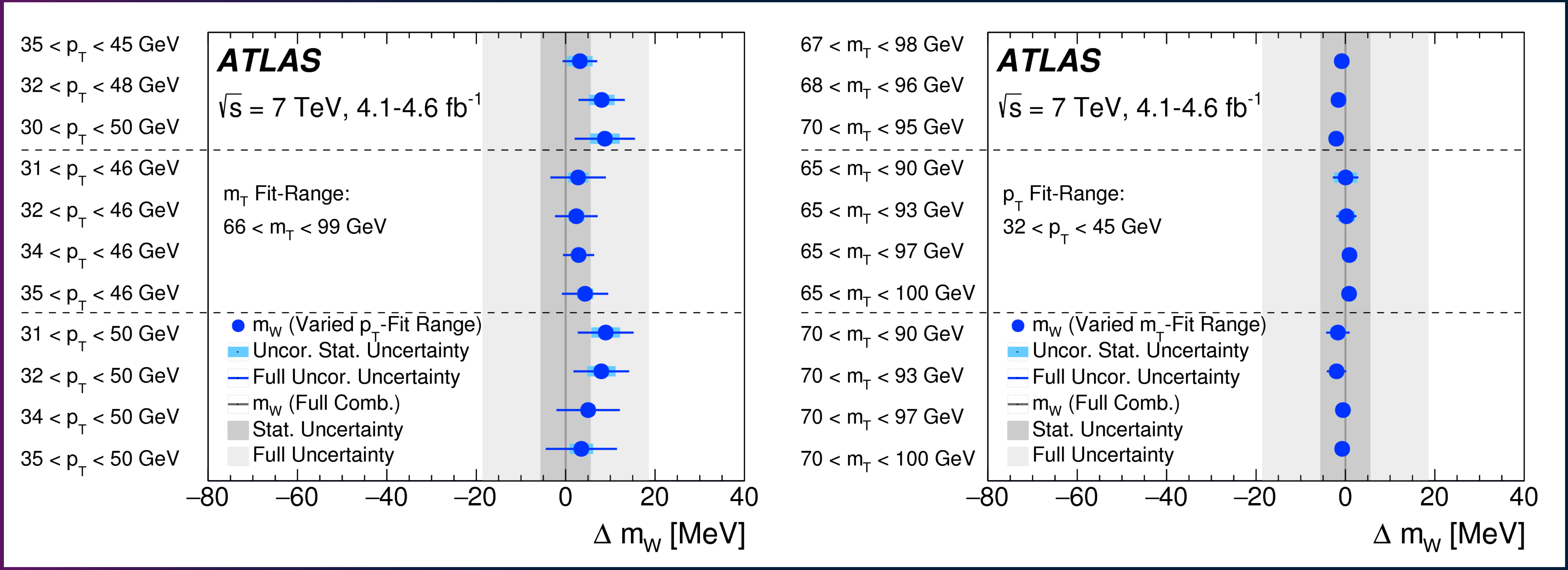

Distributions - hadronic recoil

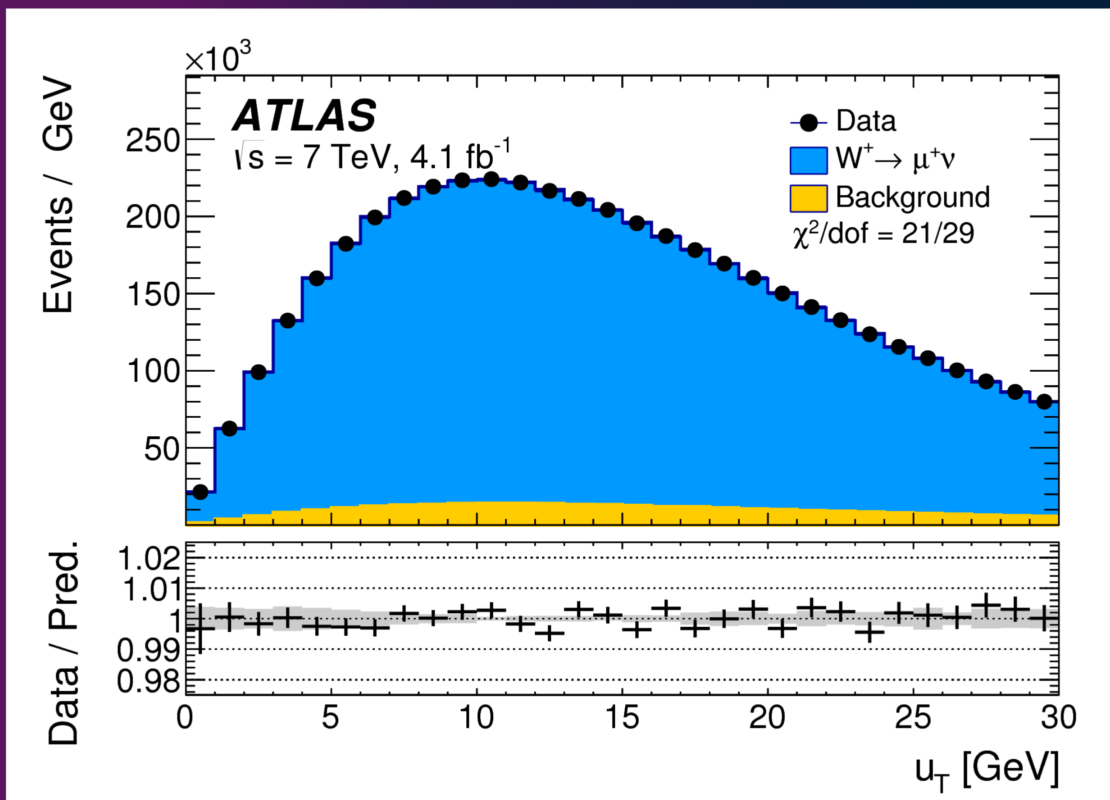

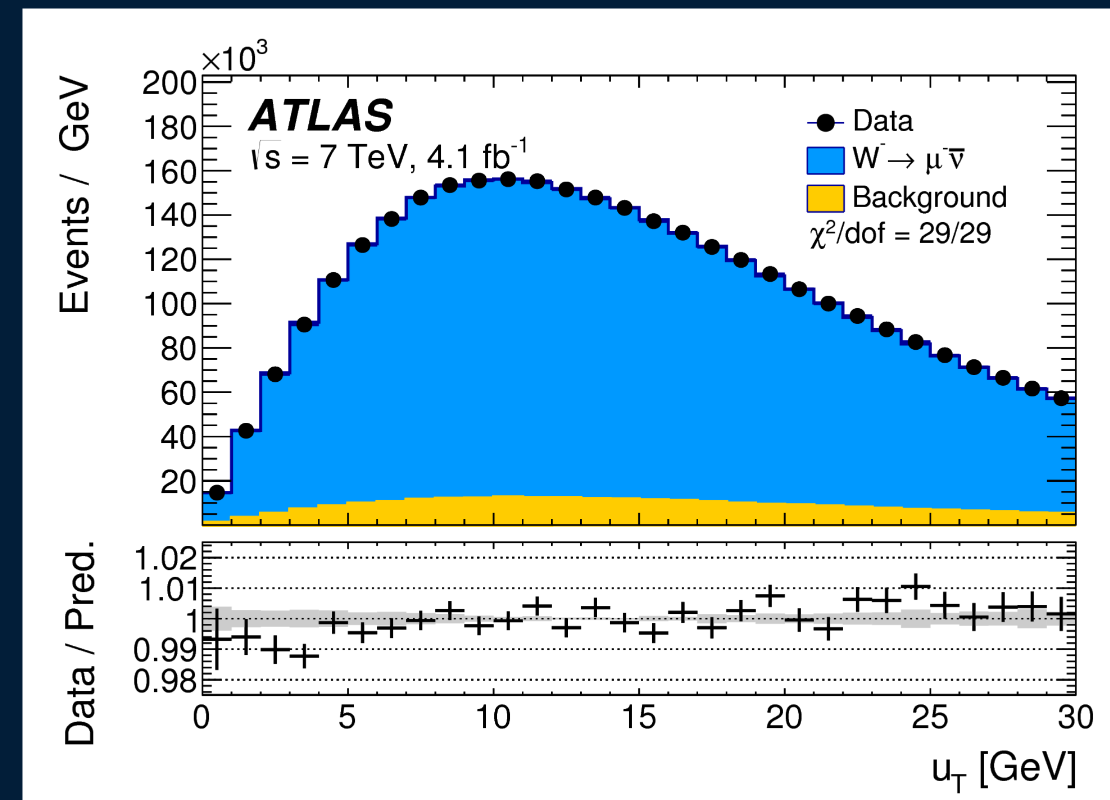

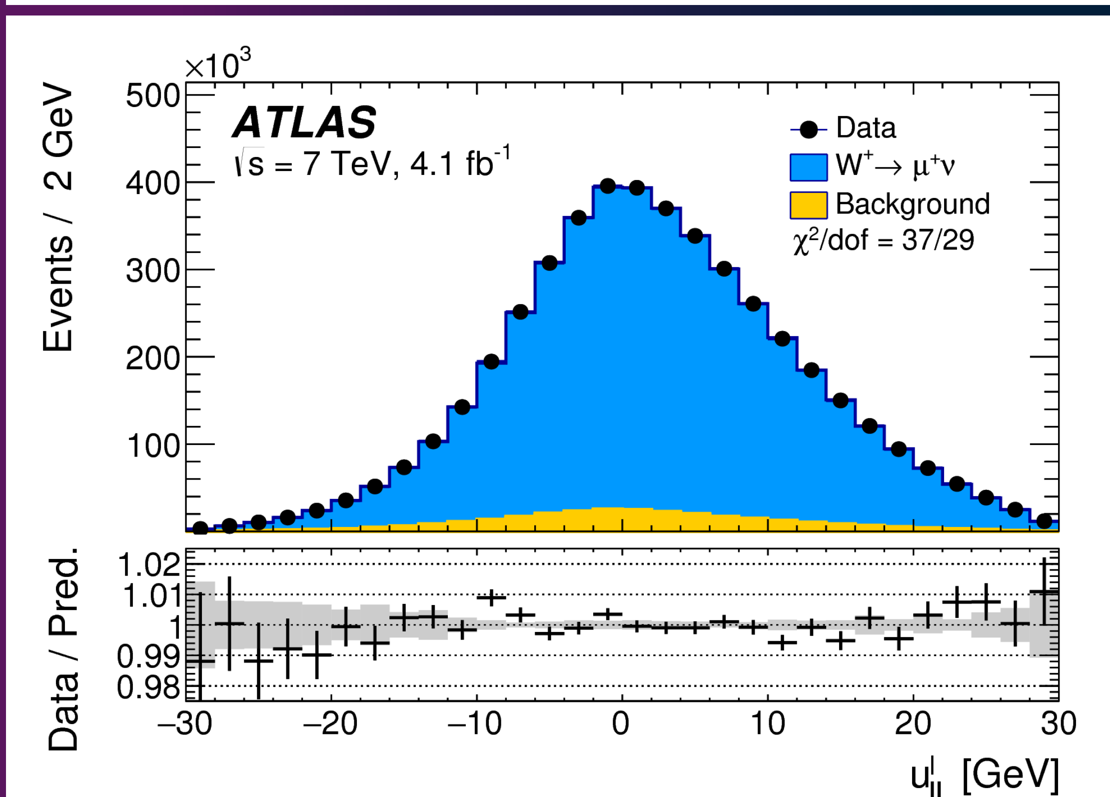

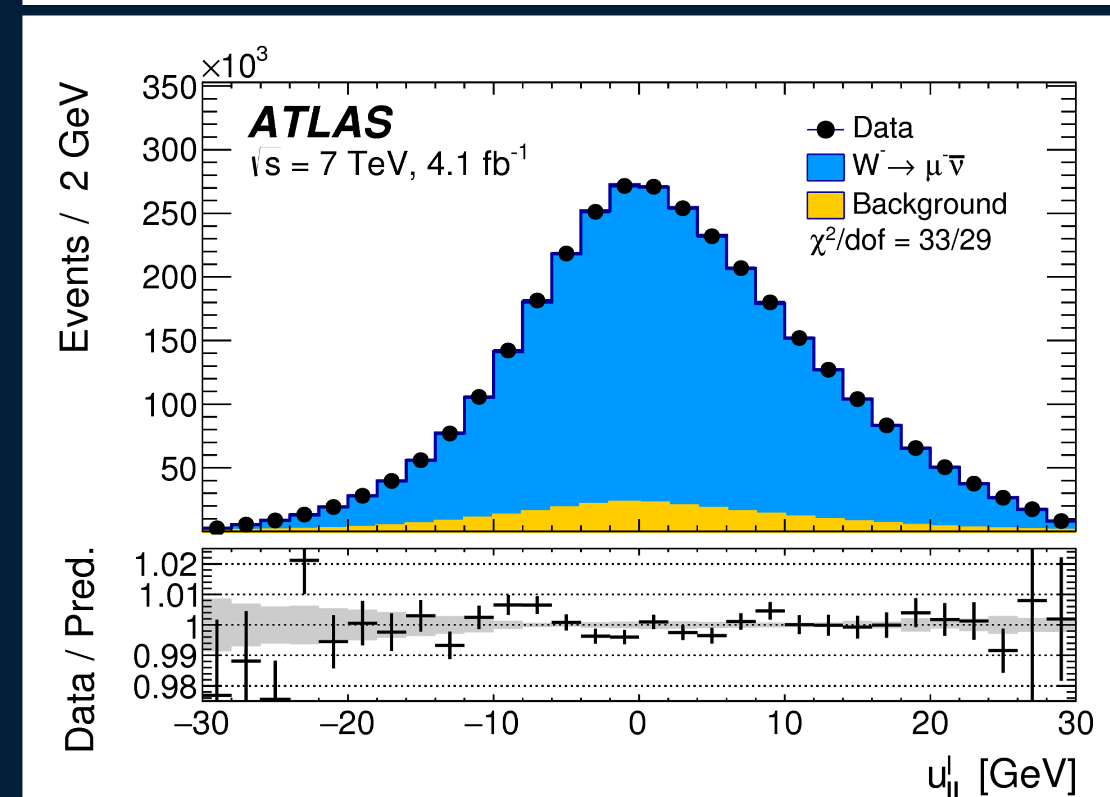

Distributions - lepton eta

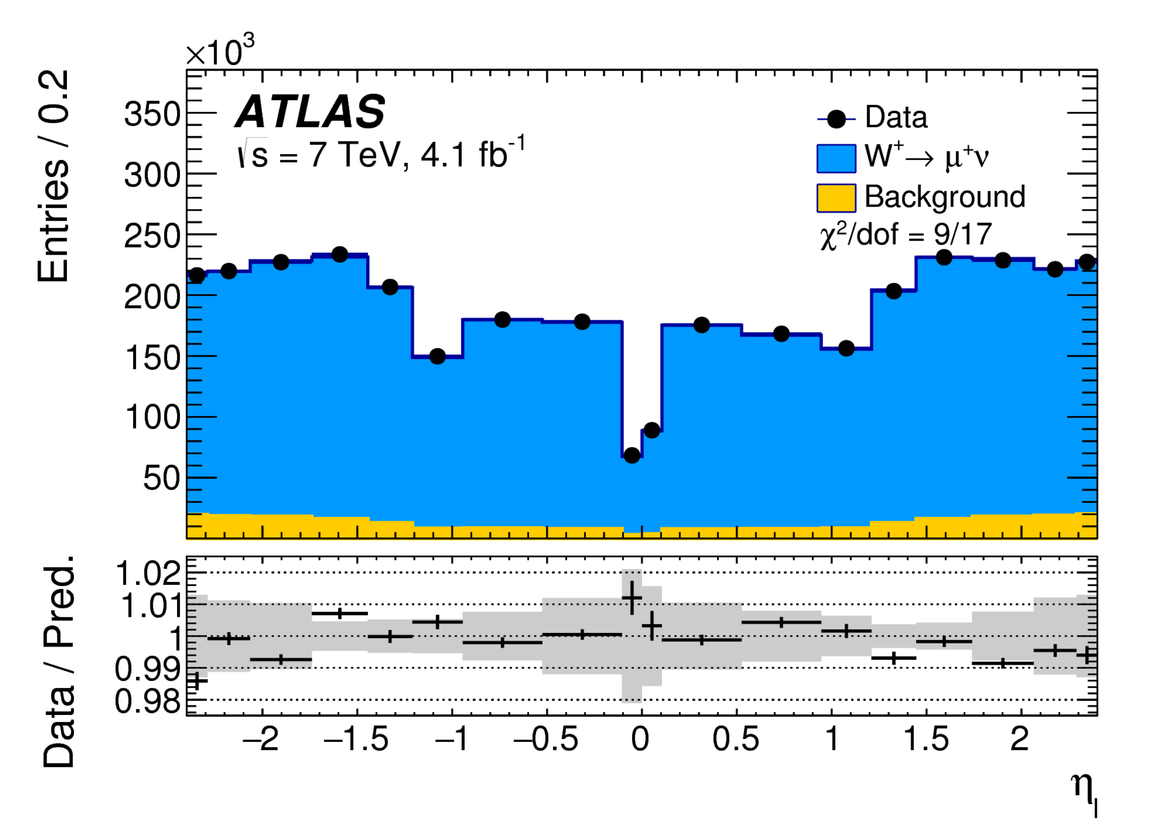

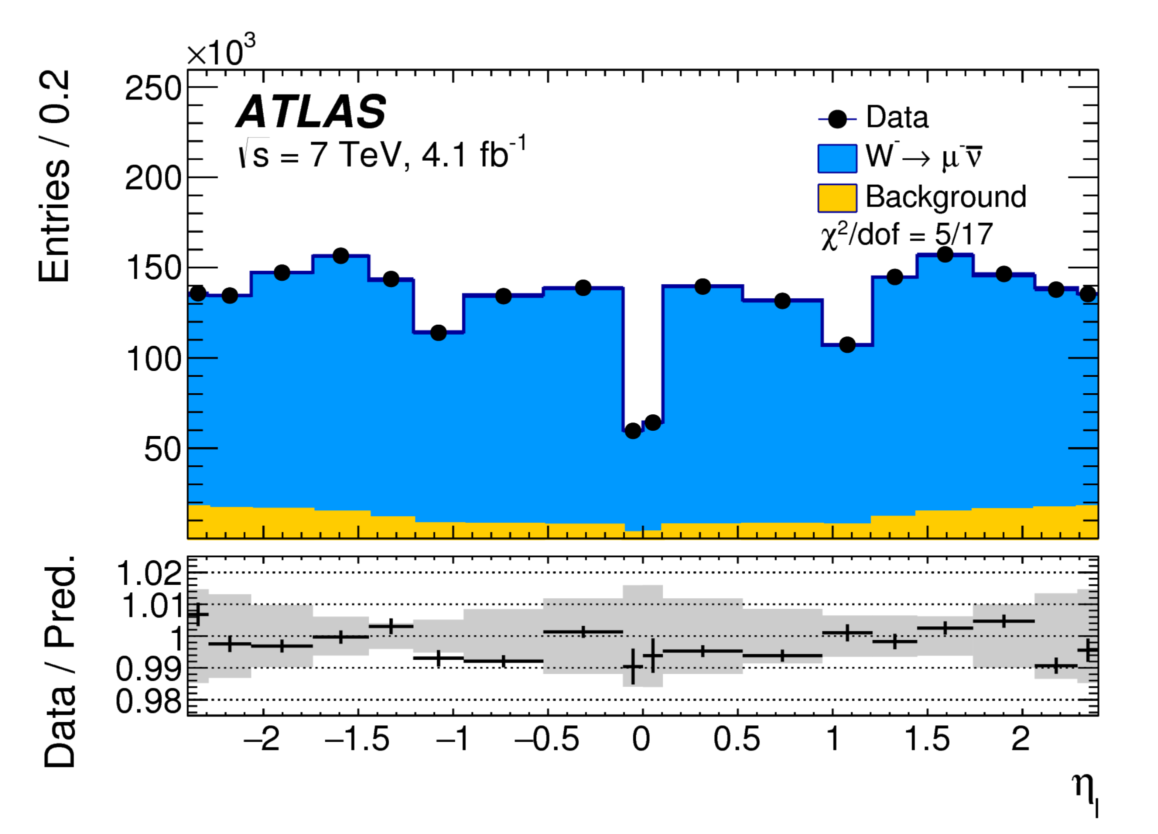

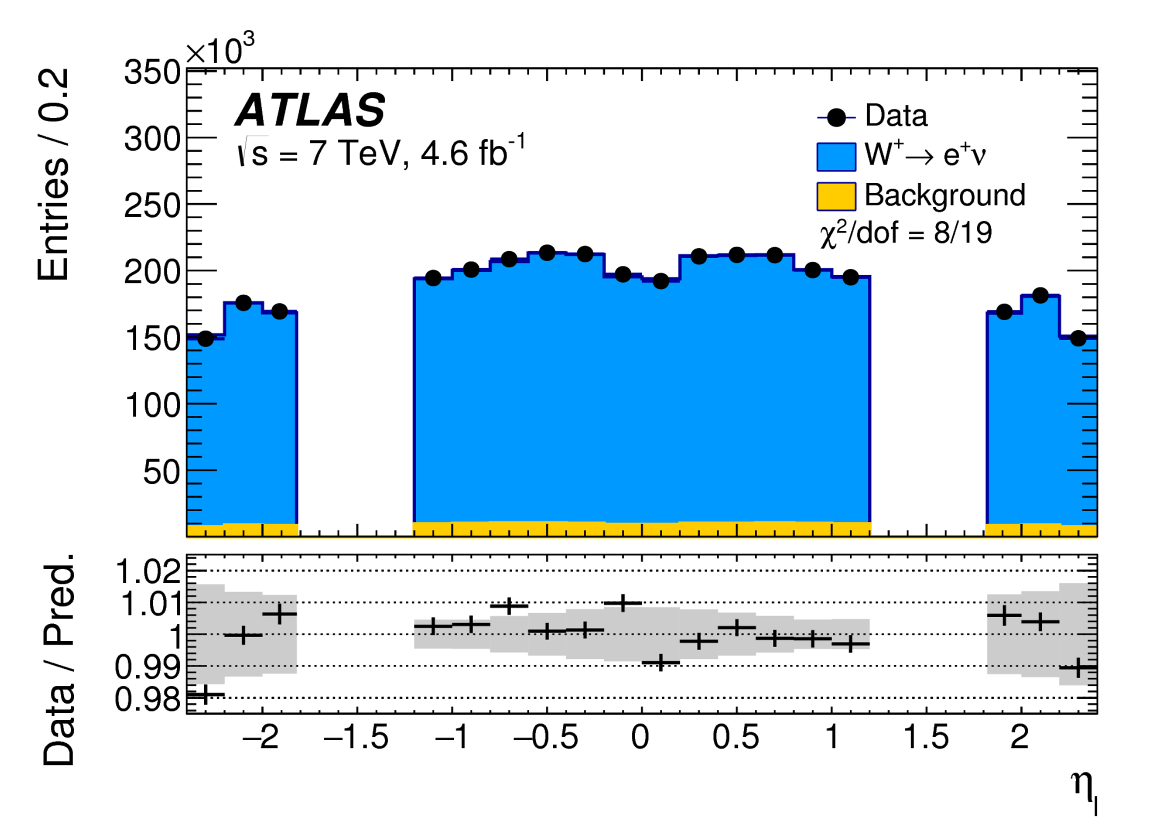

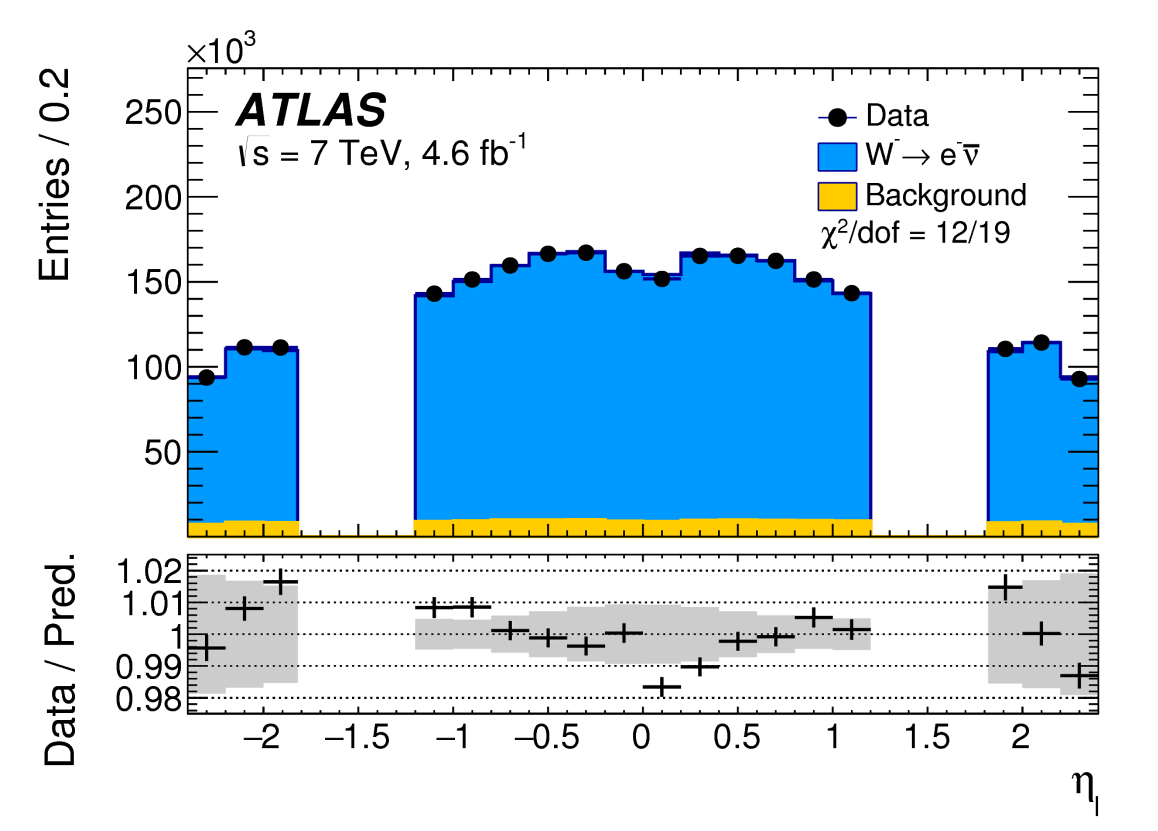

m_W extraction

- $\chi 2$ template fit to the data in each category (distribution, charge, lepton channel, η_ℓ bin)
- All categories give consistent result —> strength of detector calibration and physics modelling
- Also cross-check in more categories (bins of recoil, mu…)
- Several combinations performed, using BLUE method

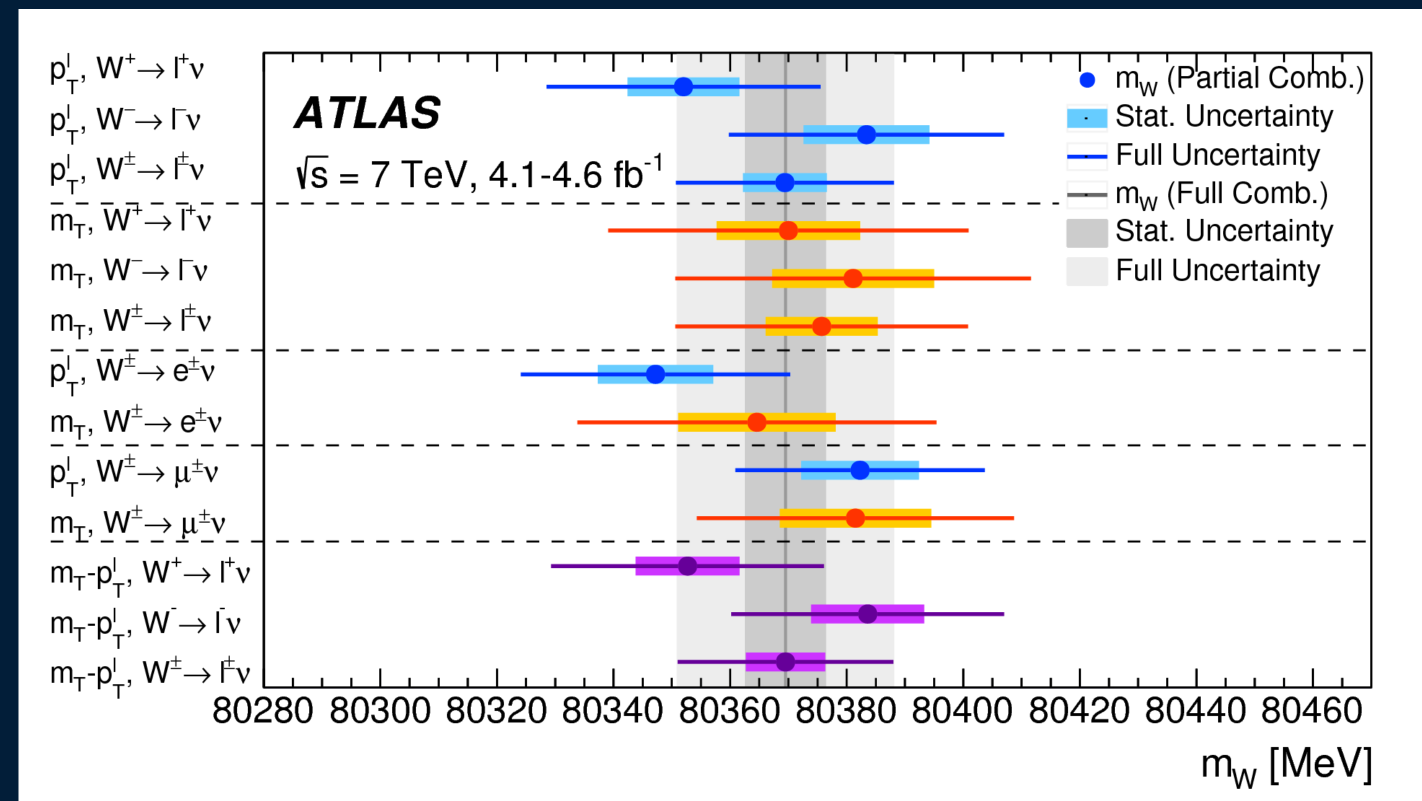

Combination	Weight
Electrons	0.427
Muons	0.573
m_T	0.144
p_T^ℓ	0.856
W^+	0.519
W^-	0.481

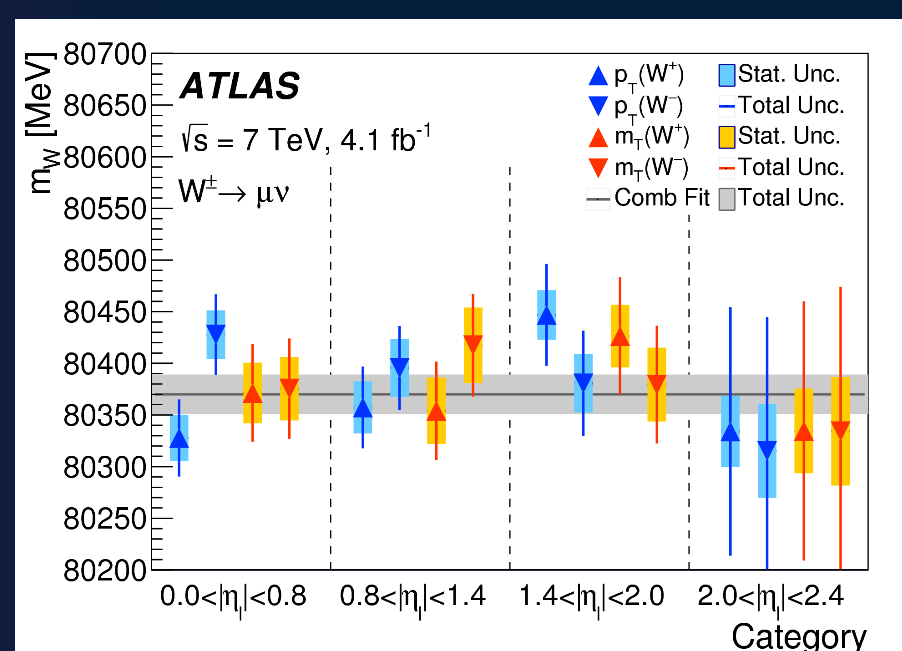

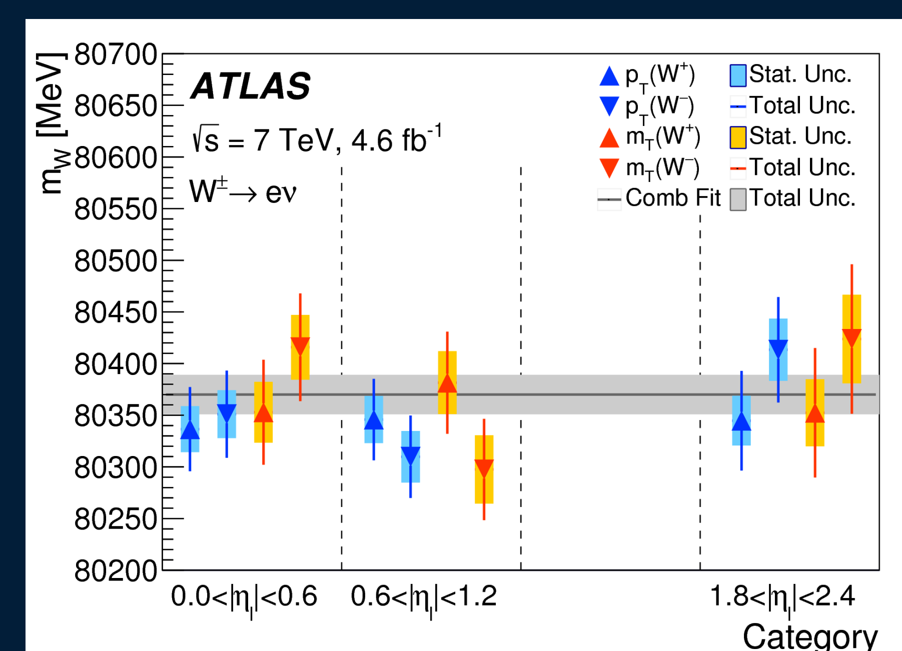

CONCLUSION AND SUMMARY

Δm_W result

- Measurement of m_{W^+} - m_{W^-}
  - Not blinded
  - Many uncertainties cancel as they are not charge-dependent
  - Dominant uncertainty from the PDFs
  - Result compatible with 0 within ~1 sigma

Channel	$m_{W^+} - m_{W^-}$ [MeV]	Stat. Unc.	Muon Unc.	Elec. Unc.	Recoil Unc.	Bckg. Unc.	QCD Unc.	EW Unc.	PDF Unc.	Total Unc.
$W \to e\nu$	-29.7	17.5	0.0	4.9	0.9	5.4	0.5	0.0	24.1	30.7
$W \to \mu\nu$	-28.6	16.3	11.7	0.0	1.1	5.0	0.4	0.0	26.0	33.2
Combined	-29.2	12.8	3.3	4.1	1.0	4.5	0.4	0.0	23.9	28.0

m_W result

m_T

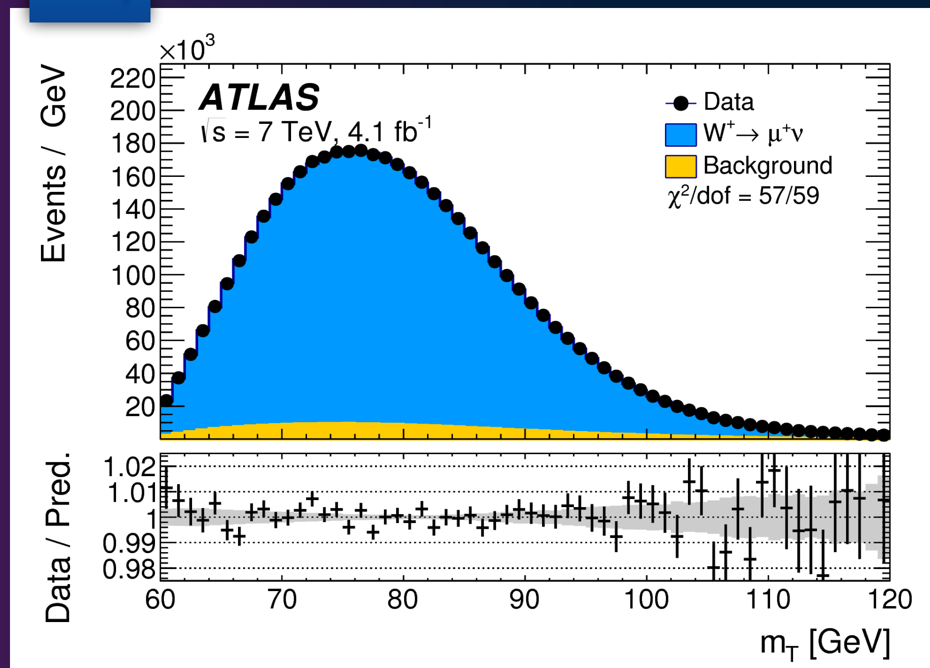

p_T^ℓ

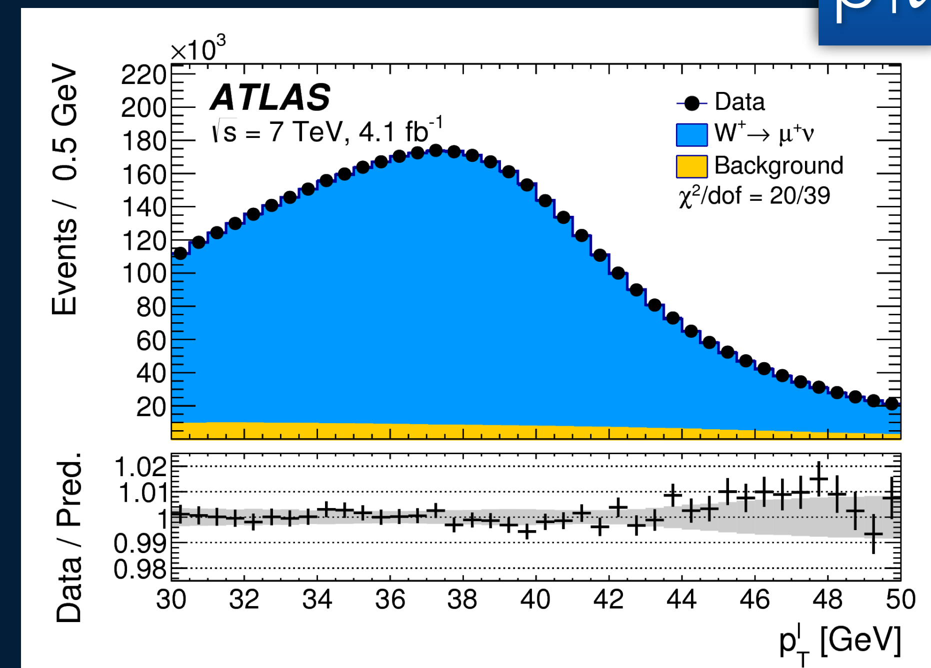

$$m_W = 80370 \pm 7\ \text{(stat.)} \pm 11\ \text{(exp. syst.)} \pm 14\ \text{(mod. syst.) MeV}$$
$$= 80370 \pm 19\ \text{MeV},$$

Combined categories	Value [MeV]	Stat. Unc.	Muon Unc.	Elec. Unc.	Recoil Unc.	Bckg. Unc.	QCD Unc.	EW Unc.	PDF Unc.	Total Unc.	χ^2/dof of Comb.
m_T-p_T^ℓ, $W^\pm$, e-μ	80369.5	6.8	6.6	6.4	2.9	4.5	8.3	5.5	9.2	18.5	29/27

- Dominant uncertainty comes from the physics modelling
  - Largest contribution from QCD

Comparison to other measurements

- Same precision as single best measurement from CDF
- Pulling the m_W towards a value close to Standard Model prediction from EW fit

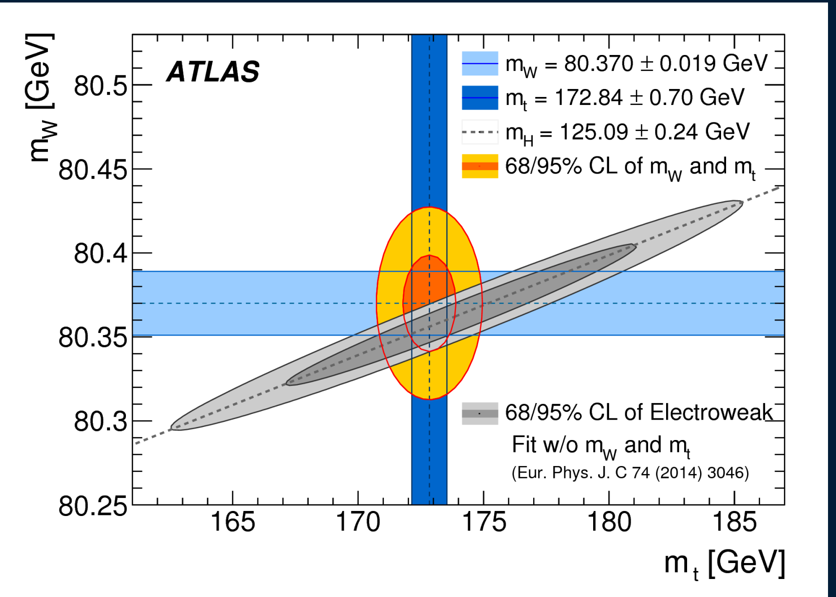

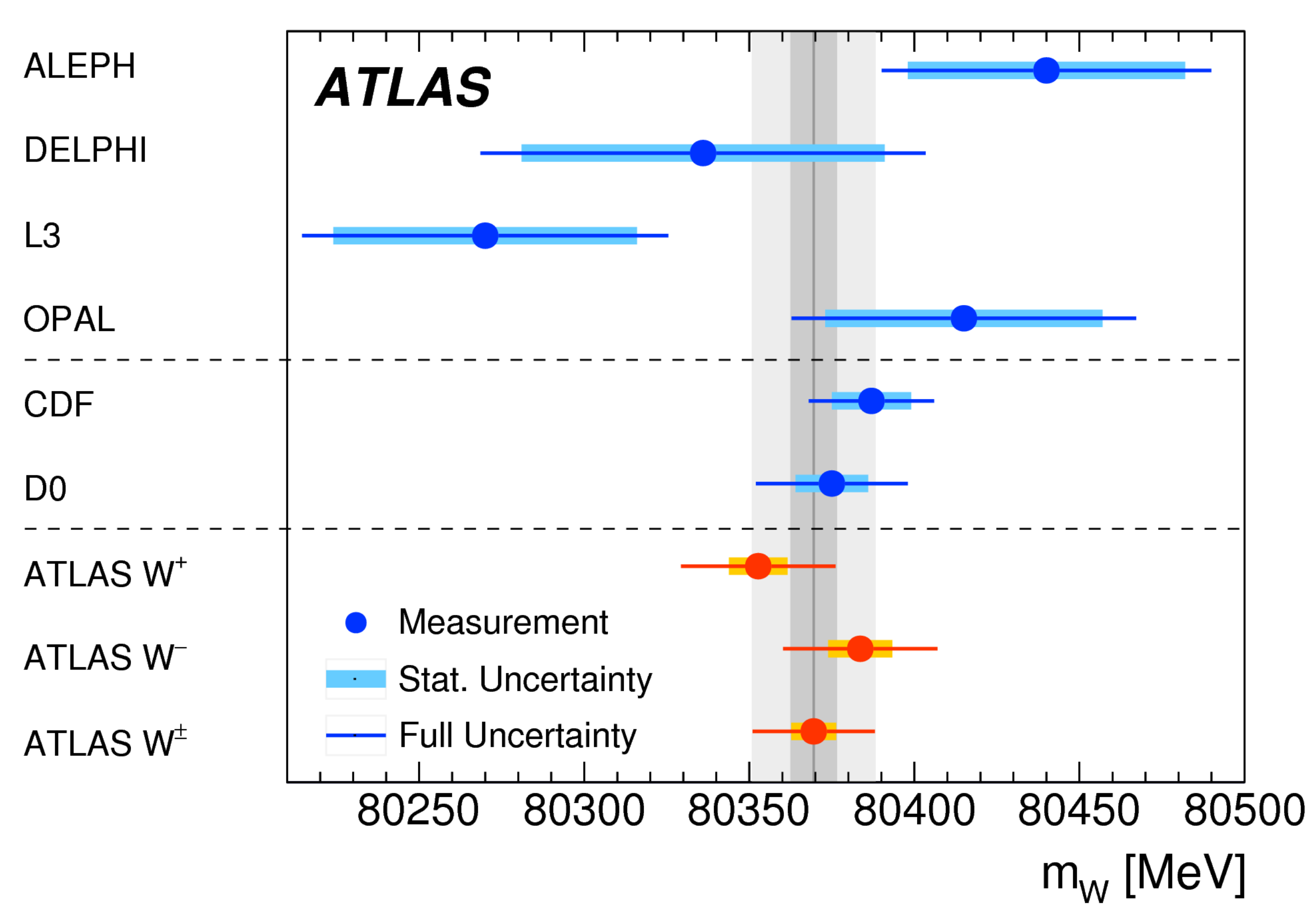

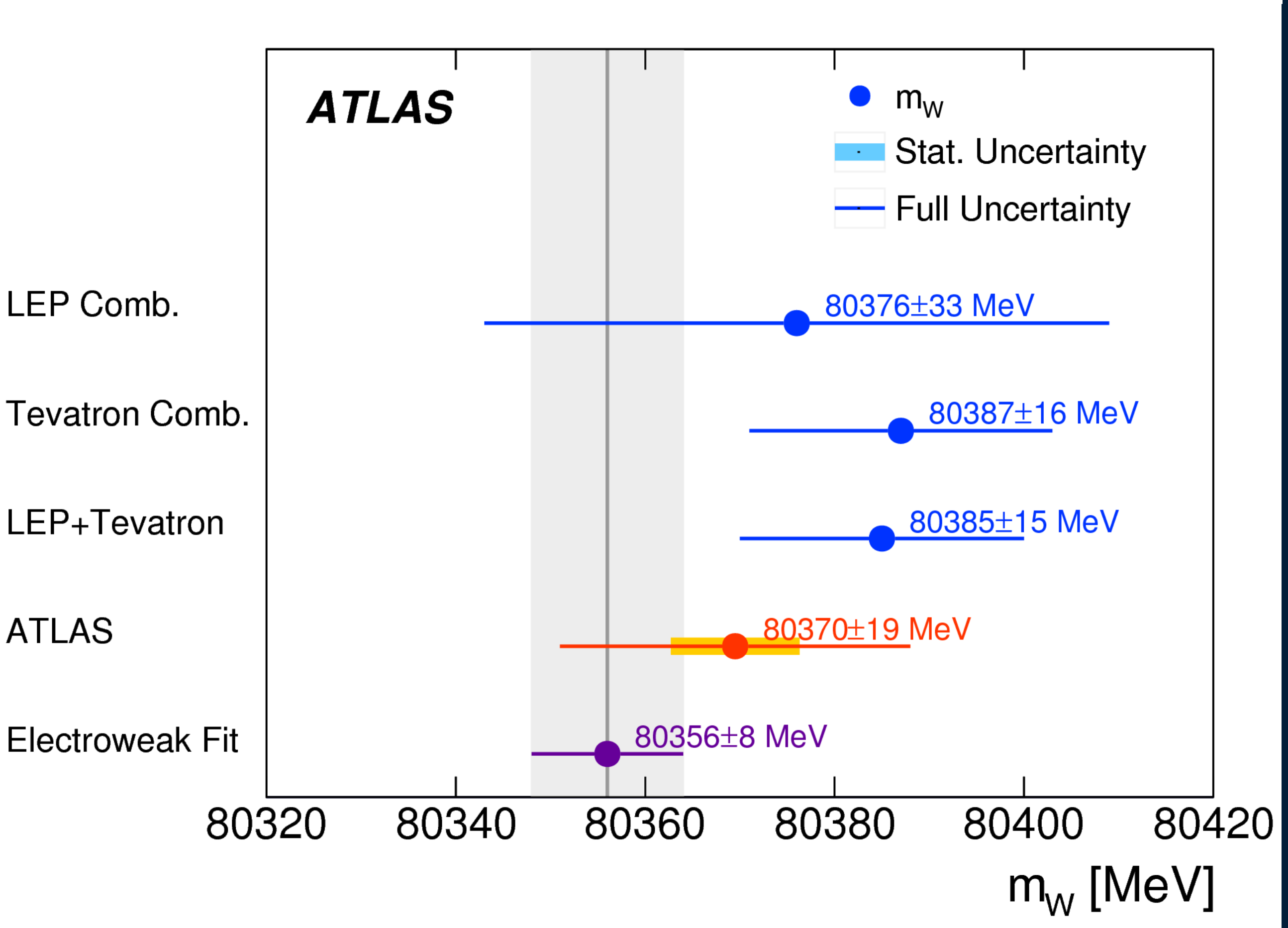

What's next ?

- What can be done to improve the precision in the coming (<10) years ?
  - **More progress on theory side : resummation, incorporation of NLO EW⊗QCD effects in simulation**
  - Experimental innovations : e.g. pile-up mitigation techniques, more and more **ancillary measurements like W p_T**, polarisation…
    - Run at low pile-up (mu~1) very interesting in this respect
  - Combinations with existing/future measurements (*e.g* Tevatron)

Low mu runs : W p_T

- Strong motivation to measure W p_T with an uncertainty below 1% in the Sudakov region (p_T ~< 20 GeV), with a resolution of ~5 GeV to catch the variation of the Sudakov peak
  - crucial input to m_W : with comparable precision, does not need to rely on Z anymore (—>no extrapolation uncertainty)
  - stringent test of resummed predictions and parton showers
- Pile-up degrades the reconstructed $p_T(W)$ resolution (== hadronic recoil) as $\sqrt{(<\mu>)}$
  - —>need very low pile-up data taking
    - ~300 pb^{-1} at 13 TeV needed for enough statistical precision
      - ~150 pb^{-1} taken in 2017, ~200 taken last month (mu~2) : stay tune!
      - 250 pb^{-1} at 5 TeV (2017) : allows to check energy dependence of the models for $p_T(W)$

ATL-PHYS-PUB-2014-015

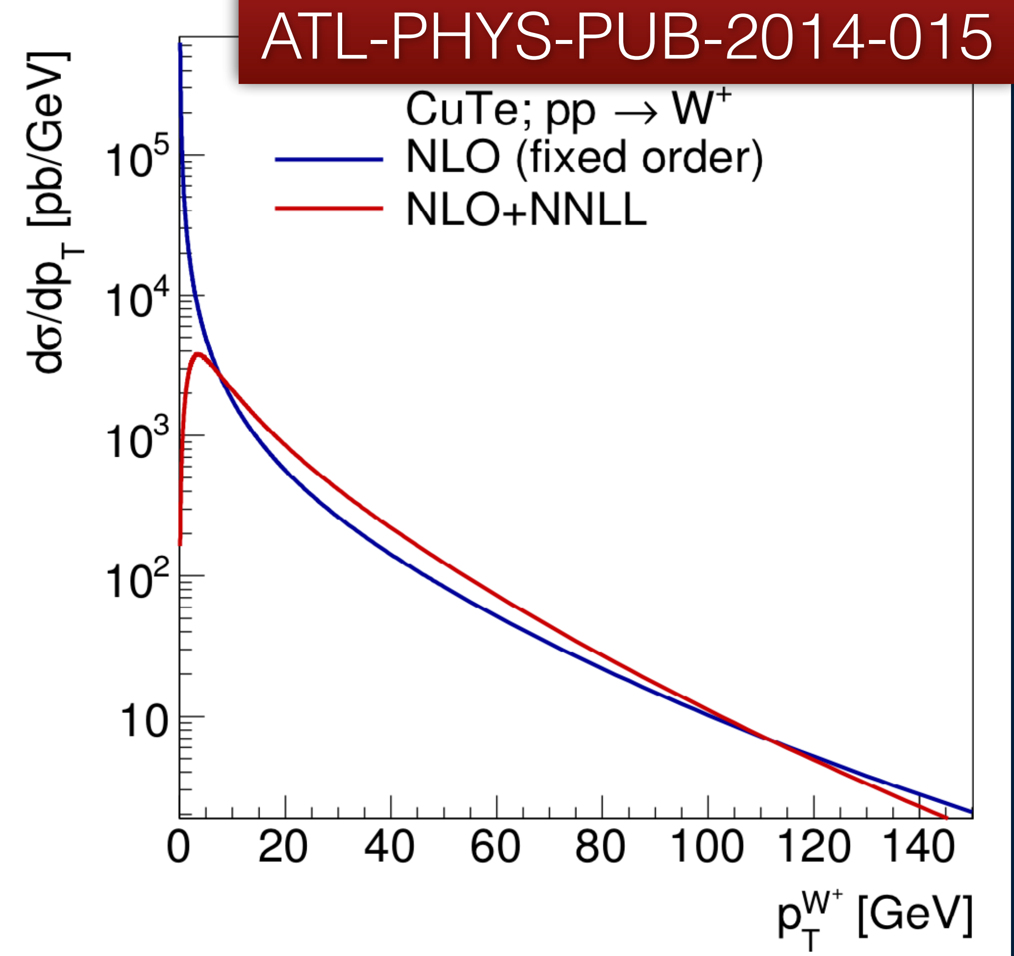

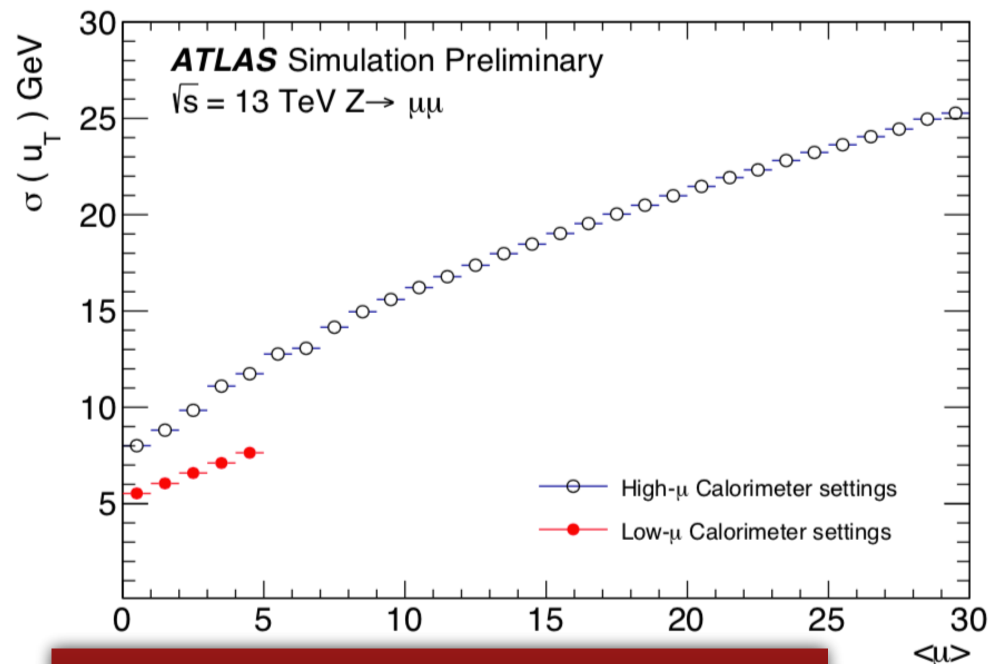

ATL-PHYS-PUB-2017-021

And now for something completely different…

Eur. Phys. J. C (2017) 77:474

Electroweak *W j j* production and constraints on anomalous gauge couplings (aGC) with 7 and 8 TeV data

- Opportunity to probe anomalous (triple) gauge couplings through VBF topology
  - probe for new fundamental interactions
  - First VBF W observation

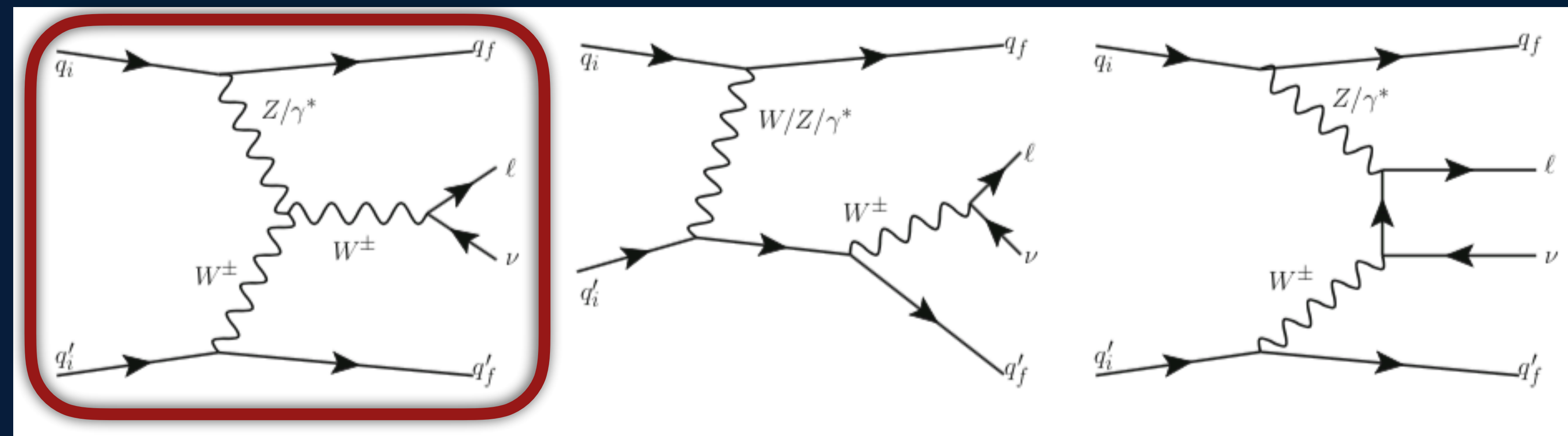

(a) Vector boson fusion (b) W bremsstrahlung (c) Non-resonant

Leading order diagrams for Wjj electroweak production

- Largest background from strong Wjj production (~O(10) times larger than EW)
- Signal :
  - Large interval in jet rapidities (rapidity gap) —>large invariant dijet mass M_{jj}
  - *W* boson in rapidity gap
  - Little hadronic activity in the rapidity gap due to the absence of colour flow between the interacting partons

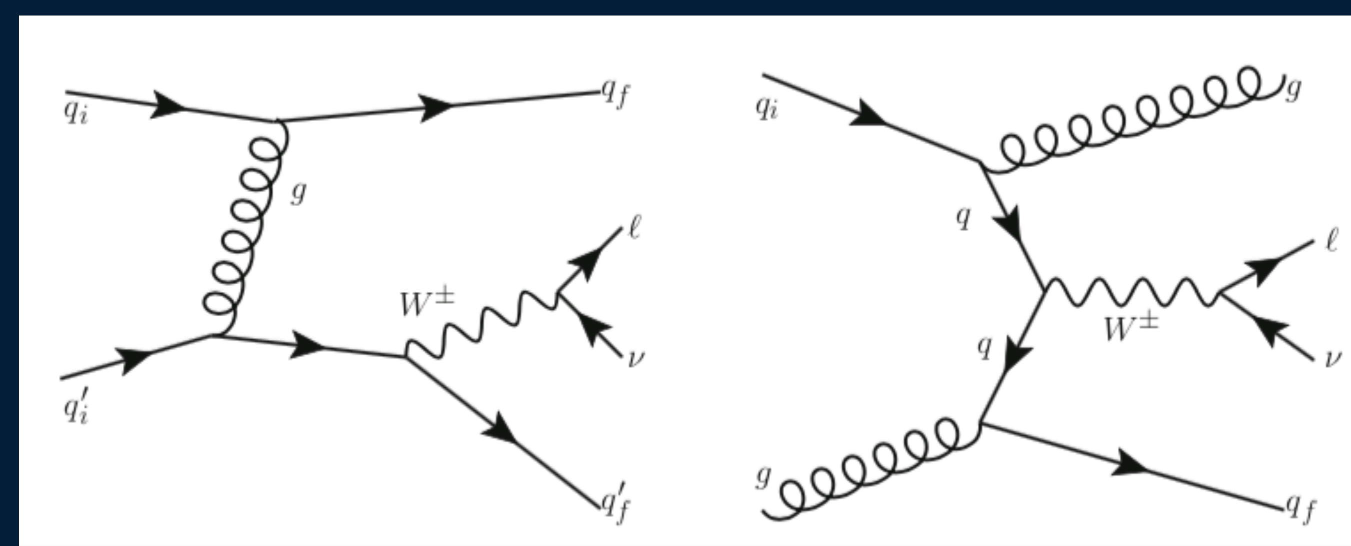

Leading order diagrams for Wjj strong production

Eur. Phys. J. C (2017) 77:474

Modeling

- Wjj MC : Powheg+Pythia8, using MiNLO for strong production (sets the QCD emission scales), PDF set is CT10
  - strong production
- Sherpa 1.4 at leading order is used to estimate interference between strong and EW (using QCD+EW vs separate QCD and EW Wjj samples)
  - Also used in cross-section comparisons
- Other backgrounds are modelled with MC except for multi jet (data-driven)

Cross-section measurement

- Binned likelihood fit to the M_{jj} distribution with Gaussian constraints to every background
- Determination of μ_i
  - i = QCD or EW
  - N_i : measured number of (background subtracted) events
  - C_i : N(reco)/N(truth) passing the selection
  - A_i : acceptance of fiducial volume

$$(\sigma_i^{\ell\nu jj} \times \mathcal{A}_i)^{\text{meas}} = \mu_i \, (\sigma_i^{\ell\nu jj} \times \mathcal{A}_i)^{\text{theo}} = \frac{N_i}{\mathcal{C}_i \mathcal{L}},$$

fiducial cross-section

normalisation factor (=1 in SM)

Event selection

- Using single lepton trigger
- Leptons and jets reconstruction/calibration/preselection similar as the W+jets analysis presented before
- Use of lepton and jet centrality defined as

$$C_{\ell(jet)} = \left| \frac{y_{\ell(jet)} - \frac{y_1 + y_2}{2}}{y_1 - y_2} \right|$$

- Such that C < Cmax = 0.4 implies y to be in the range :

$$\left[\frac{y_1 + y_2}{2} - C_{max} \times |y_1 - y_2|, \frac{y_1 + y_2}{2} + C_{max} \times |y_1 - y_2|\right]$$

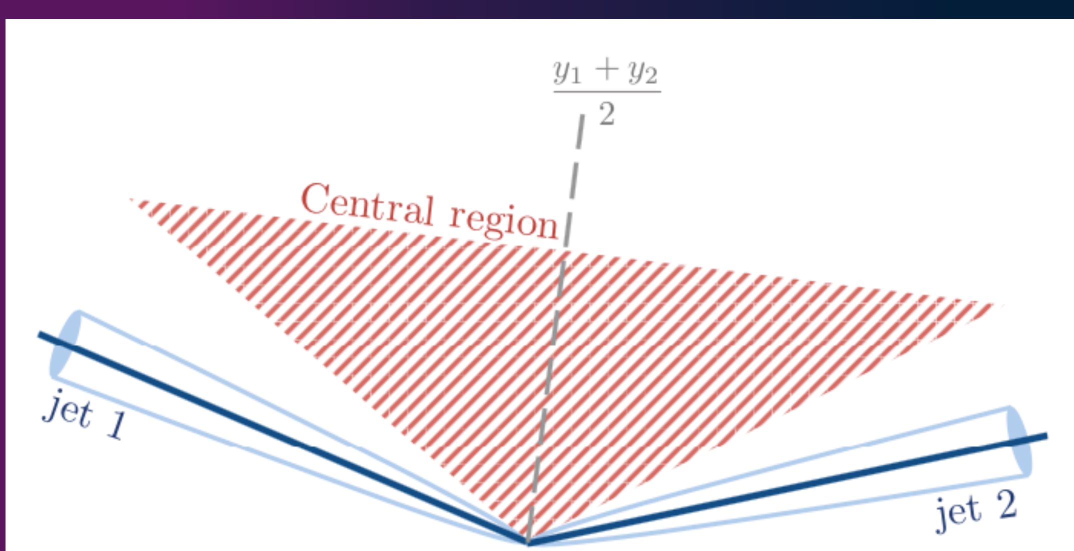

- Forward lepton CR used to constrain strong Wjj production
- Validation region (for multi jet and QCD Wjj) has >=1 central jet

Region name	Requirements
Preselection	Lepton $p_T > 25$ GeV
	Lepton $\|\eta\| < 2.5$
	$E_T^{miss} > 25$ GeV
	$m_T > 40$ GeV
	$p_T^{j_1} > 80$ GeV
	$p_T^{j_2} > 60$ GeV
	Jet $\|y\| < 4.4$
	$M_{jj} > 500$ GeV
	$\Delta y(j_1, j_2) > 2$
	$\Delta R(j, \ell) > 0.3$
Fiducial and differential measurements	
Signal region	$N_{lepton}^{cen} = 1$, $N_{jets}^{cen} = 0$
Forward-lepton control region	$N_{lepton}^{cen} = 0$, $N_{jets}^{cen} = 0$
Central-jet validation region	$N_{lepton}^{cen} = 1$, $N_{jets}^{cen} \geq 1$
Differential measurements only	
Inclusive regions	$M_{jj} > 0.5$ TeV, 1 TeV, 1.5 TeV, or 2 TeV
Forward-lepton/central-jet region	$N_{lepton}^{cen} = 0$, $N_{jets}^{cen} \geq 1$
High-mass signal region	$M_{jj} > 1$ TeV, $N_{lepton}^{cen} = 1$, $N_{jets}^{cen} = 0$
Anomalous coupling measurements only	
High-q^2 region	$M_{jj} > 1$ TeV, $N_{lepton}^{cen} = 1$, $N_{jets}^{cen} = 0$, $p_T^{j_1} > 600$ GeV

Event yields

- EW signal represents ~15 % of the total number of events
- Dominant background is strong Wjj production (~50% of total number of events)

Process	7 TeV	8 TeV
Wjj (EW)	920	5600
Wjj (QCD)	3020	19,600
Multijets	500	2350
$t\bar{t}$	430	1960
Single top	244	1470
Zjj (QCD)	470	1140
Dibosons	126	272
Zjj (EW)	5	79
Total SM	5700	32,500
Data	6063	33,719

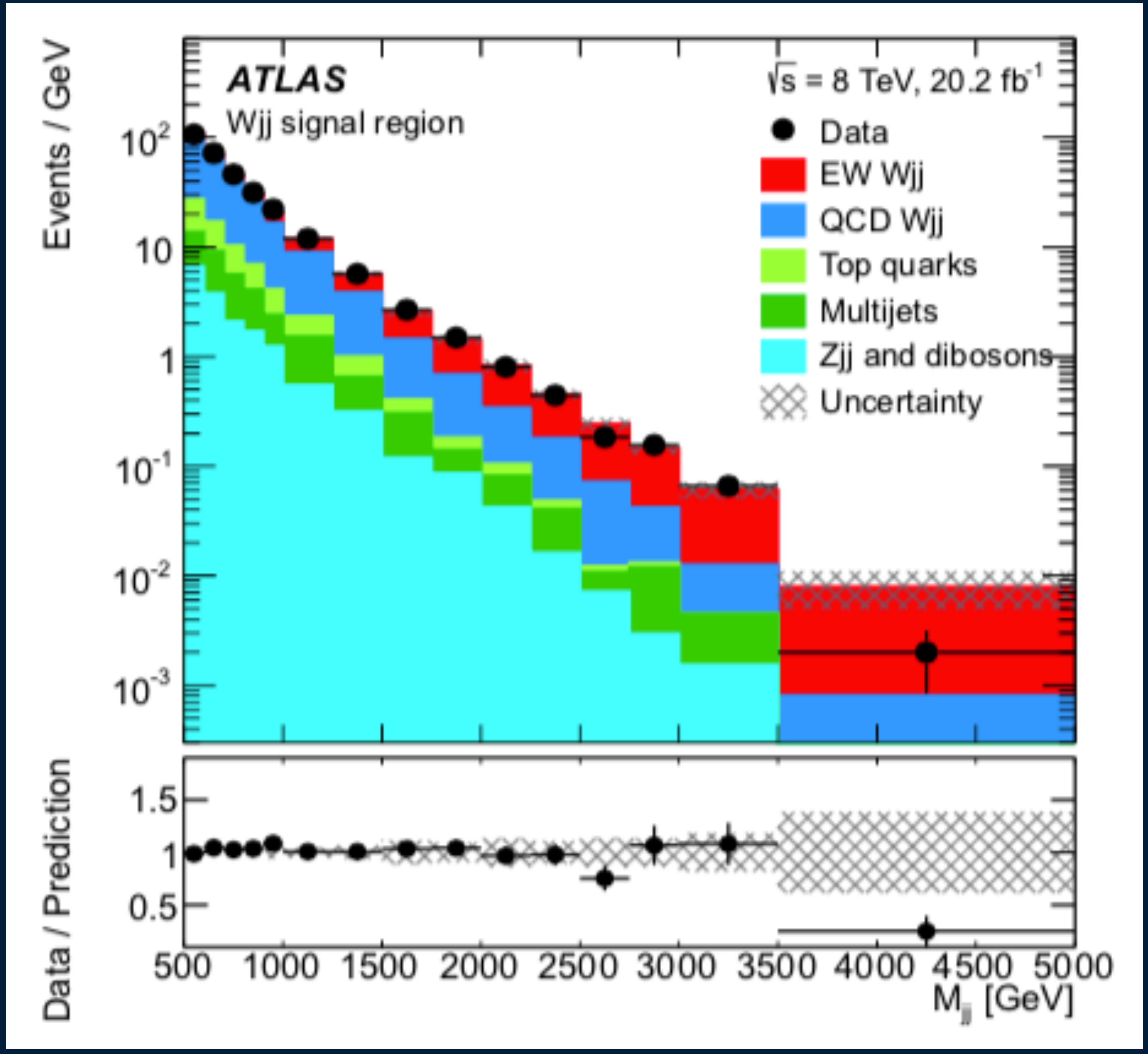

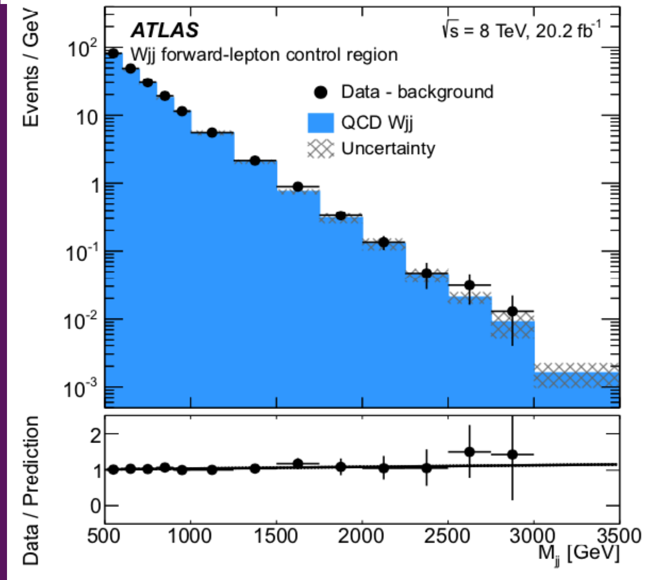

- constraint to QCD Wjj from the control region (all backgrounds subtracted)

SM Cross-section result

$\sqrt{s}$	$\sigma^{\text{fid}}_{\text{meas}}$ [fb]	$\sigma^{\text{fid}}_{\text{SM}}$ [fb]	Acceptance $\mathcal{A}$	$\sigma^{\text{inc}}_{\text{meas}}$ [fb]
7 TeV	144 ± 23 (stat) ± 23 (exp) ± 13 (th)	144 ± 11	0.053 ± 0.004	2760 ± 670
8 TeV	159 ± 10 (stat) ± 17 (exp) ± 15 (th)	198 ± 12	0.058 ± 0.003	2890 ± 510

Source	Uncertainty in μ_{EW}	
	7 TeV	8 TeV
Statistical		
Signal region	0.094	0.028
Control region	0.127	0.044
Experimental		
Jet energy scale (η intercalibration)	0.124	0.053
Jet energy scale and resolution (other)	0.096	0.059
Luminosity	0.018	0.019
Lepton and $E_{\text{T}}^{\text{miss}}$ reconstruction	0.021	0.012
Multijet background	0.064	0.019
Theoretical		
MC statistics (signal region)	0.027	0.026
MC statistics (control region)	0.029	0.019
EW Wjj (scale and parton shower)	0.012	0.031
QCD Wjj (scale and parton shower)	0.043	0.018
Interference (EW and QCD Wjj)	0.037	0.032
Parton distribution functions	0.053	0.052
Other background cross sections	0.002	0.002
EW Wjj cross section	0.076	0.061
Total	0.26	0.14

$$\mu_{\text{EW}}\ (7\ \text{TeV}) = 1.00 \pm 0.16\ (\text{stat}) \pm 0.17\ (\text{exp}) \pm 0.12\ (\text{th}),$$
$$\mu_{\text{EW}}\ (8\ \text{TeV}) = 0.81 \pm 0.05\ (\text{stat}) \pm 0.09\ (\text{exp}) \pm 0.10\ (\text{th}).$$

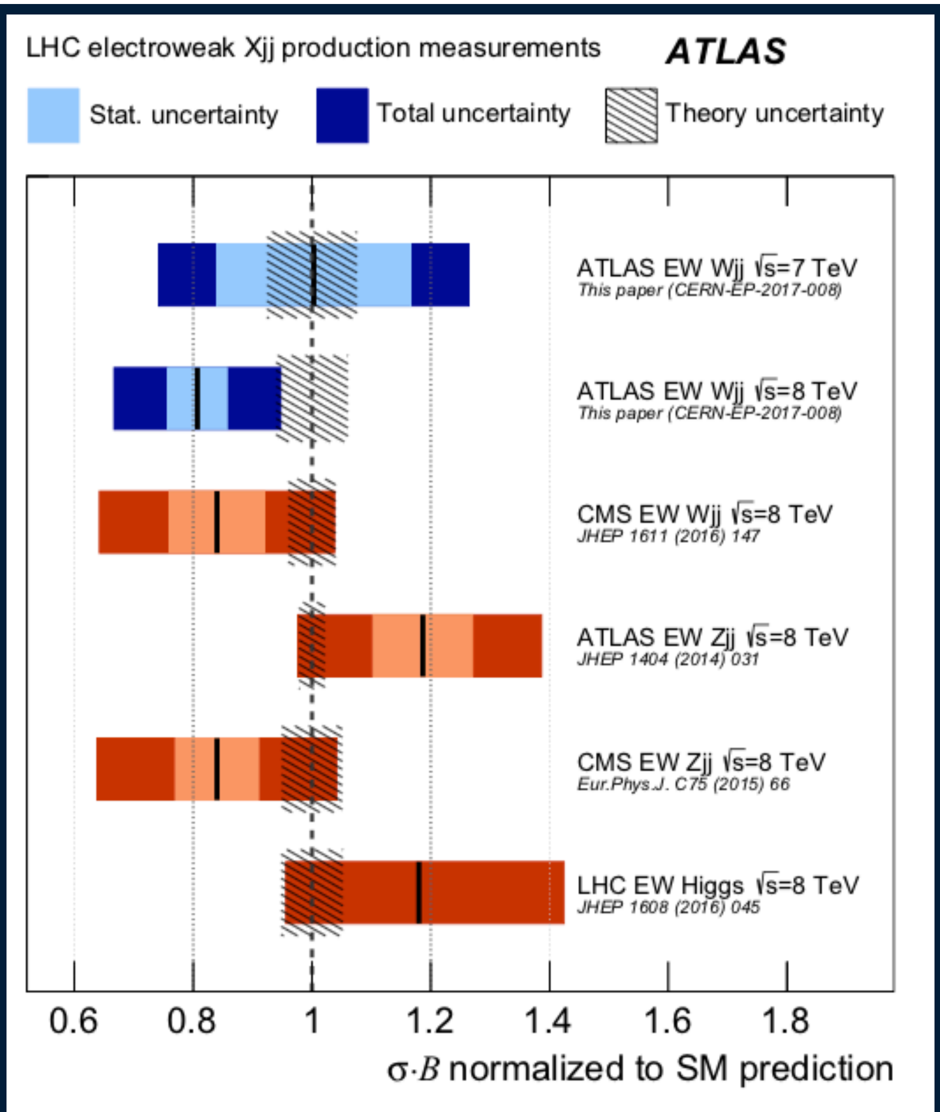

- First 5 sigma Wjj EW measurement

Unfolded differential cross-sections : Wjj EW vs QCD

- Many unfolded differential cross-sections obtained in the fiducial region
  - Direct probes of new physics
  - Here, just one exemple : for M_{jj}> 500GeV (left), dominated by QCD ; EW Wjj appears for M_{jj} > 2TeV (right) !

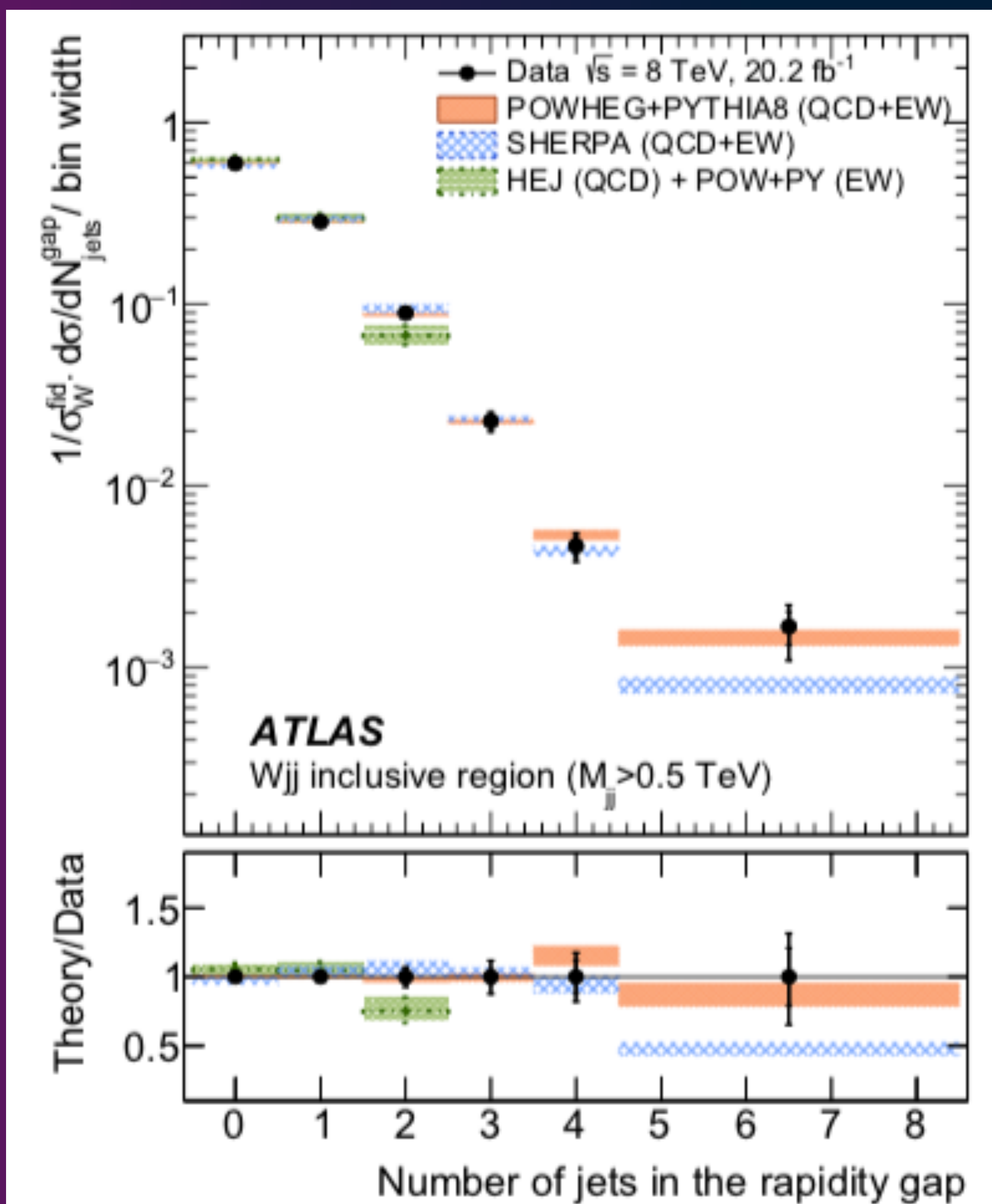

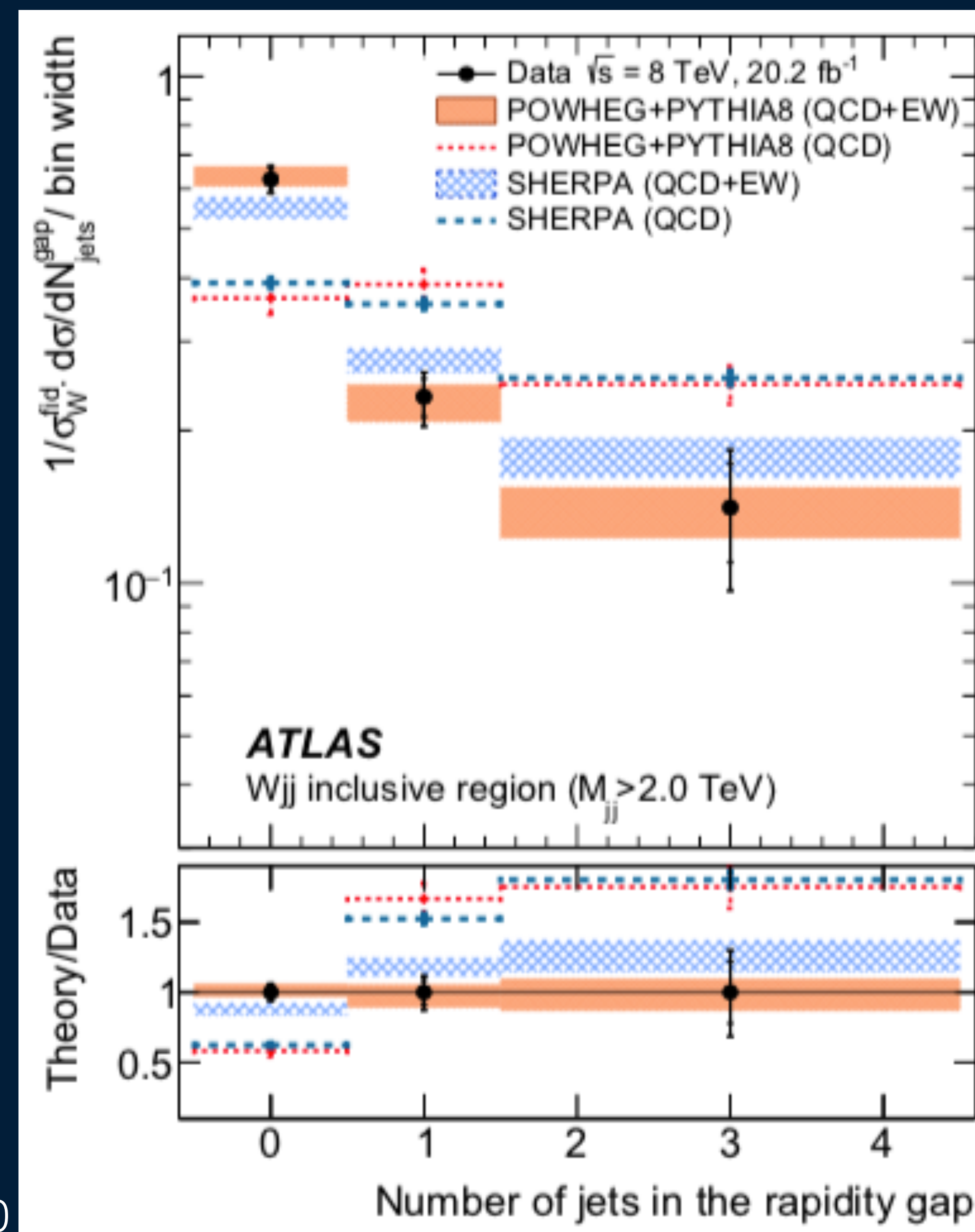

Constraints on aGC

- Effective Lagrangian for WWV coupling with operators up to dimension 6 (V=Z, gamma)
- Deviation from SM : $g_1^V \neq 1$, $\kappa_V \neq 1$, $\lambda_V \neq 0$, $\tilde{\kappa}_V \neq 0$

$$i\mathcal{L}_{\text{eff}}^{WWV} = g_{WWV}\Bigg\{\Bigg[g_1^V V^\mu (W^-_{\mu\nu}W^{+\nu} - W^+_{\mu\nu}W^{-\nu}) + \kappa_V W^+_\mu W^-_\nu V^{\mu\nu} + \frac{\lambda_V}{m_W^2} V^{\mu\nu} W_\nu^{+\rho} W^-_{\rho\mu}\Bigg] - \Bigg[\frac{\tilde{\kappa}_V}{2} W^-_\mu W^+_\nu \epsilon^{\mu\nu\rho\sigma} V_{\rho\sigma} + \frac{\tilde{\lambda}_V}{2m_W^2} W^-_{\rho\mu} W_\nu^{+\mu} \epsilon^{\nu\rho\alpha\beta} V_{\alpha\beta}\Bigg]\Bigg\},$$

CP violating

$$W^\pm_{\mu\nu} = \partial_\mu W^\pm_\nu - \partial_\nu W^\pm_\mu$$

- Gauge invariance requires :

$$\Delta g_1^Z = \Delta\kappa_Z + \Delta\kappa_\gamma \tan^2\theta_W, \quad \lambda_\gamma = \lambda_Z \equiv \lambda_V, \quad g_1^\gamma = 1,$$
$$\tilde{\kappa}_\gamma = -\tilde{\kappa}_Z \cot^2\theta_W, \quad \text{and} \quad \tilde{\lambda}_\gamma = \tilde{\lambda}_Z \equiv \tilde{\lambda}_V.$$

- To preserve unitarity one can introduce :

$$\alpha(q^2) = \frac{\alpha}{(1+q^2/\Lambda^2)^2}$$

- With Λ = 4 TeV (preserves unitarity) for all parameters in sensitivity range

- Or in EFT : assume perturbative coupling coefficients ci and scale of new interaction Λ, O_i are dimension 6 field operators :
- One can relate the c_i to the aTGC parameters

$$\mathcal{L}_{\text{EFT}} = \sum_i \frac{c_i}{\Lambda^2} O_i$$

Constraints on aGC

- Effect of anomalous couplings modelled within Sherpa
- Fit using the yield in signal region with M_{jj} > 1 TeV, p_T of leading jet > 600 GeV
  - last requirement maximises sensitivity to aTGC
  - Fit each aTGC parameter, fixing the other parameters to SM value
- No deviation from SM is observed

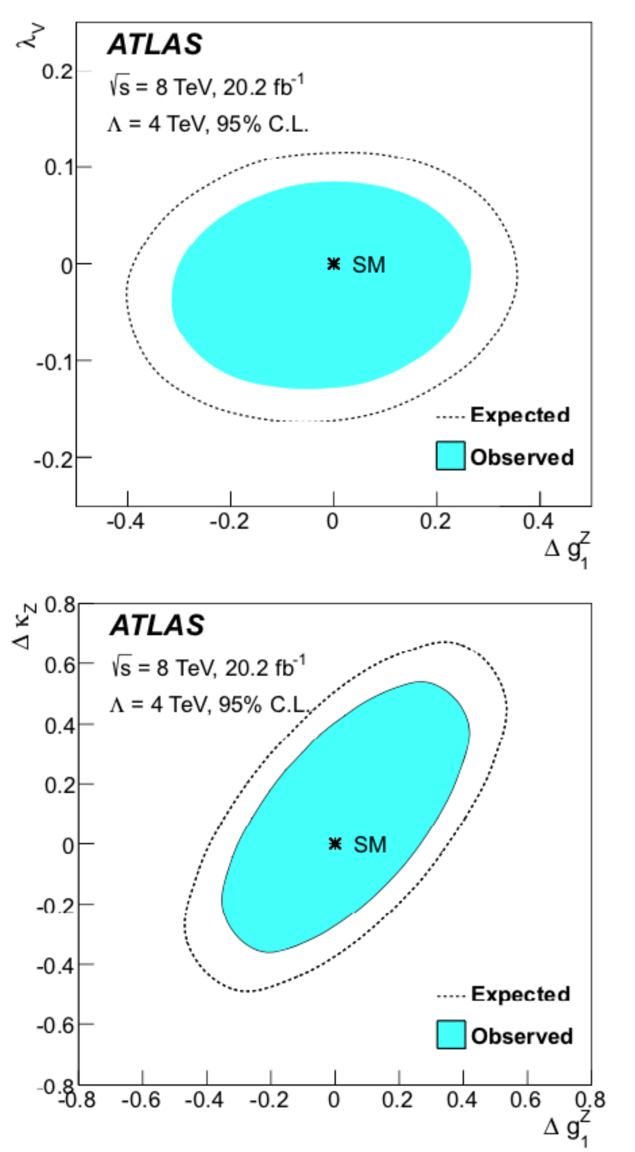

	Λ = 4 TeV	
	Expected	Observed
Δg_1^Z	[−0.39, 0.35]	[−0.32, 0.28]
$\Delta\kappa_Z$	[−0.38, 0.51]	[−0.29, 0.42]
λ_V	[−0.16, 0.12]	[−0.13, 0.090]
$\tilde{\kappa}_Z$	[−1.7, 1.8]	[−1.4, 1.4]
$\tilde{\lambda}_V$	[−0.13, 0.15]	[−0.10, 0.12]

Parameter	Expected (TeV^{-2})	Observed (TeV^{-2})
$\frac{c_W}{\Lambda^2}$	[−39, 37]	[−33, 30]
$\frac{c_B}{\Lambda^2}$	[−200, 190]	[−170, 160]
$\frac{c_{WWW}}{\Lambda^2}$	[−16, 13]	[−13, 9]
$\frac{c_{\tilde{W}}}{\Lambda^2}$	[−720, 720]	[−580, 580]
$\frac{c_{\tilde{W}WW}}{\Lambda^2}$	[−14, 14]	[−11, 11]

EW Wjj : summary

- First observation (>5 sigma) of EW Wjj
  - systematic uncertainty dominates the 8 TeV measurement
- Many unfolded differential cross-sections provided
  - Allowing to check theoretical models (high order calculations)
- aTGC constraint
  - $\boldsymbol{\lambda}_V$ intervals competitive with those from WW
  - No deviation from SM is observed

Concluding remarks

- Wide range of physics ‘touched’ using Ws at LHC
  - I just talked about a few selected items (linked with the most recent publications, mainly) …
    - Precise tests of SM
    - Key input to PDFs
    - validation of predictions that are essential for signal/background modelling in other analyses
    - W mass measurement and global EW fit
    - Wjj electroweak — direct probe of new physics
  - Many other topics
    - W+charm
    - new physics searches at high m_T
    - …

Thank you for your attention!!

BACKUP

PDF profiling : methodology

- PDF profiling and full PDF fits heavily rely on methods used in DIS experiments (esp. HERA)
- Software used is xFitter, that makes use of APPLGRID for theory predictions, together with k-factors from the accurate theory tools described before (NNLO QCD from DYNNLO 1.5, NLO EW from PHOTOS and MCSANC)
- Profiling : use of xFitter software
  - start from existing PDF set
  - Use a $\chi^2(b_{exp}, b_{th})$ that minimises difference between observed and predicted cross-section allowing nuisance parameters (b_{exp}, b_{th}) to shift
  - New PDF f_0' is :

$$f_0' = f_0 + \sum_k \left[b_{k,\mathrm{th}}^{\min} \left(\frac{f_k^+ - f_k^-}{2} \right) + (b_{k,\mathrm{th}}^{\min})^2 \left(\frac{f_k^+ + f_k^- - 2 f_0}{2} \right)^2 \right],$$

  - f_0 is the central PDF set and f_k^+ and f_k^- the corresponding up/down eigenvectors
  - Allows for quantitative estimate of the agreement between the data and the PDF sets from global fits, and study further constraining power from the new measurement
    - Best χ^2 is obtained with CT14nnlo, CT10nnlo, and reasonable with MMHT14nnlo

PDF profiling : results

Data set	n.d.f.	ABM12	CT14	MMHT14	NNPDF3.0	ATLAS-epWZ12
$W^+ \to \ell^+\nu$	11	11|21	10|26	11|37	11|18	12|15
$W^- \to \ell^-\bar{\nu}$	11	12|20	8.9|27	8.1|31	12|19	7.8|17
$Z/\gamma^* \to \ell\ell$ ($m_{\ell\ell} = 46$–66 GeV)	6	17|21	11|30	18|24	21|22	28|36
$Z/\gamma^* \to \ell\ell$ ($m_{\ell\ell} = 66$–116 GeV)	12	24|51	16|66	20|116	14|109	18|26
Forward $Z/\gamma^* \to \ell\ell$ ($m_{\ell\ell} = 66$–116 GeV)	9	7.3|9.3	10|12	12|13	14|18	6.8|7.5
$Z/\gamma^* \to \ell\ell$ ($m_{\ell\ell} = 116$–150 GeV)	6	6.1|6.6	6.3|6.1	5.9|6.6	6.1|8.8	6.7|6.6
Forward $Z/\gamma^* \to \ell\ell$ ($m_{\ell\ell} = 116$–150 GeV)	6	4.2|3.9	5.1|4.3	5.6|4.6	5.1|5.0	3.6|3.5
Correlated χ^2		57|90	39|123	43|167	69|157	31|48
Total χ^2	61	136|222	103|290	118|396	147|351	113|159

- ‘correlated chi2’ is the contribution from the penalty term
- left of ‘|’ is including PDF set uncertainties, right is excluding PDF set uncertainties

Full PDF fit

- More complex than PDF profiling
  - Requires parametrisation of the PDFs at a starting scale $Q_0^2 = 1.9\text{GeV}^2$

$$
\begin{aligned}
xu_v(x) &= A_{u_v} x^{B_{u_v}} (1-x)^{C_{u_v}} (1 + E_{u_v} x^2), \\
xd_v(x) &= A_{d_v} x^{B_{d_v}} (1-x)^{C_{d_v}}, \\
x\bar{u}(x) &= A_{\bar{u}} x^{B_{\bar{u}}} (1-x)^{C_{\bar{u}}}, \\
x\bar{d}(x) &= A_{\bar{d}} x^{B_{\bar{d}}} (1-x)^{C_{\bar{d}}}, \\
xg(x) &= A_g x^{B_g} (1-x)^{C_g} - A'_g x^{B'_g} (1-x)^{C'_g}, \\
x\bar{s}(x) &= A_{\bar{s}} x^{B_{\bar{s}}} (1-x)^{C_{\bar{s}}},
\end{aligned}
$$

- Parameter scans requiring χ^2 saturation (no χ^2 decrease when adding free parameters)
- Some constraints by sum rules
  - —>15 parameters
- $A_{\bar{s}}$ and $B_{\bar{s}}$ appear as free parameters
- assume $\bar{s} = s$

- PDFs are evolved to the scale of the measurements and convolved with hard-scattering coefficients to obtain the theoretical cross- section predictions
  - Done with a variable flavour number scheme that switches on c- and b-quark PDFs at m_c and m_b
- Then, fit using similar (but different) χ^2 as in profiling, with parameters left free
- Fit done with HERA and new ATLAS data
  - New set termed ATLAS-epWZ16
  - Includes experimental and theory uncertainties

Comparison CDF vs ATLAS

Similar PDF uncertainties

p_T W uncertainties are larger for p_T lepton than m_T at CDF, but similar in ATLAS

m_T fit uncertainties			
Source	$W \to \mu\nu$	$W \to e\nu$	Common
Lepton energy scale	7	10	5
Lepton energy resolution	1	4	0
Lepton efficiency	0	0	0
Lepton tower removal	2	3	2
Recoil scale	5	5	5
Recoil resolution	7	7	7
Backgrounds	3	4	0
PDFs	10	10	10
W boson p_T	3	3	3
Photon radiation	4	4	4
Statistical	16	19	0
Total	23	26	15

p_T^ℓ fit uncertainties			
Source	$W \to \mu\nu$	$W \to e\nu$	Common
Lepton energy scale	7	10	5
Lepton energy resolution	1	4	0
Lepton efficiency	1	2	0
Lepton tower removal	0	0	0
Recoil scale	6	6	6
Recoil resolution	5	5	5
Backgrounds	5	3	0
PDFs	9	9	9
W boson p_T	9	9	9
Photon radiation	4	4	4
Statistical	18	21	0
Total	25	28	16

Includes also Ai uncertainties

Combined categories	Value [MeV]	Stat. Unc.	Muon Unc.	Elec. Unc.	Recoil Unc.	Bckg. Unc.	QCD Unc.	EW Unc.	PDF Unc.	Total Unc.	χ^2/dof of Comb.
p_T^ℓ, $W^\pm$, e	80347.2	9.9	0.0	14.8	2.6	5.7	8.2	5.3	8.9	23.1	4/5
m_T, $W^\pm$, e	80364.6	13.5	0.0	14.4	13.2	12.8	9.5	3.4	10.2	30.8	8/5
p_T^ℓ, $W^\pm$, μ	80382.3	10.1	10.7	0.0	2.5	3.9	8.4	6.0	10.7	21.4	7/7
m_T, $W^\pm$, μ	80381.5	13.0	11.6	0.0	13.0	6.0	9.6	3.4	11.2	27.2	3/7

Comparison D0 vs ATLAS

Source	Section	m_T	p_T^e	$\not{E}_T$
Experimental				
Electron Energy Scale	VII C 4	16	17	16
Electron Energy Resolution	VII C 5	2	2	3
Electron Shower Model	V C	4	6	7
Electron Energy Loss	V D	4	4	4
Recoil Model	VII D 3	5	6	14
Electron Efficiencies	VII B 10	1	3	5
Backgrounds	VIII	2	2	2
$\sum$(Experimental)		18	20	24
W Production and Decay Model				
PDF	VI C	11	11	14
QED	VI B	7	7	9
Boson p_T	VI A	2	5	2
$\sum$(Model)		13	14	17
Systematic Uncertainty (Experimental and Model)		22	24	29
W Boson Statistics	IX	13	14	15
Total Uncertainty		26	28	33

Similar PDF uncertainties

Smaller p_T W uncertainties at D0

Includes also Ai uncertainties

Combined categories	Value [MeV]	Stat. Unc.	Muon Unc.	Elec. Unc.	Recoil Unc.	Bckg. Unc.	QCD Unc.	EW Unc.	PDF Unc.	Total Unc.	χ^2/dof of Comb.
p_T^ℓ, $W^\pm$, e	80347.2	9.9	0.0	14.8	2.6	5.7	8.2	5.3	8.9	23.1	4/5
m_T, $W^\pm$, e	80364.6	13.5	0.0	14.4	13.2	12.8	9.5	3.4	10.2	30.8	8/5
p_T^ℓ, $W^\pm$, μ	80382.3	10.1	10.7	0.0	2.5	3.9	8.4	6.0	10.7	21.4	7/7
m_T, $W^\pm$, μ	80381.5	13.0	11.6	0.0	13.0	6.0	9.6	3.4	11.2	27.2	3/7

MSSM fit

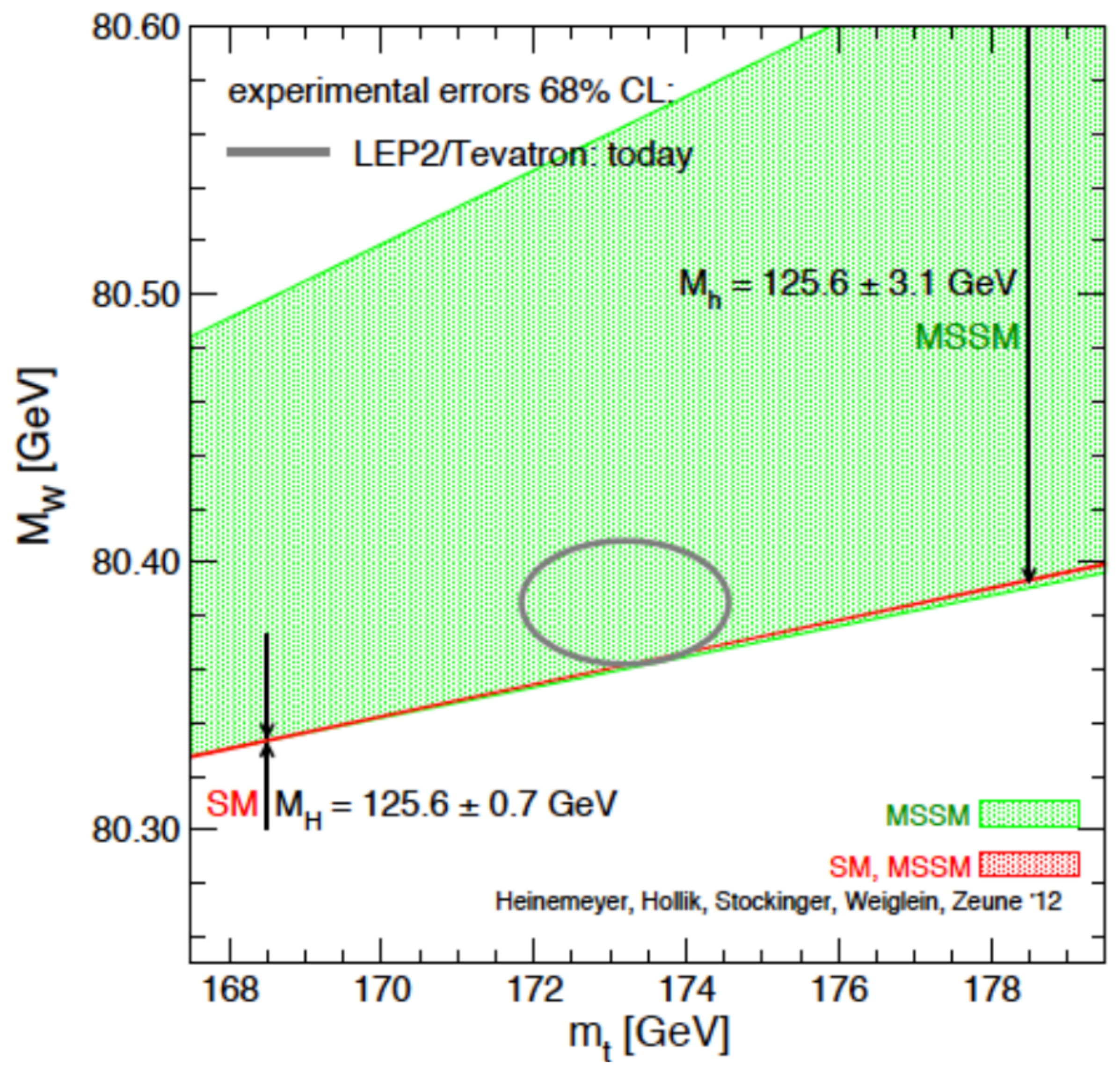

MSSM band:
scan over
SUSY masses

overlap:
SM is MSSM-like
MSSM is SM-like

SM band:
variation of M_H^{SM}

Comparison CDF vs ATLAS

Similar PDF uncertainties

courtesy of M. Boonekamp

p_T W uncertainties are larger for p_T lepton than m_T at CDF, but similar in ATLAS

m_T fit uncertainties

Source	$W \to \mu\nu$	$W \to e\nu$	Common
Lepton energy scale	7	10	5
Lepton energy resolution	1	4	0
Lepton efficiency	0	0	0
Lepton tower removal	2	3	2
Recoil scale	5	5	5
Recoil resolution	7	7	7
Backgrounds	3	4	0
PDFs	10	10	10
W boson p_T	3	3	3
Photon radiation	4	4	4
Statistical	16	19	0
Total	23	26	15

p_T^ℓ fit uncertainties

Source	$W \to \mu\nu$	$W \to e\nu$	Common
Lepton energy scale	7	10	5
Lepton energy resolution	1	4	0
Lepton efficiency	1	2	0
Lepton tower removal	0	0	0
Recoil scale	6	6	6
Recoil resolution	5	5	5
Backgrounds	5	3	0
PDFs	9	9	9
W boson p_T	9	9	9
Photon radiation	4	4	4
Statistical	18	21	0
Total	25	28	16

Includes also Ai uncertainties

Combined categories	Value [MeV]	Stat. Unc.	Muon Unc.	Elec. Unc.	Recoil Unc.	Bckg. Unc.	QCD Unc.	EW Unc.	PDF Unc.	Total Unc.	χ^2/dof of Comb.
p_T^ℓ, $W^\pm$, e	80347.2	9.9	0.0	14.8	2.6	5.7	8.2	5.3	8.9	23.1	4/5
m_T, $W^\pm$, e	80364.6	13.5	0.0	14.4	13.2	12.8	9.5	3.4	10.2	30.8	8/5
p_T^ℓ, $W^\pm$, μ	80382.3	10.1	10.7	0.0	2.5	3.9	8.4	6.0	10.7	21.4	7/7
m_T, $W^\pm$, μ	80381.5	13.0	11.6	0.0	13.0	6.0	9.6	3.4	11.2	27.2	3/7

Comparison D0 vs ATLAS

courtesy of M. Boonekamp

Source	Section	m_T	p_T^e	$\not{E}_T$
Experimental				
Electron Energy Scale	VII C 4	16	17	16
Electron Energy Resolution	VII C 5	2	2	3
Electron Shower Model	V C	4	6	7
Electron Energy Loss	V D	4	4	4
Recoil Model	VII D 3	5	6	14
Electron Efficiencies	VII B 10	1	3	5
Backgrounds	VIII	2	2	2
$\sum$(Experimental)		18	20	24
W Production and Decay Model				
PDF	VI C	11	11	14
QED	VI B	7	7	9
Boson p_T	VI A	2	5	2
$\sum$(Model)		13	14	17
Systematic Uncertainty (Experimental and Model)		22	24	29
W Boson Statistics	IX	13	14	15
Total Uncertainty		26	28	33

Similar PDF uncertainties

Smaller p_T W uncertainties at D0

Includes also Ai uncertainties

Combined categories	Value [MeV]	Stat. Unc.	Muon Unc.	Elec. Unc.	Recoil Unc.	Bckg. Unc.	QCD Unc.	EW Unc.	PDF Unc.	Total Unc.	χ^2/dof of Comb.
p_T^ℓ, $W^\pm$, e	80347.2	9.9	0.0	14.8	2.6	5.7	8.2	5.3	8.9	23.1	4/5
m_T, $W^\pm$, e	80364.6	13.5	0.0	14.4	13.2	12.8	9.5	3.4	10.2	30.8	8/5
p_T^ℓ, $W^\pm$, μ	80382.3	10.1	10.7	0.0	2.5	3.9	8.4	6.0	10.7	21.4	7/7
m_T, $W^\pm$, μ	80381.5	13.0	11.6	0.0	13.0	6.0	9.6	3.4	11.2	27.2	3/7

Difference Tevatron vs LHC

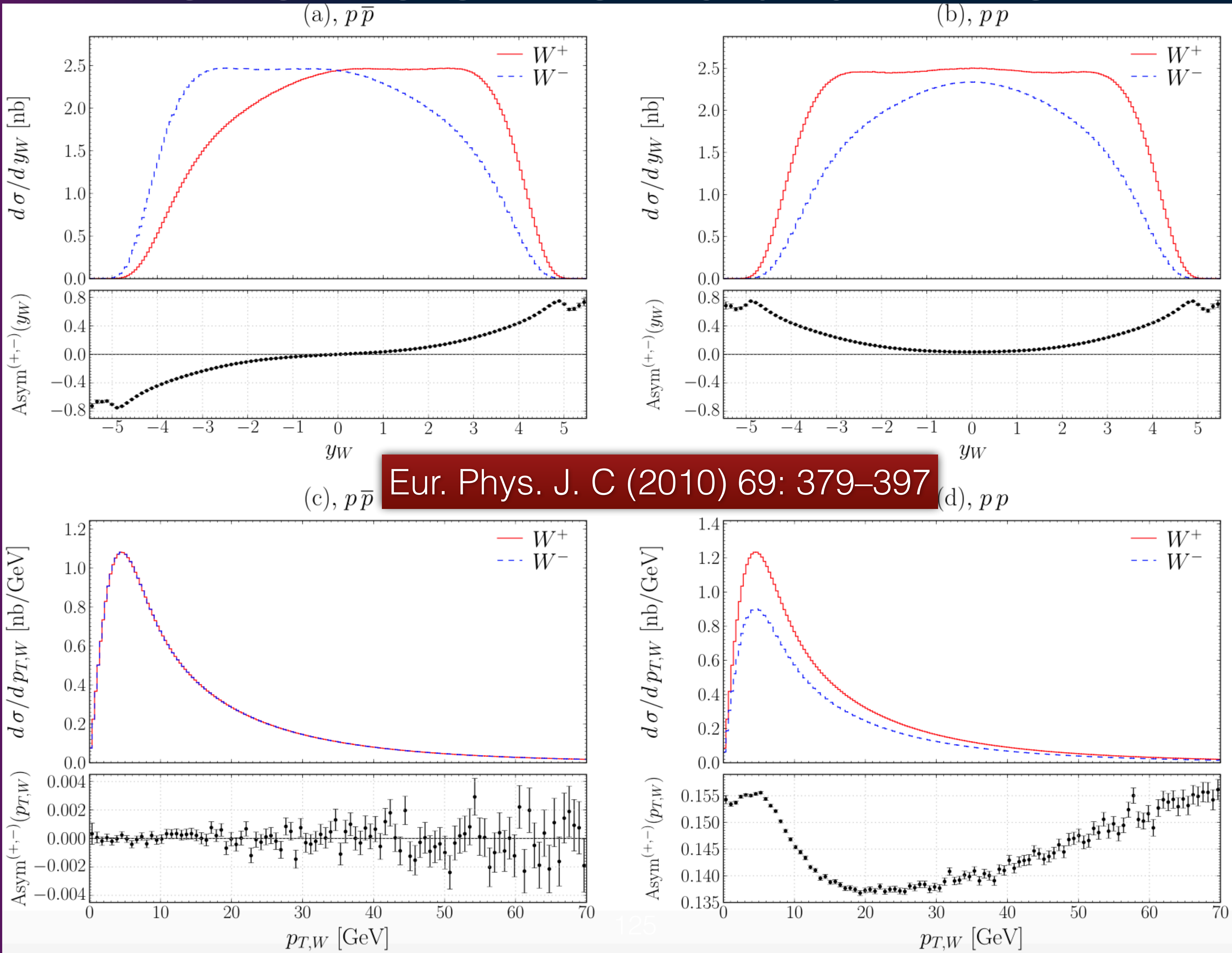

Eur. Phys. J. C (2010) 69: 379–397

Difference Tevatron vs LHC

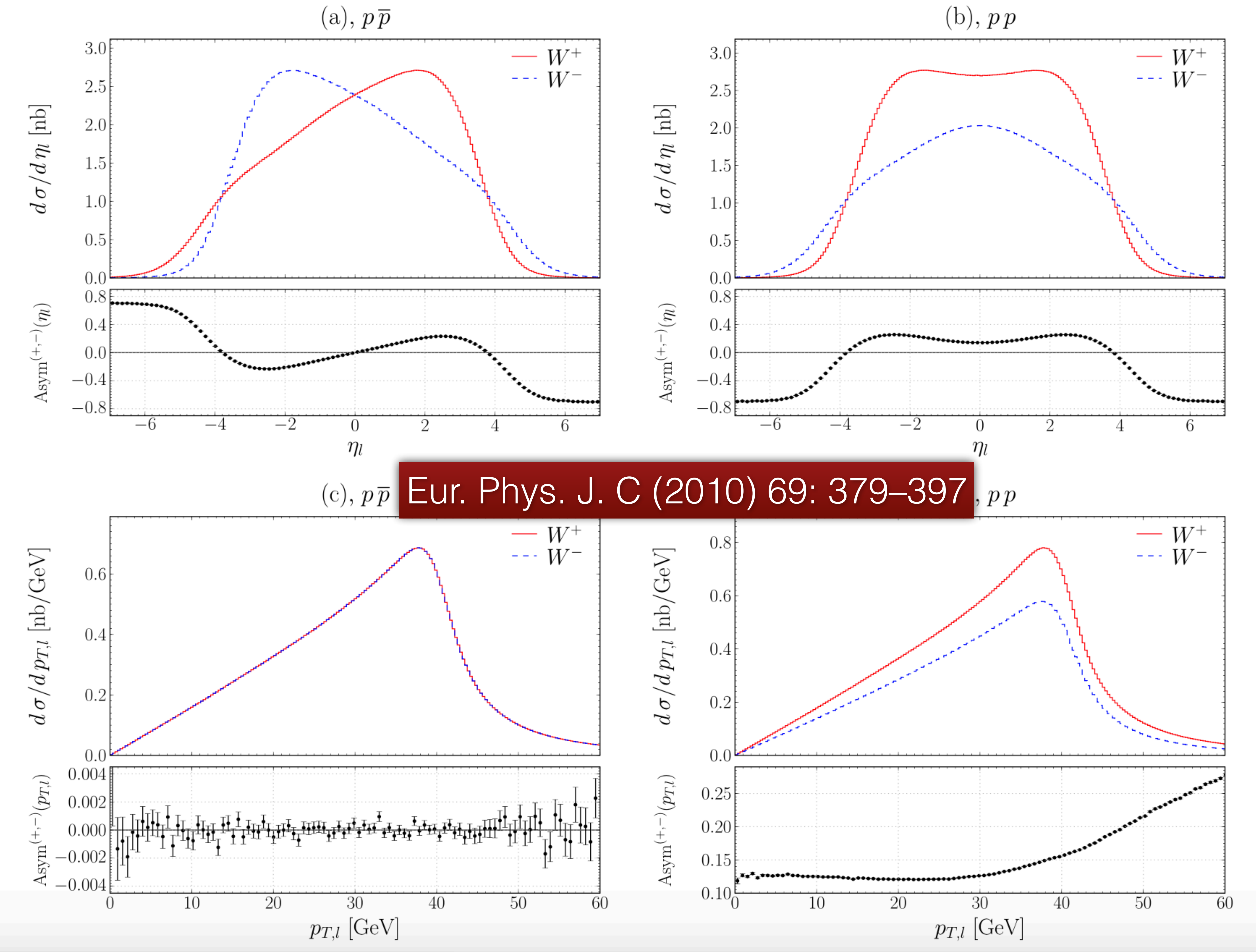

Eur. Phys. J. C (2010) 69: 379–397

Spectra differences between 'purely sea' and 'standard' quark induced W production

Eur. Phys. J. C (2010) 69: 379–397

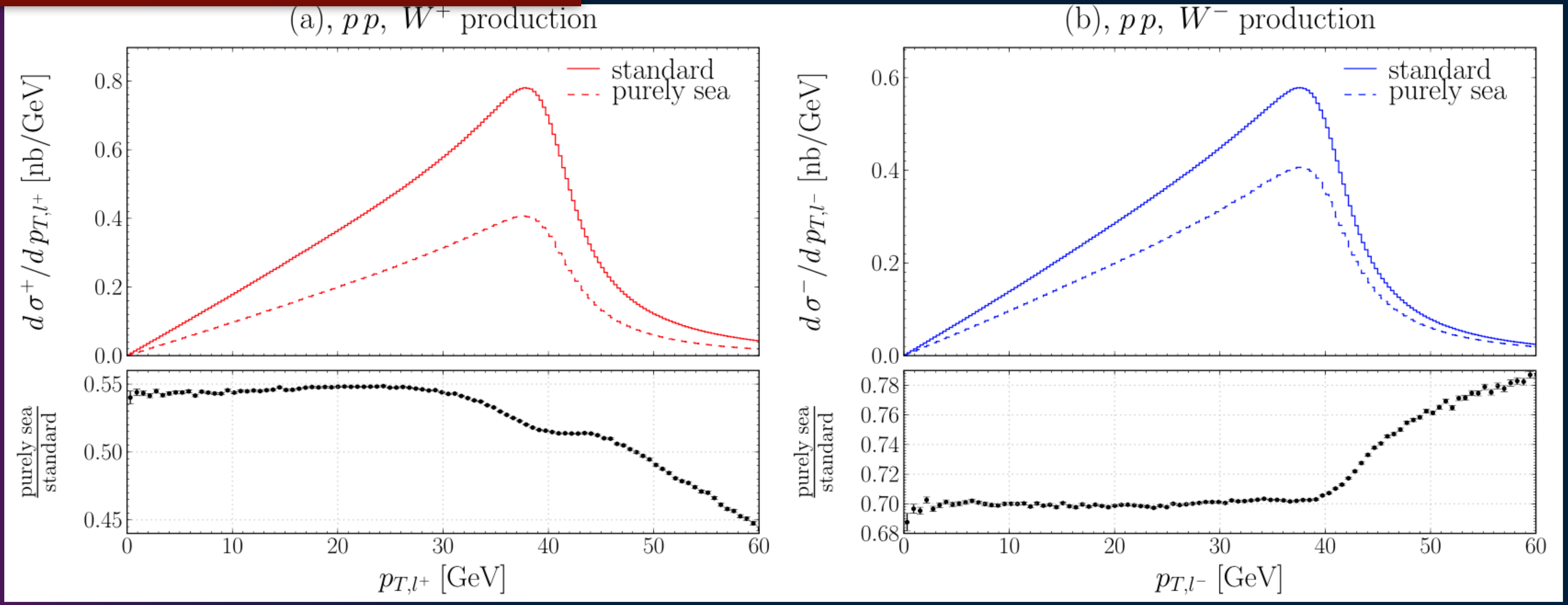

- Uncertainty on sea and valence PDFs —>uncertainty on W helicity —> on the measured spectra

$$\sigma_{W^+}(y) \propto u(x_1)\cdot\bar{d}(x_2)+\bar{d}(x_1)\cdot u(x_2)$$
$$\sigma_{W^-}(y) \propto d(x_1)\cdot\bar{u}(x_2)+\bar{u}(x_1)\cdot d(x_2)$$

Full uncertainty table

Combined categories	Value [MeV]	Stat. Unc.	Muon Unc.	Elec. Unc.	Recoil Unc.	Bckg. Unc.	QCD Unc.	EW Unc.	PDF Unc.	Total Unc.	χ^2/dof of Comb.
m_T, W^+, e-μ	80370.0	12.3	8.3	6.7	14.5	9.7	9.4	3.4	16.9	30.9	2/6
m_T, W^-, e-μ	80381.1	13.9	8.8	6.6	11.8	10.2	9.7	3.4	16.2	30.5	7/6
m_T, $W^\pm$, e-μ	80375.7	9.6	7.8	5.5	13.0	8.3	9.6	3.4	10.2	25.1	11/13
p_T^ℓ, W^+, e-μ	80352.0	9.6	6.5	8.4	2.5	5.2	8.3	5.7	14.5	23.5	5/6
p_T^ℓ, W^-, e-μ	80383.4	10.8	7.0	8.1	2.5	6.1	8.1	5.7	13.5	23.6	10/6
p_T^ℓ, $W^\pm$, e-μ	80369.4	7.2	6.3	6.7	2.5	4.6	8.3	5.7	9.0	18.7	19/13
p_T^ℓ, $W^\pm$, e	80347.2	9.9	0.0	14.8	2.6	5.7	8.2	5.3	8.9	23.1	4/5
m_T, $W^\pm$, e	80364.6	13.5	0.0	14.4	13.2	12.8	9.5	3.4	10.2	30.8	8/5
m_T-p_T^ℓ, W^+, e	80345.4	11.7	0.0	16.0	3.8	7.4	8.3	5.0	13.7	27.4	1/5
m_T-p_T^ℓ, W^-, e	80359.4	12.9	0.0	15.1	3.9	8.5	8.4	4.9	13.4	27.6	8/5
m_T-p_T^ℓ, $W^\pm$, e	80349.8	9.0	0.0	14.7	3.3	6.1	8.3	5.1	9.0	22.9	12/11
p_T^ℓ, $W^\pm$, μ	80382.3	10.1	10.7	0.0	2.5	3.9	8.4	6.0	10.7	21.4	7/7
m_T, $W^\pm$, μ	80381.5	13.0	11.6	0.0	13.0	6.0	9.6	3.4	11.2	27.2	3/7
m_T-p_T^ℓ, W^+, μ	80364.1	11.4	12.4	0.0	4.0	4.7	8.8	5.4	17.6	27.2	5/7
m_T-p_T^ℓ, W^-, μ	80398.6	12.0	13.0	0.0	4.1	5.7	8.4	5.3	16.8	27.4	3/7
m_T-p_T^ℓ, $W^\pm$, μ	80382.0	8.6	10.7	0.0	3.7	4.3	8.6	5.4	10.9	21.0	10/15
m_T-p_T^ℓ, W^+, e-μ	80352.7	8.9	6.6	8.2	3.1	5.5	8.4	5.4	14.6	23.4	7/13
m_T-p_T^ℓ, W^-, e-μ	80383.6	9.7	7.2	7.8	3.3	6.6	8.3	5.3	13.6	23.4	15/13
m_T-p_T^ℓ, $W^\pm$, e-μ	80369.5	6.8	6.6	6.4	2.9	4.5	8.3	5.5	9.2	18.5	29/27

Weights of all categories

Observable	Channel	η range	Weight
m_{T}	$W^+ \to \mu\nu$	$\|\eta\| < 0.8$	0.018
		$0.8 < \|\eta\| < 1.4$	0.022
		$1.4 < \|\eta\| < 2.0$	0.003
		$2.0 < \|\eta\| < 2.4$	0.006
	$W^- \to \mu\nu$	$\|\eta\| < 0.8$	0.020
		$0.8 < \|\eta\| < 1.4$	0.018
		$1.4 < \|\eta\| < 2.0$	0.022
		$2.0 < \|\eta\| < 2.4$	0.001
	$W^+ \to e\nu$	$\|\eta\| < 0.6$	0.013
		$0.6 < \|\eta\| < 1.2$	0.001
		$1,8 < \|\eta\| < 2.4$	0.010
	$W^- \to e\nu$	$\|\eta\| < 0.6$	0.008
		$0.6 < \|\eta\| < 1.2$	0.000
		$1.8 < \|\eta\| < 2.4$	0.002
p_{T}^{ℓ}	$W^+ \to \mu\nu$	$\|\eta\| < 0.8$	0.101
		$0.8 < \|\eta\| < 1.4$	0.076
		$1.4 < \|\eta\| < 2.0$	0.050
		$2.0 < \|\eta\| < 2.4$	0.011
	$W^- \to \mu\nu$	$\|\eta\| < 0.8$	0.097
		$0.8 < \|\eta\| < 1.4$	0.071
		$1.4 < \|\eta\| < 2.0$	0.047
		$2.0 < \|\eta\| < 2.4$	0.010
	$W^+ \to e\nu$	$\|\eta\| < 0.6$	0.056
		$0.6 < \|\eta\| < 1.2$	0.071
		$1,8 < \|\eta\| < 2.4$	0.081
	$W^- \to e\nu$	$\|\eta\| < 0.6$	0.062
		$0.6 < \|\eta\| < 1.2$	0.056
		$1.8 < \|\eta\| < 2.4$	0.067

p_T modeling strategy

various predictions of the 2 observables

Recoil distributions without modelling corrections

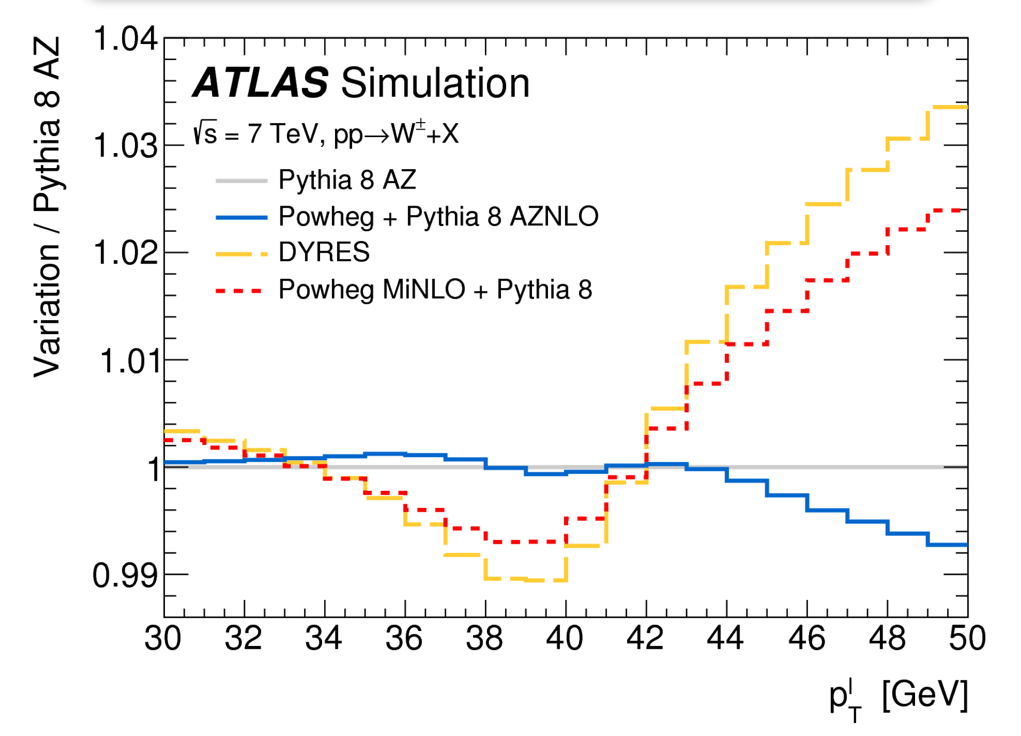

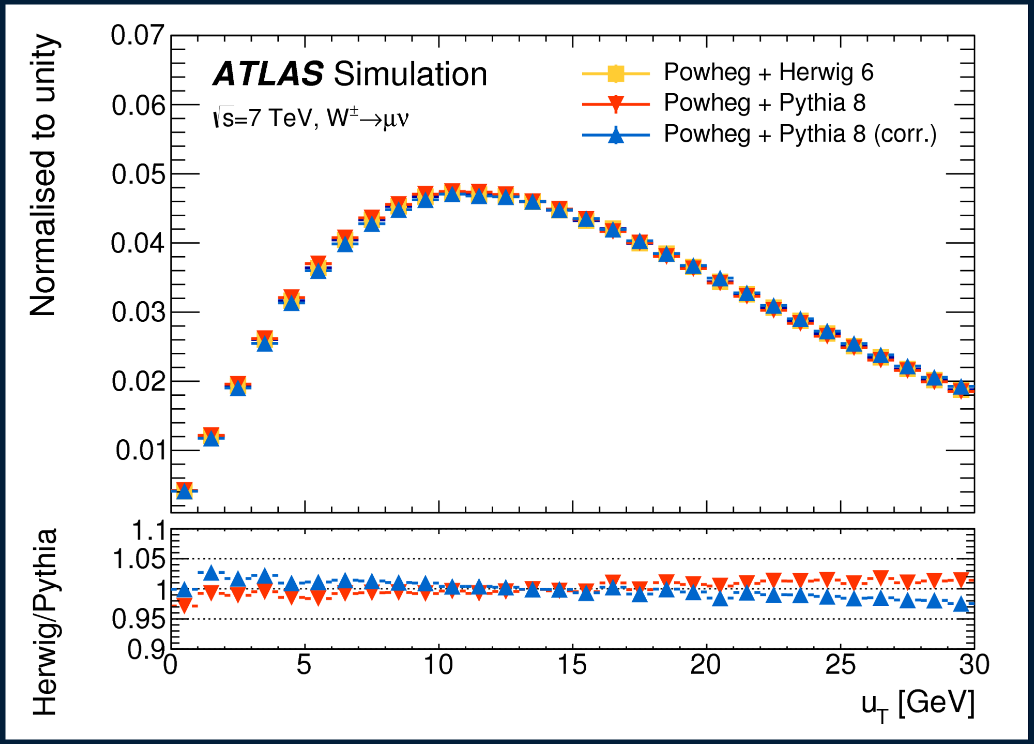

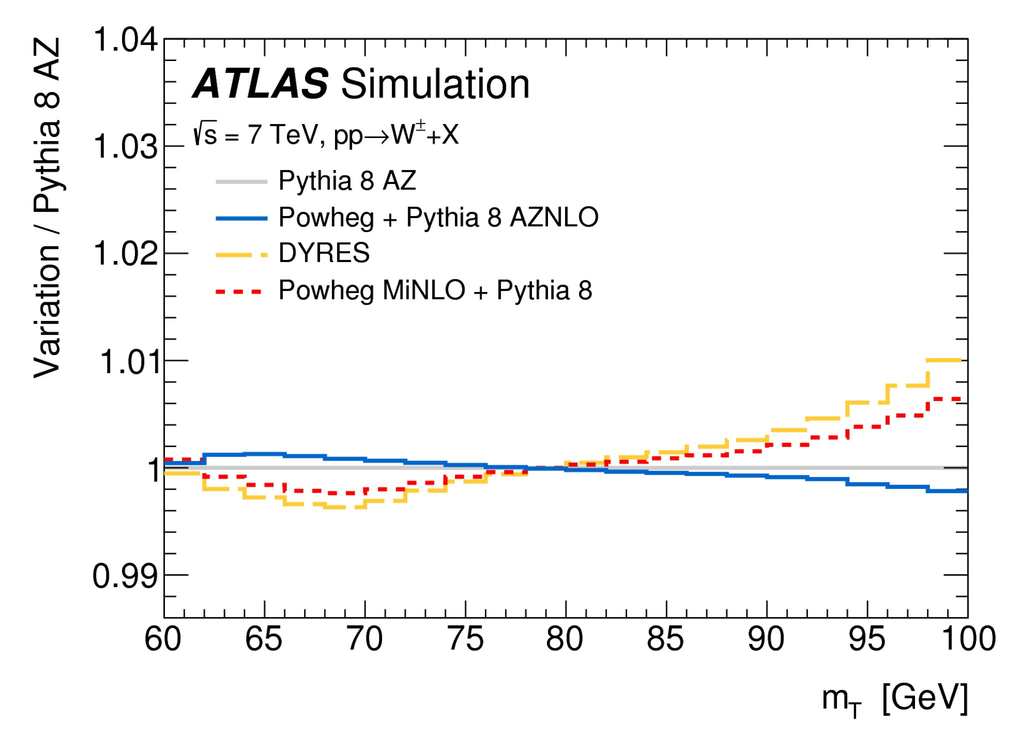

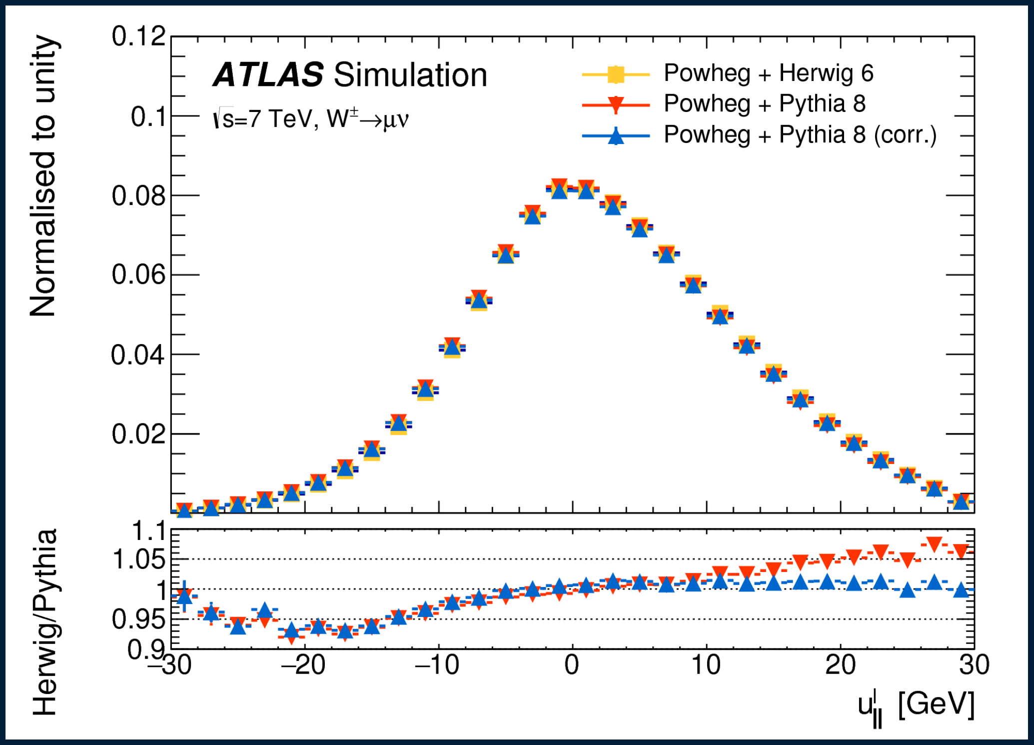

p_T modeling strategy

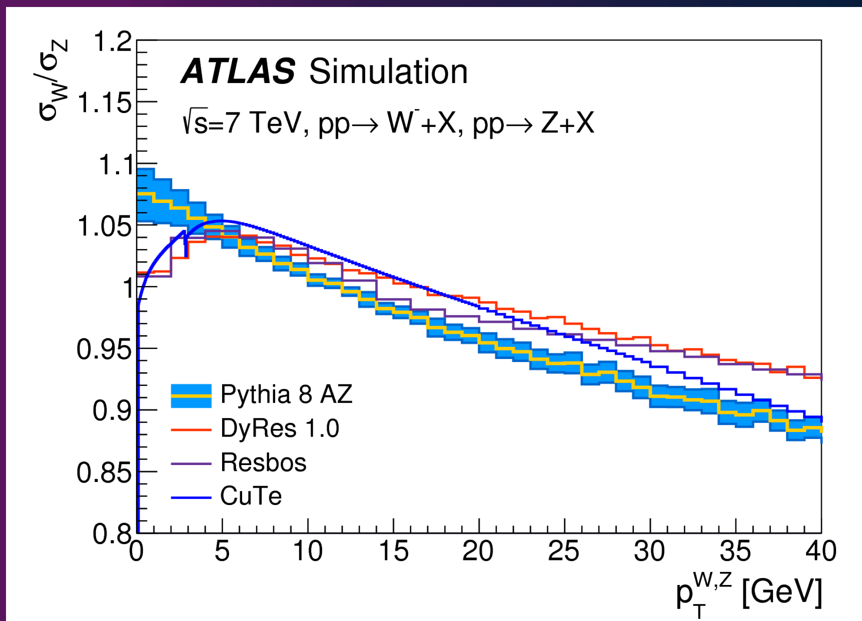

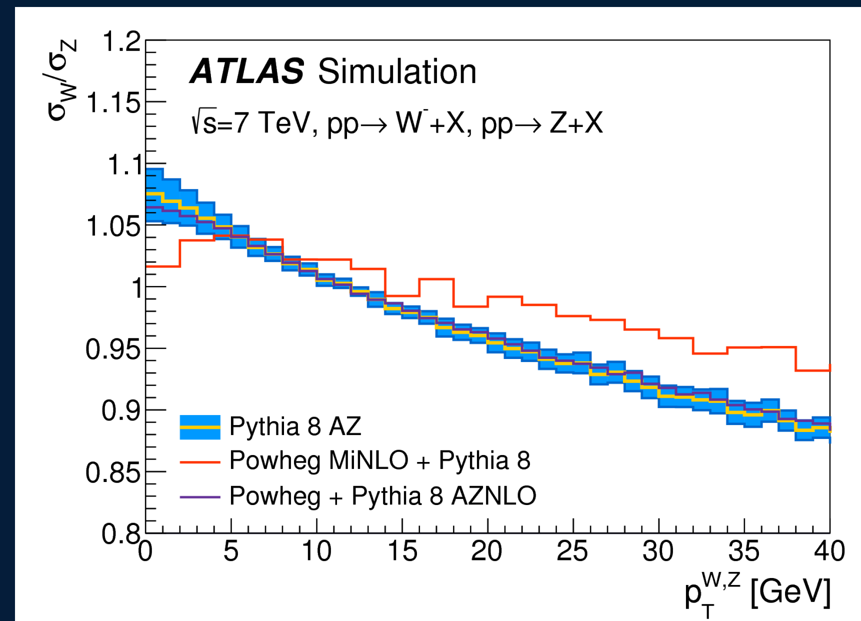

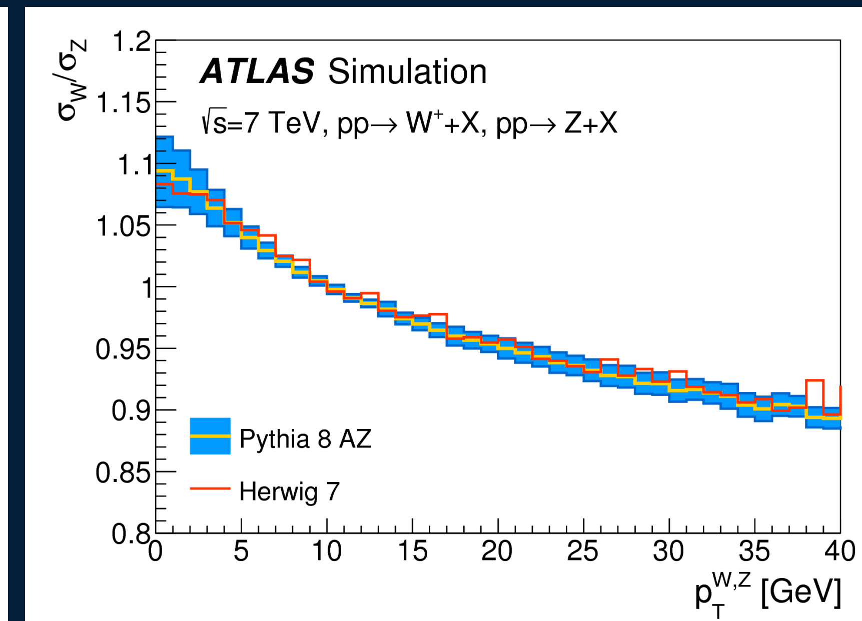

- Very different prediction of $p_T(W)/p_T(Z)$ ratio from resummed technique or Powheg MiNLO with respect to Pythia 8 AZ
  - This is a high topic of interest and subject to many discussions in the LHC EW working group
- Pythia8 AZ is validated by the data ($u_{//}$) contrary to other predictions
- Negligible impact of the parton shower model (Herwig 7)

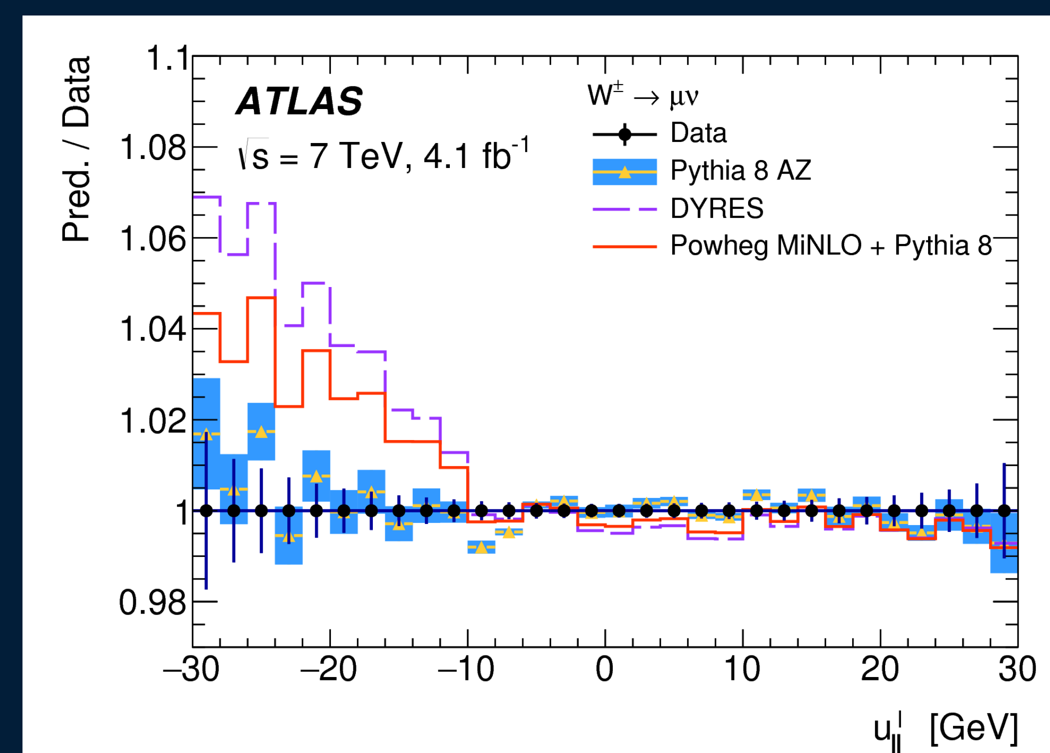

Low mu runs

- Dependence of uncertainty (statistical + recoil calibration systematic) in first pT(W) bin (0-5 GeV) vs mu for 300 pb-1 integrated luminaosity

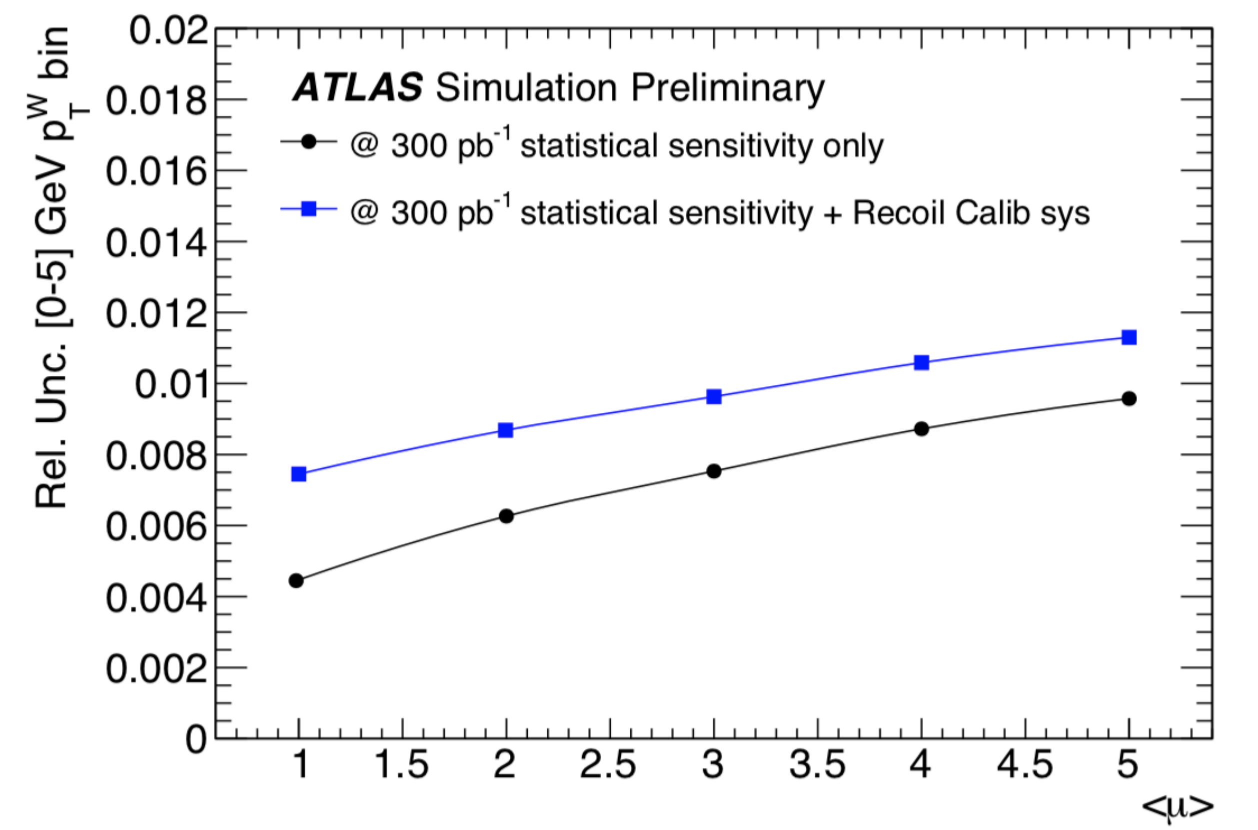

- Dependence of SET with sqrts